

This document was produced
by scanning the original publication.

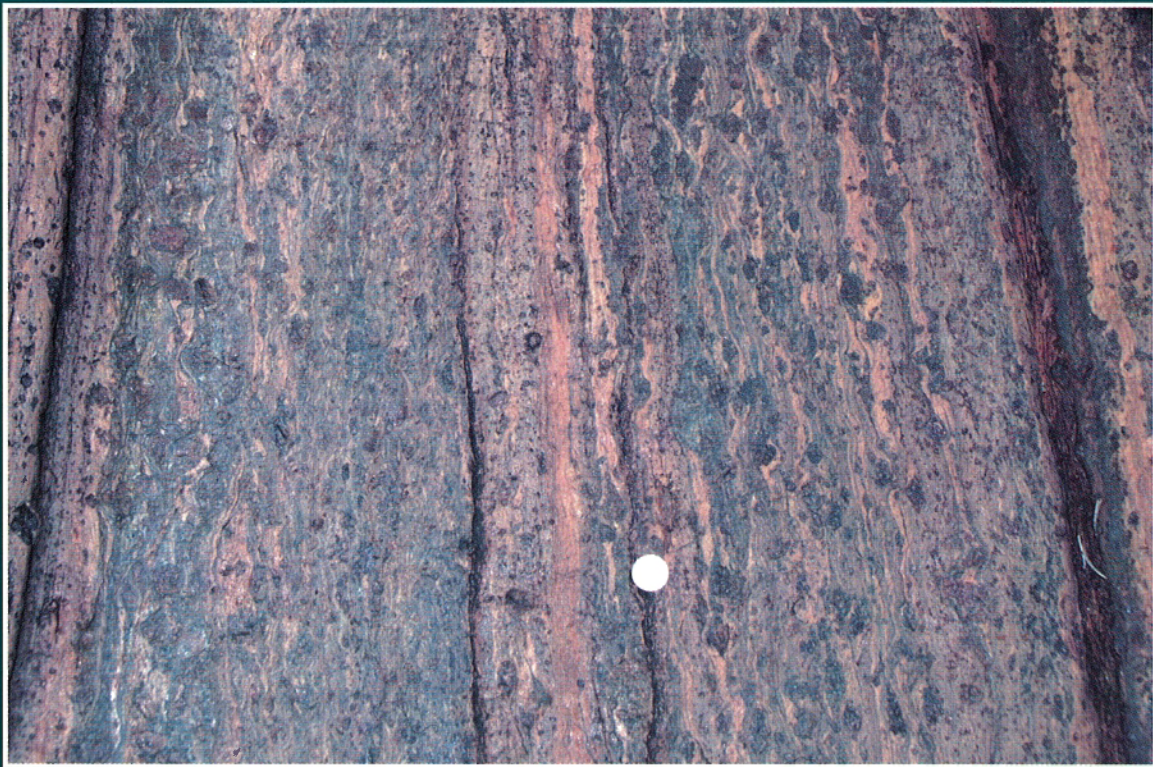
Ce document est le produit d'une
numérisation par balayage
de la publication originale.



GEOLOGICAL SURVEY OF CANADA
BULLETIN 501

**GEOLOGY OF THE STRIDING-ATHABASCA
MYLONITE ZONE, NORTHERN SASKATCHEWAN
AND SOUTHEASTERN DISTRICT OF MACKENZIE,
NORTHWEST TERRITORIES**

S. Hanmer



1997



Natural Resources
Canada

Ressources naturelles
Canada

Canada

GEOLOGICAL SURVEY OF CANADA
BULLETIN 501

**GEOLOGY OF THE STRIDING-ATHABASCA
MYLONITE ZONE, NORTHERN
SASKATCHEWAN AND SOUTHEASTERN
DISTRICT OF MACKENZIE,
NORTHWEST TERRITORIES**

Simon Hanmer

1997

© Her Majesty the Queen in Right of Canada, 1997
Cat. No. M42-501E
ISBN 0-660-16902-9

Available in Canada from
Geological Survey of Canada offices:

601 Booth Street
Ottawa, Ontario K1A 0E8

3303-33rd Street N.W.,
Calgary, Alberta T2L 2A7

101-605 Robson Street
Vancouver, B.C. V6B 5J3

or from

Canadian Government Publishing
Public Works and Government Services Canada
Ottawa, Ontario K1A 0S9

A deposit copy of this publication is also available for reference
in selected public libraries across Canada

Price subject to change without notice

Cover illustration

Garnet-sillimanite-orthopyroxene ribbon mylonite derived by deformation of
Pine Channel diatexite, north shore of Lake Athabasca. Photo by S. Hanmer.
GSC 1996-089

Author's address

Geological Survey of Canada
615 Booth Street
Ottawa, Ontario
K1A 0E8

Original manuscript submitted: 1995-03
Final version approved for publication: 1995-09

PREFACE

The Striding-Athabasca mylonite zone is one of the most remarkable faults in the Canadian Shield. Extending some 400 km from Lake Athabasca into the District of Mackenzie, Northwest Territories, it has long been the target of mapping and nickel exploration by the Geological Survey of Canada (GSC), the Saskatchewan Geological Survey and private industry, from the classical work of J.B. Tyrrell in the 1890s to prospecting and recent drilling by Devex Exploration Inc. and Noranda Exploration Co. Ltd. in 1991. This report, along with the previously published map of the East Athabasca Mylonite Triangle (GSC Map 1859A, scale 1:100 000), documents the geology of the Saskatchewan segment of the mylonite zone mapped during three-month field seasons in 1990 and 1991. Systematic observations made during a two month field season in 1992 on the Northwest Territories segment of the mylonite zone are also described.

The Striding-Athabasca mylonites form a deep-crustal fault zone which initiated during the Middle Archean (ca. 3.2 Ga) dismemberment of an island arc associated with the suturing of the Rae and Hearne continents. In the Late Archean (ca. 2.6 Ga), the mylonites and the fragments of the arc were the site of renewed shearing, plutonism, and metamorphism. Subsequently, the Archean structure was exploited by rifting during Early Proterozoic continental breakup of the Churchill continent, and served to define a major promontory-re-entrant pair which controlled accretionary tectonics (ca. 2.1-1.8 Ga) at the jagged western margin of the continent.

This report provides detailed documentation of the structural and plutonic history of the Striding-Athabasca mylonite belt, and examines its role in the Archean and Early Proterozoic tectonic evolution of the western Canadian Shield. It illustrates how geological studies are essential to the successful interpretation of crustal-scale experiments, such as LITHOPROBE.

M.D. Everell
Assistant Deputy Minister
Earth Sciences Sector

PRÉFACE

La zone mylonitique de Striding-Athabasca correspond à l'une des failles les plus remarquables du Bouclier canadien. S'allongeant sur quelque 400 km du lac Athabasca au district de Mackenzie (Territoires du Nord-Ouest), elle est depuis longtemps la cible de travaux de cartographie géologique et de prospection du nickel effectués par la Commission géologique du Canada (CGC), la Commission géologique de la Saskatchewan et l'industrie privée. Ces travaux remontent aussi loin qu'aux études classiques de J.B. Tyrrell menées dans les années 1890 et sont aussi récents que les travaux de prospection et de forage réalisés par les sociétés Devex Exploration Inc. et Explorations Noranda Limitée en 1991. Le présent rapport, comme la carte de la zone triangulaire mylonitique d'Athabasca Est (carte 1859A de la CGC, échelle de 1/100 000) publiée récemment, documente la géologie du segment de la zone mylonitique situé en Saskatchewan qui a été cartographié durant trois mois de travaux sur le terrain en 1990 et en 1991. Il contient également une description des observations systématiques faites pendant une campagne de deux mois réalisée en 1992 sur le segment de la zone mylonitique situé dans les Territoires du Nord-Ouest.

Les mylonites de la zone de Striding-Athabasca constituent une zone de failles de la croûte profonde dont la formation a débuté par le démembrement à l'Archéen moyen (vers 3,2 Ga) d'un arc insulaire associé à la suture des continents de Rae et de Hearne. À l'Archéen tardif (vers 2,6 Ga), les mylonites et les fragments de l'arc ont été le site d'un nouvel épisode de cisaillement, de plutonisme et de métamorphisme. Par la suite, au Protérozoïque précoce, la structure archéenne a été le siège d'un rifting qui a mené à la fragmentation du continent de Churchill et a donné naissance à un important couple promontoire-rentrant, qui a exercé un contrôle sur la tectonique d'accrétion (vers 2,1 -1,8 Ga) à la marge ouest dentelée du continent.

Le présent rapport fournit une documentation détaillée de l'évolution structurale et plutonique de la zone mylonitique de Striding-Athabasca et une analyse de son rôle dans l'évolution tectonique de la partie ouest du Bouclier canadien à l'Archéen et au Protérozoïque précoce. Un tel compte rendu illustre à quel point les études géologiques sont essentielles à une interprétation concluante d'expériences menées à l'échelle crustale comme celles du projet LITHOPROBE.

M.D. Everell
Sous-ministre adjoint
Secteur des sciences de la Terre

CONTENTS

1	Abstract/Résumé
2	Summary/Sommaire
3	Introduction
4	Location and access
7	Settlement
7	Climate, flora and fauna
7	Physiography
8	Previous and recent work
8	Regional geophysics
8	Regional geology
10	Regional isotopic geochemistry
11	Lake Athabasca to Snowbird Lake
12	Field methods and extent of mapping
12	Acknowledgments
13	General geology
16	Wall rocks
16	Rae crust
16	Hearne crust
17	East Athabasca mylonite triangle
17	Upper deck
17	Pine Channel diatexite
21	Axis mafic granulite
26	Lower deck
26	Reeve diatexite
27	Chipman batholith
30	Chipman dykes
34	Chipman granite
36	Bohica mafic complex
37	Garnet-pyroxene Mary granite
43	Other garnet-pyroxene granitoid bodies
45	Hornblende-biotite granitoid bodies
49	Mixed and minor map units
50	Robillard-Patterson gneiss
51	Economic geology
51	Tectonic flow
51	High temperature flow
52	Dip-slip shear zone (upper deck)
53	Conjugate strike-slip shear zones (lower deck)
54	Central septum (lower deck)
55	Medium temperature flow
57	Interface mylonites
57	Anastomosing flow
57	Lateral limits of the lower deck
59	Taylor Bay fault
59	Low temperature flow
59	Black-Bompas fault
60	Straight-Grease fault
61	Other faults
61	Heterogeneous flow

62	Syntectonic magmatism
62	Granites, extension, and accretion
64	Mafic dykes and transpression
65	Striding mylonite belt
66	Selwyn lozenge
68	Striding mylonite belt
72	Selwyn lozenge, northwest margin
73	Mylonitization
73	Shear zone geometry
75	Fault localization
75	Modest movements, spectacular fabrics
77	Tectonic significance
77	Lozenges
77	Stiff Middle Archean crust
78	Middle Archean arc?
79	Late Archean intracontinental shear zone
81	Metamorphism and uplift
81	Delamination and metamorphism
81	Uplift and exhumation
81	Continental deformation and uplift
82	Apparent vertical throw (Rae)
82	Real vertical throw (Hearne)
82	Brittle dip-slip faulting
82	Implications for Proterozoic tectonics
83	Dilational basin
84	Re-entrants, jagged margins, and transform faults
84	An internal test
85	References

Illustrations

4	1. Generalized geology of the western Canadian Shield
5	2. Spatial distribution of high grade mylonites with respect to the magnetically defined crustal-scale Athabasca, Selwyn, and Three Esker lozenges
6	3. Geographical locations in the East Athabasca mylonite triangle
8	4. Previous geometrical interpretation of the East Athabasca mylonite triangle
9	5. Snowbird tectonic zone in the horizontal gravity gradient field
9	6. Previous mapping in the vicinity of the Striding-Athabasca mylonite zone
10	7. Distribution of available U-Pb zircon dates in the western Churchill continent
11	8. Distribution of available T_{dm} -Nd model ages for the western Churchill continent
14	9. Principal map units of the East Athabasca mylonite triangle
14	10. Principal tectonic elements within the East Athabasca mylonite triangle
15	11. Principal tectonic elements of the Snowbird tectonic zone
16	12. Open to moderate folding of paragneiss banding in western (Rae) wall rock
16	13. Folded shear zone in amphibolite, western (Rae) wall rock
18	14. Porphyroblastic leucosome in eastern (Hearne) wall rock
18	15. Pelitic schist in eastern (Hearne) wall rock
18	16. Bedding-parallel cleavage in mafic flows and tuffs, in eastern (Hearne) wall rock
18	17. Coarse crenulation of bedding-parallel cleavage in eastern (Hearne) wall rock
19	18. Distribution of Pine Channel diatexite
19	19. Straight banding in Pine Channel diatexite
19	20. Ribbon mylonite fabric in Pine Channel diatexite
20	21. Garnet-rich layer in ribbon mylonite after Pine Channel diatexite

- 20 22. Variation in size of garnets in Pine Channel diatexite
- 20 23. Orthopyroxene and garnet in ribbon mylonite fabric in Pine Channel diatexite
- 21 24. Moderately deformed precursor to Pine Channel diatexite ribbon mylonite
- 21 25. Ribbon mylonite equivalent of rocks in Figure 24
- 21 26. Distribution of Axis mafic granulite
- 22 27. Bouguer gravity field in the vicinity of the East Athabasca mylonite triangle
- 22 28. Streaky aspect of finely polycrystalline Axis mafic granulite mylonite
- 23 29. Streaky aspect of Axis mafic granulite mylonite, Lake Athabasca
- 23 30. Relict coarse ophitic texture in Axis mafic granulite
- 23 31. Flattened equivalent of rocks in Figure 30
- 23 32. Branching vein of mafic granulite in Pine Channel diatexite ribbon mylonite
- 24 33. Sheets of mafic granulite in Pine Channel diatexite ribbon mylonite
- 24 34. Coarse orthopyroxene leucogranite crosscutting subtle layering in Axis mafic granulite
- 24 35. Folded vein of orthopyroxene leucogranite in Axis mafic granulite
- 24 36. Orthopyroxene leucogranite ribbon mylonite
- 25 37. Polycrystalline orthopyroxene mantle on monocrystalline orthopyroxene core
- 25 38. Distribution of Reeve diatexite
- 25 39. Low strain window in Reeve diatexite
- 26 40. Straight banded Reeve diatexite ribbon mylonite
- 26 41. Reeve diatexite ribbon mylonite
- 26 42. Distribution of Chipman tonalite batholith and the Chipman dykes
- 27 43. Distribution of structural map units within the Chipman tonalite batholith
- 28 44. Annealed tonalite mylonite (straight gneiss) in the Chipman tonalite batholith
- 28 45. Annealed tonalite mylonite (straight gneiss) in the Chipman tonalite batholith
- 29 46. Blocks of anorthosite in a tonalite matrix in the Chipman tonalite batholith
- 29 47. Tonalite mylonite enclosing lenses of coarse gabbro, Chipman tonalite batholith
- 29 48. Nebulous banding in coarse grained and weakly foliated tonalite, Chipman tonalite batholith
- 29 49. Subtle layering in coarse grained Chipman tonalite batholith
- 30 50. Progressive transposition of folded layering in the Chipman tonalite batholith
- 30 51. Coaxial refolding of annealed tonalite mylonite (straight gneiss), Chipman tonalite batholith
- 30 52. Annealed tonalite mylonite, Chipman tonalite batholith
- 31 53. Absence of shape fabrics in annealed tonalite mylonite, Chipman tonalite batholith
- 31 54. Core-and-mantle structure in annealed tonalite mylonite, Chipman tonalite batholith
- 31 55. Folding and porphyroclast in annealed tonalite mylonite, Chipman tonalite batholith
- 31 56. Coarse ophitic texture in an isotropic Chipman dyke
- 32 57. Coarse feldspar-phyric isotropic Chipman dyke
- 32 58. Spectacularly coarse garnets in banded Chipman dyke, Chipman tonalite batholith
- 32 59. Coarse garnets and tonalite melt in banded Chipman dyke, Chipman tonalite batholith
- 33 60. Garnets with tonalite melt in banded Chipman dyke, Chipman tonalite batholith
- 33 61. Garnets with tonalite melt in Chipman dyke, Chipman tonalite batholith
- 34 62. Folding of Chipman dykes, Chipman tonalite batholith
- 34 63. Disrupted dyke with very coarse garnets, Chipman tonalite batholith
- 34 64. "Cauliflower" structure in a Chipman dyke, Chipman tonalite batholith
- 35 65. Composite Chipman dykes in the Chipman tonalite batholith
- 35 66. Crosscutting Chipman dyke, Chipman tonalite batholith
- 35 67. Transposed Chipman dykes in tonalite ribbon mylonite, Chipman tonalite batholith
- 36 68. Angular mafic blocks Chipman granite vein, Chipman tonalite batholith
- 36 69. Distribution of Bohica mafic complex
- 36 70. Garnet-clinopyroxene anorthosite ribbon mylonite, Bohica mafic complex
- 37 71. Garnet-clinopyroxene anorthosite ribbon mylonite, Bohica mafic complex
- 37 72. Clinopyroxene anorthosite ribbon mylonite, Bohica mafic complex, Cora Lake
- 37 73. Igneous textural variety in isotropic garnet-bearing metanorite, Bohica mafic complex
- 37 74. Flattened relict igneous texture in metagabbro, Bohica mafic complex
- 38 75. Strongly foliated gabbro/diorite, Bohica mafic complex, Kaskawan Lake
- 38 76. Mafic dyke emplaced subconcordantly into foliated leuconorite, Bohica mafic complex
- 38 77. Leuconorite ribbon mylonite, Bohica mafic complex

- 39 78. Annealed variety of leuconorite mylonite, Bohica mafic complex
- 39 79. Streaky aspect to mylonite most frequently encountered in the field, Bohica mafic complex
- 39 80. Ribbons and relict plagioclase porphyroclasts in mylonite, Bohica mafic complex
- 39 81. Garnet-rich foliated xenoliths in weakly foliated leuconorite, Bohica mafic complex
- 40 82. Distribution of Mary granite
- 40 83. Granulite facies streaky Mary granite mylonite
- 40 84. Detail of streaky Mary granite mylonite
- 41 85. Ribbon mylonite derived from coarse grained leucocratic variant of the Mary granite
- 41 86. Detail of ribbon mylonite illustrated in Figure 85
- 41 87. Well foliated, initially very coarse grained Mary granite
- 41 88. Ribbon gneiss derived from Mary granite of the type illustrated in Figure 87
- 42 89. Low strain rate/recrystallization rate ratio in ribbon gneiss derived from Mary granite
- 42 90. Annealed porphyroclastic mylonite derived from Mary granite
- 42 91. Annealed porphyroclastic mylonite derived from Mary granite
- 42 92. Detail of annealed porphyroclastic mylonite derived from Mary granite
- 43 93. Porphyroclastic ribbon mylonite derived from Mary granite
- 43 94. Ribbon mylonite derived from Mary granite
- 43 95. Streaky annealed mylonite derived from Mary granite
- 44 96. Distribution of garnet-pyroxene granitoid bodies, excluding the Mary granite
- 44 97. Chains of pinhead garnet crystals associated with clinopyroxene in foliated Hawkes granite
- 45 98. Sketch of the geology of the area between Clut and East Hawkes lakes
- 45 99. Mechanical disaggregation of clinopyroxenite inclusions of in the Godfrey granite
- 46 100. Distribution of hornblende-biotite granitoid bodies
- 46 101. Well foliated to protomylonitic hornblende-biotite Clut granite
- 46 102. Very coarse grained, weakly foliated hornblende-biotite Melby-Turnbull granite
- 47 103. Isotropic hornblende-biotite Fehr granite
- 47 104. Detail of Figure 103 illustrating the abundant mafic inclusions
- 47 105. Well foliated, coarse grained hornblende-biotite Beed granite
- 48 106. Fehr mafic dykes cutting across the foliation of the coarse grained Fehr granite
- 48 107. Branching Fehr mafic dykes
- 48 108. Large mafic inclusions in foliated coarse grained hornblende-biotite Fehr granite
- 49 109. Relatively fine grained variety of hornblende-biotite McGillivray granite
- 49 110. Sketch map of the disposition of the Clut and McGillivray granite bodies in the Clut Lakes area
- 50 111. Distribution of Robillard-Patterson gneiss
- 50 112. Pelitic component of the Robillard-Patterson gneiss
- 52 113. Distribution of metamorphic facies within the East Athabasca mylonite triangle
- 53 114. Rare indicator of shear sense within rocks of the upper deck
- 53 115. Fabric transition at the base of the upper deck
- 54 116. Dextral winged inclusion in annealed porphyroclastic mylonite, Mary granite
- 54 117. Rotated plagioclase pressure shadows on garnets in a Chipman dyke
- 54 118. Train of back-rotated boudins in amphibolite layer, eastern (Hearne) wall rock
- 56 119. Detailed map of the Clut Lakes-East Hawkes Lake area
- 57 120. In-plane dextral winged inclusions in annealed porphyroclastic mylonite
- 57 121. Dextral winged inclusion in greenschist ribbon mylonite, Mary granite
- 58 122. Nonfissile, very fine grained porphyroclastic mylonite
- 58 123. Chlorite-bearing greenschist facies ribbon mylonite
- 58 124. Hornblende-bearing tonalite ribbon mylonite with transposed Chipman dykes
- 59 125. Sheath folding of tonalite ribbon mylonite
- 59 126. Sheath folding of tonalite ribbon mylonite and transposed branching Chipman dykes
- 60 127. Low temperature mylonite zones and faults in the East Athabasca mylonite triangle
- 60 128. Tonalite ribbon mylonite, Bompas Lake
- 61 129. Concordant pegmatite in chlorite mylonite
- 62 130. Distribution of finite strain about a stiff object in cohesive contact with a softer matrix
- 63 131. Clut and Melby-Turnbull granite bodies in relation to the displacement upper deck
- 63 132. Bifurcation of the Clut granite around the apparently younger McGillivray granite

- 64 133. Anticlockwise Chipman dyke cutting annealed tonalite mylonite, Chipman tonalite batholith
64 134. Clockwise Chipman dyke cutting annealed tonalite mylonite, Chipman tonalite batholith
65 135. Relationships between *en relais* fracture patterns, Riedel faults, and segmented dykes
66 136. Principal tectonic elements of the Striding-Athabasca mylonite zone
67 137. Weakly deformed array of tonalite veins cutting amphibolite
67 138. Geometrically complex migmatitic gneiss with irregularly shaped, angular inclusions
67 139. Microgranular xenolith in garnetiferous gabbro/diorite
68 140. Near-isotopic garnet-clinopyroxene granite
68 141. Postkinematic lamprophyre dyke
68 142. Granitic ribbon mylonite with large feldspar porphyroclast
68 143. Flaggy banded ribbon mylonite derived from diatexite
68 144. Porphyroclastic ribbon mylonite derived from granite protolith
69 145. Garnet-clinopyroxene anorthosite ribbon mylonite
69 146. Garnet-clinopyroxene anorthosite ribbon mylonite with garnet clinopyroxene bands
69 147. Sheets of leucogranite ribbon mylonite in ribbon mylonite of paragneissic origin
69 148. Garnet-clinopyroxene anorthosite ribbon mylonite with garnet-clinopyroxene bands
69 149. Garnet-clinopyroxene anorthosite ribbon mylonite with garnet clinopyroxene bands
69 150. Detail of garnet-clinopyroxene anorthosite ribbon mylonite
70 151. Porphyroclastic granite ribbon mylonite
70 152. Garnet-clinopyroxene anorthosite ribbon mylonite
71 153. Bifurcation and 90° bend in the mylonites of the Striding mylonite belt
71 154. Porphyroclastic granitic ribbon mylonite
71 155. Porphyroclastic granitic ribbon mylonite
72 156. Leucogranite ribbon mylonite with straight bands of mafic granulite
72 157. Sketch of the geology at Wholdaia Lake
73 158. Porphyroclastic ribbon mylonite derived from diorite and granitic sheets
73 159. Large garnets in streaky mylonite derived from garnet-pyroxene granite
73 160. Protomylonite with well preserved, very coarse feldspar porphyroclasts
74 161. Garnet-clinopyroxene granite ribbon mylonite
74 162. Observed and predicted distribution of shear sense in the Striding-Athabasca mylonite zone.
79 163. Distribution of shear sense, and coaxial shortening and extension
80 164. Distribution of available U-Pb zircon dates of granitic rocks in the range 2.63-2.58 Ga
83 165. Jagged boundary between Archean and the Early Proterozoic in western Churchill
85 166. Terranes docking at a jagged continental margin

Tables

- 17 1. Generalized table of geological events in the Striding-Athabasca mylonite zone
78 2. Sm/Nd data for the East Athabasca mylonite triangle



Frontispiece. Oblique aerial view looking southwest across Axis Lake towards Lake Athabasca; curvature of lakes picks out structure of the upper deck, East Athabasca mylonite triangle. Photo by S. Hanmer. GSC 1994-178

GEOLOGY OF THE STRIDING-ATHABASCA MYLONITE ZONE, NORTHERN SASKATCHEWAN AND SOUTHEASTERN DISTRICT OF MACKENZIE, NORTHWEST TERRITORIES

Abstract

Striding-Athabasca mylonite zone, northern Saskatchewan and southeastern District of Mackenzie, N.W.T., occupies a 400 km long segment of the Snowbird tectonic zone. It is a linked system of Archean granulite facies mylonite belts (East Athabasca mylonite triangle and Striding mylonite belt), which trace a sinuous course along a train of lozenges of stiff Middle Archean crust.

Middle Archean mafic and tonalitic rocks may represent part of a plutonic arc emplaced into a sedimentary accretionary wedge above a subduction zone during the early construction of the western Churchill continent, and affected by contemporaneous granulite facies mylonitization. By the Late Archean, ca. 2.62-2.60 Ga, this segment of the Snowbird tectonic zone, located well within the interior of the western Churchill continent, was invaded by voluminous mafic and granitic plutons, and subjected to further granulite facies mylonitization. Striding-Athabasca mylonite zone was not the site of an Early Proterozoic suture or orogen.

The geometry of the Archean/Early Proterozoic boundary in the western Canadian Shield may represent a jagged continental margin, composed of a pair of re-entrants defined by rifted and transform segments, inherited from Early Proterozoic break-up. Rifting may have been controlled by the Archean structure of the interior of the western Churchill continent, i.e., the Striding-Athabasca mylonite zone, with its associated Middle Archean lozenges, and Late Archean mylonites of the Great Slave Lake shear zone. The geometry of this jagged margin appears to have strongly influenced the Early Proterozoic tectonic evolution of the edge of the western Canadian Shield.

Résumé

La zone mylonitique de Striding-Athabasca dans le nord de la Saskatchewan et le sud-est du district de Mackenzie (Territoires du Nord-Ouest) occupe un segment de 400 km de longueur de la zone tectonique de Snowbird. Il s'agit d'un système composé de bandes mylonitiques archéennes du faciès des granulites (zone triangulaire mylonitique d'Athabasca Est et zone mylonitique de Striding) reliées entre elles, qui dessinent un parcours sinueux le long d'une traînée de losanges de croûte rigide de l'Archéen moyen.

Des roches mafiques et tonalitiques de l'Archéen moyen pourraient représenter une portion d'un arc plutonique mis en place dans un prisme d'accrétion sédimentaire formé au-dessus d'une zone de subduction au début de l'édification du continent de Churchill occidental et qui auraient été affectées par une mylonitisation au faciès des granulites contemporaine de leur intrusion. Avant l'Archéen tardif, soit à environ 2,62-2,60 Ga, ce segment de la zone tectonique de Snowbird, situé bien à l'intérieur du continent de Churchill occidental, avait été envahi par des plutons mafiques et granitiques de grandes dimensions et soumis à une déformation plus poussée par mylonitisation au faciès des granulites. La zone mylonitique de Striding-Athabasca n'a pas été le site d'une suture ou d'un orogène au Protérozoïque précoce.

La géométrie de la limite Archéen-Protérozoïque précoce dans l'ouest du Bouclier canadien pourrait être le reflet d'une marge continentale dentelée, composée d'une paire de rentrants correspondant à des segments d'une marge de divergence délimités par des failles transformantes, qui serait un héritage de la fragmentation continentale du Protérozoïque précoce. Le rifting a pu être contrôlé par les structures archéennes du continent de Churchill occidental, soit la zone mylonitique de Striding-Athabasca et les losanges de croûte de l'Archéen moyen associés, ainsi que les mylonites de l'Archéen tardif de la zone de cisaillement du Grand lac des Esclaves. La géométrie de la marge dentelée semble avoir exercé une forte influence sur l'évolution tectonique de la bordure ouest du Bouclier canadien au Protérozoïque précoce.

SUMMARY

Striding-Athabasca mylonite zone, northern Saskatchewan and southeastern District of Mackenzie, N.W.T., occupies a 400 km long segment of the Snowbird tectonic zone. The Snowbird tectonic zone is a northeast-southwest gravity anomaly which may be traced from the Canadian Rocky Mountains to northern Quebec. Along the Striding-Athabasca mylonite zone segment, it coincides with train of three 100 km-scale magnetically defined "lozenges" (Athabasca, Selwyn, and Three Esker). The Striding-Athabasca mylonite zone is a linked system of granulite facies mylonite belts which trace a sinuous course along the train of lozenges. The mylonite zone consists of two parts: the East Athabasca mylonite triangle, at the northeastern apex of the Athabasca lozenge, and its northeastern extension, the Striding mylonite belt.

The East Athabasca mylonite triangle, located on the north shore of the eastern end of Lake Athabasca, is structurally divided into an upper and a lower deck. The lower deck comprises three kinematic sectors; two conjugate, penetratively mylonitic, granulite facies strike-slip shear zones, each about 15 km thick, separated by a central septum. In the central septum the bulk finite strain is of relatively low magnitude, and the bulk deformation path approximates to progressive pure shear. The upper deck overlies the lower deck and was initially emplaced along a discrete basal thrust, as indicated by the presence of relict Late Archean eclogite. It is now entirely occupied by a penetratively mylonitic, 10 km thick dip-slip granulite facies shear zone. The upper deck can be described as an extensional shear zone with a lateral ramp, at least with regard to its later granulite and subgranulite facies development.

The Striding mylonite belt is a welt of through-going granulite to upper amphibolite ribbon mylonite, 5 to 10 km thick, along the southeastern side of the Selwyn lozenge, from the East Athabasca mylonite triangle to the north end of Snowbird Lake.

The geological history of the Striding-Athabasca mylonite zone began with the deposition of semipelitic to pelitic sediments. The sediments were intruded at ca. 3.4-3.2 Ga by a tonalite batholith, which dismembered an anorthosite-pyroxenite-gabbro-peridotite mafic complex during the early stages of its ascent. No geological record is preserved for the interval ca. 3.13-2.62 Ga. At ca. 2.62-2.60 Ga, the metasediments were invaded by two large mafic plutonic bodies and by a voluminous suite of syn-tectonic granitoid bodies. Two penetrative granulite facies mylonitization events are recorded. The first (about 850°C, 1.0 GPa) occurred at ca. 3.13 Ga, and is represented by annealed relict fabrics. The second (850-1000°C, 1.0-1.5+ GPa), associated with widespread, penetrative ribbon fabrics, occurred ca. 2.62-2.60 Ga, and was accompanied by voluminous mafic and granitic plutonism. During the Late

SOMMAIRE

La zone mylonitique de Striding-Athabasca dans le nord de la Saskatchewan et le sud-est du district de Mackenzie (Territoires du Nord-Ouest) occupe un segment de 400 km de longueur de la zone tectonique de Snowbird. Cette zone tectonique se manifeste par une anomalie gravimétrique d'orientation nord-est-sud-ouest que l'on peut suivre des Rocheuses canadiennes jusque dans le nord du Québec. Le long du segment de la zone mylonitique de Striding-Athabasca, l'anomalie coïncide avec une traînée de trois «losanges» (Athabasca, Selwyn et Three Esker) d'une centaine de kilomètres, qui peuvent être définis à l'aide des données magnétiques. La zone mylonitique de Striding-Athabasca est un système de zones mylonitiques du faciès des granulites reliées entre elles qui dessinent un parcours sinueux le long de la traînée de losanges. La zone mylonitique sincerely d'Athabasca Ee compose de deux parties : la zone triangulaire mylonitique st, au sommet nord-est du losange d'Athabasca, et son prolongement nord-est, la zone mylonitique de Striding.

La zone triangulaire mylonitique d'Athabasca Est, située sur la rive nord du lac Athabasca à son extrémité est, est divisée sur la base d'arguments structuraux en deux niveaux, l'un supérieur et l'autre inférieur. L'étude cinématique du niveau inférieur permet de reconnaître trois secteurs distincts. Deux d'entre eux sont des zones conjuguées de cisaillement par coulissage d'environ 15 km chacune qui renferment des roches du faciès des granulites montrant une fabrique mylonitique fortement développée. Ces deux zones sont séparées par une cloison centrale qui constitue le troisième secteur. Dans la cloison centrale, la déformation finie apparente est relativement faible et la trajectoire de la déformation apparente se rapproche de celle d'un cisaillement pur progressif. Le niveau supérieur surmonte le niveau inférieur et cette disposition résulte à l'origine du jeu d'un chevauchement basal bien individualisé dont l'existence est révélée par la présence d'éclogites reliques de l'Archéen tardif. Le site de ce chevauchement est maintenant entièrement occupé par une zone de cisaillement à rejet-pendage de 10 km d'épaisseur formée de roches du faciès des granulites qui montrent une fabrique mylonitique fortement développée. Le niveau supérieur peut être décrit comme une zone de cisaillement de régime extensif à rampe latérale, du moins si l'on se fie à la répartition des roches du faciès des granulites et celles de métamorphisme de plus faible intensité de formation ultérieure.

La zone mylonitique de Striding est un bombement de mylonites rubanées traversant toutes les unités qui témoignent d'un métamorphisme du faciès des granulites au faciès des amphibolites supérieur, dont l'épaisseur se situe entre 5 et 10 km, et qui se situe le long du flanc sud-est du losange de Selwyn, de la zone triangulaire mylonitique d'Athabasca Est à l'extrémité nord du lac Snowbird.

L'histoire géologique de la zone mylonitique de Striding-Athabasca a débuté avec le dépôt de sédiments semipélitiques à pélitiques. Les sédiments ont été traversés vers 3,4-3,2 Ga par un batholite tonalitique qui a démembré un complexe mafique d'anorthosite-pyroxénite-gabbro-péridotite durant les premiers stades de son ascension. Aucun élément géologique de l'intervalle 3,13-2,62 Ga environ n'a été préservé. Vers 2,62-2,60 Ga, les roches métasédimentaires ont été envahies par deux vastes massifs plutoniques mafiques et une suite volumineuse d'amas granitoïdes syn-tectoniques. Deux épisodes de mylonitisation pénétrative au faciès des granulites ont laissé des traces. Le premier (environ 850°C, 1,0 GPa) s'est produit vers 3,13 Ga et est représenté par des fabriques

Archean event, cooling through amphibolite to greenschist facies led to strain localization and a narrowing of the active shear zones.

Early Proterozoic activity within the Striding-Athabasca mylonite zone is limited to pluton emplacement within the lower deck, and folding of granitic veins during minor re-activation of greenschist mylonites at ca. 1.8 Ga. The absence of important Early Proterozoic regional deformation and metamorphism indicates that this segment of the Snowbird tectonic zone was not the site of an Early Proterozoic suture or orogen. The Late Archean ribbon mylonites formed as part of an intracontinental structure, far removed from the contemporaneous active plate margins. However, it is possible that the Middle Archean tonalite batholith might be part of a plutonic arc, perhaps emplaced into a sedimentary accretionary wedge, above a Middle Archean subduction zone during the early construction of the western Churchill continent.

Fragments of relatively stiff Middle Archean crust have controlled the localization, shape, and complex kinematics of the multistage, Striding-Athabasca mylonite zone during the Archean, as well as the geometry of Early Proterozoic rifting at the margin of the western Churchill continent in what is now Alberta. The geometry of the Archean/Early Proterozoic boundary in the western Canadian Shield may represent a jagged continental margin, composed of a pair of re-entrants defined by rifted and transform segments, inherited from Early Proterozoic breakup and controlled by the Archean structure of the interior of the western Churchill continent, i.e. the Striding-Athabasca mylonite zone and associated Middle Archean lozenges, and Late Archean mylonites of the Great Slave Lake shear zone. The geometry of this jagged margin appears to have strongly influenced Early Proterozoic tectonics and magmatism at the edge of the western Canadian Shield.

reliques recristallisées. Le deuxième épisode (850-1 000°C, 1,0-1,5+ GPa), auquel est associé des fabriques rubanées pénétratives de formation répandue, a eu lieu vers 2,62-2,60 Ga; il a été accompagné d'une activité plutonique mafique et granitique aux produits volumineux. Durant l'épisode remontant à l'Archéen tardif, dans la période de refroidissement qui a mené à l'atteinte de conditions du faciès des amphibolites et finalement à celles du faciès des schistes verts, la déformation est devenue plus localisée et la largeur des zones de cisaillement actives a diminué.

Au Protérozoïque précoce, l'activité dans la zone mylonitique de Striding-Athabasca a été limitée à l'injection de roches plutoniques dans le niveau inférieur et au plissement des veines granitiques durant un faible épisode de réactivation des mylonites au faciès des schistes verts à environ 1,8 Ga. L'absence, à l'échelle régionale, d'une déformation et d'un métamorphisme d'importance au Protérozoïque précoce indique que ce segment de la zone tectonique de Snowbird n'a pas été le site d'une suture ou d'un orogène à ce moment de l'histoire géologique. Les mylonites rubanées de l'Archéen tardif se sont formées dans une structure intracontinentale, très loin des marges de plaques actives à ce moment. Cependant, il est possible que le batholite tonalitique de l'Archéen moyen fasse partie d'un arc plutonique qui se serait mis en place dans un prisme d'accrétion sédimentaire, au-dessus d'une zone de subduction de l'Archéen moyen, au début de l'édification du continent de Churchill occidental.

Des fragments de croûte relativement rigide de l'Archéen moyen ont contrôlé la localisation, la forme et la cinématique complexe de la zone mylonitique de Striding-Athabasca qui s'est formée en plusieurs étapes durant l'Archéen, ainsi que la géométrie du rifting du Protérozoïque précoce à la marge du continent de Churchill occidental dans ce qui est maintenant l'Alberta. La géométrie de la limite Archéen-Protérozoïque précoce dans l'ouest du Bouclier canadien pourrait être le reflet d'une marge continentale dentelée, composée d'une paire de rentrants correspondant à des segments de marge de divergence délimités par des failles transformantes, qui serait un héritage de la fragmentation continentale du Protérozoïque précoce. Le rifting a pu être contrôlé par les structures archéennes à l'intérieur du continent de Churchill occidental, soit la zone mylonitique de Striding-Athabasca et les losanges de croûte de l'Archéen moyen associés, ainsi que les mylonites de l'Archéen tardif de la zone de cisaillement du Grand lac des Esclaves. La géométrie de la marge dentelée semble avoir exercé une forte influence sur l'activité tectonique et magmatique du Protérozoïque précoce à la bordure ouest du Bouclier canadien.

INTRODUCTION

The purpose of this project, initiated in 1983, was to investigate the displacement histories of major crustal-scale shear zones in the western part of the Churchill Province, Canadian Shield. Two principal targets were selected for systematic mapping: the southeast shore of Great Slave Lake, Northwest Territories (N.W.T.), and the eastern end of Lake Athabasca, northern Saskatchewan (Fig. 1). They were identified on the basis of examination and interpretation of the available literature and coloured aeromagnetic maps, then recently published by the Geological Survey of Canada. Fieldwork on the first target (1984, 1985, 1987) resulted in the recognition,

documentation, definition, and interpretation of the Great Slave Lake shear zone (Hanmer and Lucas, 1985; Hanmer and Connelly, 1986; Hanmer and Needham, 1988; Hanmer, 1988a, 1989, 1991; Hanmer et al., 1992a). This report is concerned with the second target, referred to in the 1983 Project Identification as the Grease River and Black Lake shear zones, northern Saskatchewan. Fieldwork began with a brief, but fruitful reconnaissance in 1986. The initial structural geological observations were surprising, to say the least, even to a confirmed student of crustal-scale faults: a large, kinematically complex, triangular area of penetratively developed granulite facies ribbon mylonite, comprising at least two conjugate shear zones (Fig. 2; Hanmer, 1987a).

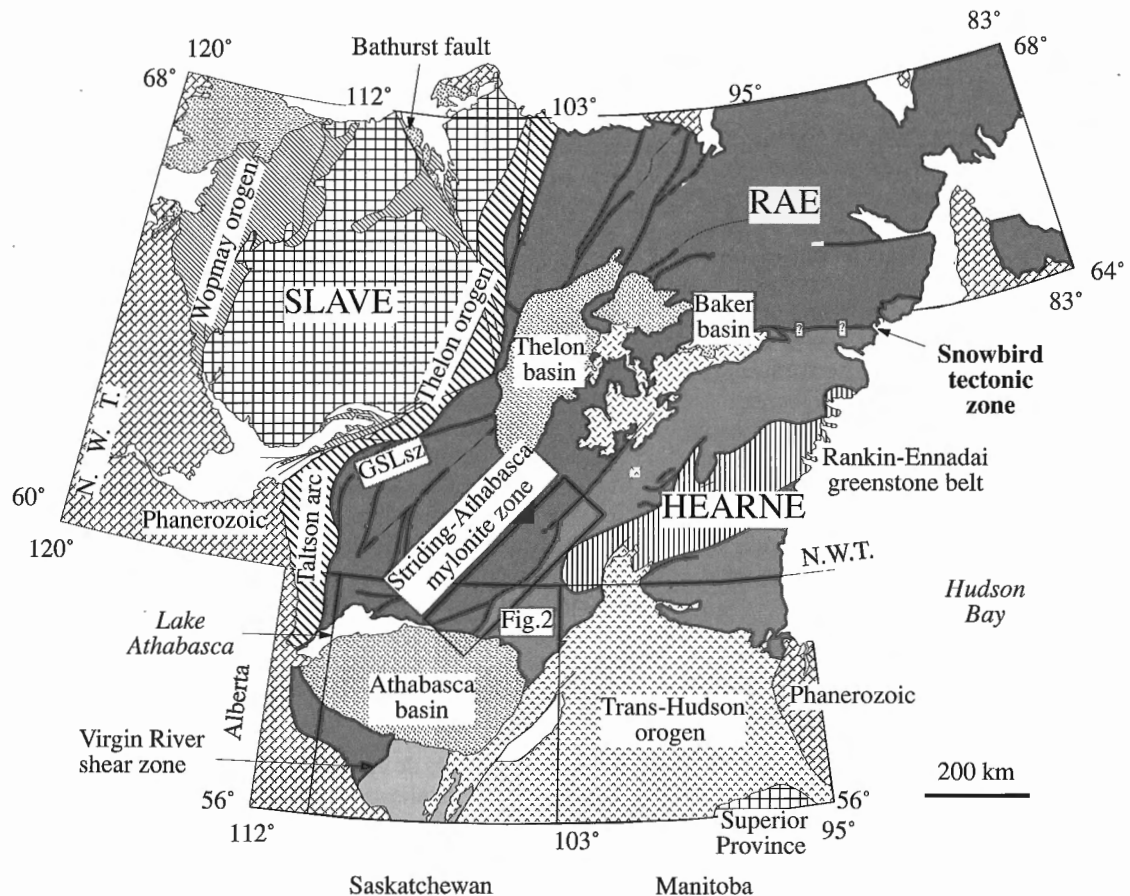


Figure 1. Generalized geology of the western Canadian Shield. The area of Rankin-Ennadai greenstone belt outliers has been grossly simplified. Modified from Hoffman (1988). Location of Figure 2 and the Striding-Athabasca mylonite zone indicated by the rectangle. GSLsz, Great Slave Lake shear zone.

Subsequent to the initial structural reconnaissance (Hanmer, 1987a), a high amplitude linear anomaly in the horizontal gravity gradient map of the Canadian Shield (Goodacre et al., 1987; Thomas et al., 1988) was baptized as the Snowbird tectonic zone by Hoffman (1988). As a geophysical anomaly, the Snowbird tectonic zone may extend almost 3000 km from the Canadian Rocky Mountains to the coast of Hudson Bay, possibly as far as northern Quebec. It has long been considered to represent a tectonically important boundary between major crustal blocks within the western Canadian Shield, variously referred to as the Rae and Hearne provinces¹ (Hoffman, 1988), or the Amer Lake (cratonic) and Cree Lake (ensialic mobile) zones (Lewry et al., 1985). By the time the main fieldwork began on this second target (1990-1992), it was appropriate to couch the project objectives

in terms of a modern structural geological investigation of the best exposed, most accessible segment of the geophysically defined Snowbird tectonic zone. The high grade mylonites discovered in 1986 (Hanmer, 1987a) were systematically mapped in northern Saskatchewan (Hanmer et al., 1991, 1992b; Hanmer, 1994) and their extension into District of Mackenzie, N.W.T., was documented during the course of this study (Hanmer and Kopf, 1993). The 400 to 500 km long geological structure was referred to as the Striding-Athabasca mylonite zone (Fig. 2; Hanmer et al., 1994, 1995a, b). This detailed report of the Striding-Athabasca mylonite zone is in part keyed to Geological Survey of Canada, Map 1859A (Hanmer, 1994).

Location and access

This report focuses upon two areas. The first is a triangle within the Fond-du-Lac and Stony Rapids map areas (NTS 74O and 74P), between longitudes 104°52'W-106°58'W and latitudes 59°15'N-59°45'N, located at the eastern end of Lake Athabasca, northern Saskatchewan (Fig. 2). The wedge-shaped area, well marked by topography and hydrology, is

¹ The original definitions of the Rae and Hearne provinces were predicated upon the interpretation of the Snowbird tectonic zone as an Early Proterozoic suture (Hoffman, 1988). However, as will be shown, the segment of the Snowbird tectonic zone studied here is intra-continental and Archean. Since the terms Rae and Hearne are now well entrenched in general usage, the Rae and Hearne nomenclature is retained.

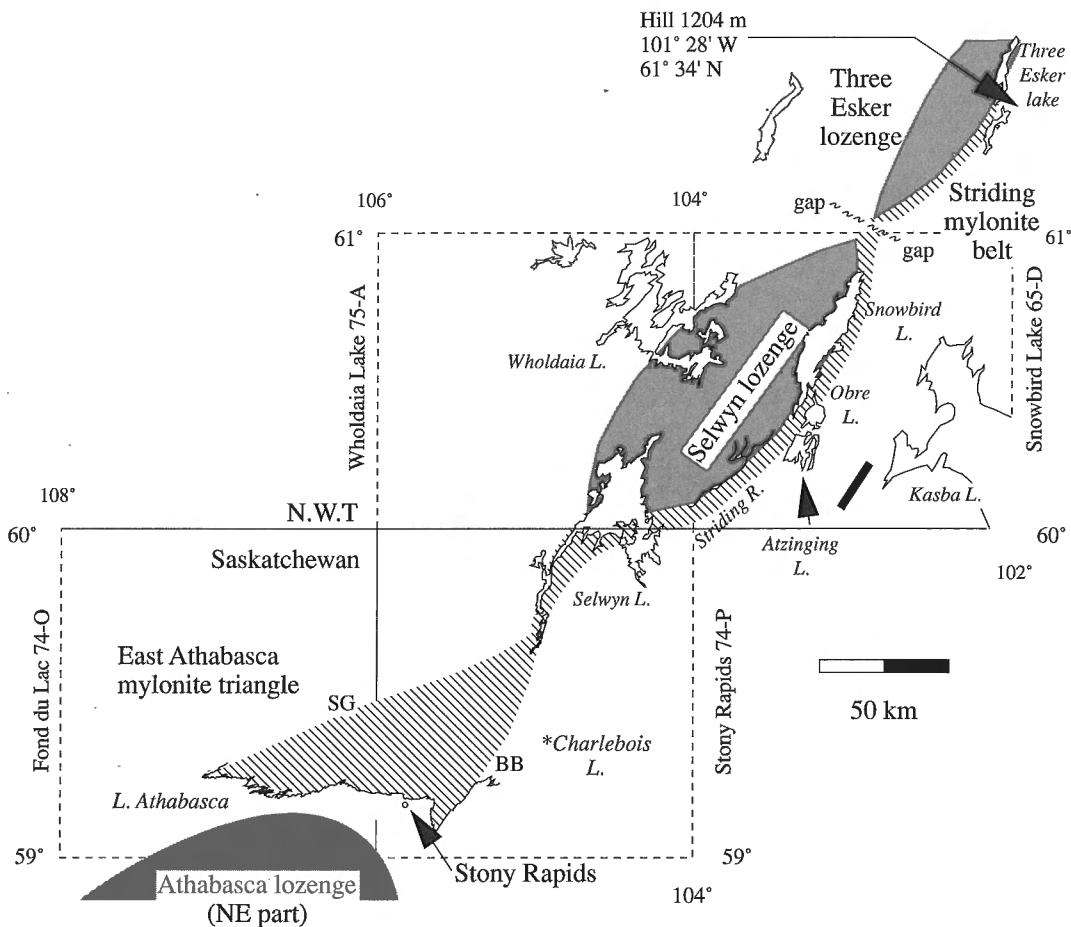


Figure 2. Sketch of the spatial distribution of laterally continuous, extensive high grade mylonite (oblique line rule) with respect to the magnetically defined crustal-scale Athabasca, Selwyn, and Three Esker lozenges (grey shading; drawn from Geological Survey of Canada, 1987; see Hanmer et al., 1995b). The East Athabasca mylonite triangle and the Striding mylonite belt are located. Outlines of 1: 250 000 scale topographic sheets are indicated. Note that the grid of latitudes and longitudes is only valid south of Snowbird Lake. SG, Straight-Grease fault; BB, Black-Bompas fault. Black bar is river section referred to in text.

referred to herein as the East Athabasca triangle. Geographically, the East Athabasca triangle is bounded by Fond du Lac¹ (eastern end of Lake Athabasca) to the south, the Grease and Straight rivers to the west, and a line linking Black and Bompas lakes to the east (Fig. 3). The second area is the narrow, triangle, across the southeastern corner of sinuous northeastward extension of the East Athabasca triangle, across the southeastern corner of District of Mackenzie (NTS 65D, 75A), N.W.T., via Selwyn Lake, the Striding River, and Snowbird Lake, to latitude 61°30'N (Fig. 2).

Access to the area is by scheduled flights with Athabasca Airways or Calm Air from Saskatoon to the village of Stony Rapids (Fig. 3). Athabasca Airways also runs scheduled

flights out of Stony Rapids to communities along Lake Athabasca. Freight, food, and field equipment can be flown daily into Stony Rapids from Points North Landing, near Lake Wollaston, at the end of the road from Prince Albert and Lac la Ronge. Fuel and heavy freight are brought from Fort McMurray to Stony Rapids by barge when Lake Athabasca breaks up (mid-June), and at the end of the summer.

From Stony Rapids, access to the field area is by float plane, except for boat access to the north shore of Fond du Lac (Lake Athabasca). Small float planes are available for charter from several companies. During the course of this project, a single engine turbine Otter, stationed in Stony Rapids to serve the local fishing lodges, was available from Athabasca Airways for camp moves. Occasionally, Athabasca Airways has a helicopter (Bell 206) available for casual charter. During the summer, a few intrepid canoeists undertake the classical overland route from Black Lake, up the Chipman

¹ Not to be confused with the village of Fond-du-Lac, Lake Athabasca, located west of the area covered by this report.

River, via Steinhauer, Woolhether, Chipman, and Bompas lakes, to Selwyn Lake (Fig. 3). From there they continue via Wholdaia Lake, the Dubawnt and Kazan rivers, eventually to arrive at Baker Lake, N.W.T. The trip, which takes several months to complete, was undertaken by several canoe parties during the duration of this project. Parts of the route are used as a skidoo trail by local Cree residents on their way to winter hunting cabins located north of Bompas Lake.

Settlement

The village of Stony Rapids (population about 500) is located just downstream of the rapids on the Fond du Lac River where it enters Fond du Lac, at the eastern end of Lake Athabasca (Fig. 3). It is supplied with electricity from Uranium City. It has a Northern Store, a Post Office, a nursing station, and a Saskatchewan Parks office where fishing licenses may be obtained. Saskatchewan Parks charges a \$40 fee per camp site. Inquiries concerning multiple camp sites for survey purposes may be addressed to the Saskatchewan Parks Regional Office in Lac la Ronge. Local entrepreneurs are able to provide reliable grocery supplies and services from Lac la Ronge. Accommodations, food, and a pay telephone are available at the Whitewater Inn. Aluminium boats and motors can be rented by special arrangement. Boat and aircraft fuel, as well as propane may be purchased from several suppliers. A secure depot facility is run by Points North Freight, where equipment storage can be arranged. A gravel road connects Stony Rapids to the village of Black Lake, located 15 km to the southeast on the lake of the same name (Fig. 3). Black Lake village is the centre of the Chicken Reservation, of which a small, unpopulated section occurs within the East Athabasca triangle, just north of Fond du Lac (Fig. 3).

Climate, flora and fauna

The study area lies within the zone of discontinuous widespread permafrost (Brown, 1967). Breakup of the larger lakes in the area occurs by mid-June in the south, and late June in the north. The summers of 1990 and 1991 were hot during the months of June and July. Early June shade temperatures were commonly in the high 20°C range. Very hot 32°-35°C shade temperatures were recorded for up to a week, several times during both field seasons. Temperatures dropped quickly in August to very comfortable daytime conditions (about 15°-20°C). Night frost and heavy morning mist became frequent by the second week in August.

The official tree line passes through the northern part of the study area, just north of Snowbird Lake (Fig. 2). However, tree cover at the latitude of Wholdaia and Snowbird lakes is very sparse, with wide barren areas separating small clumps of trees and stunted bushes in protected hollows and the leeward sides of hills. However, between Lake Athabasca and Selwyn Lake (Fig. 2), the dense forest of short pine and spruce is very difficult to traverse on foot. In places, particularly where combined with the rugged topography between Robillard River-Wiley Lake-Clut Lakes and Lake Athabasca, it is quite treacherous (Fig. 3). All of the area has been burned many times and dense recent growth of jack pine (*Pinus banksia*),

black spruce (*Picea mariana*), quaking aspen (*Populus tremuloides*), and speckled alder (*Alnus rugosa*) is mined with old deadfall. Dwarf birch (*Betula nana*) is common everywhere. In such conditions, long traverses are not feasible. Occasional stands of tall, mature white birch (*Betula papyrifera*) occur in some of the more protected valleys. Labrador tea (*Ledum groenlandicum*) and ground berries such as crowberry (*Empetrum nigrum*), bunchberry (*Cornus canadensis*), and bearberry (*Arctostaphylos uva-ursi*) are plentiful, especially cloud berries (*Rubus chamaemorus*) which thrive in swampy areas. Common flowers are harebell (*Campanula rotundifolia*), Sheep laurel (*Kalmia angustifolia*), Rugosa rose (*Rosa rugosa*), Pale corydalis (*Corydalis sempervirens*), and Silverweed (*Potentilla anserina*).

Although little wildlife was seen, there are abundant signs of the presence of black bear and moose, as well as indications of the passage of winter caribou and, more rarely, wolf. Bears were not common enough to constitute a problem, even in long term base camps. Hares and grouse were occasionally encountered, and camps were visited by mice and grey jays. The bald eagle population is thriving. Apparently, several active trap lines are maintained by local Cree trappers. Trout and grayling are present, and pike is abundant. There are active fishing lodges on the south side of Fond du Lac and on Black Lake, with satellite facilities on Selwyn Lake. Other lodges on Wholdaia Lake, Snowbird Lake, and at the narrows between Atzinging and Obrey lakes (Fig. 2) were in various states of abandon.

Physiography

The topographic relief ranges from about 300 m above sea level at Lake Athabasca, to about 500 m at Selwyn Lake. The East Athabasca triangle between Lake Athabasca, the Grease and Straight rivers, and Black and Bompas lakes is well defined by landforms and hydrology on topographic maps (NTS 74O, 74P; Fig. 2). It is markedly more rugged than the surrounding area. This is particularly so in the southern part of the East Athabasca triangle, between Robillard River-Wiley Lake-Clut Lakes and Lake Athabasca (Fig. 3), where a set of steep, concentric ridges forms a southward concave structure, with the appropriately named Axis Lake in its 'hinge zone' (see Fig. 3, 4). The terrain flanking the triangle is blanketed by extensive Pleistocene boulder moraine and drift deposits, which are only patchily present in the triangle. It would appear that the present topography is Pleistocene in age, or older, and that the ice flow from the northeast (Taylor, 1963) was diverted to either side. To the north of the triangle, the boulder deposits are succeeded by extensive sand plains. Between Selwyn Lake and Snowbird Lake, extensive simple and braided eskers are developed. North of Snowbird Lake, the sand blanket is nearly complete and outcrop is extremely sparse. However, a few culminations in the bedrock topography do penetrate the sand cover, as at Three Esker lake (Fig. 2), an informal name given to the location of the most northerly outcrop examined during this study. South of the East Athabasca triangle, the east-west ridges on the south side of Fond du Lac are held up by the sandstones and conglomerates of the Athabasca Basin (Fig. 1).

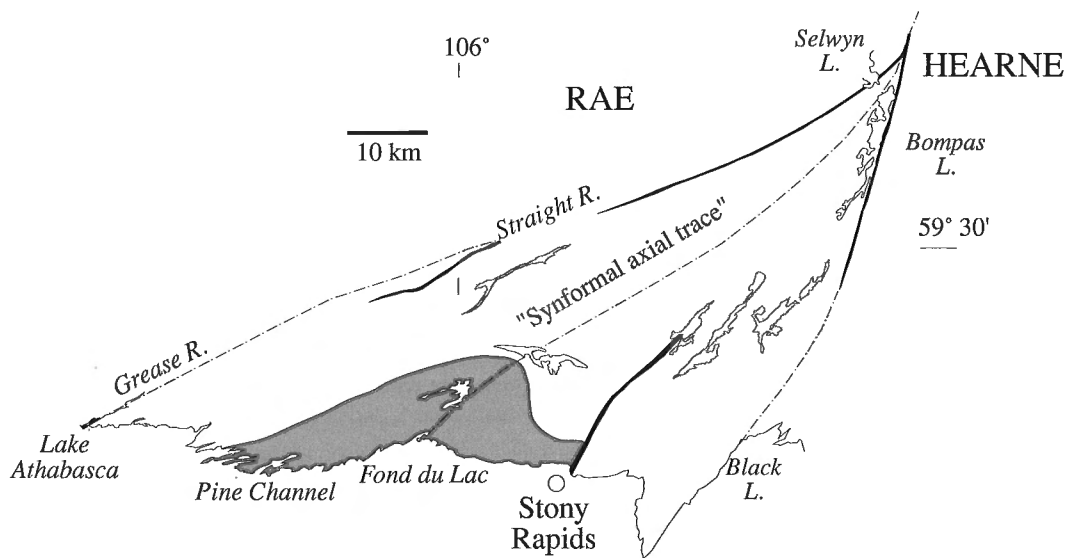


Figure 4. Previous geometrical interpretation of the East Athabasca mylonite triangle in terms of a southwest-plunging open synform. Discussed in text.

Previous and recent work

Regional geophysics

The Snowbird tectonic zone (Fig. 1) is a linear element in the regional potential field maps of the western Canadian Shield. It is well expressed as a high amplitude linear anomaly in the horizontal gravity gradient map (Fig. 5; Goodacre et al., 1987; Thomas et al., 1988). Low amplitude anastomosing linear elements in the regional magnetic field occur along the trend of the gravity anomaly and define a train of three crustal-scale elliptical features (Geological Survey of Canada, 1987; Pilkington, 1989; Hanmer et al., 1995b), referred to as the Athabasca, Selwyn, and Three Esker "lozenges" (Fig. 2; Hanmer and Kopf, 1993). These geophysical features, historically referred to as the Fond du Lac low, the Kasba Lake-Edmonton low, or the Athabasca axis, have long been familiar to regional geophysicists (Walcott, 1968; Wallis, 1970a; Walcott and Boyd, 1971; Gibb and Halliday, 1974; Teskey and Hood, 1991) and geochemists (Burwash and Culbert, 1976; Darnley, 1981).

Although the name Snowbird tectonic zone was only recently coined, many authors have long speculated on its tectonic significance. Some have interpreted the geophysical and geochemical data in terms of a cryptic, branching intracontinental rift system. Wallis (1970a) considered the rifting to be older than the Trans-Hudson orogeny (ca. 1.9-1.8 Ga, Hoffman, 1990), whereas Darnley (1981; see also Teskey and Hood, 1991) suggested that it was approximately contemporaneous with sandstone deposition in the Athabasca basin (ca. 1.7 Ga, Cumming et al., 1987). Others, referring either to apparent polar wander path determinations (Cavanaugh and Seyfert, 1977; Seyfert and Cavanaugh, 1978; Gibb et al., 1980; cf. Roy et al., 1978), apparent truncations within the regional magnetic pattern (Hoffman, 1988), or paired anomalies in the regional gravity field (Thomas and Gibb, 1985), have proposed

that the Snowbird tectonic zone marks an Early Proterozoic collisional suture. However, more recent paleomagnetic data do not support the concept of the Early Proterozoic ocean basin required by the suture model (Symons, 1991). Some workers, seeking analogues with the continental-scale indentation-related transcurrent faults of Tibet (Tapponier and Molnar, 1976; Tapponier et al., 1982, 1986), have ascribed the Snowbird tectonic zone to Early Proterozoic impingement and indentation either from the northwest (e.g. Gibb, 1978), or from the southeast (e.g. Gibb, 1983; Gibb et al., 1983).

Regional geology

Geological mapping along parts of the Snowbird tectonic zone has been undertaken at a variety of scales, both north (Tyrrell, 1897a; Lord, 1953; Wright, 1955; Taylor, 1963, 1970; Schau and Ashton, 1979; Schau et al., 1982; Eade, 1985, 1986; Tella and Eade, 1985; Gordon, 1988) and south (Tyrrell, 1897a, b; Alcock, 1936; Furnival, 1940, 1941a, b; Mawdsley, 1949, 1957; Kranck, 1955; Colborne, 1960, 1961, 1962; Johnston, 1960, 1961, 1962, 1963, 1964; Colborne and Rosenberger, 1963; Baer, 1969; Wallis, 1970b; Gilboy, 1978a, b, 1979, 1980a, b; Gilboy and Ramaekers, 1981; Slimmon and Macdonald, 1987; Crocker and Collerson, 1988; Carolan and Collerson, 1988, 1989; Slimmon, 1989) of the Northwest Territories border (Fig. 6). Understandably, early workers did not have an appropriate tectonic context within which to interpret their geological observations. However, after the early 1960s a northeast-trending array of discrete mylonitic faults (e.g. Grease River, Straight River, Black Lake, Virgin River, Snowbird, and Tulemalu) began to appear on tectonic maps of the western Canadian Shield (e.g. Byers, 1962; Douglas, 1969; Davidson, 1972; Lewry et al., 1978; Bailes and McRitchie, 1978; Eade, 1978; Tella and Eade, 1986; cf. Brown and Wright, 1957; Wright, 1967). Interpretations of

the kinematic significance of the fault system are diverse; dextral strike-slip (e.g. Byers, 1962; Carolan and Collerson, 1988, 1989), sinistral strike-slip (e.g. Taylor, 1963; Gibb, 1978), and dip-slip (e.g. Tella and Eade, 1986), although most tectonic maps remain neutral on the question.

The first *geologically based* tectonic model for the Snowbird tectonic zone was proposed by workers in central Saskatchewan, who interpreted it as the northwestern intracontinental limit of the penetrative tectonothermal influence of the Trans-Hudson orogeny (e.g. Lewry and Sibbald, 1977, 1980; Lewry et al., 1985). According to this hypothesis, the Snowbird tectonic zone is a shear zone whose location was determined by lateral rheological variation, due to the

existence of a thermal dome within the Trans-Hudson hinterland. The soft thermal dome was equated with the Cree Lake (Hearne) zone, flanked to the northwest by the stiff rocks of the Amer Lake (Rae) "cratonic" zone (Lewry et al., 1985), also referred to as the Western Granulite Domain (Lewry and Sibbald, 1977; Gibb, 1983). In Saskatchewan, the classification of the rocks within (Tantato and Western Granulite domains) and adjacent to the Snowbird tectonic zone (Virgin River, Mudjatik, Dodge, Train, and Nevins domains) has become rather complex (e.g. Macdonald, 1987). During the course of this study, it was not possible to confirm the existence of the Dodge, Train, and Nevins domains along the

Figure 5.

The geophysical expression of the Snowbird tectonic zone in the horizontal gravity gradient field west of Hudson Bay (after Goodacre et al., 1987); sz = shear zone.

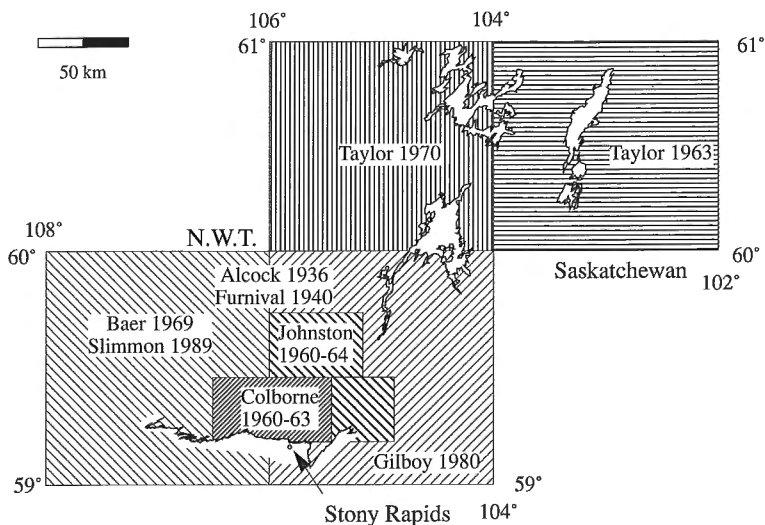
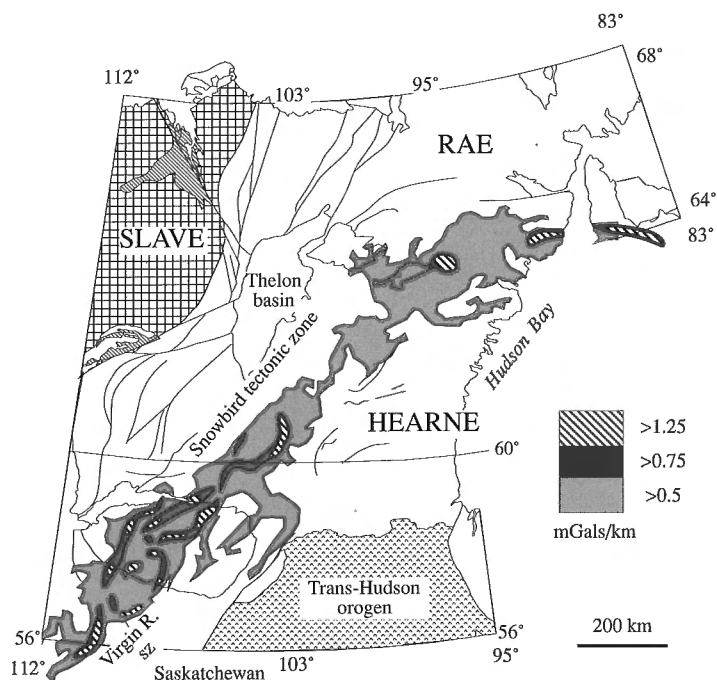


Figure 6.

Previous mapping in the vicinity of the Striding-Athabasca mylonite zone. See text.

northwestern margin of the Snowbird tectonic zone. Accordingly, in what follows, the wall rocks are referred to as the Rae and Hearne crusts.

Regional isotopic geochemistry

Previous isotopic and geochronological studies in and adjacent to the Snowbird tectonic zone have tended to focus upon the age of the basement rocks beneath the Trans-Hudson orogen and the Phanerozoic cover on the one hand, and the absence of a detectable contrast in Nd model ages across the zone, at latitudes greater than 62°N, on the other. Uranium-lead zircon age determinations within the Rae and Hearne wall rocks fall within the range ca. 3.0-2.5 Ga, according to several published summaries (Fig. 7; Macdonald, 1987; Collerson et al., 1988). A rhyolite from the southwestern extension of the Rankin-Ennadai greenstone belt (Fig. 1), just south of the Northwest Territorial border, has yielded an age of 2682 ± 6 Ma (Chiarenzelli and Macdonald, 1986). However, U-Pb zircon age determinations in the range ca. 2.0-1.89 Ga are reported from the Hearne wall rocks (Bickford et al., 1987). Late peraluminous postkinematic granitic pegmatite gave a U-Pb age of 1783 ± 47 Ma in the western part of the Hearne

crust (Orrell and Bickford, 1989). Dated materials in the Rae wall rocks are mostly located at the western end of Lake Athabasca (e.g. Van Schmus et al., 1986), well removed from the Snowbird tectonic zone.

Published U-Pb age determinations on zircon from within the Snowbird tectonic zone are the 1820 ± 19 Ma age of the Junction granite in the Virgin River shear zone (Bickford et al., 1986, 1987), and several preliminary ages in excess of ca. 2.3-2.25 Ga on gneisses from the Western Granulite Domain (Bickford et al., 1986; Macdonald and Sibbald, 1988). A Sm-Nd mineral isochron of 2.48 ± 03 Ga was obtained from the Clearwater Anorthosite within the Western Granulite Domain, south of the Athabasca Basin (Hulbert, 1988).

The range of crustal residence Nd model ages in southern Saskatchewan (Fig. 8), southeast of the Snowbird tectonic zone, is ca. 3.3-2.35 Ga, with most determinations falling between 3.0 and 2.6 Ga (Collerson et al., 1989). However, only two determinations (ca. 2.97 and 2.74 Ga; Bickford et al., 1987) fall within the Hearne crust. This broadly agrees with the 4.16-2.79 Ga spread of model ages obtained from Rae crust adjacent to the Taltson magmatic zone or arc (Fig. 1),

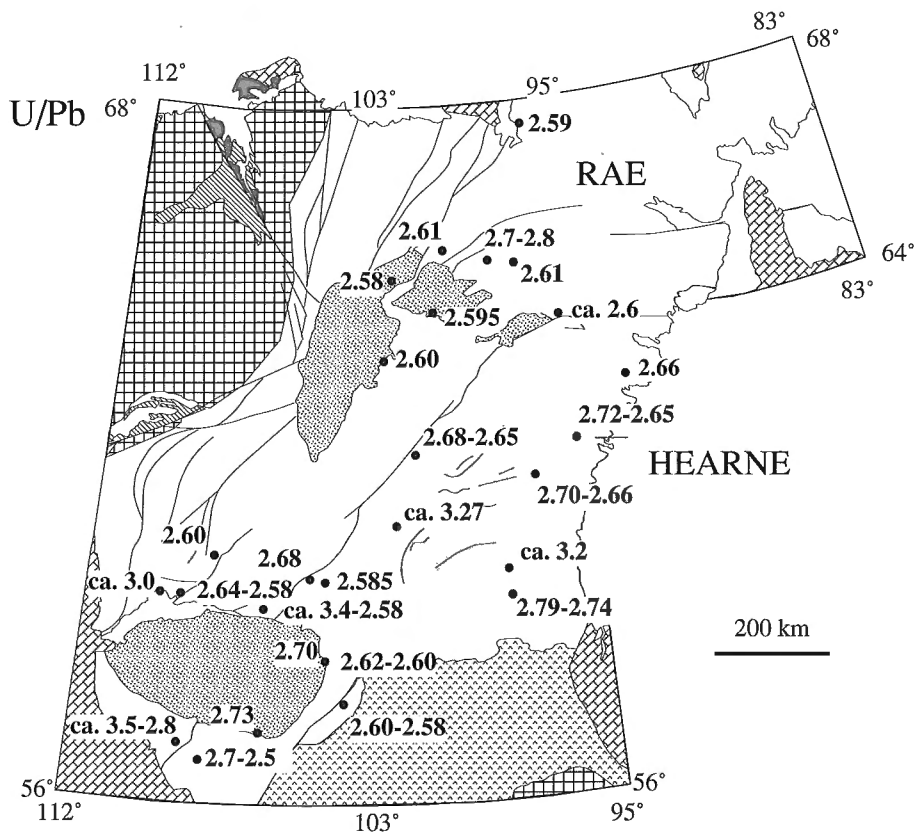


Figure 7. Distribution of available Archean U-Pb zircon dates (Ga) in the western Churchill continent. Data from Bickford et al. (1986), Van Schmus et al. (1986), Stevenson et al. (1989), Dudas et al. (1991), LeCheminant and Roddick (1991), Frisch and Parrish (1992), Roddick et al. (1992), Bickford et al. (1992), Annesley et al. (1992), Tella et al. (1992), and Crocker et al. (1993). See text for additional references.

well to the northwest of the Snowbird tectonic zone (Theriault, 1992). To the northeast, Dudas et al. (1991) examined granitoid bodies from either side of the Snowbird tectonic zone between 62°N and the Arctic Circle. They obtained a younger range of Nd model ages compared with the material to the southwest, ca. 2.91-2.4 Ga, with no indication of Middle Archean age crust.

Lake Athabasca to Snowbird Lake

Parts of the East Athabasca triangle, and its extension to the northeast into District of Mackenzie, have been systematically mapped since the late 1930s by the Geological Survey of Canada and the Saskatchewan Department of Mineral Resources, now the Saskatchewan Geological Survey (Fig. 5; see "Regional geology"). Prior to the initiation of the present study (Hanmer, 1987a), much of the East Athabasca triangle was erroneously mapped as metavolcanic and metasedimentary rocks. Furnival (1940) gave detailed descriptions of conglomerate along the southwest arm of Reeve Lake (Fig. 3), and described a detailed volcanic stratigraphy along the northwestern side of the East Athabasca triangle. Colborne (1961) described similar conglomerate from Mary Lake (Fig. 3).

Kranck (1955) considered that mafic granulites north of Fond du Lac (Fig. 3) were of supracrustal origin. After detecting "high" levels of Na in a single clinopyroxene sample, he prophetically speculated on the possibility of the presence of eclogite (see Snoeyenbos et al., 1995). Colborne (1960, 1961, 1962; see also Colborne and Rosenberger, 1963) described thick, stratified arkose and greywacke sandstones in and around Clut Lakes (Fig. 3). Johnston (1960, 1961, 1962) recognized the presence of greenschist mylonite and cast doubt upon Furnival's (1940) identification of volcanic rocks along the west side of the East Athabasca triangle, although he equivocated and continued to describe them as tuffs and flows. Johnston (1962, 1963; see also Colborne, 1960) referred to the eastern third of the triangle by the equivocal epithet "hybrid gneiss".

Much of this earlier work was incorporated into the 1:250 000 scale compilation of Gilbo (1980b). Gilbo and Ramaekers (1981) introduced the term "Tantato Domain" to refer to the geology of the East Athabasca triangle. They explicitly stated that the rocks of the Tantato Domain appear to be largely volcanoclastic in origin and suggested that granulite facies metamorphism had occurred at the end of the Archean. The

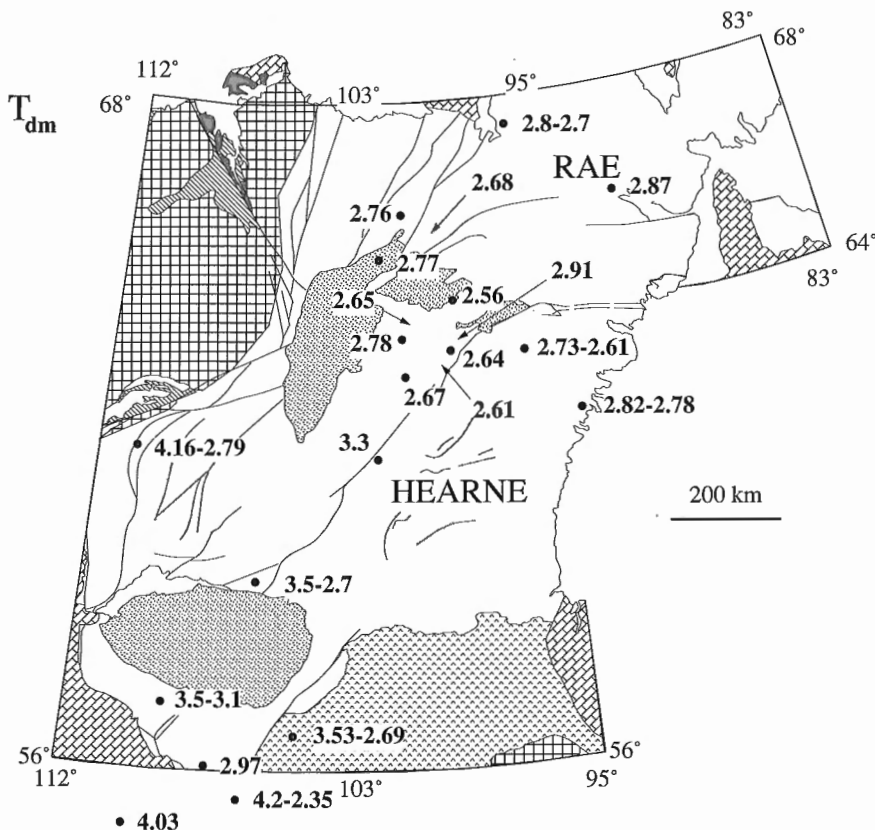


Figure 8. Distribution of available T_{dm} -Nd model ages (Ga) for the western Churchill continent. Note the broader range of ages to the southwest and the younger ages to the northeast in both Rae and Hearne crusts. Discussed in text. Data from Bickford et al. (1987), Collerson et al. (1989), Stevenson et al. (1989), Dudas et al. (1991), Frisch and Parrish (1992), Bickford et al. (1992), and Crocker et al. (1993). Patterns as in Figure 1.

compilation map correctly shows the greenschist mylonite of the Black-Bompas, Straight-Grease, and Platt-Kaskawan fault zones (see Fig. 10, Fig. 127), already identified by the above cited mappers. However, it incorrectly extended the gently southwesterly plunging synformal structure, identified by Colborne (1960) between Clut Lakes and Lake Athabasca (Fig. 3), to the entire East Athabasca triangle by extrapolating the hybrid gneiss along the west side of the triangle (Fig. 4).

The poorly exposed Snowbird Lake and Wholdaia Lake map areas in southeast District of Mackenzie (Fig. 2) were each mapped in single field season by Taylor (Taylor, 1963, 1970). He identified important swaths of paragneiss over large parts of the map areas, largely under-representing the real proportion of intermediate to mafic rocks which occupy the area between Selwyn, Wholdaia, and Snowbird lakes. Mylonite along the Snowbird tectonic zone was first referred to by Johnston (1960, 1961, 1962, 1964), Colborne (1960, 1962), and Taylor (1963). While Johnston and Colborne mapped the Straight River, Black Lake, and Platt Creek shear zones as narrow greenschist facies mylonitic faults (see Fig. 10), Taylor drew a discrete fault along the Striding River and through Snowbird Lake (Fig. 2), to the east of which he mentioned the presence of mylonite. After the initial recognition of extensive high grade mylonite (Hanmer, 1987a), Slimmon and Macdonald (1987) confirmed the observation during detailed mapping of the auriferous area around Sucker Bay (Fig. 3). Slimmon (1989) also incorporated the observation in a 1:250 000 scale compilation of the Fond du Lac map area (Fig. 2).

In 1990-1992, systematic structural geological studies were undertaken of the East Athabasca triangle and its geological extension into southeastern District of Mackenzie, N.W.T. (Fig. 2; Hanmer et al., 1991, 1992b; Hanmer and Kopf, 1993; Hanmer, 1994). They revealed that the geophysical expression of the Snowbird tectonic zone corresponds to two main geological components: mafic to intermediate composition Middle Archean gneisses which underlie the magnetically defined crustal-scale lozenges, and sinuous belts of principally Late Archean, dextral transpressive, high grade ribbon mylonite which bound them. Understanding the origin of, and the causal relationship between these two components is the keystone to the view of this segment of the Snowbird tectonic zone espoused during this work (Hanmer et al., 1994, 1995a, b; see also Williams et al., 1995; Snoeyenbos et al., 1995), and will be discussed at the end of this report.

Field methods and extent of mapping

Fieldwork for this project was carried out in two stages. An initial three week reconnaissance was undertaken during the summer of 1986. Two-person camps were established at Bompas and Tantato lakes (Fig. 3). Combined foot traverses and boat supported examination of lake shore outcrops, supplemented by two days of aircraft supported investigation, were sufficient to indicate the extent, high metamorphic grade, and kinematic complexity of the rocks (Hanmer, 1987a).

Two full field seasons of systematic mapping in the East Athabasca triangle were undertaken in 1990 and 1991. In both years, the main crew comprised Simon Hanmer (Geological Survey of Canada), Chris Kopf (University of California at Santa Cruz), and Mark Darrach (University of Massachusetts). In 1992, Hanmer, Kopf, and Williams, with one assistant, undertook six weeks of fieldwork in the Northwest Territories during June and July (Hanmer and Kopf, 1993).

During the 1990 field season, base camps were set up on Bompas, Chipman, Clut, and Reeve lakes (Fig. 3). A boat supported fly camp was established at Cora Lake (Fig. 3). During the 1991 field season, a permanent base camp was set up at the Chipman Lake site. Throughout the summer, trios of two person fly camps, equipped with small inflatable boats, were set out by Beaver for periods of 4 to 7 days at Athabasca, Bompas, East Hawkes, Father, Gunderson, Kaskawan, Little Farad, Mary, Tilden, Turnbull, Wiley, and Woolhether lakes, and the Grease River (Fig. 3). During both summers, provisions were purchased directly from Robertson's Trading in Lac la Ronge, transported by road and DC-3 to Stony Rapids, and then flown into camp by float plane. The aim of this part of the study was to systematically map the East Athabasca triangle. Most mapping was by foot traversing, supplemented by boat work. Observations were recorded directly onto vintage (1940s-1950s) black and white air photographs of variable scale (about 1:35 000). All information was then compiled at the base camp using a Macintosh SE-30 computer and MiniCad+ CAD software (for details see Peterson and Hanmer, 1992). At the end of the fieldwork, the digital data was transferred to ArcInfo and a final colour map produced at 1:100 000 scale (Hanmer, 1994).

During the 1992 field season, camps were established on the Striding River, in the northwestern bays of Selwyn Lake, and at the central narrows on Wholdaia Lake (Fig. 2). Emphasis was placed upon boat-supported examination of good quality lakeshore outcrops. Foot traverses in otherwise inaccessible areas were supported by fixed wing aircraft. The aim of this section of the study was to trace the important geological elements discovered during the systematic mapping of the East Athabasca triangle along strike to the northeast. Exposure north of the Territorial border is poor and not very extensive, and the area had been mapped by the Geological Survey of Canada during the 1960s (Taylor, 1963, 1970). Accordingly, the intent here was to upgrade the structural geological database, as opposed to launching a new systematic mapping program.

Acknowledgments

I am indebted to a number of people who, through their efforts and enthusiasm, interest, and dedication, have contributed to the success of this project, but in particular to Chris Kopf (ex-UCSC, presently at University of Massachusetts) whose unflagging support as a senior mapping assistant was exemplary throughout all three field seasons. I am also much indebted to Mark Darrach, an enthusiastic senior mapping assistant during 1990 and 1991 and source of some of our more memorable, humorous moments. To Shaocheng Ji, I express my thanks for his efforts on behalf of the project. Our assistants

Katherina Ross (1986); Matt Reinke, Guillaume Couture, Julie Lavoie, and cook Darcie Casselman (1990); Melanie Kells, Brent Loney, Mike Peshko, and Dave Ross (1991); and Andrea Dorval (1992), were a pleasure to work with and a source of great companionship and joie de vivre, in base camps, fly camps, and long wet traverses. Their sense of responsibility and self motivation has been subsequently reflected in the successful pursuit of their geological studies and the demand for their services as assistants on other field parties.

I am most grateful to the people of Stony Rapids who went to great effort to offer us excellent service and welcome assistance; the pilots of Athabasca Airways who flew us out and brought us home, Bob, Dan, Jason, Kelly, Kevin, and Twain, but most especially Keith Norstrom (Turbo Otter pilot), Ed and Margie White (Whitewater Inn), Kwan and Emily (Emily's Place), Jerry Cameron, Rick and Carl (Points North Freight), Al (Petrocan), and Scott Hale (Stony Rapids Snowmobile Centre). Their many helping hands were always appreciated.

I am also indebted to my colleagues for their presence and participation in various facets of this study. To Rick Law (Virginia Polytechnic) who visited us in the field (1990) and is working on those parts of the rocks most of us can't even see. To Randy Parrish (GSC) for his companionship and participation in the field (1990), and for his work and dedication in the geochronology laboratory at the Geological Survey of Canada, producing timely results which we had the opportunity to follow up on during the next field season. Most particularly I want to acknowledge my gratitude to Mike Williams (University of Massachusetts). He has acted as foil and sounding board as I thought aloud, sharing fly camps and bumpy, wet boats, and has freely contributed his own evolving metamorphic ideas on the Striding-Athabasca mylonite zone throughout the project, from its inception.

We welcomed visits in 1990 by Bill Slimmon (Saskatchewan Geological Survey) and Ken Collerson (UCSC). Even the District Nurse was welcome when she arrived, unannounced, to vaccinate the entire crew, on the beach in front of the cook tent, against an outbreak of meningitis which had struck northern Saskatchewan. In 1991 we were visited by Sandy Colvine (Geological Survey of Canada), accompanied by Bob Macdonald (Saskatchewan Geological Survey). In particular, we appreciated the visit by Subhas Tella, Mikkel Schau (Geological Survey of Canada), and Terry Gordon (University of Calgary), the first step in an ongoing comparative study of the geological histories of the Striding-Athabasca mylonite zone and the Chesterfield Inlet segment of the Snowbird tectonic zone.

Finally, I am indebted to Subhas Tella for undertaking the task of critically reading and commenting on the manuscript. His thorough and painstaking efforts have significantly contributed to improving this report.

GENERAL GEOLOGY

In the Stony Rapids area, the geophysical expression of the Snowbird tectonic zone is geologically underlain by the *East Athabasca mylonite triangle* (Fig. 9 and 10; Hanmer, 1987a, 1994; Hanmer et al., 1991, 1992b), a 75 km by 80 km by

125 km wedge-shaped area of high grade mylonite located at the northeastern end of the magnetically defined, 300 km by 100 km Athabasca lozenge (Fig. 2, 11). The simple lines of the foliation trajectories and the trace of layering within the East Athabasca mylonite triangle contrast strongly with the convoluted, curvilinear trajectories of foliations and lithological traces in the Rae (e.g. Slimmon, 1989) and Hearne wall rocks (e.g. Gilboy, 1980b).

The East Athabasca mylonite triangle is structurally divided into an upper and a lower deck¹, both of which were extensively and penetratively mylonitized at granulite facies (Fig. 10). Layering and foliations in the lower deck are steeply dipping with moderately southwest-plunging extension lineations. The lower deck comprises three kinematic sectors; a central septum² which has experienced bulk progressive pure shear and relatively low finite strain, flanked by sinistral and dextral shear zones to the east and west, respectively. The upper deck is entirely composed of a shallowly southwest-dipping, dip-slip shear zone in the east, which progressively becomes a steeply dipping dextral shear zone in the west. Layering and foliations are parallel to the shear zone boundaries. Extension lineations plunge down-dip in the east and porpoise moderately about the strike direction in the west. The dip-lined mylonites were associated with top-side-down displacements, at least during the later stages of their high grade deformation history. However, as discussed below, the earlier stages of mylonite development appear to have been associated with lineation-parallel thrusting. Accordingly, the upper deck is entirely occupied by a geometrically simple, though kinematically complex, dip-slip shear zone with a lateral ramp.

Lithologically, the East Athabasca triangle is composed of diatexite of semipelitic origin, intruded by a tonalitic batholith, two mafic complexes, numerous large granitic plutons, and at least two mafic dyke swarms (Fig. 9). These lithologies are distinct from those of the Rae and Hearne wall rocks. Along with their associated mylonite fabrics they can be followed to the northeast, across the territorial border, along the geophysical trace of the Snowbird tectonic zone. There, they form the *Striding mylonite belt*, a sinuous, upright dextral shear zone with subhorizontal extension lineations which

¹ I refer to upper and lower decks to convey the image of two structural compartments with geometrically distinct internal fabrics, separated by a sharp discontinuity. As will be explained, the upper deck was apparently initially emplaced as a hanging wall along a shallowly dipping, discrete thrust plane at its base. Subsequently, a dip-slip mylonite zone, at least 10 km thick, developed in the lower part of the hanging wall, parallel to the shallowly dipping basal thrust. The hanging wall to the dip-slip mylonites (the Athabasca lozenge?) is still buried beneath the overlying Athabasca basin (ca. 1.7 Ga, Cumming et al., 1987; Cumming and Krstic, 1992). Finally the mylonites were displaced as a rigid hanging wall to later localized dip-slip mylonites. Accordingly, in order to avoid repetitious clarification of which hanging wall is being referred to throughout the text, the descriptions are couched in terms of upper and lower decks.

² The term septum is used in the sense of a relatively narrow panel separating two volumes, specifically the two shear zones within the lower deck.

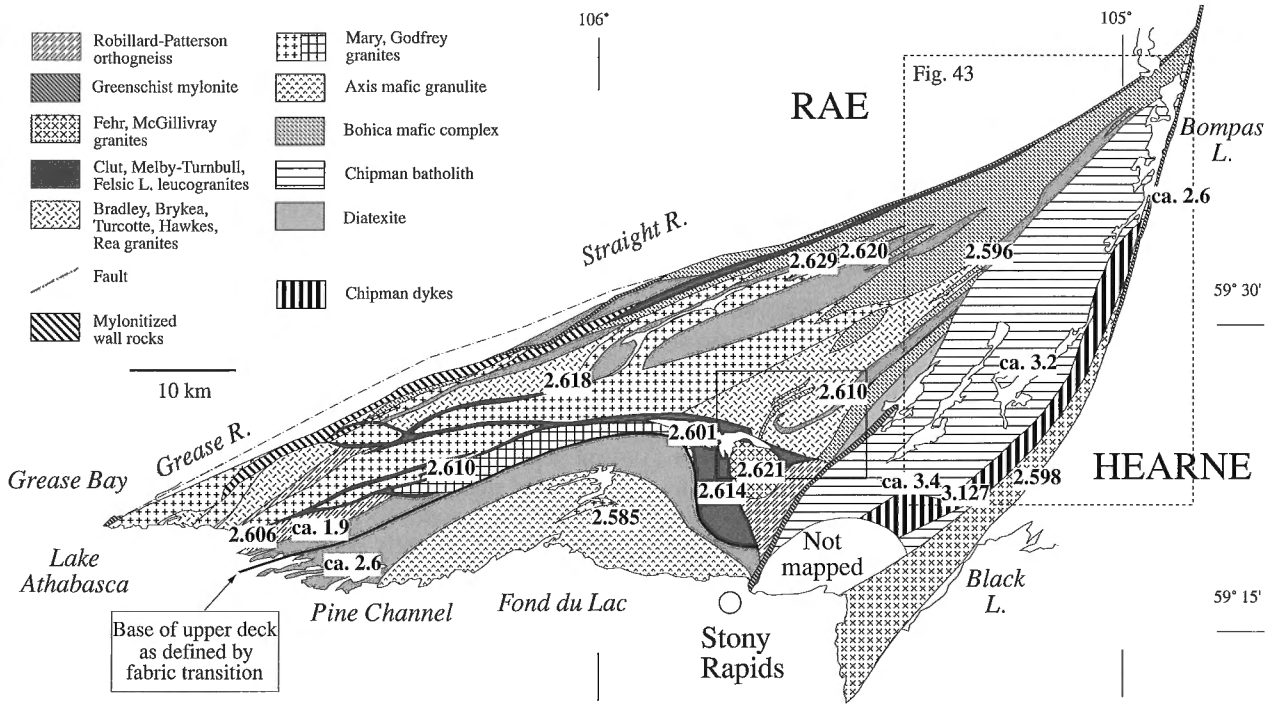
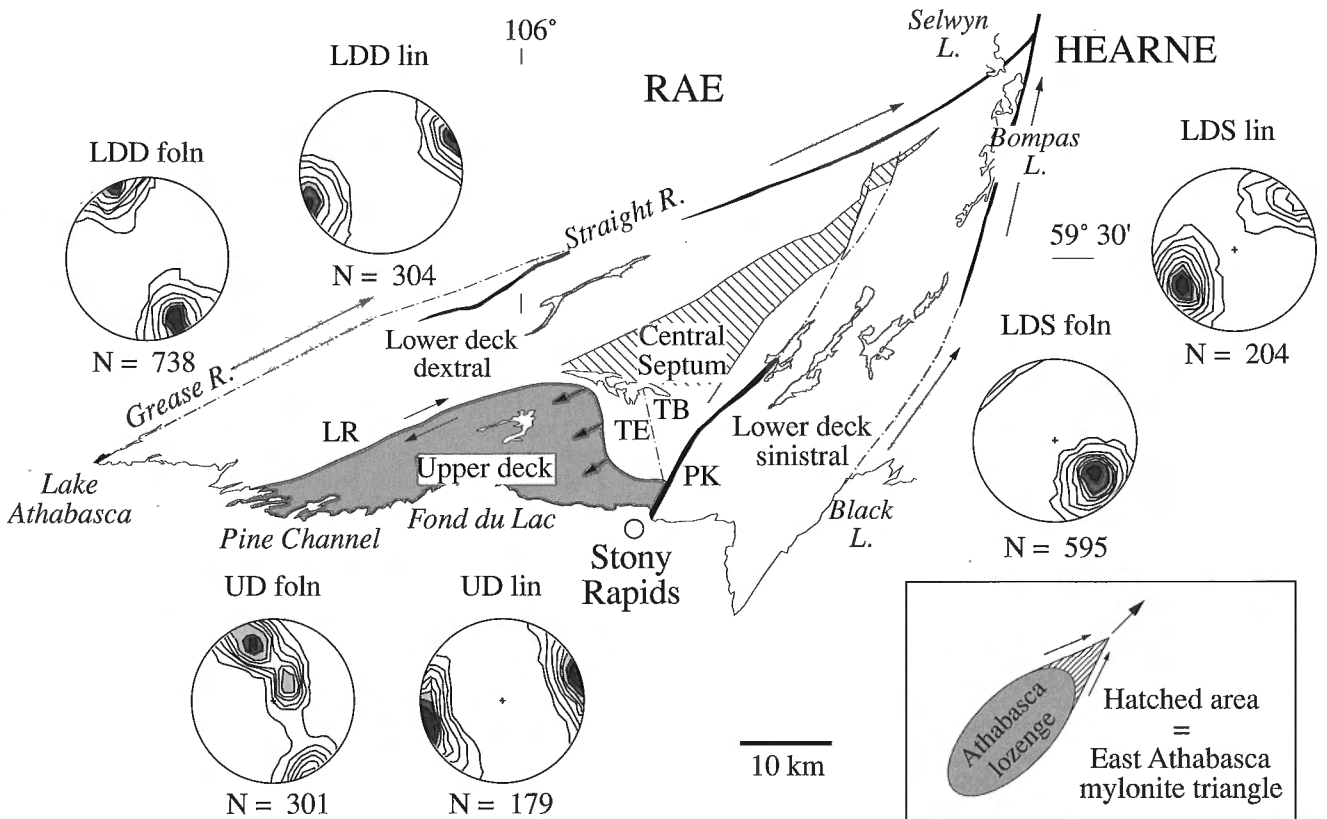


Figure 9. Principal map units of the East Athabasca mylonite triangle, after Hanmer (1994). U-Pb zircon magmatic crystallization ages are indicated in Ga. Small box is general location of Figures 98 and 119, large box is general location of Figure 43.



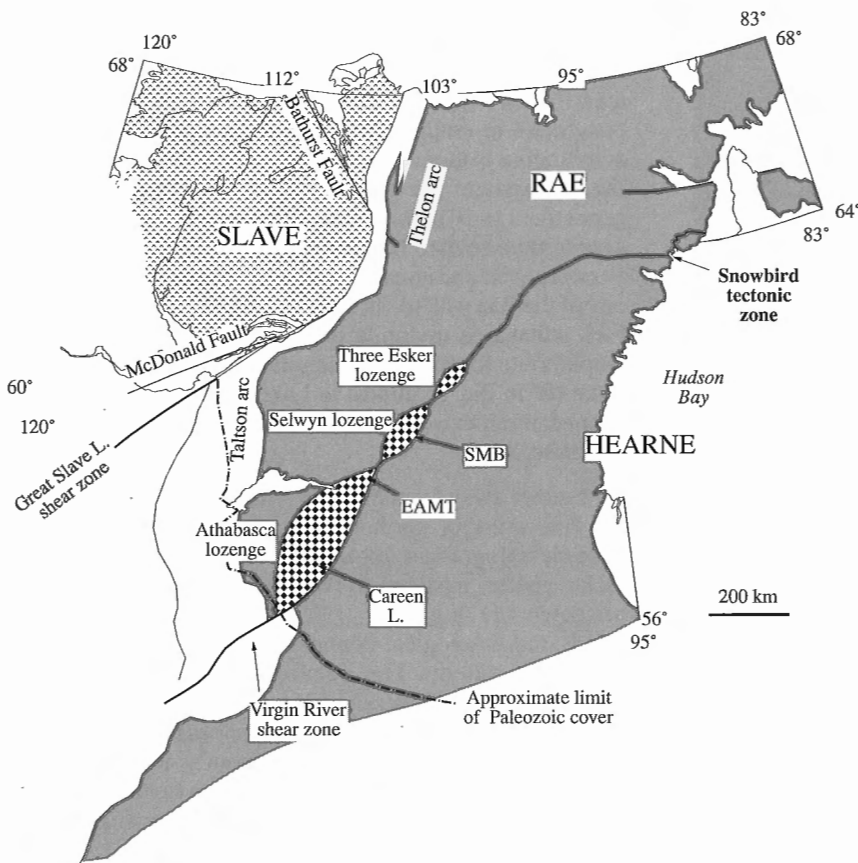


Figure 11.

Principal tectonic elements of the Snowbird tectonic zone set in the context of the western Churchill continent, itself composed of the Rae and Hearne crusts. The Athabasca, Selwyn, and Three Esker lozenges are bounded by the East Athabasca mylonite triangle (EAMT) and the Striding mylonite belt (SMB). Discussed in text.

closely follows the southeastern margins of the magnetically defined Selwyn and Three Esker lozenges (Fig. 2). The East Athabasca mylonite triangle and Striding mylonite belt are contiguous segments of the same structure, collectively referred to as the *Striding-Athabasca mylonite zone* (Fig. 2). Geochronological data demonstrates that the Striding-Athabasca mylonite zone is a composite structure of Mid- to Late Archean age (ca. 3.2 to ca. 2.6 Ga).

←

Figure 10 (opposite). Principal tectonic elements within the East Athabasca mylonite triangle (see Fig. 9 for geology). Arrows indicate directions of relative tectonic displacement. The lateral ramp (LR) and trailing edge (TE) of the upper deck are indicated. Stereoplots are of poles to foliation and extension lineations for the upper deck (UD), lower deck dextral (LDD), and lower deck sinistral (LDS) kinematic sectors. Inset is a schematic representation of the location of the East Athabasca mylonite triangle at the northeastern apex of the crustal-scale Athabasca lozenge and the general pattern of flow resolved adjacent to the apex. Taylor Bay (TB) and Platt-Kaskawan (PK) faults are specifically indicated by initials. Discussed in text.

All unreferenced magmatic crystallization and metamorphic ages cited herein are U-Pb from zircon and monazite (Table 1; data of R. Parrish, Geological Survey of Canada, tabulated in Hanmer et al., 1994, 1995a). I am well aware of the internal contradictions in the details of the emplacement sequence determined from geological observation and the Late Archean syntectonic geochronological data (see below). Therefore, I shall confine interpretation of the geochronological data to delimiting the approximate time windows within which the geological events associated with the formation of the Striding-Athabasca mylonite occurred.

This report will first deal briefly with the wall rocks on either side of the Striding-Athabasca mylonite zone. Then the geology of the East Athabasca mylonite triangle will be examined in detail. This is followed by a presentation of observations made in the Striding mylonite belt, the interior of the Selwyn lozenge, and relatively minor mylonites located on the northwest side of the Selwyn lozenge. Subsequently, a structural analysis of the geometrical and kinematic aspects of the Striding-Athabasca mylonite zone, and their significance for understanding deep-seated, crustal-scale mylonite zones in general, will be given. The report will close with a tectonic analysis of the role of the Striding-Athabasca mylonite zone in the growth of the western Churchill Province.

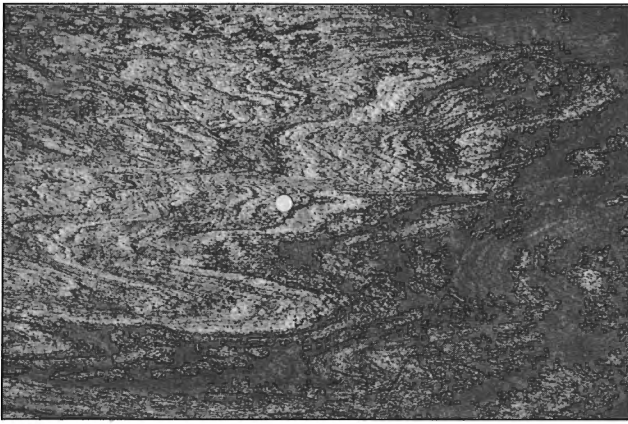


Figure 12. Open to moderate folding of paragneiss banding in western (Rae) wall rock, north of Tantato Lake. Coin for scale 2.5 cm. GSC 1994-186



Figure 13. Folded shear zone in amphibolite, with well foliated granitoid vein in shear zone, western (Rae) wall rock, north of Tantato Lake. Coin for scale 2.5 cm. GSC 1994-187

WALL ROCKS

Rae crust

On the west side of the East Athabasca mylonite triangle, the immediately adjacent wall rocks of the Rae crust in the Faraud Lake area (Fig. 3) are predominantly composed of folded two-mica schist, feldspar porphyroblastic paragneiss with abundant coarse granitic sweats or veins, and subordinate amphibolite (Fig. 12, 13; Faraud gneiss, *Afp*¹). The schist and paragneiss represent retrograde equivalents of locally preserved sillimanite-garnet-andalusite metapelitic migmatite, with abundant, crosscutting, coarse grained, muscovite leucogranite which either forms discrete plutonic masses, or is intimately mixed with the metasediments at the outcrop scale. A crosscutting, but foliated vein of leucogranite from

Little Faraud Lake has yielded a magmatic crystallization age of 2181 ± 5 Ma (Table 1). A similar association occurs along strike to the southwest in the McConville-Margetts Lakes area (Mt in Fig. 3), except that the relative proportions of paragneiss to amphibolite are inverted (*Afa*). Much of the amphibolite is monotonous and extensively replaced by biotite, to the extent that it forms a biotite-hornblende schist with pervasive 1 to 10 m thick sheets of moderately foliated leucogranite \pm muscovite. Northwest of Turnbull Lake (Fig. 3), Faraud gneiss and amphibolite are, in part, separated from the rest of the Rae wall rocks by intercalated granitic rocks of the East Athabasca mylonite triangle (Fig. 9). The gneiss and amphibolite form a train of lenses extending from Wakeman Lake (W in Fig. 3) almost to Lake Athabasca, in part transformed into spectacular banded ribbon ultramylonite (Faraud mylonite, *Afm*).

Further away from the East Athabasca mylonite triangle, the Rae crust in northern Saskatchewan is composed of strongly retrogressed, apparently complexly folded, granulite facies gneiss, intruded by voluminous granitic plutons, of unknown age (e.g. Baer, 1969; Slimmon, 1989). Foliation trends and lithological boundaries describe swirling, curvilinear map patterns. This lithological assemblage extends to the northeast, into District of Mackenzie, N.W.T., where the wall rock to the Selwyn lozenge comprises folded and injected granitoid gneiss, associated with poorly foliated, undated granitoid plutons (Taylor, 1970). Foliation trends in the granitoid gneiss are highly variable, but are predominantly east.

Hearne crust

On the east side of the East Athabasca mylonite triangle, the Hearne wall rocks are sillimanite-garnet pelite, and semipelite, rhythmically layered on a 50 cm scale, with incipient development of partial melt and concordant leucogranite sheets (Black Lake paragneiss, *Abp*). Abundant feldspar porphyroblasts and granitic veinlets and segregations are preferentially developed in pelitic horizons, giving the rock a metatextitic aspect (Fig. 14). The pelite units are best exposed along the western shore of Black Lake, where they form intensely crenulated schists with coarse (5 cm) pseudomorphs possibly after cordierite porphyroblasts (Fig. 15). The porphyroblasts contain fossilized inclusion trails representing preserved open fold hinges of a first foliation, protected within the relatively stiff crystals from transposition into the second, dominant foliation. The contact with the eastern margin of the East Athabasca mylonite zone (Fehr granite), exposed in the cliff section, is a discrete fault.

The schist and paragneiss pass eastward into cordierite-garnet metapelite with coarse grained cordierite-bearing quartz sweats. The pelite is intruded by concordant sheets of foliated leucogranite, several metres wide. Further east, large plutons of isotropic to poorly foliated to isotropic medium grained leucocratic to biotite-hornblende granite intrude the metasediments. The plutons are dome-like, with an anastomosing carapace of foliated, coarsely annealed pelitic, carbonate, and amphibolitic supracrustal rocks, preserved as narrow (1 km) keels (Mawdsley, 1957). Beyond a few kilometres from the East Athabasca mylonite triangle, these

¹ Note that the italicized map unit designators accompanying the detailed descriptions are included for ease of reference to the 1:100 000 geological map of the East Athabasca mylonite triangle (Hanmer, 1994).

plutons are the dominant feature of the Hearne crust in northern Saskatchewan and impart a markedly curvilinear map pattern. One of the plutons, centred upon Charlebois Lake (Fig. 2), has yielded an approximate magmatic crystallization age of ca. 1840 Ma (Table 1).

To the northeast, in District of Mackenzie, N.W.T., the Hearne crust is very poorly exposed at the latitude of the Selwyn lozenge (Fig. 2). It is apparently dominated by the voluminous mass of isotropic biotite granite around Kasba Lake (Taylor, 1963). Between the granite and the Selwyn lozenge is a 10 km wide belt of amphibolite and finely laminated pelitic and volcanoclastic sediments which were only examined along a river section at the latitude of Atzinging Lake (black bar in Fig. 2). The enveloping surfaces of the stratification and a penetratively developed bedding-parallel cleavage are generally flat-lying (Fig. 16), and a mineral extension lineation is oriented about 030°. The cleavage is locally deformed about later 1 cm to 10 m scale, lineation-parallel, open folds (Fig. 17). The fold axial planes are shallowly to moderately east- or west-dipping, and the folds verge in both directions. No associated axial planar cleavage is present. The principal metamorphic mineral assemblage

(hornblende-chlorite) is indicative of upper greenschist to lower amphibolite facies, although 1 m thick cleavage-parallel zones of chlorite schist, crenulated by the later folds, suggest that retrogression to lower greenschist facies occurred between the cleavage- and crenulation-forming events. In brief, these are typical greenstone belt rocks which form an outlier at the southwestern end of the Rankin-Ennadai supra-crustal belt (Fig. 1; e.g. Wright, 1967; Park and Ralsler, 1992).

EAST ATHABASCA MYLONITE TRIANGLE

Upper deck

Pine Channel diatexite

The Pine Channel diatexite (*Apdm*; Fig. 18) is a leucocratic, straight banded rock (Fig. 19), with extremely well developed 0.5 mm by up to 10 cm ribbons of quartz and feldspar which deflect around abundant 2 to 20 mm garnets (Fig. 20). Although present throughout the upper deck, the diatexite is the principal map unit of the 4 km thick lower structural level. It is white to tan and comprises a banded, leucocratic, quartzofeldspathic matrix with a highly variable content of lilac to

Table 1. Generalized table of geological events in the Striding-Athabasca mylonite zone.

	Million years
Minor reactivation of Straight-Grease fault	1788 +28/-15
Intrusion of isotropic granites into Hearne wall rock	ca. 1840
Robillard-Patterson gneissic plutons	ca. 1900
Garnet-pyroxene granite, Whooldaia Lake ⁿ	1907 ± 8
Minor dextral shearing in Rae wall rock	2181 ± 5
<hr/>	
Bompas granite, localized greenschist facies mylonitization	D ca. 2600
McGillivray granite	2621 ± 3
<hr/>	
Fehr dykes	
Fehr granite	2598 ± 3
Clut and Melby-Turnbull granites	D 2614 +9/-7, 2610 ± 2
Felsic Lake leucogranite sheets	ca. 2629 +26/-20
Localization of flow	
<hr/>	
End of pervasive granulite facies mylonitisation (ca. 700°C ^m)	D 2619 +9/-6 ^l , 2629 ± 2 ^u
Leucogranite, south Snowbird lake ⁿ	2558 ± 25
Selwyn Lake granite ⁿ	2585 ± 2
Hawkes granite*	ca. 2610, 2604 ± 1
Rea granite*	2584 +40/-15
Bradley and Brykea granites*	2601 ± 4
Godfrey granite*	2618 ± 4, 2606 +13/-11
Mary granite (multiphase)*	
<hr/>	
Beginning of syngranulite facies pervasive mylonitization	
Axis gabbro/horite (mafic granulite)	ca. 2600
Bohica mafic complex	2596 ± 12, 2620 +34/-21
<hr/>	
Syngranulite facies mylonitization, Chipman dykes and granites	D 3126 +6/-5
Striding River granite ⁿ	ca. 3300-3100
<hr/>	
Chipman batholith	
Layered anorthositic mafic complex	3149 ± 100,
Pelitic/semipelitic sediments	3466 +327/-80
<hr/>	
(m) Monazite: see Parrish (1990)	
(l) lower deck	
(u) upper deck	
(n) Northwest Territories	
(*) granulite facies metagranite	
(D) Major mylonitization event (between dashed lines)	



Figure 14. Development of porphyroblastic leucosome in more pelitic horizons of rhythmically layered semipelitic paragneiss in eastern (Hearne) wall rock, east of Bompas Lake. Coin for scale 2.5 cm. GSC 1994-192

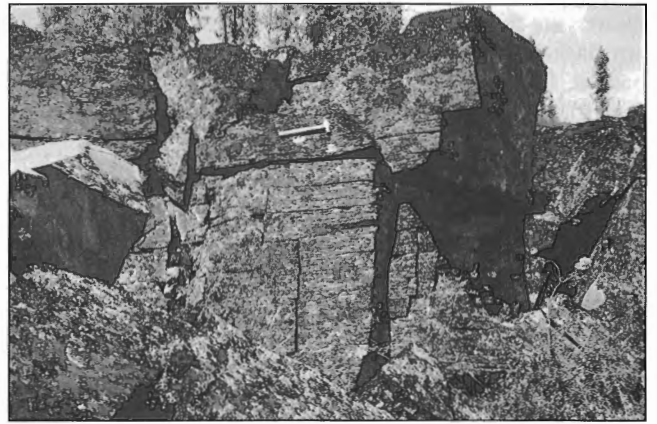


Figure 16. Subhorizontal planar bedding-parallel cleavage in mafic flows and tuffs, in eastern (Hearne) wall rock, between Atzinging and Kasba lakes (Fig. 2). Hammer for scale. GSC 1992-241

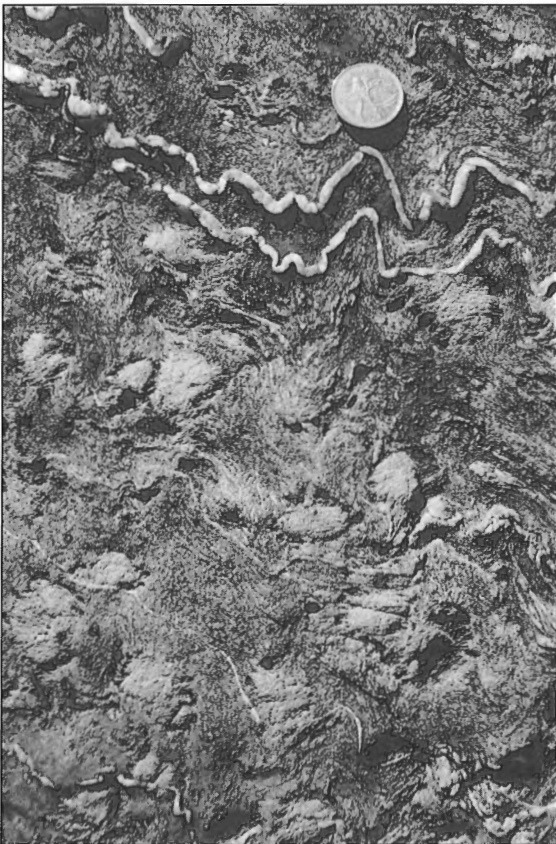


Figure 15. Crenulated cleavage in pelitic schist with 2 cm pseudomorphs after cordierite(?) which fossilize straight cleavage segments in eastern (Hearne) wall rock, Black Lake. Coin for scale 2.5 cm. GSC 1991-577N



Figure 17. Coarse crenulation of bedding-parallel cleavage (see Fig. 16) by open, kink-like folds whose axial planes dip moderately east (left). Vertical section in eastern (Hearne) wall rock, between Atzinging and Kasba lakes (Fig. 2). Hammer for scale. GSC 1994-194

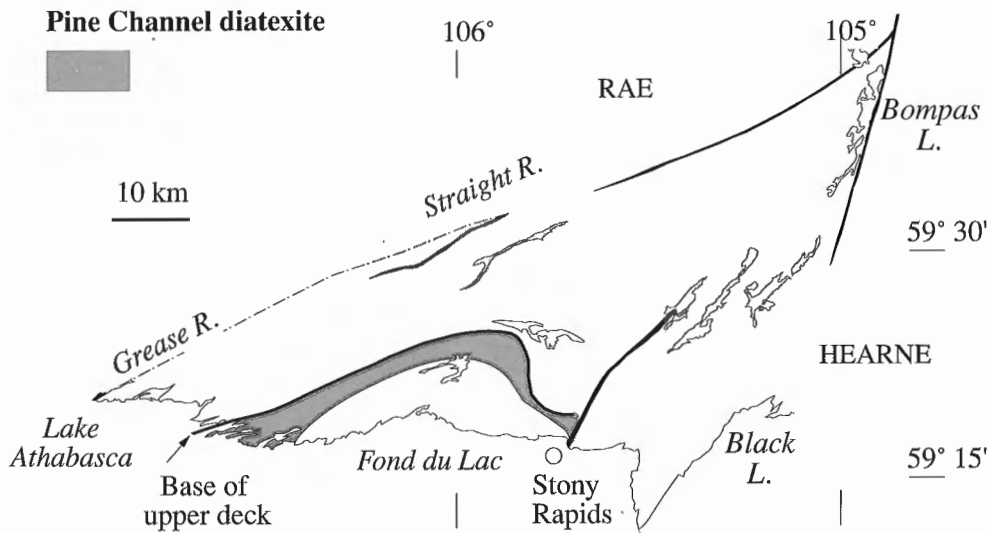


Figure 18. Distribution of Pine Channel diatexite (cf. Fig. 9 and 10).



Figure 19. Straight banding in Pine Channel diatexite, Lake Athabasca. Note the absence of feldspar porphyroclasts. Hammer for scale. GSC 1994-103

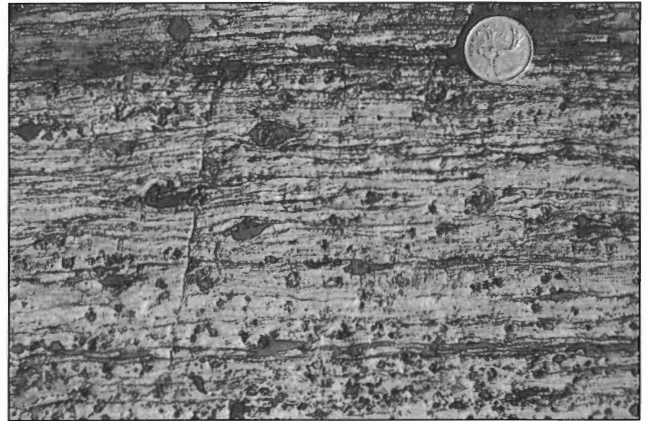


Figure 20. Ribbon mylonite fabric in Pine Channel diatexite, Lake Athabasca, with elongate orthopyroxene, quartz, and feldspar ribbons wrapping around garnet porphyroclasts. Note the absence of feldspar porphyroclasts. Coin for scale 2.5 cm. GSC 1994-097

pink garnets (Fig. 21, 22), local orthopyroxene (Fig. 23), graphite, and sprays of coarse sillimanite. Clear yellow monazite crystals, up to 1 mm in size, are visible in outcrop. The term diatexite should be understood *sensu lato*, because a variable proportion of mesosome (modified parent rock) is locally present in sufficient proportion for the rock to be a metatexite (see Mehnert, 1971; Brown, 1973). Nevertheless, globally the map unit has undergone extreme melting. The banding is defined by alternation of 0.1 to 1.0 m thick bands of ultramylonitic garnet granitoid leucosome, mesosome, garnet-quartz±clinopyroxene, garnet-clinopyroxene±quartz



Figure 21. Garnet-rich layer (bottom) in garnetiferous ribbon mylonite after Pine Channel diatexite, Lake Athabasca. Note the absence of feldspar porphyroclasts. Coin for scale 2.5 cm. GSC 1994-099

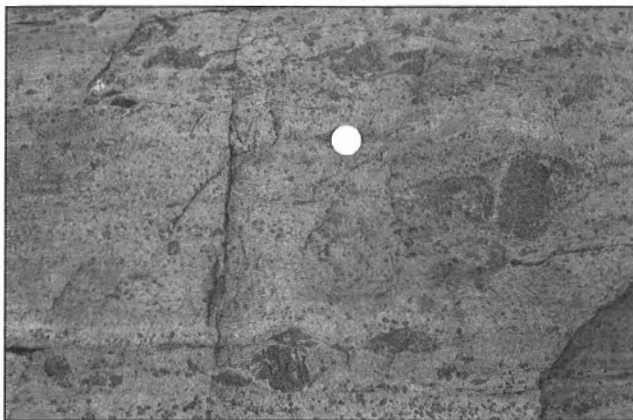


Figure 22. Variation in size of garnets (dark grey) in Pine Channel diatexite, Lake Athabasca. Note the absence of feldspar porphyroclasts. Coin for scale 2.5 cm. GSC 1994-098

and mafic granulite, with concordant 10 to 20 cm thick sheets of isotropic to strongly foliated garnet pegmatite. Some layers, up to a metre thick are extremely garnet-rich (<90% volume) and are either composed of garnet-quartz±magnetite, or garnet-clinopyroxene±magnetite (iron formation of authors; e.g. Slimmon and Macdonald, 1987). The granitic leucosome is generally a fine grained ribbon mylonite to ultramylonite, banded on a 5 to 10 cm scale due to variation in grain size, garnet content, composition, and colour. The pegmatites are compositionally identical to the mylonitic leucosome. Accordingly, the contrast in the degree of their fabric development, combined with their intimate spatial association, suggests that migmatization was, at least in part, syntectonic with respect to the mylonitization. Monazite from the diatexite at McBride Bay, Axis Lake (Fig. 3) has been dated at 2629 ± 2 Ma (Table 1). In light of the high estimated blocking



Figure 23. Ribbon mylonite fabric in Pine Channel diatexite, Lake Athabasca, with elongate orthopyroxene ribbons especially well developed in lower field, and garnet porphyroclasts. Note the absence of feldspar porphyroclasts. Coin for scale 2.5 cm. GSC 1993-221F

temperature for U-Pb diffusion in monazite (e.g. Parrish, 1990; Heaman and Parrish, 1991; Mezger et al., 1991), this date suggests that the granulite facies anatexis and mylonitization occurred at about that time.

Sillimanite is widespread in the diatexite, but it is particularly well developed in garnet-rich bands, up to a metre thick, which occur above a structurally defined horizon running from Camille Bay, Lake Athabasca (Fig. 3) to the north shore of McBride Bay, Axis Lake (Camille-McBride line). Kyanite is confined to the lower structural levels of the upper deck, below the Camille-McBride line. It occurs in intimate association with quartz, plagioclase, and K-feldspar as inclusions within garnets in the diatexite. The same association also occurs within the diatexite mylonite matrix. At two widely separated outcrops in the kyanite-bearing diatexite, mafic bands of omphacitic clinopyroxene-garnet, partially retrogressed to orthopyroxene-albite symplectite, were identified. These rocks are relict eclogite, retrogressed to granulite facies, which may have experienced peak pressures of at least 1.5 GPa (Snoeyenbos et al., 1995).

Mylonitic to ultramylonitic ribbon fabrics are penetratively developed throughout the Pine Channel diatexite, except between Pine Channel and Algold Bay (Fig. 3). There, the pronounced embayments in the Lake Athabasca shoreline highlight kilometre-scale, relatively low strain lenses of highly irregular, folded migmatite (*Apd*; Fig. 24). They are comprised of a stack of steeply southeast-dipping 'horses', individually and collectively bounded above and below by their highly attenuated ultramylonitized equivalents (Fig. 25). The diatexite is cut by two types of discrete concordant sheets (1-10 m thick) of orthopyroxene±garnet leucogranite; white and medium grained, and buff-pink and very coarse grained. Both types occur in the low strain 'horses', as well as in the ribbon mylonites. The white orthopyroxene leucogranite is everywhere concordant in the diatexite mylonite. The buff orthopyroxene leucogranite is usually

reduced to a ribbon ultramylonite. However, it is also seen to crosscut both the white orthopyroxene leucogranite and the diatexite mylonite fabric, albeit at a low angle. The above observations suggest that the buff orthopyroxene leucogranite is syntectonic with respect to the granulite facies mylonitization. Two samples of the leucogranite from south of Sucker Bay, Lake Athabasca (Fig. 3), yielded approximate magmatic crystallization ages of ca. 2600 Ma (Table 1), indicative of the approximate time of mylonitization.

Axis mafic granulite

The Axis mafic granulite (*Aam*; Fig. 26) constitutes the principal map unit in the structurally higher part of the upper deck. It forms a stack of sheets, essentially composed of

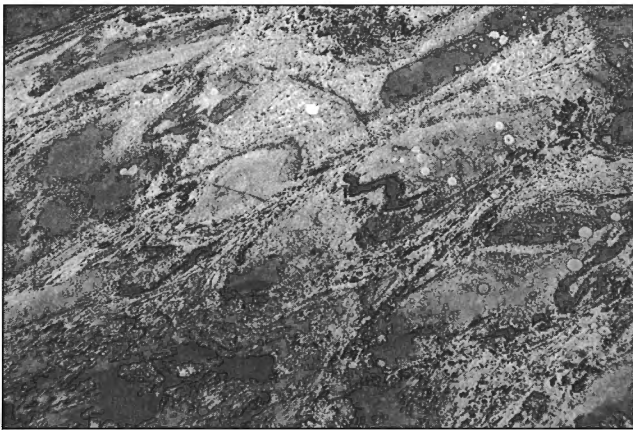


Figure 24. Moderately deformed migmatite of irregular aspect, precursor to Pine Channel diatexite ribbon mylonite, Sucker Bay, Lake Athabasca. Coin for scale 2.5 cm. GSC 1991-577G

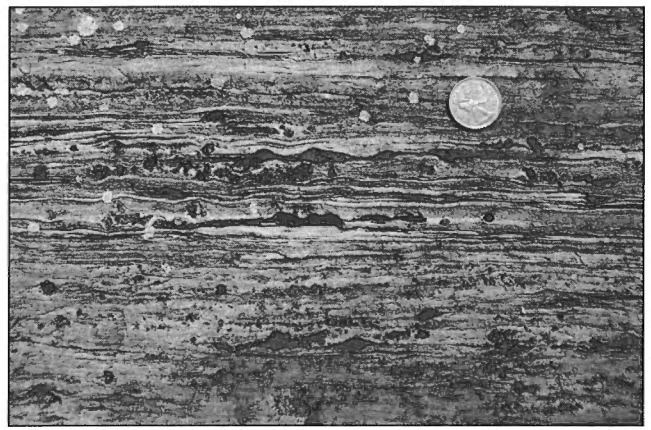


Figure 25. Ribbon mylonite equivalent of Figure 24. General streakiness is due to quartz-feldspar ribbons. Dark streaks are orthopyroxene ribbons, whereas grey spots are garnets. Sucker Bay, Lake Athabasca. Coin for scale 2.5 cm. GSC 1991-577J

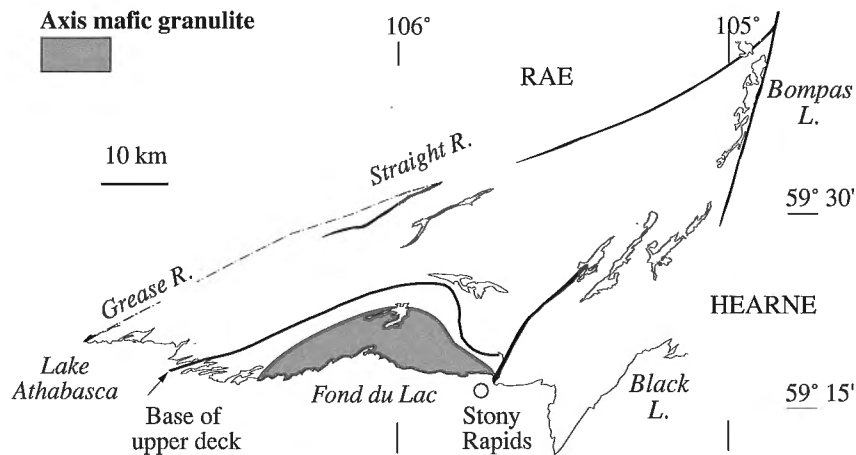


Figure 26. Distribution of Axis mafic granulite (cf. Fig. 9 and 10).

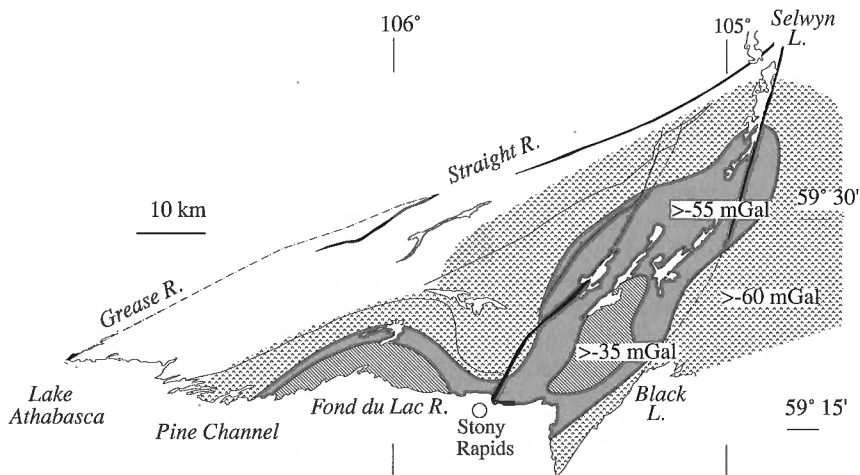


Figure 27. Generalized representation of the Bouguer gravity field in the vicinity of the East Athabasca mylonite triangle. Unpublished 1:50 000 scale Bouguer anomaly compilation, Geophysics Division, Geological Survey of Canada. Discussed in text.



Figure 28. Streaky aspect of finely polycrystalline Axis mafic granulite mylonite, Lake Athabasca. Dark grey is orthopyroxene, light grey is plagioclase. Note absence of porphyroclasts. Coin for scale 2.5 cm. GSC 1993-221G

orthopyroxene-plagioclase-magnetite±clinopyroxene±garnet±quartz, separated from one another by thin, but often mappable, horizons of diatexite ribbon mylonite. It is spatially coincident with a positive gravity anomaly which extends under the northern margin of the overlying Athabasca Basin (Fig. 27). At structurally lower levels of the upper deck, below a line linking Camille and McBride bays (Fig. 3), volumetrically subordinate clinopyroxene-garnet-plagioclase bands, possibly unrelated to the main structurally overlying volume of mafic granulite, contain the relict eclogite assemblage.

The individual mafic granulite sheets, 100 m to almost 2 km thick, collectively constitute a stack 5 km thick. The mafic granulite is a dark grey to brown, fine grained, sugary

textured rock, with 30 mm by 2 mm polycrystalline streaks of orthopyroxene or plagioclase (Fig. 28, 29). Quartz ribbons derived from the deformation of syntectonically introduced quartz veinlets are widespread in a strike-parallel band stretching from the southern bay of Axis Lake to Fond du Lac (Fig. 3). Coarse gabbroic to microgabbroic ophitic textures, indicative of a plutonic origin, are locally preserved in the mafic granulite through a thickness of more than a kilometre to the south and east of Axis Lake (Fig. 30, 31). Subtle compositional banding is only locally visible, suggesting that the protolith was not a layered mafic complex, although orthopyroxene layers, tens of metres thick, do occur at Axis Lake. Because it was locally possible to trace the mafic tectonite into coarse, plutonic textured protoliths, the mafic granulite bodies are interpreted as mylonite. In the field, the nature of the mafic granulite (grain size, relict plutonic igneous textures, coronitic metamorphic textures) varies abruptly from sheet to sheet in the Axis Lake area, although such marked variation is less apparent elsewhere.

The relationship of the Axis mafic granulite protolith to the Pine Channel diatexite has been the subject of disagreement between partisans of an intrusive relationship (e.g. Alcock, 1936; Furnival, 1940; Mawdsley, 1949) and those who interpret the mafic rocks as supracrustal in origin and stratigraphically intercalated with the diatexite protolith (e.g. Kranck, 1955). Baer (1969) stated that, due to the scarcity of crosscutting contacts, field relationships are equivocal. Contacts between the mafic granulite and the diatexite ribbon mylonites are either abrupt or sheeted. At the contacts, the mafic granulite is often a ribbon ultramylonite. However, it may also preserve moderate angles between subtle compositional layering and tectonic foliation (shape fabric). In the Axis Lake area (Fig. 3), thin diatexite mylonite intervals separate mafic granulite sheets of very different composition and fabric. This suggests that the present disposition of the

mafic granulite sheets may be, in part, the result of tectonic juxtaposition (stacking). Intrusion of the igneous protolith of the mafic granulite into the diatexite was directly observed at only one locality southeast of Axis Lake. There, a 1.5 m thick branching sheet of mafic granulite cuts across the ribbon fabric of thoroughly mylonitized diatexite and includes a



Figure 29. Streaky aspect of Axis mafic granulite mylonite, Lake Athabasca. Note absence of porphyroclasts. Coin for scale 2.5 cm. GSC 1994-106

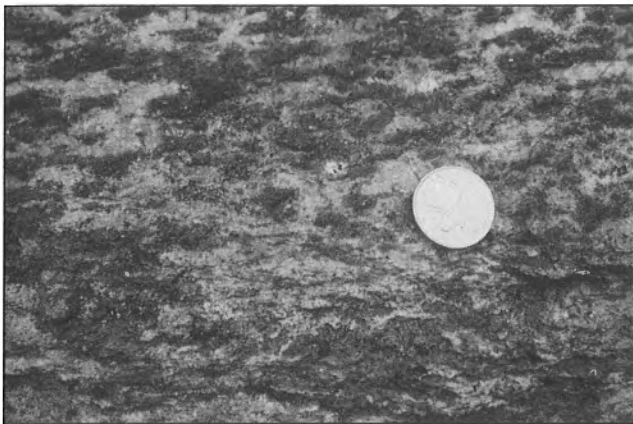


Figure 30. Relict coarse ophitic texture in Axis mafic granulite, southeast of Axis Lake. Coin for scale 2.5 cm. GSC 1994-101

small fragment of the same (Fig. 32, 33). At another locality in Camille Bay, Lake Athabasca (Fig. 3), an isolated very thin (5 cm) mafic dyke cuts the diatexite mylonitic fabric at a very low angle. Although it is probably a vein of the mafic granulite, the correlation is not unequivocal. Recognizing the restricted nature of the data set, it nevertheless appears that the protolith to the mafic granulite was syntectonically emplaced into the diatexite during mylonitization. The mafic granulite has yielded zircons which are dated at ca. 2600 Ma (Table 1). In the absence of inherited material, if the zircon age is indicative of the approximate time of magmatic crystallization, it would lend support to the interpretation of the mafic granulite as syntectonic with respect to mylonitization of the Pine Channel diatexite. Elsewhere in the upper deck, the diatexite visibly intrudes fractured mafic granulite sheets as arrays of thin (<25 cm) veins. These observations do not necessarily contradict the foregoing, given that the solidus temperatures of mafic melts are much greater than those of granite compositions.



Figure 31. Flattened equivalent of Figure 30 with relict coarse orthopyroxene crystals set in a recrystallized plagioclase matrix, Lake Athabasca. Coin for scale 2.5 cm. GSC 1994-100

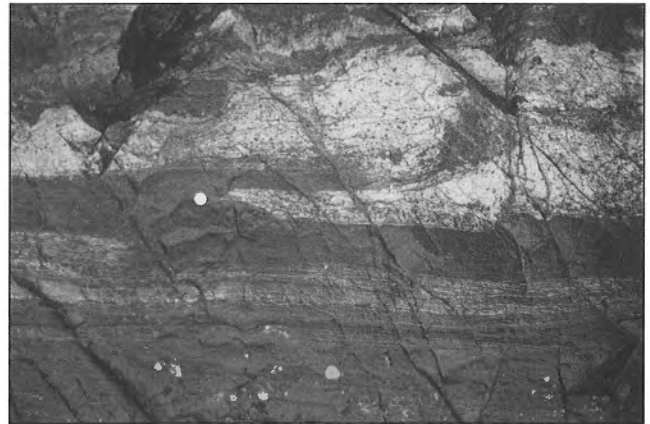


Figure 32. Branching vein of mafic granulite in Pine Channel diatexite ribbon mylonite, southeast of Axis Lake. Coin for scale 2.5 cm. GSC 1994-104

Two types of felsic rock occur within the Axis mafic granulite between Axis Lake and Fond du Lac (Fig. 3). Compositionally homogeneous, locally clinopyroxene-bearing leucocratic Rea granite (*Argm*) outcrops along the south shore of Axis Lake and west of Rea Lake. Contact relations with the mafic granulite are not exposed, and the granite is penetratively mylonitized with an excellent ribbon fabric. The 2584 +40/-15 Ma (Table 1) date obtained for the granite indicates a maximum age for its own mylonitization, and presumably for that of the Axis mafic granulite as well. Along the shore of Fond du Lac, the mafic granulite is cut by veinlets and <10 m thick sheets of coarse grained, buff orthopyroxene

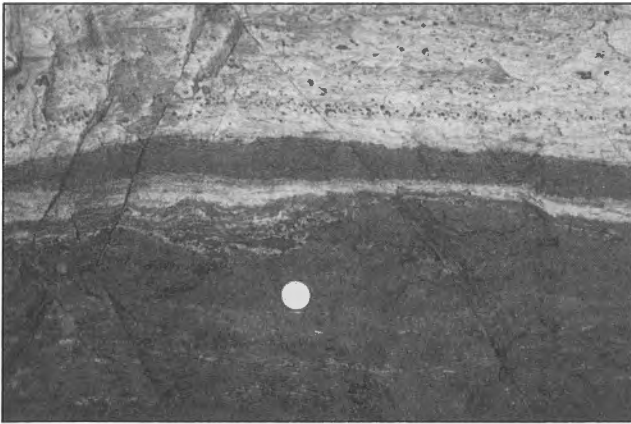


Figure 33. Two sheets of mafic granulite in Pine Channel diatexite ribbon mylonite, southeast of Axis Lake. The thicker sheet contains quartzofeldspathic streaks, possibly fragments of the diatexite. Its upper subconcordant contact crosscuts and truncates layering in the diatexite. This mafic granulite appears to intrude the diatexite mylonite. Coin for scale 2.5 cm. GSC 1994-105



Figure 34. A branching sheet of coarse orthopyroxene leucogranite crosscutting subtle layering in Axis mafic granulite at a low angle, Lake Athabasca. Note the shape fabric parallel to the pen, axial planar with respect to open folding of the layering. Pen for scale. GSC 1994-183

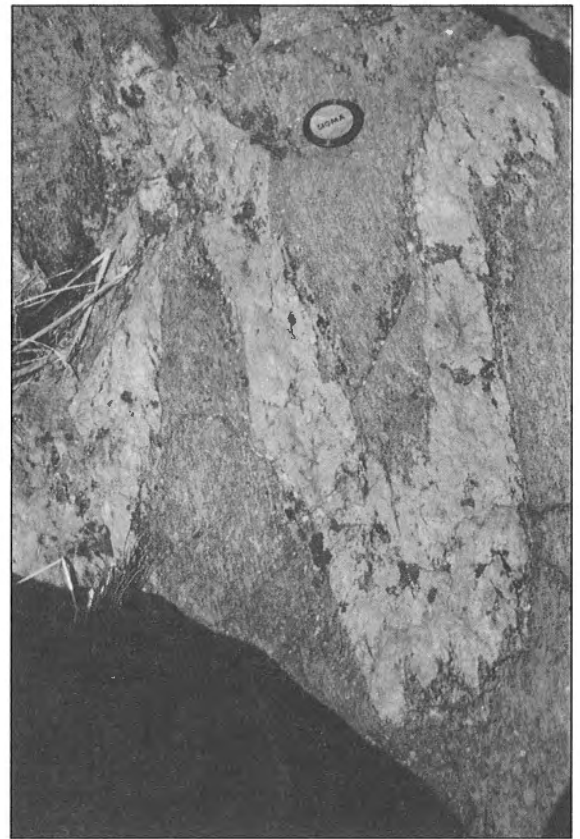


Figure 35. Folded vein of orthopyroxene leucogranite with Axis mafic granulite foliation aligned in the axial plane, Lake Athabasca. Lens cap for scale. GSC 1994-184

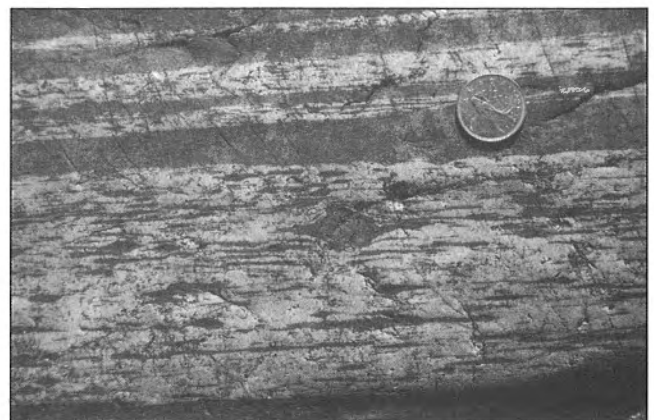


Figure 36. Orthopyroxene leucogranite ribbon mylonite, Lake Athabasca. Note the absence of feldspar porphyroclasts, the highly attenuated orthopyroxene ribbons, and the large orthopyroxene porphyroclast in the centre. Subconcordant sheet of mafic granulite crosscuts the ribbon foliation just left of the coin, scale 2.5 cm. GSC 1994-185

leucogranite, lithologically identical to that described above for the Pine Channel diatexite. Some of the leucogranite sheets which cut across the mafic mylonite are near isotropic (Fig. 34), others are folded with an axial planar fabric marked by the coarse quartz, feldspar, and orthopyroxene (Fig. 35). However, most of the orthopyroxene leucogranite is strongly mylonitized (Fig. 36, 37). Locally the mylonitic fabric is so intense that the rock resembles a "paper-schist". The above observations indicate that the leucogranite is syntectonic with respect to the mylonitization of the Axis mafic granulite. In brief, the combined data for the Axis mafic granulite, the Pine Channel diatexite, and the orthopyroxene leucogranite indicate that they were mylonitized together at ca. 2600 Ma.



Figure 37. Detail of Figure 36 to show the polycrystalline orthopyroxene mantle developed around the monocrystalline orthopyroxene core. Such core-and-mantle structures are often taken as diagnostic of dynamic recrystallization (however, see Nyman et al., 1992). Coin for scale 2.5 cm in diameter. GSC 1991-5770



Figure 39. Mafic sheets cutting across (top-right to bottom-left) coarse grained folded Reeve diatexite (*sensu lato*) with layers of pelitic paleosome observed in a rare low strain window, Tantato Lake. Note the axial plane fabric in the diatexite. Looking along the fold axis, coaxial with the extension lineation. Coin for scale 2.5 cm. GSC 1994-126

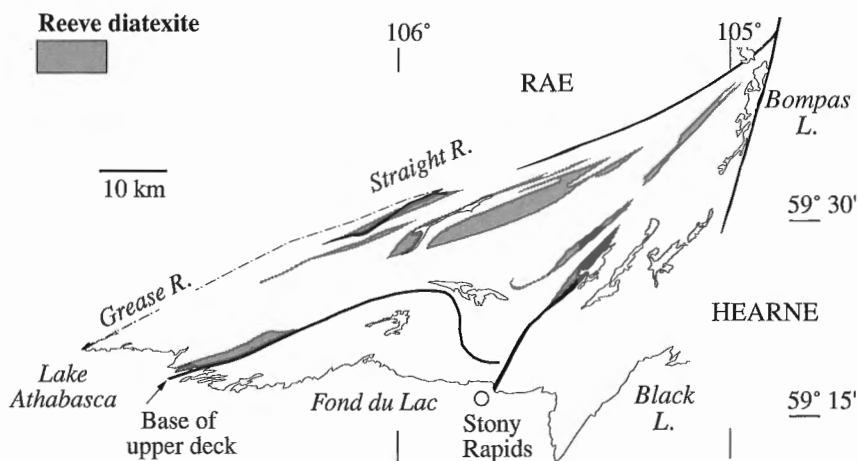


Figure 38. Distribution of Reeve diatexite (cf. Fig. 9 and 10).

Lower deck

Reeve diatexite

The garnet-sillimanite±orthopyroxene Reeve diatexite (Fig. 38) is lithologically and structurally very similar to that described above for the upper deck (see “Pine Channel diatexite”), except for the absence of orthopyroxene±garnet leucogranite sheets. The Reeve diatexite is a leucocratic, straight banded, quartzofeldspathic ribbon mylonite (Ardm; Fig. 39, 40). It is white to tan with a highly variable content (0-50%+) of lilac to delicate pink garnets, local orthopyroxene, graphite, and microscopic sillimanite. Monazite crystals are visible in outcrop. The banding is a complex alternation of 0.1-1 m thick bands of ultramylonitic garnet granitoid leucosome, mesosome, garnet-quartz±clinopyroxene,



Figure 40. Straight banded Reeve diatexite ribbon mylonite, derived by the deformation and transposition of the material illustrated in Figure 39, Tantato Lake. Note the absence of porphyroclasts. Lens cap for scale. GSC 204337-S

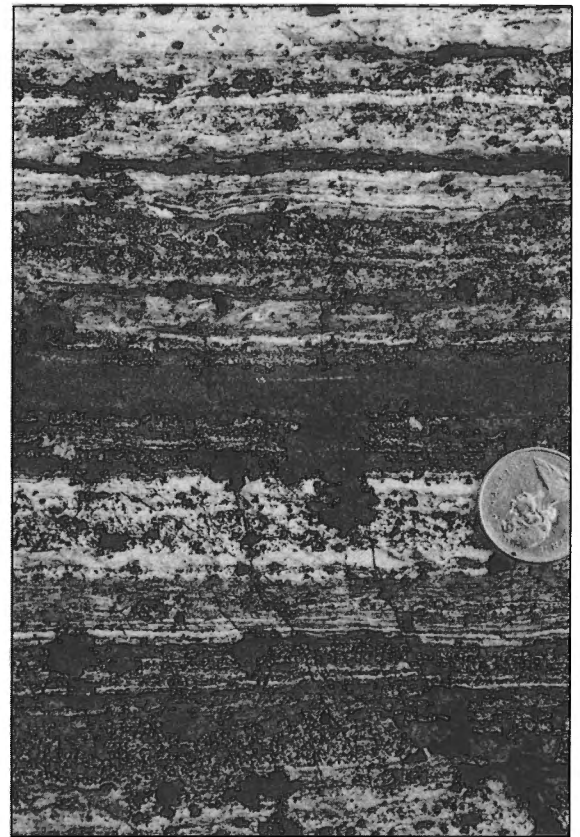


Figure 41. Reeve diatexite ribbon mylonite, Tantato Lake. Banding is principally due to variation in garnet content; compare the dispersal of garnets (dark spots) in the light layer beneath the coin with the dense packing of the garnet in the dark layer just above it. Coin for scale 2.5 cm. GSC 1994-130

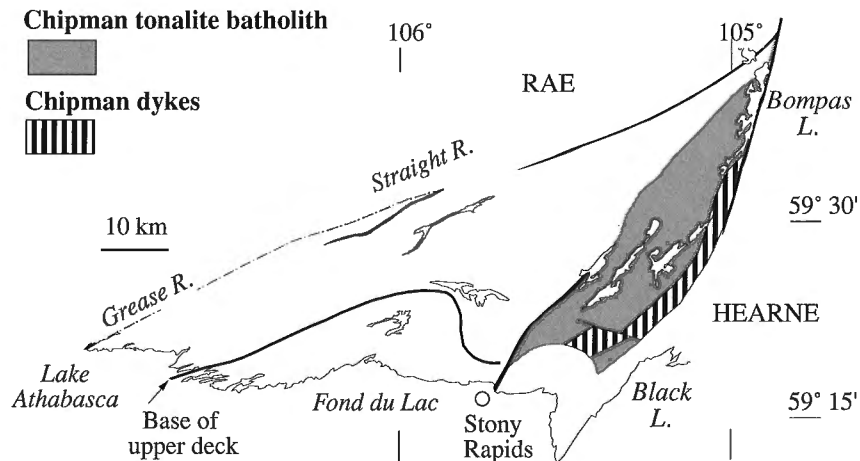


Figure 42. Distribution of Chipman tonalite batholith and the Chipman dykes (cf. Fig. 9 and 10).

garnet-clinopyroxene±quartz, and mafic granulite (Fig. 41), with concordant 10-20 cm thick sheets of isotropic to strongly foliated garnet pegmatite. Mylonitic ribbon fabrics are penetratively developed throughout the Reeve diatexite, except in a lens-like pod, 2 km by 1 km, which separates the southwest arms of Reeve Lake (Fig. 3). There, the diatexite is a compositionally monotonous, isotropic, coarse grained garnet±sillimanite leucogranite (*Ard*). Monazite from Reeve Lake yielded a 2619 ±9/-6 Ma age (Table 1) which, by the same reasoning as outlined above (see "Pine Channel diatexite"), is interpreted as the approximate time of granulite facies anatexis and mylonitization.

Chipman batholith

The Chipman batholith (Fig. 42; "hybrid gneiss" of authors; see Gilbo 1980b; Gilbo and Ramaekers, 1981) is apparently a single magmatic body, divided into several structurally and metamorphically defined map units (Fig. 43).

Deformation fabrics within the tonalite (*Acu*, *Act*) are composite, comprising an older straight gneiss (*Acgn*; Fig. 44, 45; Hanmer, 1988b) preserved in the eastern part of the batholith, reworked by younger ribbon mylonite (*Acm*) principally in the western part of the batholith. All units of the Chipman batholith contain abundant, dispersed, fist-size to map-scale inclusions of variably deformed anorthosite (*Aan*), layered amphibolite (*Aca*), orthopyroxenite, garnet clinopyroxenite, cummingtonite-anthophyllite rock, and fresh peridotite (*Ap*), the majority of which are concentrated in the eastern half of the batholith (Fig. 46, 47). These appear to represent fragments of a magmatically dismembered layered mafic complex, dispersed throughout the tonalite. A single greater than ten metre xenolithic raft of garnetiferous paragneiss, which superficially resembles the Reeve diatexite, was observed in the tonalite on the southeast side of Chipman Lake.

The central part of the batholith, a lenticular area (5 x 30 km) between Chipman and Bompas lakes (Fig. 43), is occupied by coarse (>2 cm) hornblende tonalite with a coarse

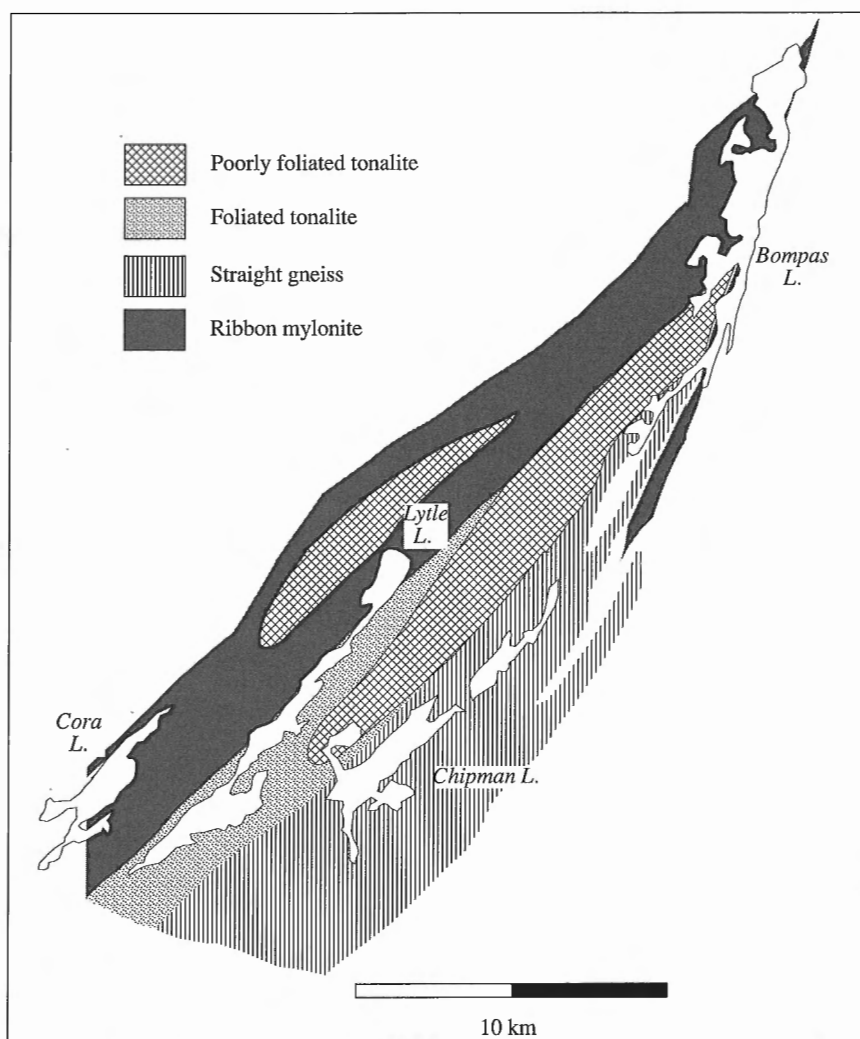


Figure 43. Sketch map of the distribution of structurally determined map units identified within the Chipman tonalite batholith. See Figure 9 for location.



Figure 44. Annealed tonalite mylonite (straight gneiss) in the eastern part of the Chipman tonalite batholith, Woolhether Lake. Note the absence of porphyroclasts. Lens cap for scale. GSC 1994-129

igneous texture, a moderate shape fabric, and a nebulous banding of dispersed amphibolite and clinopyroxenite inclusions (*Ac*; Fig. 48, 49). Compositional banding, defined by thin (<25 cm) lenses or concordant layers of the included mafic material, reflects flow during magmatic emplacement. The banding is folded with an upright, northeast-trending shape fabric developed in the fold axial planes. Fold axes are parallel to a penetrative, generally southwest-plunging extension lineation, irrespective of fold tightness. The foliation, accompanied by a general tightening and transposition of the associated folds, passes progressively (*Act*) into quartz and feldspar ribbon tonalitic mylonite (*Acm*; Fig. 50). This is well exposed in large outcrops west of south Bompas Lake (Fig. 3), where 50 m to 100 m wide lenses of moderately deformed tonalite are wrapped around by anastomosing belts of quartz and feldspar ribbon mylonite, even at the scale of a single outcrop. A similar transition can be followed at the map scale as the tonalite west of Lytle Lake (Fig. 3) passes progressively into fine grained garnet-clinopyroxene tonalitic ultramylonite at Cora Lake (Fig. 3). There, the tonalitic mylonite is associated with thick (10-100 m), laterally extensive, concordant layers of clinopyroxenite, orthopyroxenite, garnet-magnetite clinopyroxenite, amphibolite, anorthosite, and garnet-sillimanite diatexite.

To the east of Chipman Lake (Fig. 3) most of the tonalite is transformed into an annealed hornblende±garnet straight gneiss (e.g. Hanmer, 1988b), devoid of shape fabrics, and with a sugary texture and a medium to fine grain size (<1 mm). The straight layering is derived by the transposition of locally preserved metre-scale folds which deform an earlier banding, similar to that described above for the batholith core (Fig. 51, 52). Locally, plagioclase occurs as polycrystalline streaks and ribbons, or as 1 to 5 cm porphyroclasts disposed as isolated grains or arranged in trains along the plane of the layering (Fig. 53, 54). These observations indicate the initially coarse grain size of parts of the tonalitic straight gneiss, and the strong deformation and grain size reduction that it has undergone. Therefore, the straight gneiss is an annealed tonalitic mylonite (e.g. Hanmer, 1987b) in which the quartz shape fabric has apparently been destroyed (e.g. Hanmer, 1984a). Thin, concordant amphibolite, hornblende, clinopyroxenite, and anorthosite layers, derived by the deformation of inclusions, as well as mafic dykes and granitic veins (see “Chipman dykes” and “Chipman granite” below), are an integral part of the annealed mylonite banding (Fig. 55). However, after the straight mylonitic layering had

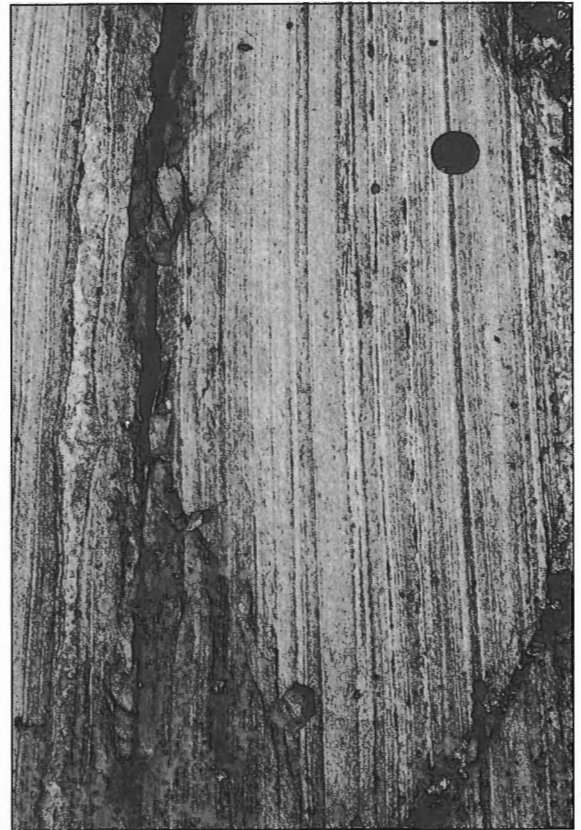


Figure 45. Annealed tonalite mylonite (straight gneiss) in the eastern part of the Chipman tonalite batholith, Woolhether Lake. Although streaky in appearance due to compositional variation, no shape fabrics are preserved. Note the absence of porphyroclasts in the tonalite, but their presence in the narrow attenuated granite vein to the left. Lens cap for scale. GSC 1994-128



Figure 46. Misoriented, internally layered angular blocks of anorthosite in a hornblende-bearing tonalite matrix in the Chipman tonalite batholith, west of the upper Chipman rapids. Coin for scale 2.5 cm. GSC 1994-133

formed, thicker mafic layers (>1 m) tended to behave more competently than the bounding tonalitic mylonite and extended heterogeneously, probably in response to changing deformation conditions (e.g. decreasing temperature, increasing strain rate). Coarse tonalite and granitic pegmatite have crystallized in the gaps between competent blocks. Locally, heterogeneous flow around blocks of competent material has led to the initiation and amplification of folds of the once straight layering. The result is a disrupted gneiss of highly irregular aspect.

The presence of the common assemblage of mafic and ultramafic inclusions in the straight gneiss, the moderately foliated tonalite, and the tonalitic ribbon mylonite suggests that all the tonalitic map units are components of the same

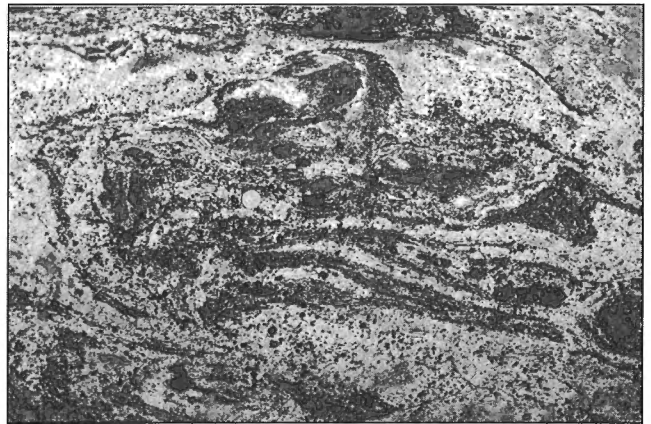


Figure 48. Nebulous banding marked by streaks of amphibolite ± clinopyroxene contained in coarse grained and weakly foliated tonalite, Chipman tonalite batholith, west of the upper Chipman rapids. Coin for scale 2.5 cm. GSC 1994-131



Figure 47. Strands of streaky annealed tonalite mylonite wrapping around lenses of very coarse grained gabbro, Chipman tonalite batholith, Chipman Lake: strongly deformed equivalent of the material illustrated in Figure 46. Note the absence of shape fabrics in the mylonite. Coin for scale 2.5 cm. GSC 1994-146

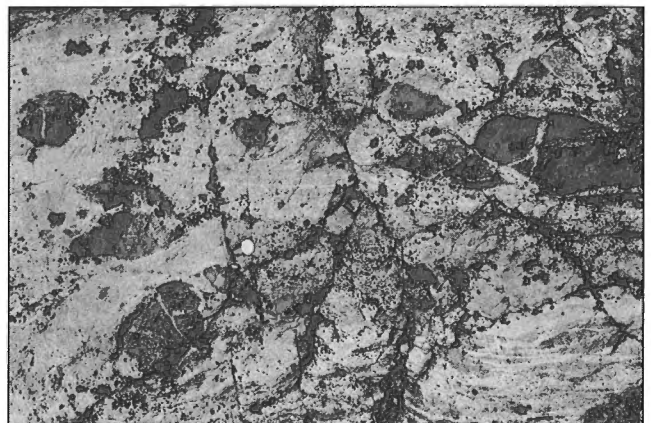


Figure 49. Subtle, discontinuous layering marked by streaks of amphibolite in coarse grained and weakly foliated tonalite, associated with randomly oriented subangular fragments of clinopyroxenite, Chipman tonalite batholith, west of the upper Chipman rapids. Coin for scale 2.5 cm. GSC 1994-132

body. The principal differences between them are reflections of spatial variation in total strain, degree of annealing, and the volume of inclusions and syntectonic intrusions. Attempts have been made to date several samples of the tonalite. Folded tonalitic straight gneiss (*Acgn*) from Steinhauer Lake (Fig. 3) has yielded a poorly constrained age of $3466 + 327 / - 80$ Ma (Table 1). A sample of poorly foliated tonalite from the core of the batholith at Chipman Lake (Fig. 3) has yielded an equally poorly constrained age of 3149 ± 100 Ma (Table 1). All of the map units of the Chipman batholith are truncated by the strike of the eastern boundary of the East Athabasca mylonite triangle. At Bompas Lake (Fig. 3) they abut against a 750 m wide belt of hornblende tonalitic ribbon mylonite to ultramylonite, derived from the same tonalite precursor.

Chipman dykes

The Chipman batholith is intruded by a swarm of subconcordant, 1 to 100 m thick mafic dykes, referred to here as the Chipman dykes (Chipman Sill Swarm of Macdonald, 1980). These dykes are pivotal to understanding the structural and metamorphic history of the Chipman batholith and will therefore



Figure 50. Progressive transposition of folded layering (top) with an axial planar foliation, into streaky annealed tonalite mylonite, in the Chipman tonalite batholith, west of the upper Chipman rapids. Note the absence of porphyroclasts and shape fabric in the mylonite. Coin for scale 2.5 cm. GSC 1994-134

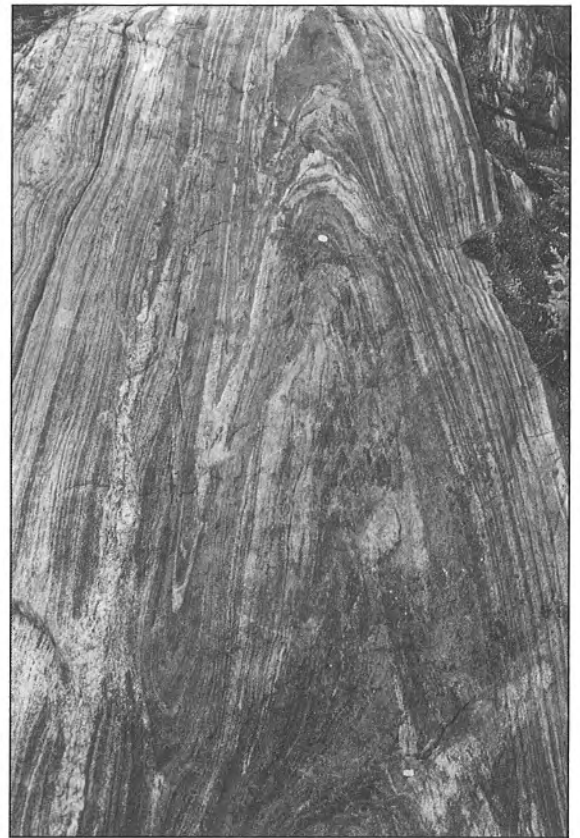


Figure 51. Coaxial refolding of lineation-parallel isoclinal fold of annealed tonalite mylonite (straight gneiss), Chipman tonalite batholith, Chipman Lake. Note the absence of porphyroclasts and of shape fabrics. Coin for scale 2.5 cm. GSC 1994-147

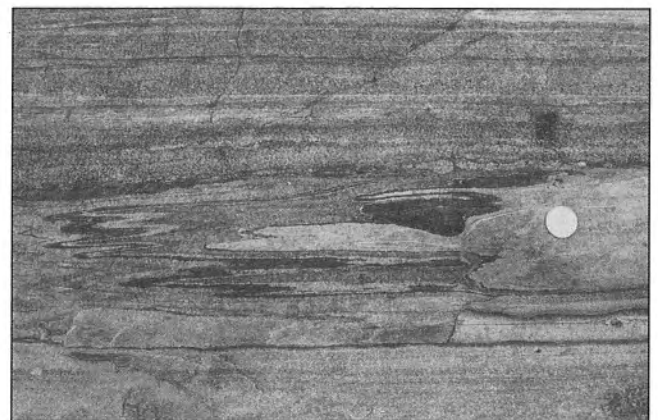


Figure 52. Annealed tonalite mylonite, Chipman tonalite batholith, Chipman Lake, illustrates the straight attenuated banding, very tight to isoclinal folding, absence of shape fabrics, and the local preservation of feldspar porphyroclasts (lower right). Coin for scale 2.5 cm. GSC 1994-123

be examined in some detail (see also Williams et al., 1995 for detailed analysis). The dykes may be so closely spaced as to occupy 60 to 100% of the outcrop, thereby constituting a mappable unit (Fig. 42). The main part of the swarm is spatially coincident with the tonalitic straight gneiss, east of Chipman Lake (Fig. 3), though dykes are present in the western part of the batholith. Without implying any correlation with the Axis mafic granulite, the main part of the swarm also coincides with a lateral extension of the positive gravity anomaly, centred on the mafic rocks of the upper deck (Fig. 27; see "Axis mafic granulite"). This suggests that the volume of dyke material may increase with depth. Chilled margins and concentrations of plagioclase

phenocrysts near the centres of the dykes are common. The dykes are variably deformed. Some are well foliated and subsequently isoclinally folded, whereas others preserve misoriented wall rock inclusions, joint-controlled irregularities decorating their contacts, and apophyses projecting into the wall rocks.

Metamorphism of the Chipman dykes has resulted in a variety of mineral assemblages, even within adjacent, cross-cutting sheets. Many of the dykes are texturally homogeneous, fine- to medium-grained and composed of hornblende-plagioclase (Fig. 56). A small number of dykes, generally found along the eastern margin of the Chipman

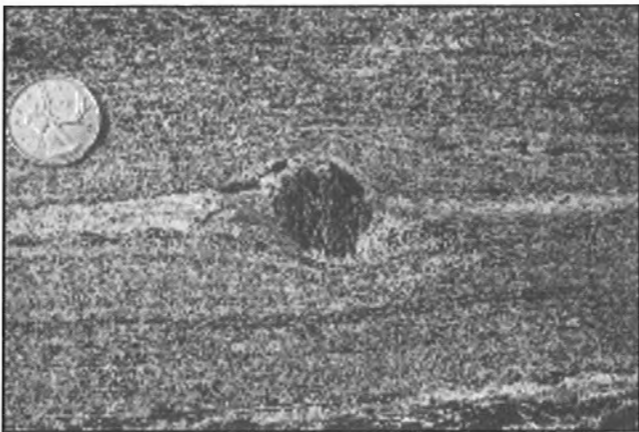


Figure 53. Annealed tonalite mylonite, Chipman tonalite batholith, Chipman Lake, illustrates the absence of shape fabrics, yet a relict planar structure wrapping around a locally preserved feldspar porphyroblast. Coin for scale 2.5 cm. GSC 1991-577E



Figure 55. Annealed tonalite mylonite, Chipman tonalite batholith, Chipman Lake, illustrates the absence of shape fabrics, yet a relict planar structure wrapping around a heterogeneously extended mylonitic granite sheet (left of coin) and an isolated mafic boudin (top-right), as well locally preserved feldspar porphyroclasts (far-left and far-right of coin, scale 2.5 cm). GSC 1991-577H

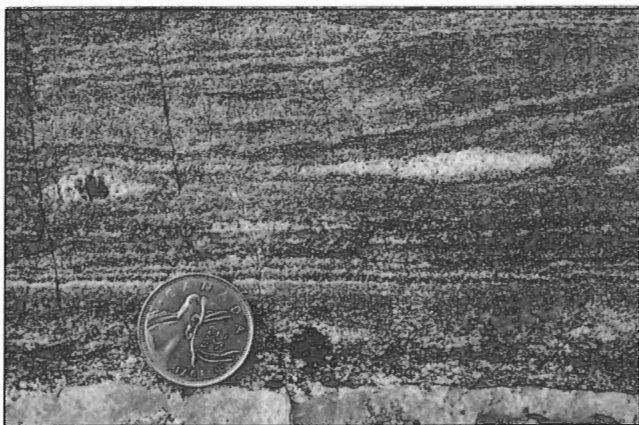


Figure 54. Annealed tonalite mylonite, Chipman tonalite batholith, Chipman Lake, illustrates the absence of shape fabrics and the local preservation of core-and-mantle structure developed on feldspar porphyroclasts. Coin for scale 2.5 cm. GSC 1994-124

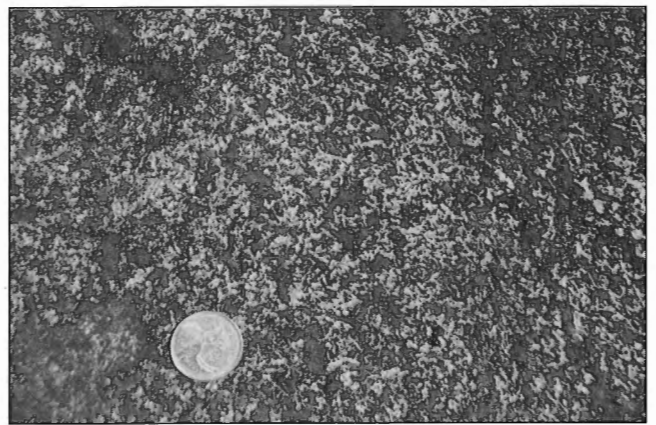


Figure 56. Coarse ophitic texture in an isotropic Chipman dyke, Chipman tonalite batholith, Stallard Lake. Coin for scale 2.5 cm. GSC 1994-109

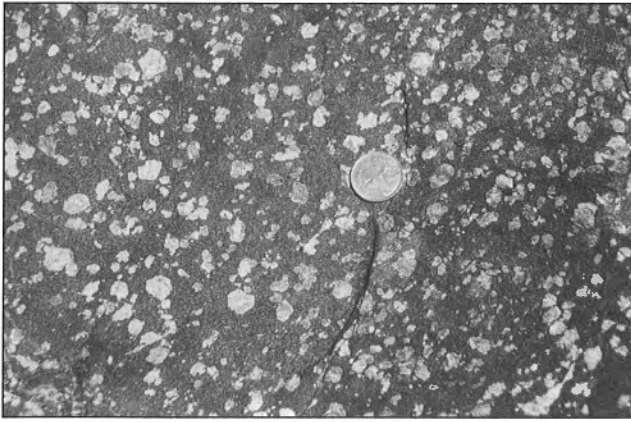


Figure 57. Coarse feldspar-phyric isotropic Chipman dyke, Chipman tonalite batholith, Stallard Lake. Coin for scale 2.5 cm. GSC 1994-108

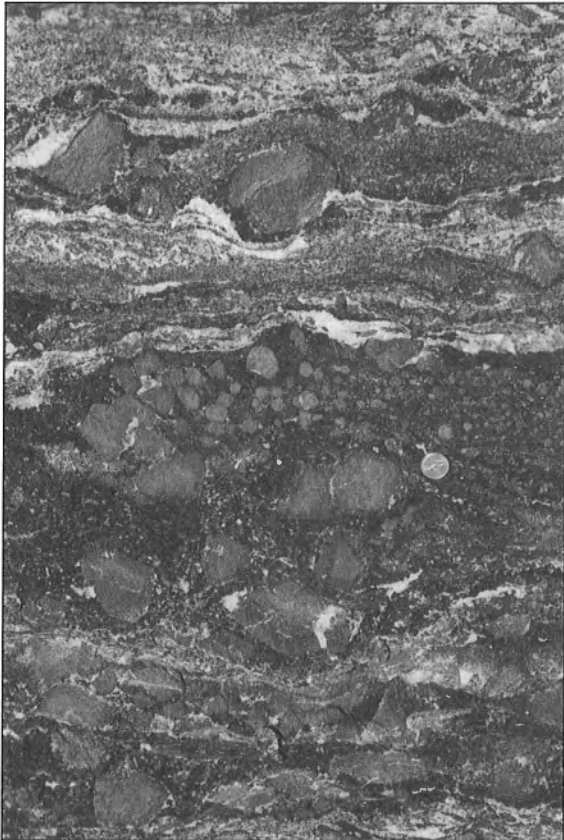


Figure 58. Spectacularly coarse garnets set in hornblende-rich matrix (lower field) and associated with tonalite melt (upper field) in banded Chipman dyke, Chipman tonalite batholith, Woolhether Lake. Coin for scale 2.5 cm. GSC 1994-577M

batholith, are plagioclase-phyric, with 2 to 5 cm feldspar phenocrysts concentrated in the centres of the dykes (Fig. 57). The phyric dykes may contain clinopyroxene, and 1 mm garnet forms necklace-like rims on the plagioclase phenocrysts. However, others contain several distinctive garnet-bearing metamorphic assemblages, which facilitate identification of the components of the swarm.

The most spectacular dykes contain euhedral garnet crystals of uniform grain size up to 10 cm across, derived at the expense of an earlier, fine- to medium-grained hornblende-plagioclase assemblage. The matrix surrounding the garnets shows clear evidence of a marked increase in the hornblende/plagioclase ratio, often associated with a coarsening of the hornblende component. Regular variation in garnet grain size within a given dyke may impart a banded or lenticular structure parallel to the dyke walls (Fig. 58, 59). In many examples, elongate tails of quartz-plagioclase (tonalitic melt; see Wolf and Wyllie, 1993) develop at the garnet/matrix interface and constitute the principal tectonic fabric-forming elements within the dyke (Fig. 60, 61). The garnet-melt assemblage is derived by the reaction plagioclase+hornblende I \rightarrow garnet+hornblende II+tonalite melt. It is present in dykes spanning the complete range of deformation states from transposed, isoclinally folded and dismembered (Fig. 62, 63), to crosscutting and nondeformed. Because they are both part of, and crosscut the straight gneiss of the Chipman batholith, even within a single outcrop, these dykes were emplaced during the deformation which produced the annealed mylonite.

The commonest garnetiferous assemblage in the mafic dykes is clinopyroxene-garnet-plagioclase \pm hornblende, with a uniform 1 mm to 2 mm grain size. It is often possible to observe that an initial hornblende-plagioclase assemblage was replaced by fine- to medium-grained clinopyroxene-garnet-plagioclase \pm hornblende. In such examples, the reaction is arrested and it is clear that the new anhydrous assemblage forms in small, 1 cm diameter bud-like volumes, resembling

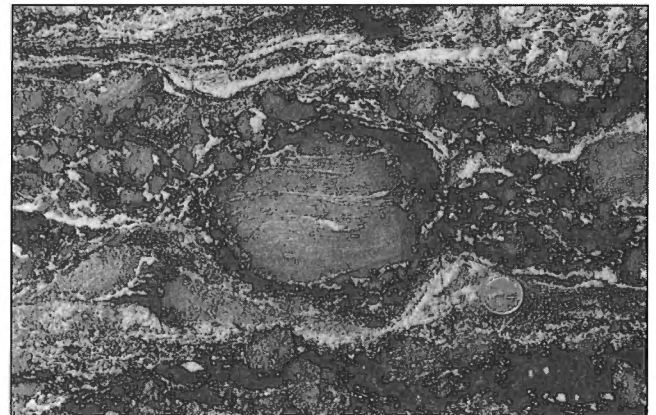


Figure 59. Coarse garnets set in hornblende-rich matrix (lower field) and associated with tonalite melt (upper field) in banded Chipman dyke, Chipman tonalite batholith, Woolhether Lake. Note the inclusion trails in the large garnet and the symplectite developed at its margins. The reactions illustrated here are thought to be hornblende+plagioclase \rightarrow garnet+new hornblende+tonalite melt. Coin for scale 2.5 cm. GSC 1994-494



Figure 60. Garnets with associated tails of tonalite melt set in hornblende-rich matrix in banded Chipman dyke, Chipman tonalite batholith, Woolhether Lake. The shape fabric (top-left to bottom right) marked by the tonalite melt tails is oblique to the compositional layering, itself parallel to the dyke wall (not shown) in this example. Coin for scale 2 cm. GSC 1993-221A

the form of a “cauliflower” (Fig. 64). The boundary between the old hydrous and new anhydrous assemblages is sharply delimited by a distinct necklace-like rim of 1 mm garnets. Where the bud-like volumes have coalesced, only the outermost rims show the garnet necklaces. In many dykes, the reactions have gone to completion, the entire dyke is occupied by the anhydrous assemblage, and all trace of the “cauliflower” structure is lost.

The structurally isotropic and compositionally homogeneous nature of the clinopyroxene-garnet-plagioclase assemblage combine to make it difficult to unequivocally determine its relationship to the straight gneiss structure of the host Chipman batholith, because it does not preserve internal shape fabrics. Where the dykes are crosscutting and associated with well preserved, joint-defined relief along their contacts, they are clearly late- to postkinematic (Fig. 65). However, where the dykes are concordant to the host gneissosity, it is not clear whether they were emplaced along the gneissosity, or rotated into parallelism with it by deformation. However, folded, foliated dykes with the spectacular garnet-melt assemblage locally crosscut dykes with

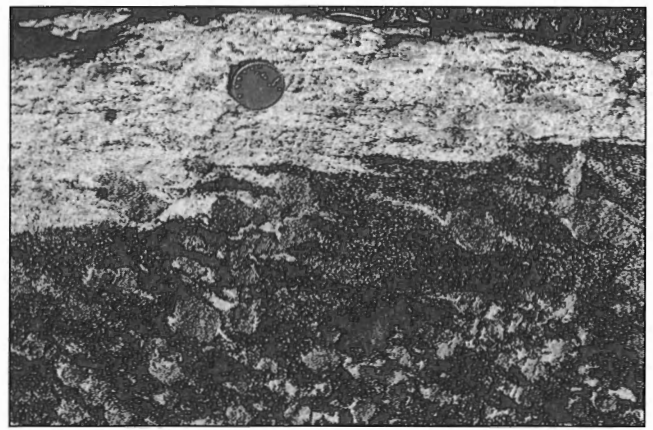


Figure 61. Garnets with associated tails of tonalite melt set in hornblende-rich matrix in a Chipman dyke whose contact makes a low angle with the foliation in tonalite host rock, Chipman tonalite batholith, Woolhether Lake. Looking down on horizontal surface. The shape fabric (top-left to bottom-right) marked by the tonalite melt tails is oblique to the dyke boundary and curves progressively anticlockwise to pass with continuity into the host foliation. In view of the subconcordant relationship of the dyke to the host foliation, this appears to represent rotation of the principle directions of finite strain with respect to the kinematic reference frame, i.e. a sinistral sense of shear (e.g. Hammer and Passchier, 1991). Coin for scale 2.5 cm. GSC 1994-114

the “cauliflower” assemblage, while the latter clearly crosscut older, transposed and disrupted equivalents of the former (Fig. 66). Accordingly, the garnet-melt and garnet-clinopyroxene assemblages are mutually contemporaneous, intimately spatially associated, syntectonic and quasi-synmagmatic with respect to the emplacement of the dykes. Since the garnet-clinopyroxene assemblage was clearly stable under granulite facies conditions, so too was the garnet-hornblende assemblage (see also Wolf and Wyllie, 1993). It is probable that subtle compositional variations within the dykes determine which of the two assemblages formed under the ambient metamorphic conditions. Moreover, because the dykes were emplaced syntectonically with respect to the development of the straight gneiss banding in the tonalitic host rocks, the hornblende-bearing assemblages of the central and eastern parts of the Chipman batholith must also have developed under granulite facies conditions.

The mafic dykes are numerically and volumetrically more important in the eastern part of the Chipman batholith, compared with the west. Furthermore, a greater proportion of them are crosscutting and less deformed in the east, compared with the west. Indeed, the syntectonic features of the dyke swarm are totally obliterated in the ribbon mylonite of the western part of the Chipman batholith (Fig. 67). Therefore, postdyke deformation, which resulted in ribbon mylonite in the western part of the batholith, is younger than the annealed mylonite fabrics in the east.

Chipman granite

Pinkish-red, coarsely equigranular leucogranite cuts the Chipman tonalite, east of Chipman Lake and to the southwest of Woolhether Lake (Fig. 3), and is referred to there as Chipman granite. Although some large, discontinuous bodies outcrop between Chipman Lake and upper Chipman rapids (Fig. 3), most of the granite within the tonalite batholith occurs as thin (0.1-1 m) sheets. Some of the better preserved and thicker examples at the east end of Steinhauer Lake contain 50 cm, rounded blocks of amphibolite (Fig. 68), unlike any of the material in the local tonalitic host rocks. The granite is variably deformed, ranging from unfoliated sheets which cut across the annealed straight gneiss fabric of the host tonalite, to transposed layers in the straight gneiss banding (Fig. 55). Isotropic to variably foliated granite is associated with



Figure 62. A complex folding relationship illustrating the syntectonic nature of some Chipman dykes, Chipman tonalite batholith, Woolhether Lake. A well defined dyke with very coarse garnets, similar to material illustrated in Figures 58-61, defines a fold (axial trace top-left to bottom right). However, annealed tonalite mylonite and mafic layers describe a very similar fold whose lower limb is truncated by the coarse garnet dyke. Inspection of the core of the "inner" fold shows that the laminated appearance of some of the mafic layers is due to strong attenuation of an early garnet-tonalite melt texture. Accordingly, Chipman dykes were emplaced and metamorphosed during the growth of the fold shown here. Short dimension of photograph about 1 m. GSC 1994-113

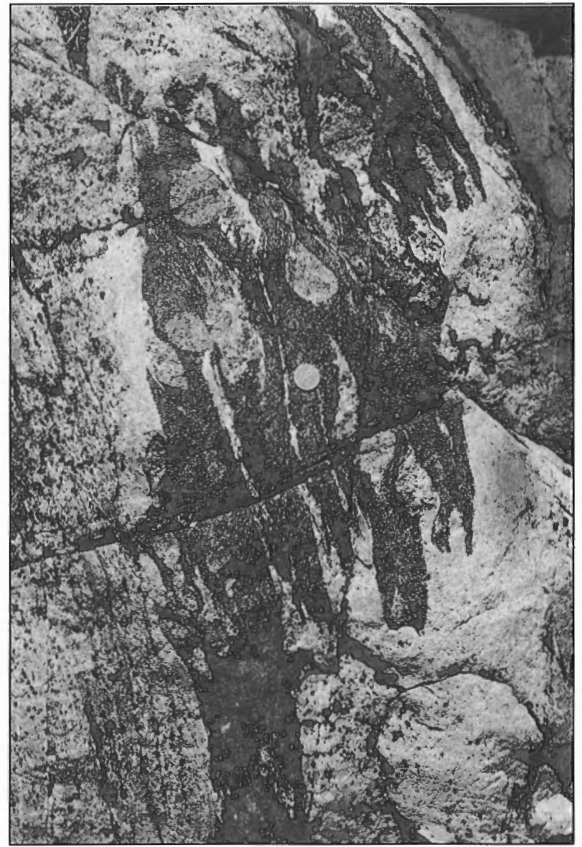


Figure 63. Strongly folded and mechanically disrupted dyke with very coarse garnets, similar to material illustrated in Figures 58-62, set in a tonalite host, Chipman tonalite batholith, Woolhether Lake. Coin for scale 2.5 cm. GSC 1994-107

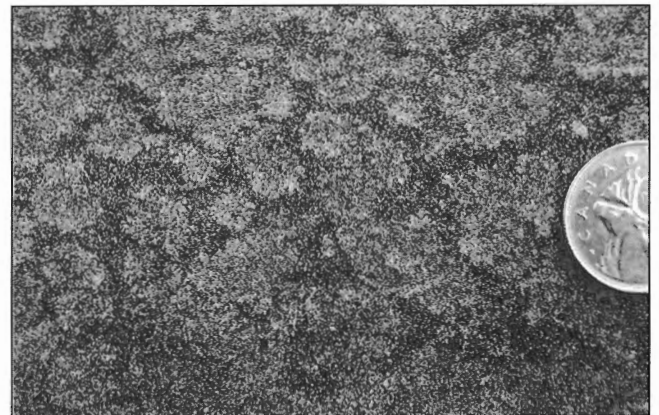


Figure 64. Detail of the isotropic fabric and metamorphic texture of a Chipman dyke, Chipman tonalite batholith, Woolhether Lake. Light coloured, partially coalesced patches ("cauliflower" structure) are principally plagioclase-clinopyroxene±garnet±hornblende separated from the darker hornblende-plagioclase matrix by a thin chain-like rim of equant garnet crystals. Coin for scale 2.5 cm. GSC 1991-577B

disrupted parts of the annealed tonalitic mylonite and with heterogeneous extension of the competent mafic inclusions. Locally, the granite forms sheets which are thick enough to be represented at the map scale, for example, northeast of Chipman Lake (Fig. 3), but even there they comprise a densely packed set of discrete veins intruded into tonalitic gneiss.

Sheets of Chipman granite crosscut strongly deformed early members of the Chipman dyke swarm, but are systematically crosscut by later, less deformed to undeformed Chipman dykes. Accordingly, the Chipman batholith was intruded by broadly coeval granite and mafic sheets, such that the emplacement of the latter outlasted that of the former. A 1 m thick sheet of isotropic Chipman granite, crosscutting with respect to the annealed tonalitic straight gneiss at



Figure 65. Composite Chipman dykes in the Chipman tonalite batholith, Woolhether Lake. A dyke with coarse garnets and tonalite melt tails marking a well developed, oblique planar internal foliation, is bounded on either side by finer grained dyke material across well defined, sharp contacts. The dyke material on the far right has the “cauliflower” metamorphic texture illustrated in Figure 64. The material separating the garnet-melt dyke from the tonalite host (light grey) is less well characterized, but it is possible that the garnet-melt dyke cut and split the “cauliflower” dyke. The internal obliquity and the horizontal lineation are compatible with sinistral strike-slip postdyke shearing, but the planar nature of the garnet-melt foliation remains enigmatic. Photograph short dimension 1 m. GSC 1994-152



Figure 66. Strong foliation in deformed garnet-tonalite melt-bearing Chipman dyke (upper field) crosscut by a homogeneous garnet-clinopyroxene-bearing Chipman dyke, Chipman tonalite batholith, Woolhether Lake. Compare with Figure 65. Coin for scale 2.5 cm. GSC 1994-150

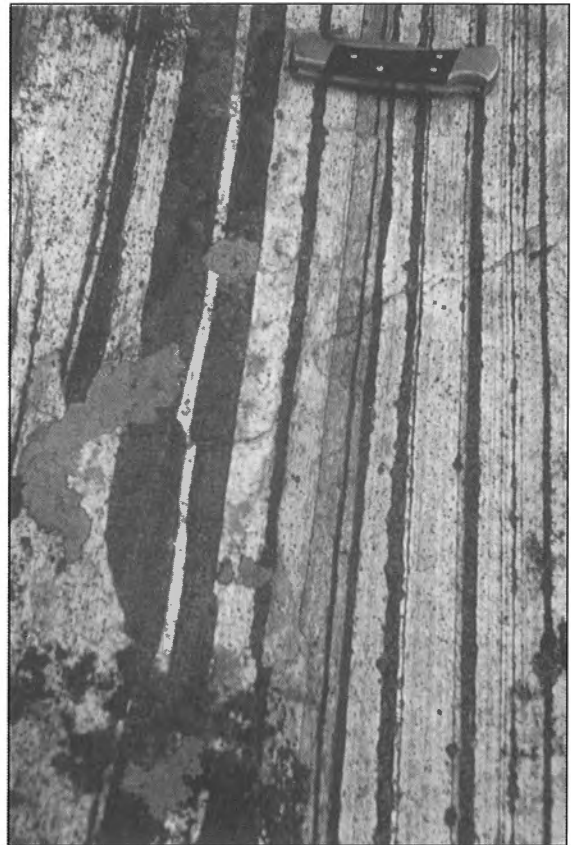


Figure 67. Attenuated and transposed Chipman dykes in garnet-clinopyroxene tonalite ribbon mylonite, Chipman tonalite batholith, Cora Lake. Knife for scale. GSC 1994-118

Steinhauer Lake (Fig. 3), has yielded a magmatic crystallization age of 3126 \pm 6/-5 Ma (Table 1). Because the granite sheets are contemporaneous with the syntectonic Chipman dykes, this date indicates the approximate time of granulite facies metamorphism and mylonitization represented by the annealed straight gneiss of the eastern part of the Chipman batholith. It also confirms the older vintage of the straight gneiss, compared to the ribbon mylonite in the western part of the Chipman batholith, deduced from field observations of the Chipman dykes (see "Chipman dykes"). Lastly, it indicates the approximate time of emplacement of the Chipman dykes.

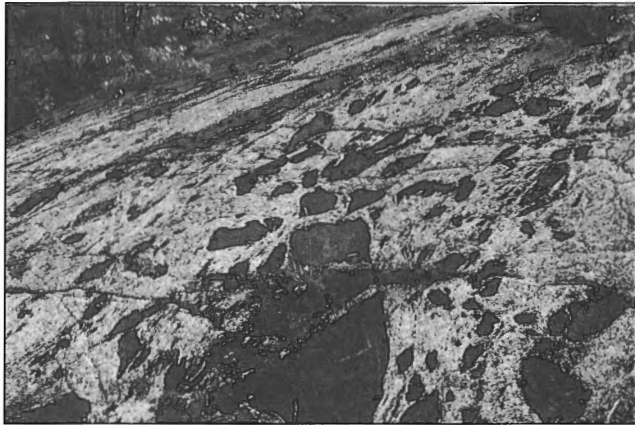


Figure 68. A dense swarm of angular blocks of amphibolite and hornblende floating in a weakly foliated Chipman granite vein (foreground) which was emplaced subconcordantly into annealed tonalite straight gneiss (background), Chipman tonalite batholith, Steinhauer Lake. In this photograph the tonalite/granite contact can only be perceived from the distribution of the mafic inclusions. Hammer for scale (centre). GSC 1994-116

Bohica mafic complex

The Bohica mafic complex (Fig. 69) is an association of orthopyroxene-plagioclase and clinopyroxene-garnet-plagioclase metanorite, metagabbro, metadiorite, and meta-anorthosite, with metric-scale, garnet pyroxenite bands. Two large bodies, up to 2 km thick, of clinopyroxene-garnet anorthosite, gabbroic anorthosite, and garnet pyroxenite ultramylonite (*Aba, Abam*), locally with splendid ribbon fabrics (Fig. 70, 71, 72), locally strongly annealed, outcrop at Cora Lake and west of Bompas Lake (Fig. 3) along the southeast side of the principal Bohica mafic complex outcrop, separated from it by a strip of diatexite. Similar anorthosite mylonites can be traced along strike to the southwest, almost to Fond du Lac (Fig. 3). They are spatially associated with, and were mapped as part of, the Bohica complex. However, further petrological study may show that they are related to



Figure 70. Garnet-clinopyroxene anorthosite ribbon mylonite with concordant bands of garnet-clinopyroxenite, Bohica mafic complex, Cora Lake. Note the absence of feldspar porphyroclasts. Coin for scale 2 cm. GSC 1991-577C

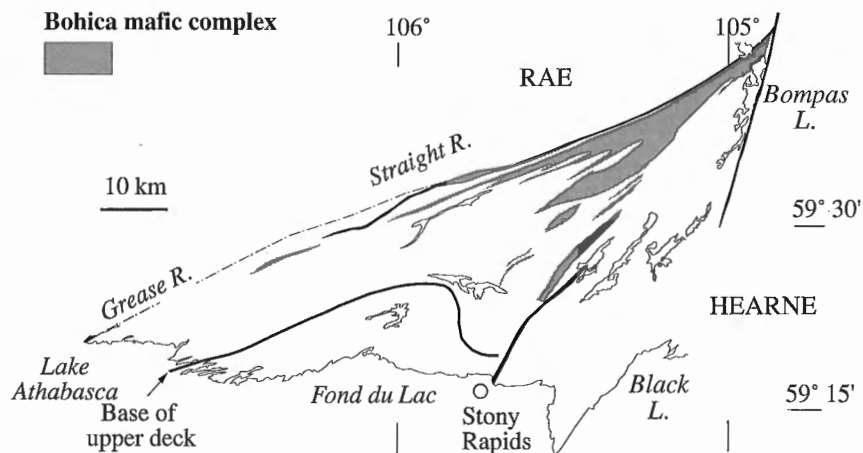


Figure 69. Distribution of Bohica mafic complex (cf. Fig. 9 and 10).

the anorthosite inclusions scattered throughout the Chipman tonalite batholith (see “Chipman batholith”). The main body of the Bohica complex is divided into well foliated garnet-pyroxene metanorite, metagabbro, and metadiorite, with relict igneous textures (*Ab*; Fig. 73, 74, 75, 76), flanked to the northwest by garnet-clinopyroxene mafic mylonite (*Abm*; Fig. 77, 78, 79, 80). Coarse ophitic textures to strongly flattened flaser fabrics are locally preserved, especially in the central septum from southwest of East Hawkes Lake to northeast of Kaskawan Lake (Fig. 3). Large garnet-rich pyroxene-feldspar xenoliths that are locally preserved in poorly foliated norite, northeast of Tantato Lake (Fig. 3), suggest that the Bohica complex may have intruded the diatexite (Fig. 81). An isotropic, ophitic sample from Kaskawan Lake (Fig. 3) has yielded an age of 2596 ± 12 Ma (Table 1), interpreted as the approximate time of emplacement of the Bohica mafic complex.



Figure 71. Naturally etched garnet-clinopyroxene anorthosite ribbon mylonite, Bohica mafic complex, Cora Lake. Note the absence of feldspar porphyroclasts. Coin for scale 2 cm. GSC 1994-121

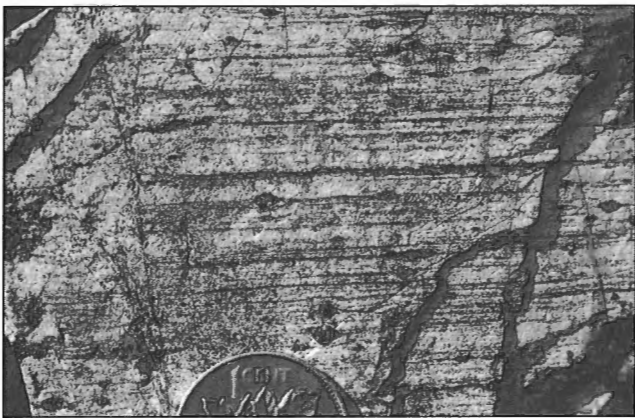


Figure 72. Clinopyroxene anorthosite ribbon mylonite, Bohica mafic complex, Cora Lake. Note the absence of feldspar porphyroclasts. Coin for scale 2 cm. GSC 1994-148

The coarse igneous textures within the Bohica mafic complex can be followed progressively into mylonite (Fig. 73-80). Although much of the mylonite is principally composed of hornblende-plagioclase, anhydrous garnet-clinopyroxene and ortho/clinopyroxene-bearing assemblages are well preserved. Small 1 mm garnet and clinopyroxene often form long monomineralic necklaces along the boundaries of polycrystalline plagioclase streaks and ribbons. There is a spatial relationship between the intensity of the mylonitization and the proportion of free quartz, up to ca. 20% (volume). This may either reflect selective deformation of the more quartz-rich parts of a lithologically variable mafic complex, or the introduction of silica during deformation as in the Axis mafic granulite (see “Axis mafic granulite”).

Garnet-pyroxene Mary granite

In the western and central parts of the lower deck (Fig. 10), the Reeve diatexite and the Bohica mafic complex are intruded by a contiguous suite of metamorphosed hornblende-garnet-biotite,

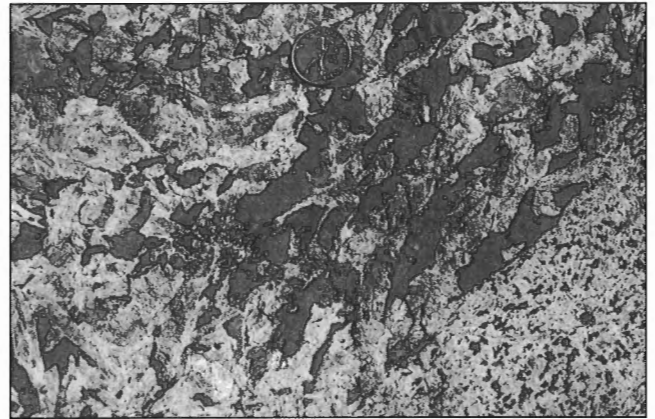


Figure 73. Igneous textural variety in isotropic garnet-bearing metanorite, Bohica mafic complex, Tantato Lake. Coin for scale 2.5 cm. GSC 1991-577A



Figure 74. Flattened relict igneous texture in metagabbro, Bohica mafic complex, Kaskawan Lake. Coin for scale 2.5 cm. GSC 1994-122

hornblende-garnet-clinopyroxene-orthopyroxene, and garnet-clinopyroxene granite, granodiorite, tonalite, and monzonite, and their mylonitized equivalents (Fig. 9). A number of discrete map units have been distinguished, apparently corresponding to deformed plutons (see below). Much of this granitic material shows variations on a rather distinctive textural and compositional theme, although it is as yet unclear to what extent these reflect primary or metamorphic features of the rocks. Some of these plutons were previously grouped together as the *Mary batholith* (Hanmer et al., 1991, 1992b). On-going petrological studies may eventually lead to the inclusion of most of these garnet-bearing metamorphosed plutons within such a batholith. However, the geological value of the term “batholith” in this context remains to be demonstrated.

The Mary granite (*sensu lato*; Fig. 82), the largest compositionally coherent granitic body (*Amg*), occupies much of the western lower deck from Mary Lake to Lake Athabasca (Fig. 3). Outcrop-scale observations in windows of relatively low strain, show that more strongly mylonitized parts of the Mary granite are crosscut by less strongly mylonitized components. From this, one may deduce that the Mary granite is syntectonic with respect to the granulite facies mylonitization which affects it.

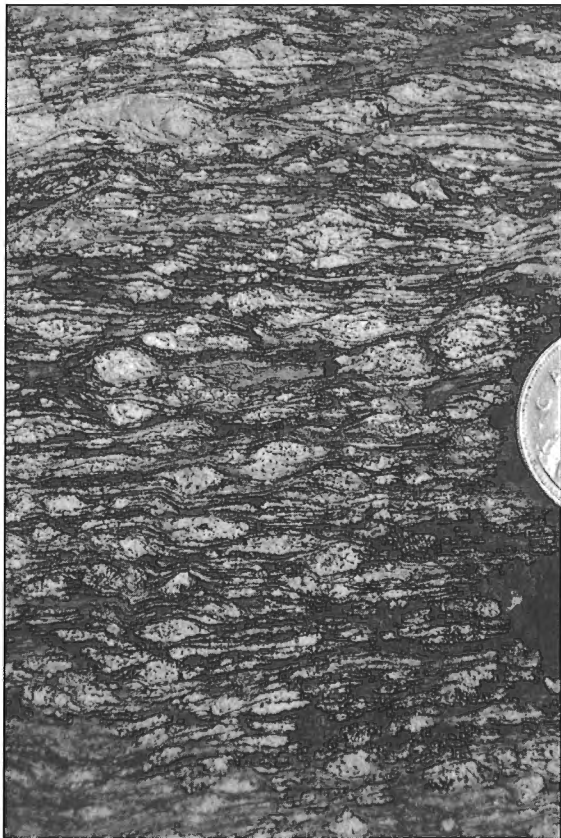


Figure 75. Strongly foliated gabbro/diorite with relict plagioclase crystals, Bohica mafic complex, Kaskawan Lake. Looking down on horizontal surface. The fabric could be termed protomylonitic. Note the sinistral shear bands. Coin for scale 2.5 cm in diameter. GSC 1994-170



Figure 76. Mafic dyke with apophyses emplaced subconcordantly into foliated leuconorite, Bohica mafic complex, Tantato Lake. Coin for scale 2.5 cm. GSC 1994-145



Figure 77. Leuconorite ribbon mylonite, Bohica mafic complex, Tantato Lake. The dark streaks are orthopyroxene ribbons. Note the absence of porphyroclasts. Compare with Figure 73. Coin for scale 2.5 cm. GSC 1991-577D

On fresh surfaces, the Mary granite is composed of white streaks and ribbons of polycrystalline feldspar, separated by a 'steel' grey, fine matrix of macroscopically indistinguishable feldspar-quartz-hornblende-garnet-clinopyroxene-orthopyroxene, studded with 2 to 5 mm hornblende, blood-red garnet and occasionally clinopyroxene porphyroclasts (Fig. 83). The granite is rich in mafic minerals; garnet alone may volumetrically account for 5 to 20% (Fig. 84), whereas amphibole and pyroxene commonly represent more than 20%, often forming polycrystalline rims on garnet cores. Some of the garnet is present as either dispersed or clustered aggregates within the polycrystalline mantles of dynamically recrystallized plagioclase surrounding monocrystalline plagioclase garnet-free cores. Such garnets may be interpreted as reaction products derived at the expense of the actively recrystallizing plagioclase (Spear and Florence, 1992), and therefore indicative of mylonitization under conditions of increasing pressure.

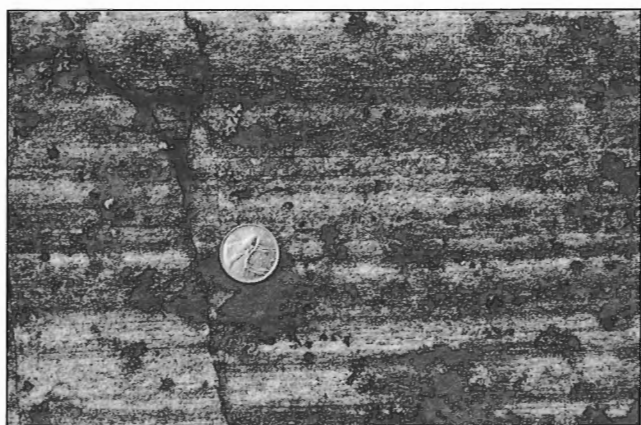


Figure 78. Annealed variety of leuconorite mylonite, Bohica mafic complex, Kaskawan Lake. Note the absence of porphyroclasts. Coin for scale 2.5 cm. GSC 1994-119



Figure 79. Streaky aspect to plagioclase-hornblende-garnet±clinopyroxene mylonite most frequently encountered in the field, Bohica mafic complex, Kaskawan Lake. Note the absence of porphyroclasts. It can be seen as a hybrid of the fabrics illustrated in Figures 77 and 80. Coin for scale 2.5 cm. GSC 1994-144

Throughout the granite, the pyroxenes, especially orthopyroxene, are extensively replaced by hornblende, giving the rock such a dark colour that parts of it was originally mapped as a mafic gneiss (see "Previous and recent work" for references). Elsewhere, the granite is leucocratic. Clearly the Mary granite is highly variable with respect to the proportion

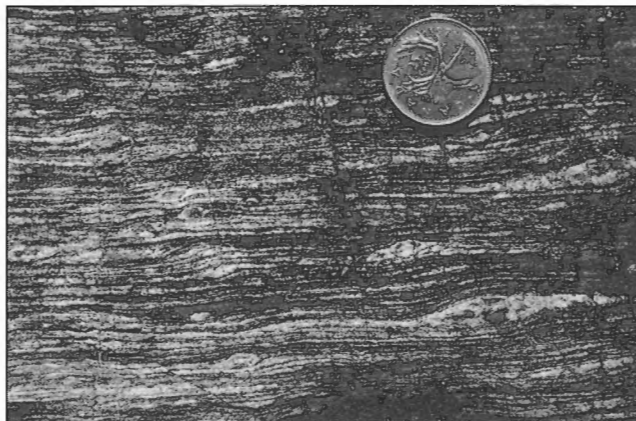


Figure 80. Well developed ribbons and relict plagioclase porphyroclasts in plagioclase-hornblende-garnet±clinopyroxene mylonite, Bohica mafic complex, east of Tantato Lake. Coin for scale 2.5 cm. GSC 1994-120

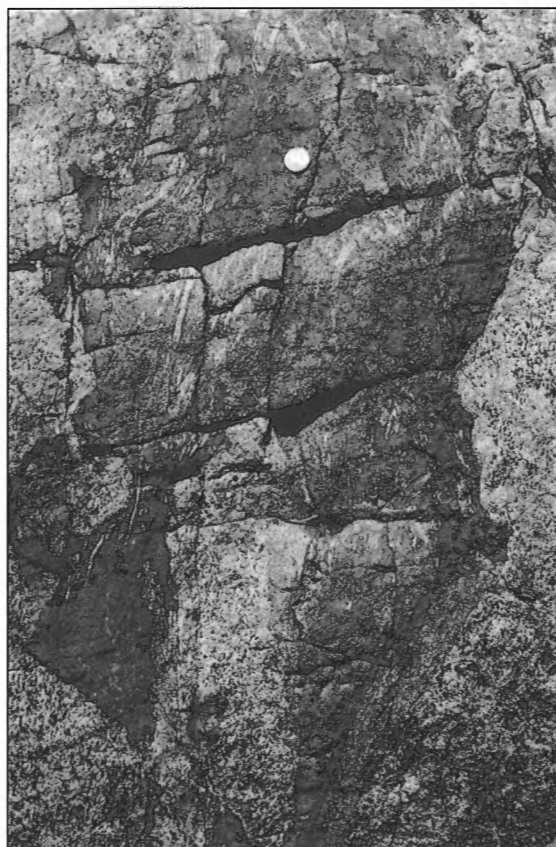


Figure 81. Garnet-rich foliated xenoliths in weakly foliated leuconorite, Bohica mafic complex, Tantato Lake. Coin for scale 2.5 cm. GSC 1994-143

of coloured minerals. Outcrop is not continuous enough to follow the variation progressively, but its heterogeneity and changes in colour index (ca. 30+ to <5) from outcrop to outcrop suggest either that the granite is made of multiple injections, or that the magma was poorly mixed. This latter suggestion stems from the local preservation, in rare windows of relatively low strain, of clusters of garnet pyroxenite fragments included and dismembered within a leucocratic granitic matrix (cf. Fig. 99). Similar clustered rock fragments are also observed in thin section. It would appear that the granite carries

a significant charge of mafic xenolithic to xenocrystic material, possibly derived from its source region. A second, common variant is similar to the first, except that the garnet is present as chains of 1 to 2 mm cherry-red crystals, adjacent to either hornblende or clinopyroxene (cf. Fig. 97). In a common subvariety, chains of very fine pinhead-sized garnets outline polycrystalline ribbons of feldspar, themselves indicative of a very coarse megacrystic protolith (Fig. 85, 86). One such sample from Turnbull Lake (Fig. 3) has yielded an age of 2618 ± 4 Ma (Table 1), interpreted as the time of magmatic emplacement.

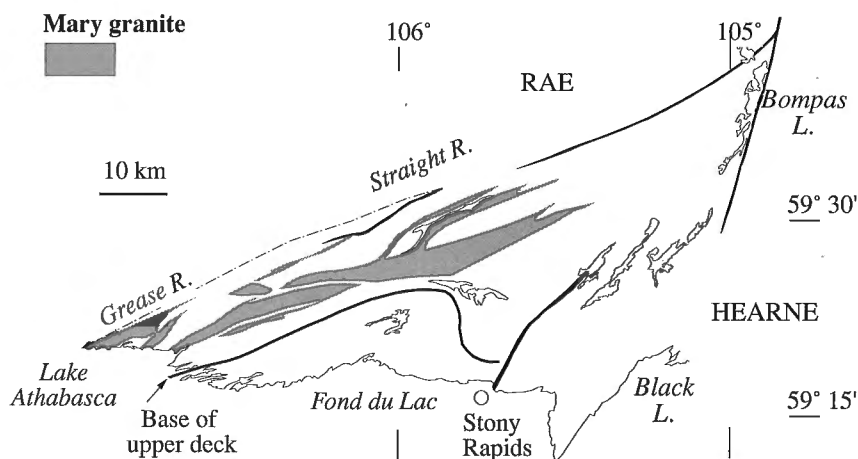


Figure 82. Distribution of Mary granite (cf. Fig. 9 and 10).

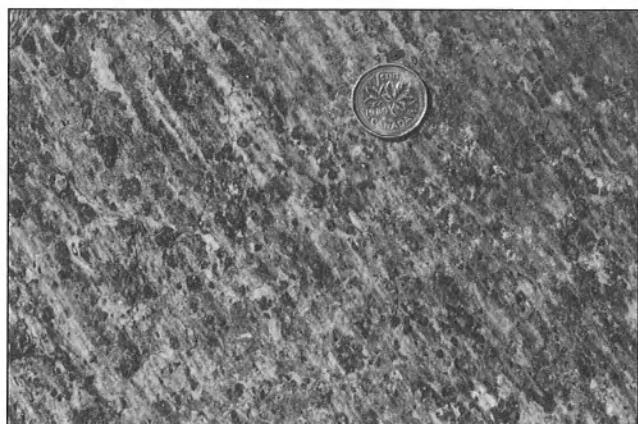


Figure 83. Granulite facies streaky Mary granite mylonite, MacLachlan Lake. The dark 'studs' are garnet, clinopyroxene, and orthopyroxene porphyroclasts. Note the absence of feldspar porphyroclasts. Coin for scale 2 cm. GSC 1993-065C



Figure 84. Detail of streaky Mary granite mylonite, Turnbull Lake. The cores of the dark 'studs' are garnets with hornblende rims and tails pulled out along the mylonitic foliation. The winged inclusions formed by the cores and tails indicate sinistral shear in the photograph (upper centre), but this loose block is probably inverted. Note the absence of feldspar porphyroclasts. In thin section, the assemblages are more complex: the cores of garnet are in textural equilibrium with spatially associated orthopyroxene-clinopyroxene and hornblende. The orthopyroxene is more readily replaced by amphibole than is the clinopyroxene. Coin for scale 2.5 cm. GSC 1994-214

In the west, particularly between Wiley and Harper lakes and at Turnbull Lake (Fig. 3), the Mary granite is locally preserved as a very coarse grained (>5 cm) hornblende±clinopyroxene±garnet granitoid (Fig. 87), the protolith to two distinctive types of tectonite. One is a coarse ribbon gneiss (*Arm*), whose igneous feldspars have been deformed into thick polycrystalline ribbons, 100 by 5 mm, and which contains very few feldspar porphyroclasts (Fig. 88, 89). The thickness of the ribbons and the uniform nature of the fabric engendered the informal, but evocative field term “pin-stripe gneiss”. The ribbon gneiss forms large map-scale lenses, ranging in size from 25 km by 3 km to 4 km by 1 km. A sample from Robillard Bay, Lake Athabasca (Fig. 3), has yielded a magmatic crystallization age of 2606 ±13/-11 Ma (Table 1). The other tectonite is a very fine grained, thoroughly annealed porphyroclastic

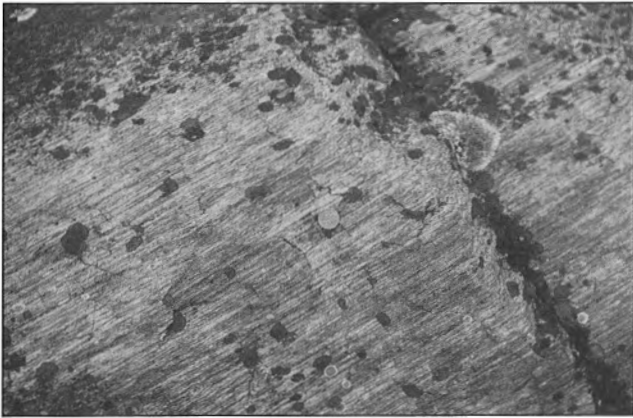


Figure 85. Ribbon mylonite derived from an extremely coarse grained leucocratic variant of the Mary granite, Turnbull Lake. Note the absence of feldspar porphyroclasts. Coin for scale 2 cm. GSC 1993-221J



Figure 86. Detail of ribbon mylonite illustrated in Figure 85. Thick polycrystalline ribbons of alkali and plagioclase feldspar are separated by very thin quartz ribbons (medium grey) and dark lines. The dark lines are chains of tiny garnet crystals interspersed with clinopyroxene readily identifiable in the field. Note the absence of feldspar porphyroclasts. Coin for scale 2 cm. GSC 1994-215



Figure 87. Well foliated, initially very coarse grained hornblende±clinopyroxene±garnet Mary granite, north of Wiley Lake. Note the large feldspar porphyroclast. Coin for scale 2.5 cm. GSC 1991-577L



Figure 88. Hornblende±garnet±clinopyroxene ribbon gneiss, north of Wiley Lake, derived from Mary granite of the type illustrated in Figure 87. Note the very thick polycrystalline feldspar ribbons and the absence of porphyroclasts which together lend a “pin-stripe” aspect to the fabric. Coin for scale 2.5 cm. GSC 1991-577I

mylonite (Fig. 90, 91, 92), with 5 to 50 mm feldspar porphyroclasts, and smaller porphyroclasts of hornblende and garnet (*Ampg*). The mylonitic matrix does not preserve a strong shape fabric. The porphyroclastic mylonite constitutes a network of 0.5 to 1.5 km wide vertical anastomosing belts which bound the lenses of ribbon gneiss, along the Robillard River, Wiley and Harper lakes, and parts of Turnbull and Reeve lakes (Fig. 3). A wide triangular area of the porphyroclastic mylonite in the southwestern corner of the map area is superbly exposed along the shore of Lake Athabasca, east of Grease Bay (Fig. 3; Fig. 93, 94). There, the geometry

of the mylonitic foliation is complex. Locally the dip of the foliation ranges from steep to very shallow and the strike may vary irregularly. However, passing eastward from Grease Bay (Fig. 3), the regional strike of the foliation swings progressively to a southeasterly direction, describing an open, shallowly southwest-plunging synform. By analogy with the vertical belts to the east-northeast, the foliation of the porphyroclastic mylonite appears to have wrapped around the base of a structurally higher, now eroded, lens-like body, perhaps composed of ribbon gneiss.

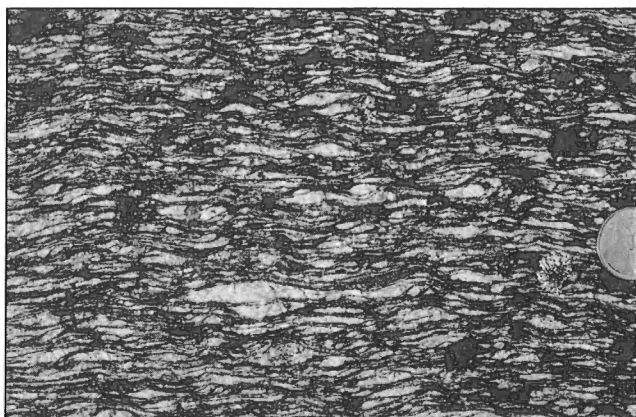


Figure 89. Hornblende ± garnet ± clinopyroxene ribbon gneiss, north of Wiley Lake, derived from Mary granite of the type illustrated in Figure 87 and similar to the example in Figure 88. In this example, the thick polycrystalline ribbon feldspars are clearly derived by the deformation and recrystallization of single feldspar grains from the protolith. One can describe this fabric in terms of a low strain rate/recrystallization rate ratio. Coin for scale 2.5 cm. GSC 1993-065B

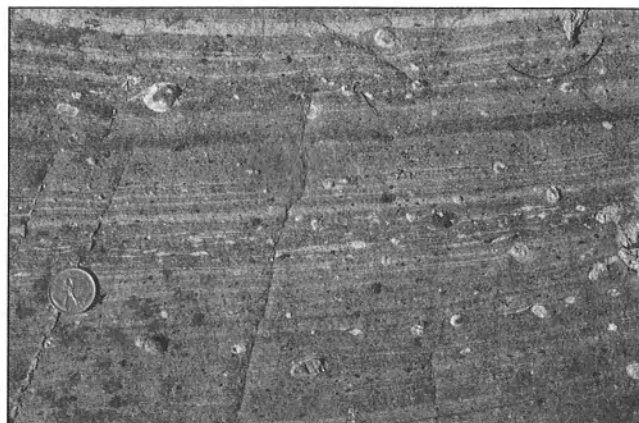


Figure 91. Annealed porphyroclastic mylonite, west of Robillard Bay, derived from Mary granite of the type illustrated in Figure 87. The light grey porphyroclasts are feldspar, the small dark ones are hornblende and garnet. Looking down onto a horizontal surface. Note the numerous dextral winged inclusions and the well preserved, very thin and continuous laminations. Coin for scale 2.5 cm. GSC 1994-213

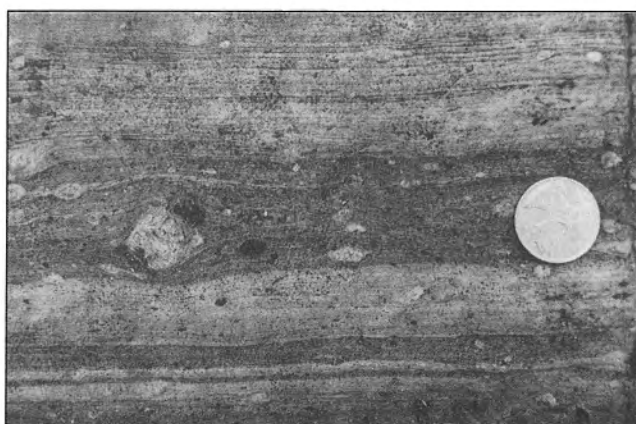


Figure 90. Annealed porphyroclastic mylonite, Wiley Lake, derived from Mary granite of the type illustrated in Figure 87. The light grey porphyroclasts are feldspar, the small dark ones are hornblende and garnet. Note the well preserved, very thin and continuous laminations in the lighter coloured layers. Coin for scale 2.5 cm. GSC 1991-577F



Figure 92. Detail of annealed porphyroclastic mylonite, Robillard Bay, derived from Mary granite of the type illustrated in Figure 87. The light grey porphyroclasts are feldspar, the small dark ones are hornblende and garnet. Looking down onto a horizontal surface. Note the stair-step geometry of the dextral winged inclusion (see Hanmer and Passchier, 1991). Coin for scale 2.5 cm. GSC 1991-577K

According to locally preserved low strain inclusions, both the ribbon gneiss and the porphyroclastic mylonite are derived from the same coarse grained Mary granite protolith. However, the absence of preserved feldspar megacrysts in the ribbon gneiss means that it does not represent an intermediate stage in the development of the porphyroclastic mylonite. The inference is that the two tectonite fabrics represent the products of two different fabric paths. Moreover, the metamorphic assemblages of the ribbon gneiss and the porphyroclastic mylonite reflect different reaction paths. Although both carry the assemblage hornblende-garnet-biotite-plagioclase, the garnet is only locally present as very small crystals in the ribbon gneiss, whereas it forms abundant 2 to 10 mm grains in the porphyroclastic mylonite. Indeed, the presence of blood-red garnet and black hornblende porphyroclasts is a diagnostic feature of the porphyroclastic mylonite (Fig. 95). These observations suggest either that the porphyroclastic mylonite developed in those parts of the protolith which were compositionally more susceptible to the formation of garnet, or that the garnet-forming reactions were enhanced by the deformation. Having specifically searched the superb, extensive outcrops along the shore of Lake Athabasca for an example of garnet-rich ribbon gneiss, without success, it is suggested that the different reaction paths were deformation controlled (see "Synkinematic magmatism"). It is also noteworthy that clinopyroxene is locally present in the ribbon gneiss, but absent in the porphyroclastic mylonite. This observation will be discussed below (see "Medium temperature flow").

Other garnet-pyroxene granitoid bodies

The Mary granite apparently grades into the Hawkes leucogranite (Ahl; H in Fig. 96) to the east. The relationship between the two remains uncertain because of the compositional variability of the Mary granite itself. Indeed, Hanmer et al. (1992b) included the Hawkes granite with the Mary granite in their original definition of *Mary batholith*. The Hawkes granite varies structurally from an isotropic,

equigranular, medium grained (1-2 cm) plutonic rock, to a ribbon ultramylonite (Ahg). However, all the structural variants carry the same metamorphic mineral assemblages and metamorphic textures (e.g. Fig. 97) as those described for the Mary granite. Because of the leucocratic nature of the Hawkes granite, it is easy to observe that the spatial distribution of the mafic minerals is very patchy. Spatial variation of mineral proportions, degree of hydration and of texture occur rapidly both within and between outcrops and is well exemplified by the shoreline at East Hawkes Lake (Fig. 3). There, the granite colour index varies over the range 0 to 30 from outcrop to outcrop. Where such variations occur within a given outcrop, they appear to be gradational. This suggests that the granite melt was compositionally heterogeneous, i.e., poorly mixed, in the sense implied for the Mary granite



Figure 94. Porphyroclastic ribbon mylonite, Lake Athabasca west of Robillard Bay, derived from Mary granite of the type illustrated in Figure 87 (dark grey), associated with less porphyroclastic leucogranite sheets (light grey). The light grey porphyroclasts are feldspar. Coin for scale 2.5 cm. GSC 1994-220



Figure 93. Porphyroclastic ribbon mylonite, Lake Athabasca west of Robillard Bay, derived from Mary granite of the type illustrated in Figure 87. The light grey porphyroclasts are feldspar, the small dark ones are hornblende and garnet. Coin for scale 2.5 cm. GSC 1994-217



Figure 95. Sreaky annealed mylonite, Lake Athabasca west of Robillard Bay, derived from Mary granite of the type illustrated in Figure 87. The abundant small dark spots are hornblende and garnet. Coin for scale 2.5 cm. GSC 1994-218

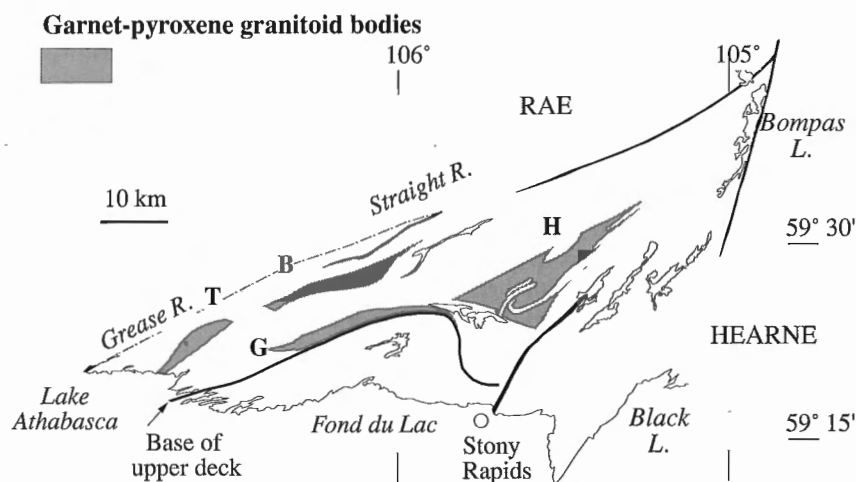


Figure 96. Distribution of garnet-pyroxene granitoid bodies, excluding the Mary granite (cf. Fig. 9 and 10). Bradley and Brykea granites (B), Godfrey granite (G), Hawkes leucogranite (H) and Turcotte granite (T) are discussed in the text.

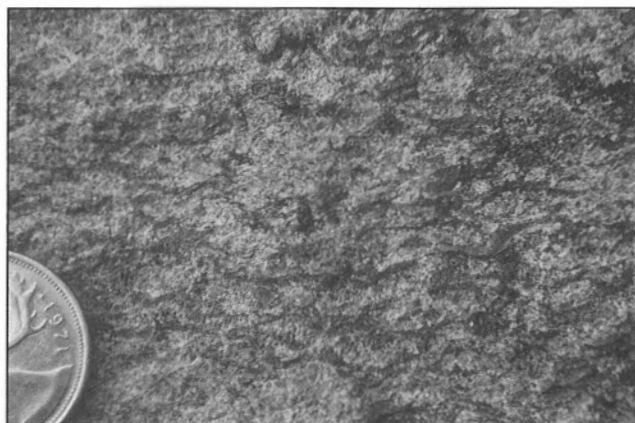


Figure 97. The thin grey laminae in this photograph are chains of pinhead garnet crystals associated with clinopyroxene in foliated Hawkes granite, East Hawkes Lake. Coin for scale 2.5 cm. GSC 1994-216

(see "Garnet-pyroxene Mary granite"). A sample of the Hawkes leucogranite from West Hawkes Lake (Fig. 3) yielded an approximate magmatic crystallization age of ca. 2610 Ma (Table 1). A thick sheet of leucogranite from Kaskawan Lake (Fig. 3), mapped as part of the mixed Bohica mafic complex/Hawkes granite map unit (Abg), gave a magmatic crystallization age of 2604 ± 1 Ma (Table 1).

A thin, kilometre-scale panel of Reeve diatexite with internally concordant gneissic banding occurs within a very poorly foliated to isotropic, garnet-pyroxene-bearing facies of the Hawkes leucogranite southeast of East Hawkes Lake (Fig. 3). The diatexite panel describes a shallowly southwest-plunging upright antiform to which the leucogranite foliation is axial planar (Fig. 98). Therefore, the Late Archean

leucogranite was intruded into already gneissic Late Archean diatexite. Accordingly, whether the Hawkes granite is part of the Mary granite, or an independent pluton of similar age, it is syntectonic with respect to the ca. 2600 Ma granulite facies deformation.

To the south, the Mary granite is partly flanked by the garnet-hornblende±clinopyroxene Godfrey granite (Agg; G in Fig. 96). The latter is structurally variable, grading progressively from well foliated coarse granite in the west to ribbon ultramylonite in the east. It strongly resembles the garnet and hornblende studded variant of the Mary granite, with local development of garnet rims on coarse (1 cm) clinopyroxene. It even contains similar disaggregated xenoliths of garnet pyroxenite (Fig. 99). The principal difference between the two granites is the uniformly larger size of the individual polycrystalline streaks and ribbons of feldspar, which appears to be a reflection of the coarse grain size of the protolith in the Godfrey granite. One cannot exclude the possibility that while this granite is a separate pluton, it may be closely linked to the Mary granite. This suggestion is reinforced by the 2601 ± 4 Ma magmatic crystallization age (Table 1) obtained from a sample at the entrance to Godfrey Bay, Clut Lakes.

Three distinctive granite plutons occur on the west side of the Mary granite. The Bradley (Abdg) and Brykea (Abkg) leucogranite bodies (B in Fig. 96) are both garnet-clinopyroxene-bearing, and penetratively mylonitized. They are both compositionally and texturally variable, and it is possible that their separation as distinct map units is more a reflection of the spatial distribution of the dominant metamorphic and structural fabrics than the existence of two distinct plutons. The Brykea granite is everywhere an L/S mylonite, locally with 100 mm by 2 mm feldspar ribbons, often with 1 to 2 cm stubby feldspar porphyroclasts. It contains

abundant chains of 1 mm garnets arranged along the feldspar ribbons, or rimming attenuated clinopyroxene aggregates. In places it is a striking salmon pink granite ultramylonite with abundant, 1 mm cherry-red garnets set in a fine grained, sugary annealed matrix with variable proportions of small feldspar porphyroclasts. The Bradley granite is predominantly an L>>S pencil mylonite, with only local preservation of feldspar porphyroclasts. The long (5-10 cm) quartz and feldspar 'pencils' suggest a coarse grained protolith. Although it locally contains fine garnet chains, the garnets occur more commonly as 2 mm cherry-red crystals scattered throughout the mylonite. The contact between the two granite bodies is progressive and thoroughly mylonitized. To the southwest, the Turcotte granite (*Atg*; T in Fig. 96) shares many of the characteristics of both the Bradley and Brykea granite units, but it is predominantly biotite-garnet-hornblende-bearing, and the intensity of the mylonite fabric is more variable. Locally the rock is simply a well foliated equigranular granite.

Hornblende-biotite granitoid bodies

A linked network of hornblende-biotite granite bodies, and their mylonitic equivalents (Fig. 100), cuts the garnet-pyroxene granite units (Fig. 96). They contain no trace of relict pyroxene. The most voluminous is the Clut granite (*Acgm*; C in Fig. 100), which forms a shallowly south- and west-dipping sheet under the Godfrey granite, immediately

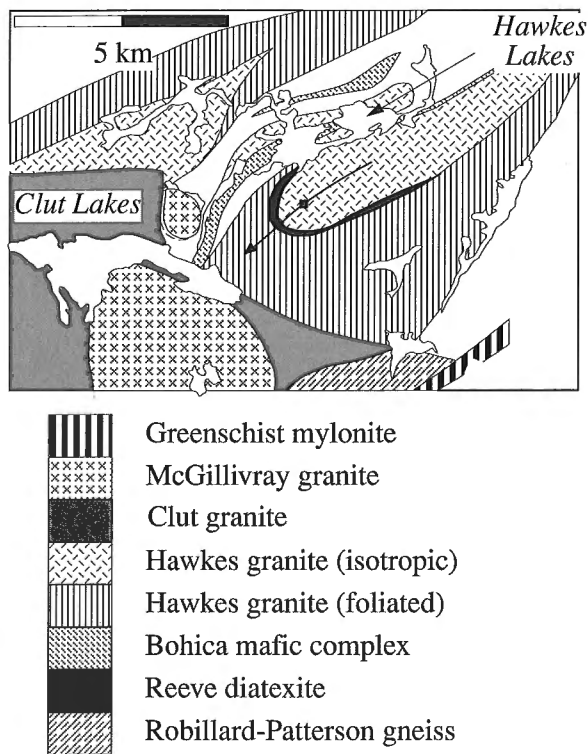


Figure 98. Detailed sketch of the geology of the area between Clut and East Hawkes lakes to illustrate the relationship between the folded panel of Reeve diatexite and the isotropic and foliated variants of Hawkes granite. See Figure 9 for location. Discussed in text.



Figure 99. Xenolithic inclusions of garnet-clinopyroxenite caught in the process of mechanical disaggregation in weakly foliated low strain window in the Godfrey granite, south of Wiley Lake. Coin for scale 2.5 cm. GSC 1994-212

beneath the eastern part of the upper deck. It is in general a mylonite to protomylonite, derived from a medium grained equigranular granite (Fig. 101), with local megacrystic phases developed in the centre of the sheet. Very locally, it contains xenolithic rafts of banded amphibolitic gneiss. It carries a concordant mylonitic foliation and a dip-parallel extension lineation. Abundant asymmetrical extensional shear bands indicate that mylonitization was associated with top-down to the south and west displacements (Fig. 101). A sample from Clut Lakes (Fig. 3) has yielded a magmatic crystallization age of 2614 +9/-7 Ma (Table 1).

The Clut granite extends into the western part of the lower deck as an anastomosing vertical array of sheets of hornblende-biotite Melby-Turnbull granite (*Amtg*; MT in Fig. 100). The latter comprise two principal branches. The more northerly branch extends due west from the Clut granite. The more southerly one lies subparallel to the lateral ramp of the upper deck, but within the lower deck. They were exclusively emplaced into the network of annealed porphyroclastic mylonite belts in the Mary granite (see "Garnet-pyroxene Mary granite"). The isotropic to poorly foliated parts of the granite sheets have abrupt intrusive contacts, locally preserve coarse plutonic textures (Fig. 102), and contain misoriented xenoliths of the adjacent porphyroclastic

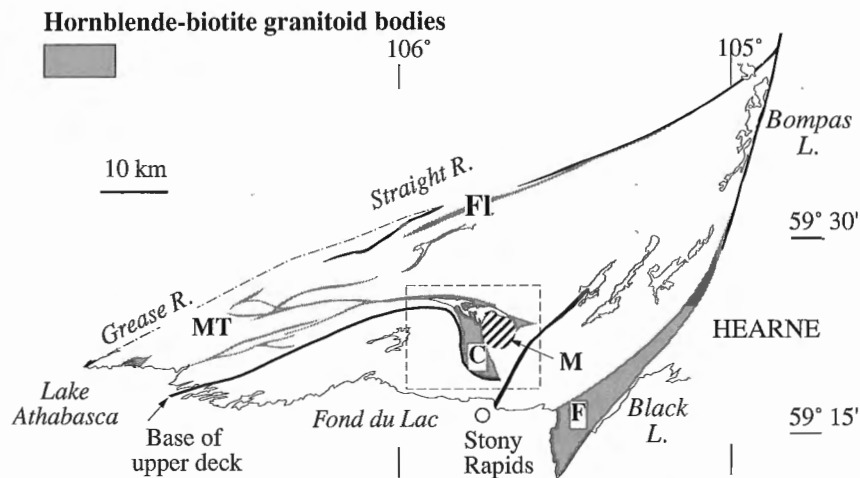


Figure 100. Distribution of hornblende-biotite granitoid bodies, excluding the Mary granite (cf. Fig. 9 and 10). Clut granite (C), Fehr granite (F), Felsic Lake granite (Fl), McGillivray granite (M), and Melby-Turnbull granite (MT) are discussed in the text. Box is location of Figures 110 and 132.



Figure 101. Well foliated to protomylonitic hornblende-biotite Clut granite, Clut Lakes. Looking to the northwest at a subvertical surface. Note the well developed asymmetrical extensional shear bands indicating top-down to the southwest displacement. Coin for scale 2.5 cm. GSC 1994-222

mylonites. Nevertheless, they are themselves locally to extensively mylonitized. They are concordantly foliated and strike-lined. From the structural control of their emplacement, and their internal strain state, the Melby-Turnbull granite sheets were syntectonically emplaced within an array of still-active shear zones. A poorly foliated, coarse grained sample from Wiley Lake (Fig. 3) yielded a magmatic crystallization age of 2610 ± 2 Ma (Table 1).

Along the southeast margin of the lower deck, the hornblende-biotite±garnet Fehr granite (F in Fig. 100) cuts the Chipman batholith and its associated mafic dykes, but is itself cut by a later set of subconcordant hornblende-plagioclase-garnet mafic metadykes (Fehr dykes). To the southwest, the granite is isotropic and coarse grained, with



Figure 102. Very coarse grained, weakly foliated hornblende-biotite Melby-Turnbull granite, Wiley Lake. Coin for scale 2.5 cm. GSC 1994-221

feldspars typically >5 cm in size (*Afg*). Locally it is cut by narrow, discrete shear zones with upright fabrics, which trend subparallel to the regional strike. In places, the granite contains abundant coarse grained, metre-scale, amoeboid inclusions, essentially composed of hornblende, rare relict orthopyroxene, and garnet (Fig. 103). It also contains smaller (5-10 cm), equant microgranular inclusions of quartz-biotite or hornblende-plagioclase (Fig. 103, 104). The inclusions appear to represent restitic material (*sensu lato*). The amoeboid xenoliths are mechanically broken up to yield abundant smaller clots of coarse, polycrystalline hornblende±orthopyroxene which become indistinguishable from the mafic mineral content of the granite. These observations clearly point to the poor mechanical mixing of the granitic melt and

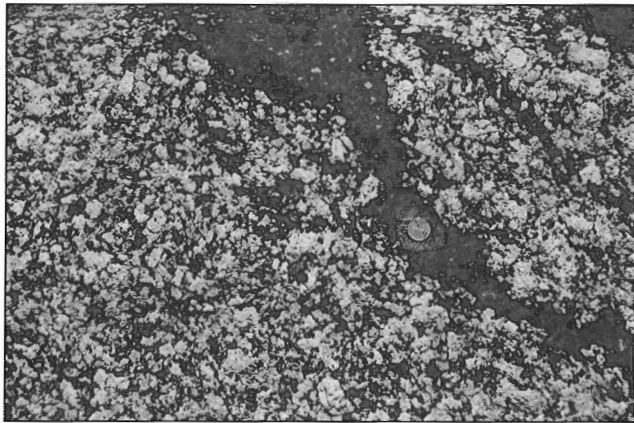


Figure 103. Isotropic hornblende-biotite Fehr granite, Stallard Lake. Note the abundant amoeboid inclusions of hornblende and biotite±garnet±orthopyroxene (small dark patches), identical to the larger xenolithic inclusion. The xenolith has ill-defined margins and itself contains an angular microgranular enclave beneath the coin. Coin for scale 2.5 cm. GSC 1994-223

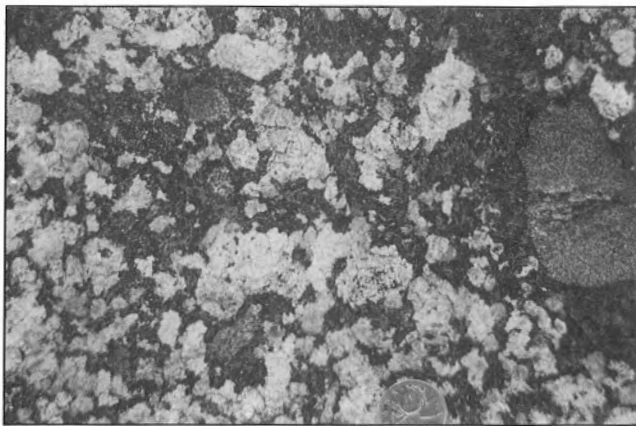


Figure 104. Detail of Figure 103 illustrating the abundant inclusions of hornblende and biotite±garnet±orthopyroxene. Note that microgranular enclaves occur throughout these inclusions. Coin for scale 2.5 cm. GSC 1994-224

its included mafic material, and are suggestive of the process already inferred to account for the compositional variation in the Mary, Godfrey, and Hawkes granites. To the north, the Fehr granite narrows in width and becomes a hornblende-garnet-bearing amphibolite facies ribbon ultramylonite (*Afgm*). A transitional protomylonitic sample has yielded an age of 2598 ± 3 Ma (Table 1), interpreted to indicate the time of magmatic crystallization. On the west side of the lower deck, north of Kaskawan Lake (Fig. 3), the variably foliated, coarse grained, biotite-hornblende Beed granite (*Abeg*; Fig. 105) closely resembles the poorly mixed, southern variant of the Fehr granite. It contains rare mafic mylonite xenoliths, presumably derived from the Bohica mafic complex.

The Fehr granite is cut by a swarm of strike-parallel mafic dykes, each 1 m to tens of metres thick, which may locally account for 20% (volume) of the outcrop (Fehr dykes). Some of the dykes carry abundant 2 to 4 mm garnets, often replaced by plagioclase. Although the contact of the granite with the Chipman batholith is abrupt, veins of Fehr granite cut across both the batholith structure and the Chipman dykes. Accordingly, there are at least two dyke swarms in the eastern part of the lower deck. The Fehr dykes clearly crosscut the foliation in the mildly deformed part of the Fehr granite (Fig. 106, 107), but are themselves transposed where the granite is transformed to mylonite. Furthermore, mildly foliated parts of the Fehr granite contain trains of large, irregular-shaped amphibolite inclusions which resemble disrupted mafic dykes (Fig. 108). If this is the case, the state of mechanical disaggregation of the mafic material is disproportionately high when compared to the state of strain reflected by the shape fabric in the granite host. Accordingly, it is possible that the inclusions represent mafic dykes emplaced into the subolidus Fehr granite while it was still capable of plastic flow, associated with its own magmatic emplacement. Such an interpretation has been proposed for dyke-granite relations elsewhere (e.g. Hanmer and Scott, 1990; Talbot and Sokoutis, 1992; McLelland et al., 1992). In the present case, it would

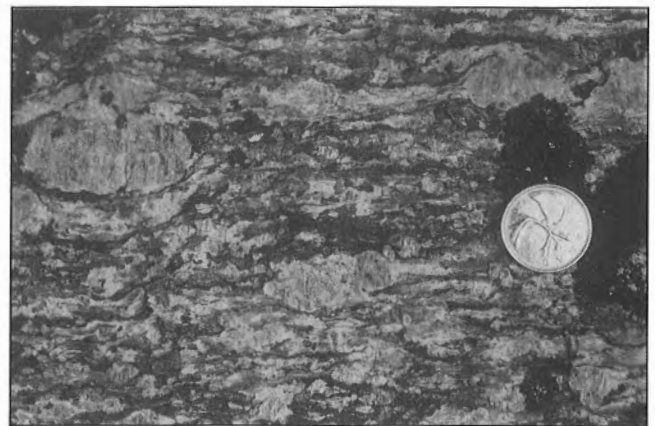


Figure 105. Well foliated, coarse grained hornblende-biotite Beed granite, Beed Lake. Coin for scale 2.5 cm. GSC 1994-142

imply that both the Fehr granite and the Fehr dykes are synkinematic with respect to shearing in the eastern part of the lower deck.

Intrusive sheets of equigranular, fine- to medium-grained, biotite leucogranite (*Alg*) form a concordant swarm throughout the western lower deck, particularly in the Clut-Reeve-Father-Kaskawan lakes area (Fig. 3). Individual sheets rarely exceed 10 m in thickness, and the density of the swarm varies greatly from outcrop to outcrop. The leucogranite is everywhere reduced to a quartz ribbon mylonite, remarkable for its very fine grained dark matrix and rarely preserved feldspar porphyroclasts. Locally, mylonitized later members of the leucogranite swarm crosscut earlier, concordant, mylonitized leucogranite sheets at a low angle. This indicates that the leucogranite was emplaced during mylonitization. One such sample from west of Lake Tantato (Fig. 3) has yielded an age of $2625 \pm 26/-20$ Ma (Table 1), indicative of the approximate

time of magmatic crystallization. The Felsic Lake leucogranite ultramylonite (*A/flg*, Fl in Fig. 100, located along the western boundary of the lower deck (Fig. 9), is identical to the granite sheets and probably represents a map-scale component of the swarm.

The biotite-hornblende megacrystic McGillivray granite (*Am*, M in Fig. 100) cuts the Clut granite. It is very coarse grained, with very little internal tectonic fabric development (Fig. 109) and a locally preserved magmatic alignment of euhedral feldspar megacrysts. Although its circular outcrop pattern and internal deformation state are suggestive of post-kinematic emplacement, the pluton is in fact syntectonic. It contains misoriented rafts of mylonitic Clut granite near its western margin, yet is itself cut by a narrow, less than 100 m thick, dip-lineated, west-side-down hornblende-bearing porphyroclastic ribbon mylonite zone (Taylor Bay fault; see Fig. 127), extending along the length of the western contact. Moreover, the mylonitic foliation within the Clut granite bifurcates around the McGillivray pluton (Fig. 110). This strongly suggests that the McGillivray granite exerted a mechanical influence on the pattern of tectonic flow within its wall rocks prior to its final emplacement, presumably during its ascent. A sample of the McGillivray granite from Clut

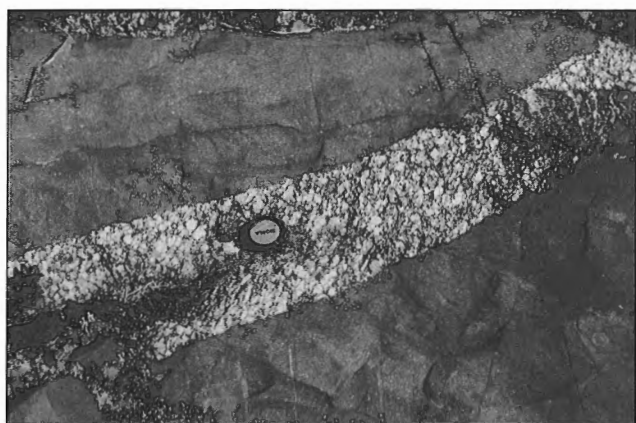


Figure 106. Fehr mafic dykes cutting across the foliation of the coarse grained hornblende-biotite Fehr granite, Stallard Lake. Lens cap for scale. GSC 1994-135

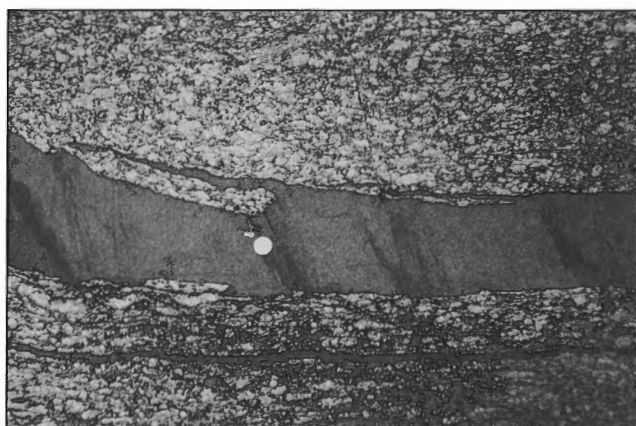


Figure 107. Branching Fehr mafic dykes, composed of left-stepping segments, emplaced subconcordantly along the foliation of the coarse grained hornblende-biotite Fehr granite, Stallard Lake. Coin for scale 2.5 cm. GSC 1994-137

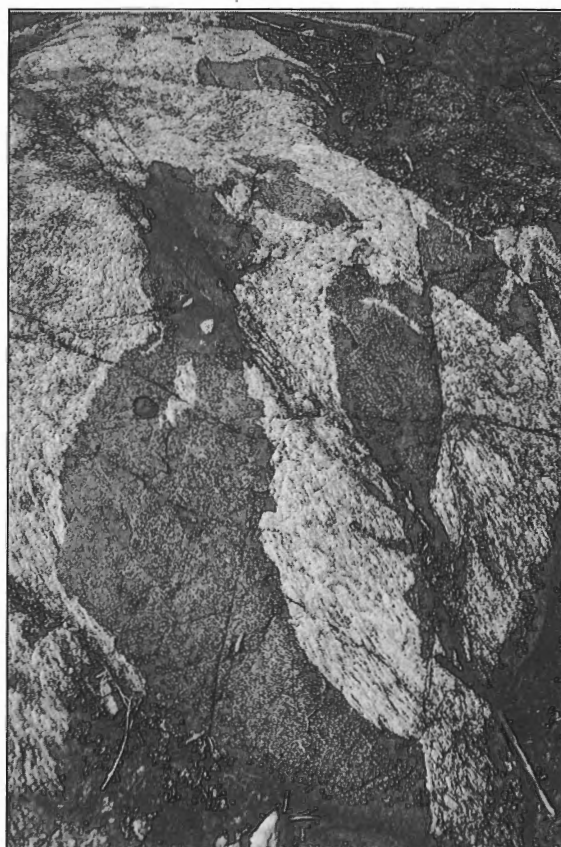


Figure 108. Large mafic inclusions in foliated coarse grained hornblende-biotite Fehr granite, Stallard Lake. From their aspect ratio and the presence of granite inclusions, they resemble dismembered mafic dykes emplaced into the granite. Lens cap for scale. GSC 1994-138

Lakes (Fig. 3) has yielded an apparent magmatic crystallization age of 2621 ± 3 Ma (Table 1). However, at face value, this determination would suggest that the McGillivray granite is older than the Clut granite and Melby-Turnbull granite which it clearly cuts. A smaller elliptical body of poorly foliated megacrystic hornblende-biotite granite, outcropping on the south side of MacLachlan Lake (Fig. 3), is flanked along its west margin by a 50 m thick, shallowly to moderately west-dipping, dip-lineated, coarsely porphyroclastic hornblende-bearing mylonite. The similarity to the situation of the McGillivray granite is obvious, and it would appear to be a stock of the same pluton.



Figure 109. Relatively fine grained variety of the normally much coarser megacrystic hornblende-biotite McGillivray granite, Clut Lakes. Note the well developed composite C/S fabric, indicating local development of dextral shear sense (see Hanmer and Passchier, 1991). Lens cap for scale. GSC 1994-136

Other biotite leucogranite units occur along the eastern margin of the lower deck. The Stevenson granite (*Asg*) lies to the east of the principal strand of the mylonitic, greenschist facies Black-Bompas fault (Fig. 10; see "Low temperature flow"). Although it is itself cut by greenschist mylonite (*Ags*), it may be more properly considered as part of the Cree Lake zone (Lewry et al., 1985) wall rock to the East Athabasca mylonite triangle. Of greater significance are the smaller, 10 to 50 m sheets of biotite leucogranite (*Agm*) which outcrop along the eastern shore of Bompas Lake (Fig. 3), informally referred to here as the Bompas granite. At the south end of the lake, a 50 m wide sheet of Bompas granite cuts two-mica mylonitic metatexite and biotitized amphibolite, which it includes as misoriented xenoliths. The metatexite and amphibolite are part of the Hearne wall rock assemblage, retrogressed to biotite grade adjacent to the Black-Bompas fault. The leucogranite and xenoliths were subsequently transformed to chlorite-sericite ultramylonite, effectively acting as a soft medium within which shearing was localized. The leucogranite would have been anomalously soft if it was in a warm, subsolidus state immediately following magmatic crystallization. Accordingly, the Bompas granite would be syntectonic. A sample of the granite from Bompas Lake (Fig. 3) has yielded an approximate magmatic crystallization age of ca. 2600 Ma (Table 1), indicative of the approximate time of greenschist mylonitization.

Mixed and minor map units

Although most of the map units in the East Athabasca mylonite triangle can be identified as distinct lithological entities, ranging from dykes to batholiths, some represent composites within which the individual lithological units are either not thick or continuous enough to be distinguished at the map-scale. Hawkes leucogranite with subordinate Bohica mafic complex rocks (*Ahb*) is differentiated from a similar unit in

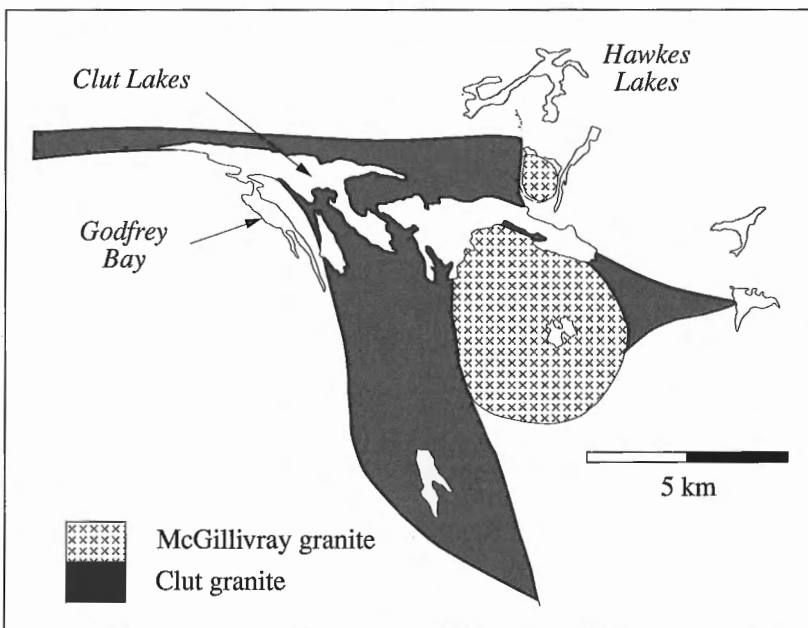


Figure 110.

Sketch map of the disposition of the Clut and McGillivray granites in the Clut Lakes area. A small stock of McGillivray granite occurs in the north side of the eastern Clut Lake. Note how the Clut granite bifurcates around the McGillivray granite, even though the McGillivray granite is nominally younger. See Figure 100 for location. Discussed in text.

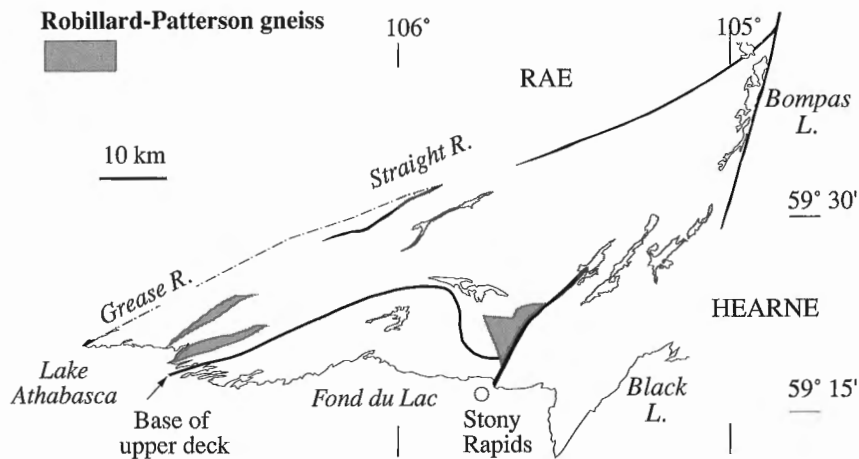


Figure 111. Distribution of Robillard-Patterson gneiss (cf. Fig. 9 and 10).



Figure 112. Pelitic component of the Robillard-Patterson gneiss, Robillard Bay, Lake Athabasca. Note the large size of the characteristic round garnet porphyroblasts. Coin for scale 2.5 cm. GSC 1994-204

which subordinate Hawkes leucogranite sheets intrude Bohica mafic complex (*Abg*). Unit *Arm* represents Reeve diatexite with Mary granite in approximately equal proportions. Unit *Abc* is a mixture of Bohica mafic complex and tonalite of the Chipman batholith. Other minor mafic map units are garnet-clinopyroxene-plagioclase granulite (*Amp*), and a hornblende-plagioclase-garnet mafic gneiss derived from a pluton in which cumulate layering is locally preserved (*Ahm*). Both are of uncertain affiliation. The latter occurs as a single sheet between Robillard Bay and Wiley Lake (Fig. 3). The former is really a broad lithological designation for xenoliths within the Chipman batholith, certain anhydrous parts of the Bohica mafic complex, and some of the larger mafic inclusions in the Mary granite.

Robillard-Patterson gneiss

Three panels of coarse grained, white granitic orthogneiss (*Arg*) are collectively referred to as the Robillard-Patterson gneiss (Fig. 111). The gneiss is remarkable for the size and diversity of its inclusions, but more specifically for its well developed banding, despite the absence of shape fabrics in its quartzofeldspathic component. It forms a large, apparently fault bounded mass to the southeast of Clut Lakes and two concordant panels north of Sucker Bay, Lake Athabasca (Fig. 3). Xenolithic rafts of rhythmically layered garnet-sillimanite metatexitic semipelite to pelite (*Arp*) are common to all panels (Fig. 112). The Robillard-Patterson gneiss is best exposed along the east shore of Robillard Bay, Lake Athabasca. Upright layering in the granitoid gneiss is defined by concordant bands of amphibolite up to several metres in thickness, variably deformed metre-scale pegmatite sheets, and variable proportions of hornblende and biotite. It may be folded with axes parallel to a very coarse, moderately southwest-plunging rodding lineation. At the grain-scale, the rock is coarsely recrystallized and generally lacks a shape fabric. Pegmatite veins are common and locally crosscut both banding and folding in the gneiss. Locally, the metapelite rafts preserve a rhythmic compositional layering, apparently of primary origin; for example west of Robillard Bay (Fig. 3). The 1 to 2 cm garnets within the migmatitic paragneiss rafts (Fig. 112) are distinct from those of the Pine Channel and Reeve diatexite units. The eastern panel is very difficult to access on foot on account of extensive swamp and surface water, and could only be examined by helicopter supported spot checking. It contains white granitoid and paragneissic components identical to those described from the western panels. However, it differs from them because (i) it contains large rafts of isotropic metagabbro intruded by very coarse grained isotropic hornblende-biotite granite and (ii) its internal fabrics are oriented at a high angle to the regional strike.

The Robillard-Patterson gneiss does not resemble any of the other map units of the East Athabasca mylonite triangle. It carries no evidence of a granulite facies mineral assemblage, nor of a ribbon fabric. There is no evidence that it is an annealed mylonite. The gneiss is frankly enigmatic. Hanmer et al. (1992b) speculated tentatively that its apparently transitional contact with the diatexite to the southeast indicated that it is a precursor to the diatexite, although they point out that the contact is poorly exposed. A sample of the white granitoid from Robillard Bay (Fig. 3), yielded an approximate magmatic crystallization age of ca. 1900 Ma (Table 1), indicating that the gneiss was magmatically emplaced well after the granulite facies mylonitization of the East Athabasca mylonite triangle. The poorly exposed boundaries with the adjacent mylonites are broad, ill-defined zones and could be progressive intrusive contacts. In the absence of Early Proterozoic regional deformation in the adjacent high grade mylonite, it would appear that the deformation of the Robillard-Patterson gneiss is local and related to plutonic emplacement, perhaps in a manner analogous to that described for the Donegal Granite in Ireland by Pitcher and Berger (1972). Indeed, in Robillard Bay, the gneiss contains a map-scale raft of spectacular Mary granite mylonite.

Economic geology

Alcock (1936) and Furnival (1940) reported that initial claims related to copper-nickel mineralization were staked in the mafic granulite of the upper deck as early as 1910. In 1929 a copper-nickel sulphide deposit was found in the southwestern part of Axis Lake (Fig. 3). Much of the presently visible trenching there (see Colborne, 1960) was undertaken in 1929-1930, although sporadic work has continued until very recently. In 1991, a detailed geophysical, ground survey, and drilling operation in the Axis-Rea lakes area (Fig. 3) was undertaken by Devex Exploration Inc. and Noranda Exploration Co. Ltd. A similar nickel exploration program had previously been undertaken in 1957, just south of Currie Lake (Ce in Fig. 3; Colborne (1962)).

Postmetamorphic 170°/90° trending veins of blue quartz, cutting across upper deck mylonite fabrics, have long been known for their gold potential. Furnival (1940) reported staking around Sucker Bay (Fig. 3), an area recently mapped in detail by Slimmon and Macdonald (1987). According to Johnston (1963), the Black-Bompas fault at Black Lake (Fig. 3) was prospected for pitchblende mineralization in 1948-1950. He also reported minor nickel mineralization from northeast of Woolhether Lake (Fig. 3). Copper-nickel mineralization associated with Bohica norite, northeast of Tantato Lake and at Father Lake (Fig. 3), was staked, trenched, and drilled in 1956 (Johnston, 1962). During the present study, trenches and abandoned drill core were found on the north shore of Day Lake (D in Fig. 3) at the site of rare bull quartz veins in mylonitized Reeve diatexite. The drill core, marked and dated 1975, appeared to have come exclusively from the diatexite. Anomalously radioactive pegmatites in the Hearne wall rock north of Black Lake have been examined for uranium, as well as molybdenite (Johnston, 1964; Thomas, 1983).

TECTONIC FLOW

The tectonic fabric pattern and vorticity (shear sense) distribution in the East Athabasca mylonite triangle appears complex. It could hardly be otherwise in a triangular field of mylonite. Nonetheless, this apparent complexity is readily unravelled by systematically considering the following observations, listed here in point form, but examined in detail below.

- (i) Geometrically, the East Athabasca mylonite triangle is divided into an upper and a lower deck, such that the upper deck forms the base of the triangle (Fig. 10). This is most clearly seen at Clut Lakes (Fig. 3), where the shallowly dipping foliation of the upper deck is discordant to upright foliations and lithological contacts within the lower deck.
- (ii) The upper deck, in its entirety, corresponds to a single dip-slip shear zone, whose hanging wall is still buried beneath the overlying Athabasca Basin (Fig. 1).
- (iii) The lower deck comprises a pair of conjugate strike-slip shear zones, separated by a central septum of relatively low finite strain (Fig. 10).
- (iv) The strike-slip and extensional shear zones are contemporaneous.
- (v) Despite the apparent geometrical and kinematic complexity, the finite extension lineations throughout the upper and lower decks are arranged about an average extension direction plunging moderately to the southwest (Fig. 10). This corresponds to the principal direction of regional-scale finite extension which one would predict from the coeval operation of the observed shear zones in three dimensions.

Mylonites within the East Athabasca triangle formed at all metamorphic grades from eclogite and granulite to lower greenschist facies (Fig. 113). The same geometrical and kinematic pattern is reflected by the mylonites formed at high, medium, or low temperatures. Older high temperature mylonites are developed throughout the East Athabasca mylonite triangle, but younger medium and low temperature fabrics occur in progressively narrower zones with decreasing metamorphic grade. This trend is explained by the well known process of increasing localization with cooling (e.g. Hanmer, 1988a; Hanmer et al., 1992a). The next section of this report will examine this pattern of flow, beginning with the older, hotter mylonites.

High temperature flow

Granulite facies garnet-pyroxene-bearing metamorphic mineral assemblages are developed throughout the mafic and quartzofeldspathic rocks of the upper and lower decks in the East Athabasca mylonite triangle. The mylonite fabrics of the upper deck are exclusively developed in anhydrous plagioclase-pyroxene-, garnet-pyroxene-, garnet-sillimanite-, and garnet-orthopyroxene-sillimanite-bearing assemblages. Polycrystalline ribbons of feldspar, quartz, sillimanite, and pyroxene are aligned in the mylonitic foliations and wrap around rigid, anhedral to euhedral garnets. Pyroxene and garnet

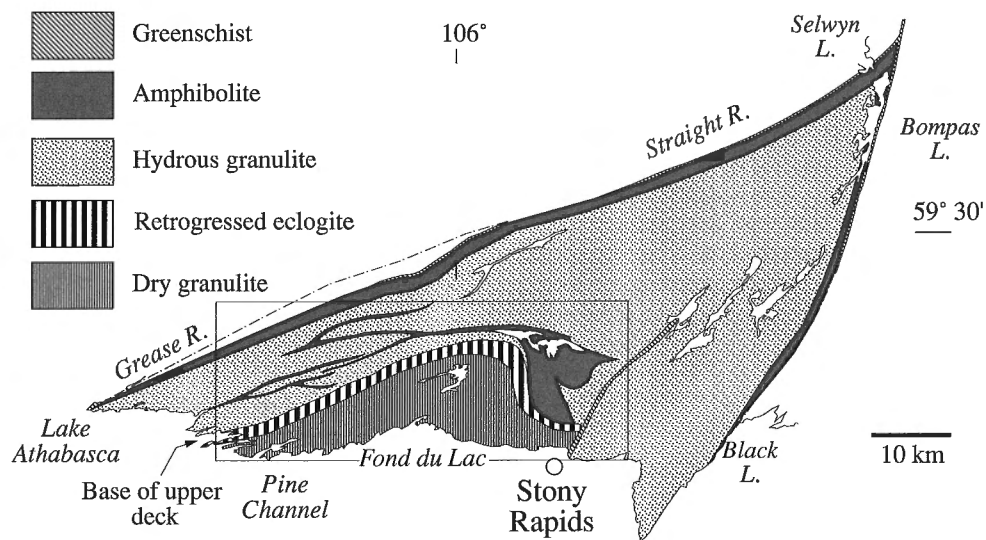


Figure 113. Distribution of metamorphic facies within the East Athabasca mylonite triangle. Box is general location of Figures 115 and 131.

are commonly replaced by amphiboles and biotite indicating hydration of the mineral assemblage with cooling. The systematic observation of mylonitic ribbons wrapping around undeformed polycrystalline pseudomorphs after equant garnet demonstrates that the retrogression is entirely postkinematic.

In the lower deck, hornblende is practically ubiquitous as a porphyroclastic or foliation-forming phase, even in garnet-pyroxene-bearing units such as the Mary granite, Godfrey granite, and the Bohica mafic complex. In the granites, biotite generally participates in the mylonitic foliation, but it also commonly forms polycrystalline postkinematic pseudomorphs after garnet. The principal exceptions are the mafic lenses of garnet-clinopyroxene-plagioclase±orthopyroxene granulite (*Amp*), mostly found in the north and east, but present across the width of the lower deck. Examination of metamorphic textures in thin sections from throughout the western and central parts of the lower deck demonstrates that the initial metamorphic assemblages in the garnet- and hornblende-bearing granite and mafic rocks were garnet-clinopyroxene-orthopyroxene-hornblende. However, much of the now visible hornblende is secondary and derived at the expense of the earlier pyroxenes. Part of the secondary hornblende population is postkinematic, but hornblende is commonly a foliation-forming phase.

Dip-slip shear zone (upper deck)

Geometrically, the upper deck can be considered in two parts (Fig. 10). In the east it is essentially a shallowly west- to southwest-dipping homocline. The foliation and layering progressively steepen and change azimuth westwards to form an upright panel, for the most part characterized by steep southeastward dips, but with local reversals. Fold closures within the western panel which could account for the variations in dip direction have not been observed. In the east, the

extension lineations are approximately down-dip, whereas in the west they are subparallel to the strike. Although the extension lineations mostly plunge to the southwest, there is a significant segment within the steep panel where they plunge toward the northeast. Layer-parallel ribbon mylonite fabrics are penetratively developed throughout the upper deck (Fig. 21, 23, 25, 28), except for the lenses of migmatite near Sucker Bay (Fig. 24). In the vicinity of these low-strain lenses, the plunge of the extension lineation is markedly steeper than elsewhere within the western panel of the upper deck. In other words, the localized decrease in finite strain in the southwestern part of the upper deck is associated with an increasingly heterogeneous strain pattern.

From a purely structural perspective, the entire upper deck forms part of a penetratively mylonitic segment of a curved shear zone, whose hanging wall has not yet been identified. The striking feature of the mylonite fabrics is their homogeneity at all scales (e.g. Fig. 19). Feldspar porphyroclasts are extremely rare. Minor folds, boudins, and asymmetrical extensional shear bands are practically absent, despite the abundance of potentially stiff layers, such as the garnet-quartz and garnet-clinopyroxene bands, or stress raisers, such as large garnet crystals (e.g. Fig. 22). One implication of this observation is that the spatial distribution of strain rate was remarkably homogeneous, and that perturbations in the flow failed to amplify. Such a flow requires a very homogeneous, weak rheology, incapable of sustaining spatial variations in mean stress, even over a relatively short time interval. An unfortunate consequence is that visible shear-sense indicators (e.g. Hanmer and Passchier, 1991) are rare. Nevertheless the few that have been found, mostly asymmetrical extensional shear bands, are consistent and uniformly indicate a top-down to the southwest sense of shear (Fig. 114).

As with any shear zone, the lower boundary of the upper deck must be defined by a strain gradient, and/or a discontinuity. In the west (Fig. 115), the base of the upper deck has been

mapped at a fabric transition from penetratively, but relatively heterogeneously, mylonitized, folded and veined Reeve diatexite in the lower deck, into the remarkably homogeneous Pine Channel diatexite mylonite. Passing eastward to Currie Lake, the basal fabric transition initially coincides with the lithological contact between the Pine Channel diatexite and the underlying Godfrey granite, then transgresses the lithological contact to lie within the Godfrey granite

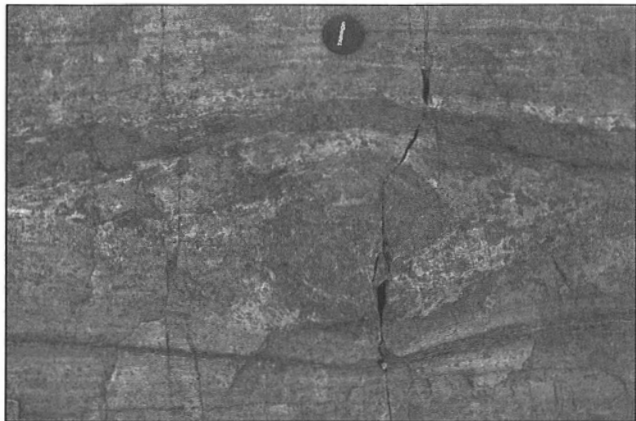


Figure 114. Rare indicator of shear sense within rocks of the upper deck. A lens of garnet-sillimanite in Pine Channel diatexite mylonite, Camille Bay, Lake Athabasca, has rolled up into a winged inclusion. Observed looking down onto a horizontal surface. Note the well developed matrix tucks present in the lower-right and upper-left quadrants, indicative of dextral shear, i.e. upper deck displaced towards the southwest (towards the left in photograph). Lens cap for scale. GSC 1994-102

west of Godfrey Bay. South of Godfrey Bay, the fabric transition has been intruded by the younger, mylonitic Clut granite. The continuity of lithological units across the fabric transition in the west might suggest that the upper deck is parautochthonous with respect to the lower deck. However, from a metamorphic perspective, the contrast in the high grade assemblages across the boundary between the structural decks (Fig. 113; see "Reeve diatexite") strongly suggests that the upper deck is allochthonous and relatively far-travelled. Therefore, the original base of the upper deck may have lain at the lower limit of the diatexite, including the panel of Reeve diatexite which now occurs immediately on the lower deck side of the fabric transition (Fig. 38, 116), southwest of Wiley Lake (Fig. 3). The original contact has been subsequently obscured by the emplacement of the Godfrey granite and the Robillard-Patterson gneissic pluton. This would imply that the upper deck was initially emplaced as a thrust hanging wall, whose lower level evolved into the 10 km thick shear zone, within which the marginal fabric transition is preserved. Although the early kinematic evolution of the shear zone is masked by the homogeneity of the ribbon fabrics, it acted as an extensional shear zone, at least during the latter part of its history. However, the extensive development of mylonite under conditions of increasing pressure in the lower deck (see "Garnet-pyroxene Mary granite"), coupled with the geochronological results (Table 1), suggest that mylonitization in the upper deck was, at least in part, related to thrusting.

Conjugate strike-slip shear zones (lower deck)

The tripartite geometrical subdivision of the lower deck represents three kinematic sectors (Fig. 10). The northwestern side of the triangular lower deck is a ca. 15 km wide belt of upright mylonitic foliations and lithological contacts, which

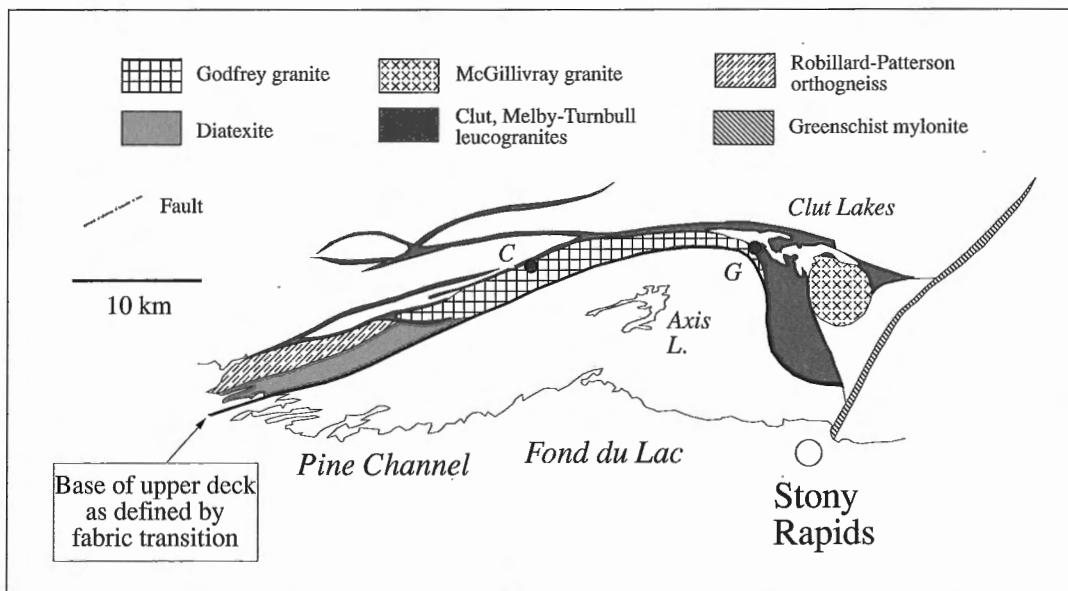


Figure 115. The spatial relationship between the base of the upper deck, as defined by a fabric transition, and the lithological map units along the upper deck-lower deck interface. Currie Lake (C) and Godfrey Bay (G) are indicated. See Figure 113 for location.

strike about 060-070°. The foliations dip moderately to very steeply both to the northwest and the southeast and appear to reflect an anastomosing flow pattern. The eastern side is a 20 km wide belt of about 020-050° trending, moderately to very steeply northwest-dipping mylonitic fabrics. As in the northwestern shear zone, variation in dip reflects the anastomosing nature of the flow planes. This is especially well exposed on a 100 to 1000 m scale at and west of southern Bompas Lake (Fig. 3). The two belts are separated from each other by a wedge-shaped area of anastomosing mylonite belts, about 15 km across the base, called the central septum. Outside of the central septum, ca. 2.6 Ga ribbon mylonite (Fig. 40, 41, 67, 70, 71, 72, 77-80, 83, 85) and ca. 3.13 Ga annealed mylonite fabrics (Fig. 44, 45, 53, 54, 55) are extensively developed. Diverse assemblages of shear-sense indicators, such as winged porphyroclasts, asymmetrical extensional shear bands, asymmetrical pull-aparts, pressure shadows, oblique boudin trains and oblique internal fabrics in

shear-parallel veins (e.g. White et al., 1980; Platt and Vissers, 1980; Hanmer, 1984b, 1986, 1990; Passchier and Simpson, 1986; see Hanmer and Passchier, 1991 for review) occur throughout the lower deck (e.g. Fig. 61, 65, 87, 91, 92, 116, 117, 118; see also Fig. 121, 122, 129, 133). The northwestern and eastern mylonite belts are strike-slip dextral and sinistral shear zones, respectively, with gently to moderately southwestward plunging finite extension lineations. At the northern apex of the lower deck, where the dextral and sinistral shear zones meet, exposure is very poor and it is not possible to observe their time relations directly. Nevertheless, within each shear zone, the sense of shear is consistent, regardless of deformation intensity. In other words, there is no evidence of shear-sense reversal during the histories of either shear zone.

Central septum (lower deck)

In general, mylonite fabrics are penetratively developed throughout the dextral and sinistral shear zones of the lower deck. The main exception is the core of moderately foliated tonalite within the Chipman batholith (Fig. 43; see "Chipman batholith"). However, the central septum (Fig. 10) is principally composed of mylonitic to isotropic Hawkes leucogranite, associated with panels and rafts of moderately deformed Bohica mafic complex. The deformation state of the Bohica



Figure 116. Dextral winged inclusion in annealed porphyroclastic mylonite derived from the Mary granite, Wiley Lake. A feldspar core-and-mantle structure, indicating dextral shear sense. Coin for scale 2.5 cm. GSC 1993-166J



Figure 117. Rotated plagioclase pressure shadows on garnets in a Chipman dyke, Chipman tonalite batholith, Square Lake, indicative of sinistral sense of shear. Coin for scale 2.5 cm. GSC 204775-H

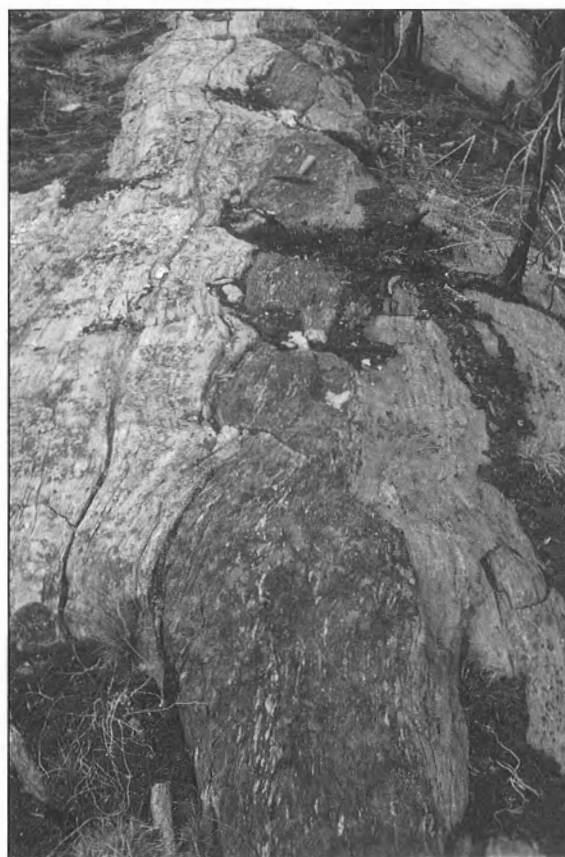


Figure 118. Train of back-rotated boudins in amphibolite layer in pelitic metasediments, eastern (Hearne) wall rock, Bompas Lake, indicative of sinistral sense of shear (see Hanmer and Passchier, 1991). Hammer for scale. GSC 1994-171

mafic complex material is reflected in the frequent preservation of relict, coarse ophitic textures in a *flaser* fabric. In part, the Hawkes granite occurs as well preserved plutons and it is demonstrably intrusive with respect to the Bohica mafic complex material, which it cuts and includes as xenoliths. Indeed, southwest of Kaskawan Lake (Fig. 3), the relative proportions of Bohica mafic complex and Hawkes granite material are such that it is not feasible to discriminate between heavily veined wall rock on the one hand, and granite charged with xenolithic rafts on the other. However, much of the Hawkes granite is penetratively mylonitized. The contacts between the nonmylonitic (plutonic) and mylonitic parts of the granite are gradational and no xenoliths of the latter have been found in the former. The same is true for the relationship between the nonmylonitic Hawkes granite and the mylonitic Mary granite. It is conceivable that the Hawkes granite is simply a large scale example of the compositional variation observed elsewhere throughout the Mary granite (see "Garnet-pyroxene Mary granite"). However, it is equally possible that it represents a distinct magma body, emplaced into the Mary granite. If this is the case, then the discrete plutons of Hawkes granite might also be intrusive with respect to its own mylonitic equivalent. The point being made here is that the complex pattern of lithologies and deformation fabrics in the central septum reflects either the syntectonic nature of the Hawkes granite, or the spatial distribution of tectonic flow.

The following observations serve to illustrate that, in contrast to the flanking, kinematically homogeneous, dextral and sinistral shear zones, the spatial distribution of strain and shear sense within the central septum is heterogeneous, but reflects the distribution of flow and vorticity in the East Athabasca mylonite triangle as a whole. A large panel of Mary granite occupies the middle of the central septum. It encloses a map-scale raft of moderately deformed Bohica mafic complex, yet is itself mylonitized. This is presumably a function of the greater ability of the softer quartzofeldspathic Mary granite to accommodate the imposed deformation, thus protecting the relatively minor volume of the mafic raft. South of East Hawkes Lake, the Hawkes granite contains a large folded panel of annealed straight banded diatexite, whose fold axis plunges gently to the southwest (Fig. 119). The granite on the concave side of the panel is poorly foliated to isotropic and clearly intrusive with respect to the diatexite, whereas the granite on the convex side is mylonitic. The diatexite panel has either guided the intrusion of the isotropic granite, or it has acted to partition the deformation within its host granite (e.g. Bell, 1981, 1985; Lister and Williams, 1983). The panels of both Bohica mafic complex and diatexite have acted as guides for the flow patterns in their host granites. Between East Hawkes Lake and Clut Lakes, a steeply dipping panel of Bohica mafic complex, striking about 020°, is associated with sinistral strike-slip shearing in the adjacent mylonitic Mary granite (Fig. 119). At East Hawkes Lake itself, the same Mary granite, associated with about 070° striking upright panels of Bohica mafic complex contains dextral shear-sense indicators (Fig. 119). In the hinge zone of the folded diatexite panel within the Hawkes granite, the diatexite and the immediately overlying granite are transformed to ribbon mylonite associated with a top-down to the southwest sense of shear. At the scale of the central septum as

a whole, although the mylonitic fabrics of the northwest side tends to reflect dextral noncoaxial flow and the southeast side tends to be sinistral, unequivocal contradictory shear-sense indicators (see Hanmer and Passchier, 1991) also occur locally.

Precise definition of the extent of the central septum is somewhat problematical. It is readily determined in its southwestern part where there is a spatial coincidence of mixed shear sense, variable foliation development, and frequent preservation of recognizable relict igneous textures. Given the fairly coarse resolution of the data, it is probably futile to try to define the precise location of the lateral limits of the central septum on structural grounds alone. Accordingly, as a reasonable approximation, the limits of the central septum are taken to correspond to the eastern and western contacts of the Hawkes granite. To the northeast, mixed shear-sense determinations, preservation of relict ophitic texture in the Bohica mafic complex and the presence of abundant Hawkes leucogranite suggest that Kaskawan Lake (Fig. 3) spans the width of the central septum. Having thus broadly defined the limits of the central septum, the dextral and sinistral shear zones are those parts of the lower deck which lie to the northwest and east of it, respectively (Fig. 10). However, at the northern end of the lower deck, a combination of poor outcrop and late faulting makes it particularly difficult to precisely define the boundary between the dextral and sinistral shear zones.

In summary, the timing and shear sense of principal kinematic components of the East Athabasca mylonite triangle as a whole are reflected within the central septum. While recognizing that the magnitude of some of the geochronological error envelopes (Table 1), kinematic compatibility, and similarity of metamorphic grade of the various shear zones within the central septum suggest that some of the flow in the conjugate strike-slip shear zones was contemporaneous with the normal (extensional) component of dip-slip flow within the upper deck. The strike-slip shear zones acted to accommodate a subhorizontal northwest-southeast oriented direction of principal shortening, whereas the normal shearing would have accommodated a steeply plunging direction of principal shortening. The two directions of principal shortening are compatible with the gently southwest-plunging direction of principal extension manifested in the extension lineations throughout the East Athabasca mylonite triangle (Fig. 10). Collectively, these three principal stretching directions define a bulk constrictional flow. This is precisely the symmetry that would be predicted for flow around the termination of a northeast-southwest oriented stiff lozenge-like volume set in a bulk extensional flow parallel to its axis (Fig. 10).

Medium temperature flow

Hornblende-biotite±garnet-bearing amphibolite facies mylonites occur at four specific sites (Fig. 113): (i) the interface between the upper and lower decks, (ii) bounding the lenses of Mary granite ribbon gneiss in the southwestern part of the lower deck (Fig. 82), (iii) adjacent to the lateral limits of the lower deck (Fig. 10), and (iv) along the western margin of the McGillivray granite (Fig. 100).

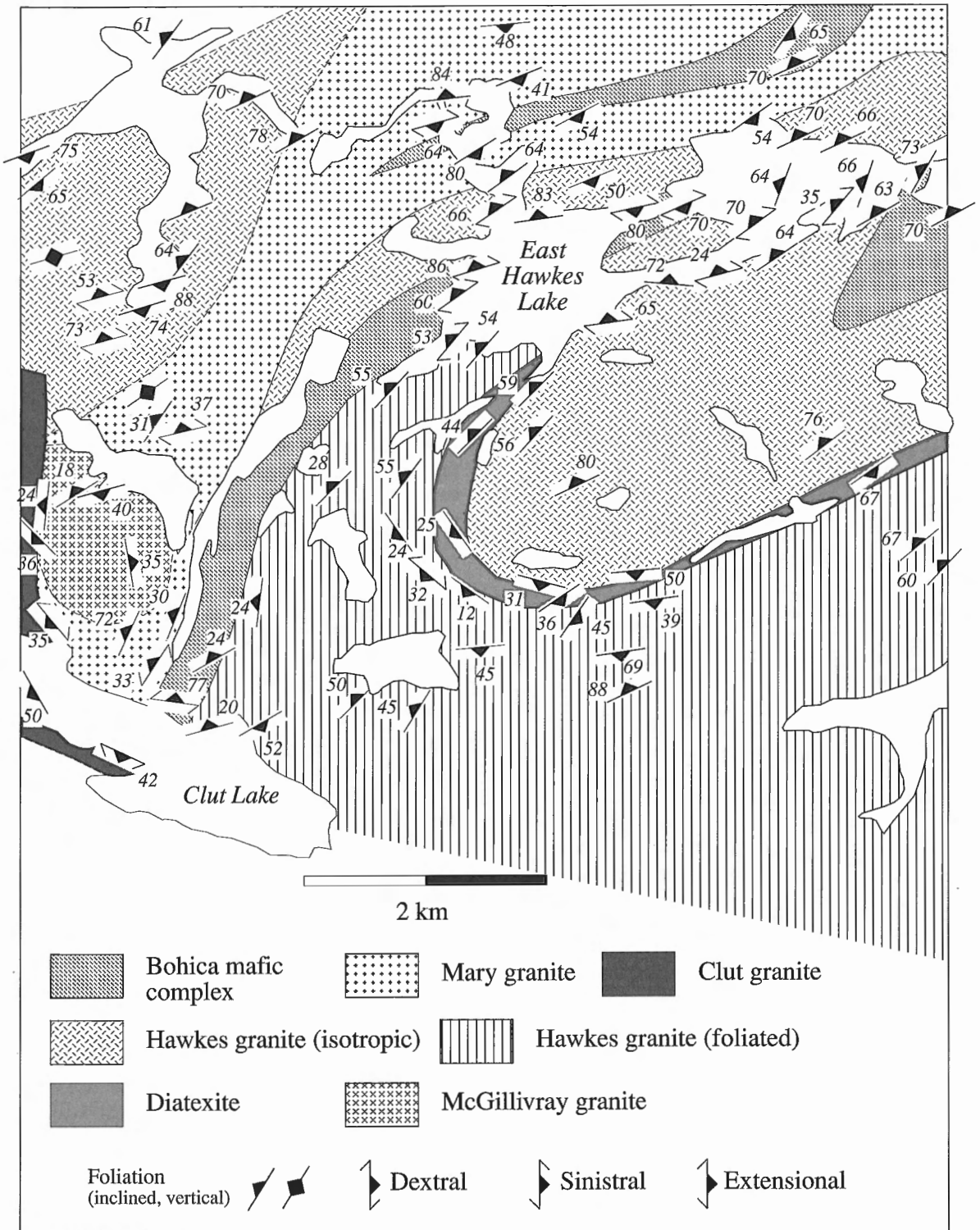


Figure 119. Detailed map of the Clut Lakes-East Hawkes Lake area to illustrate the relationship between locally resolved vorticity (shear sense) and the orientation of rheologically important map units. See Figure 9 for location.

Interface mylonites

The protomylonitic to mylonitic Clut granite occupies a significant segment of the contact between the upper and lower decks (Fig. 10). The south- and west-dipping fabrics carry hornblende and biotite, with no trace of relict pyroxene or garnet. In local low strain windows, the mylonite is clearly seen to be derived from a hornblende-biotite granite. In other words, the emplacement and deformation of the granite postdate granulite facies metamorphism. In contrast to the overlying granulite facies mylonite units of the upper deck and the Godfrey granite, the Clut granite contains abundant, often penetratively developed asymmetrical extensional shear bands, all of which indicate top-side-down displacement along the dip-parallel extension lineation (Fig. 101). The granite contact and its internal mylonitic foliation are discordant with respect to the lower deck structures and map units (Fig. 9). Clearly, a component of top-side-southwest relative displacement of the upper deck was accommodated by localized deformation within the Clut granite at amphibolite to upper greenschist facies. In the absence of firm constraints, transitional deformational behaviour of the feldspar population of the granite is suggestive of temperatures of about 500°C (White, 1975; Tullis and Yund, 1980; Hanmer, 1982; Tullis, 1983).

Anastomosing flow

In general, feldspar porphyroclasts are not a common component of the rather uniform, high temperature mylonite fabrics of the lower deck (Fig. 40, 41, 67, 70, 71, 72, 77, 78, 79, 83, 85, 88). However, between Reeve Lake and Lake Athabasca (Fig. 3), the homogenous fabric pattern is replaced by a heterogeneous one, reflecting partitioning of the flow at all scales (e.g. Lister and Williams, 1983). Mappable lenses of ribbon gneiss are enclosed by belts of annealed porphyroclastic mylonite (Fig. 90-94; see "Garnet-pyroxene Mary granite"), along which sheets of hornblende-biotite Melby-Turnbull granite were preferentially emplaced and variably mylonitized (Fig. 100; see "Hornblende-biotite granitoid bodies"). The hornblende-bearing ribbon gneiss contains garnet and clinopyroxene. In contrast, the porphyroclastic mylonite only contains biotite-hornblende-garnet. The absence of feldspar porphyroclasts in the ribbon gneiss means that it is not part of the fabric path leading to the porphyroclastic mylonite. On the other hand, the lower metamorphic grade of the porphyroclastic mylonite means that the *preserved* fabrics are younger than those of the ribbon gneisses. Note that the anastomosing geometry is also reflected in the three-dimensional orientations of mylonitic foliation along the shore of Lake Athabasca, west of Robillard Bay (Fig. 3), where flat-lying fabrics, uncharacteristic of the lower deck, are common (see "Garnet-pyroxene Mary granite").

A possible interpretation of these fabrics is suggested here, predicated on the known strain-rate sensitivity of the strength of rock-forming minerals (e.g. Nicolas and Poirier, 1976; Poirier, 1985), assuming initially uniform metamorphic conditions. The map pattern in the southwestern part of the lower deck (Fig. 9, 82, 100; see also Hanmer, 1994) indicates that during high temperature (hornblende-clinopyroxene-garnet) deformation, the normally homogeneous pattern of flow was perturbed for reasons discussed below (see "Heterogeneous flow"). Flow

would therefore have been partitioned between relatively slowly deforming volumes (Bell, 1981, 1985) of ribbon gneiss, in which all the rock-forming minerals participated, and narrow bounding zones of faster strain rate, in which the feldspar component acted as stiff porphyroclasts. With cooling, deformation ceased in the ribbon gneiss and continued in the porphyroclastic mylonite. Melby-Turnbull granite sheets were preferentially emplaced into those zones where shearing was active. In brief, although deformation partitioning had initiated at higher (granulite) temperatures, flow was further localized with cooling to amphibolite facies (Hanmer, 1988a).

Lateral limits of the lower deck

On the west side of the lower deck, the transition from granulite facies ribbon mylonite to greenschist mylonite occurs progressively over a zone up to 1.5 to 2 km wide. It is particularly



Figure 120. In-plane dextral winged inclusions (see Hanmer and Passchier, 1991) in annealed porphyroclastic mylonite, Tantato Lake. A feldspar core-and-mantle structure, indicating dextral shear sense. Coin for scale 2.5 cm. GSC 1993-166D



Figure 121. Dextral winged inclusion, adjacent to coin, in greenschist ribbon mylonite derived from the Mary granite, Grease Bay. A feldspar core-and-mantle structure, indicating dextral shear sense. Note also the dispersed dark amphibole crystals aligned anticlockwise with respect to the mylonitic foliation. Coin for scale 2.5 cm. GSC 1994-188

well preserved north and west of Reeve Lake (Fig. 3). Garnet-hornblende-clinopyroxene-orthopyroxene ribbon mylonites derived from diatexite, Mary granite, and Bohica mafic complex protoliths become progressively finer grained towards the western limit of the lower deck, such that their ribbon structure is imperceptible to the naked eye and the rocks are distinctively nonfissile (Fig. 120, 121). Within these fine nonfissile mylonites, occasional coarser grained bands with visible garnet and pyroxene, which occur to the east, are not found to the west. The garnet-hornblende studded Mary granite ribbon mylonite is replaced by a very fine grained, nonfissile rock with an annealed sugary matrix, scattered hornblende porphyroclasts, and very fine disseminated biotite (Fig. 122). Within this fine grained hornblende-porphyroclastic mylonite



Figure 122. Nonfissile, very fine grained porphyroclastic mylonite, Straight River, northwest of Tantato Lake. Note that ribbons are not visible to the unaided eye. Larger white porphyroclasts are plagioclase, more numerous smaller black porphyroclasts are hornblende. Coin for scale 2.5 cm. GSC 1994-189

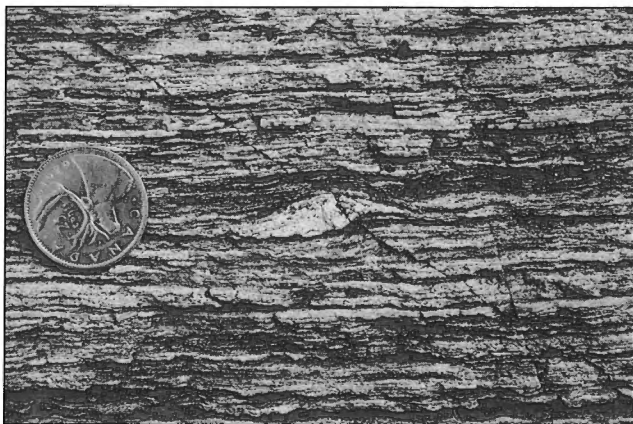


Figure 123. Chlorite-bearing greenschist facies ribbon mylonite, Straight River, north of Tantato Lake. Looking down on horizontal surface. Note the solitary feldspar fish which, by analogy with foliation fish, can be interpreted in terms of dextral shear sense (see Hanmer and Passchier, 1991). Coin for scale 2.5 cm. GSC 1994-190

lies the Felsic Lake leucogranite (Fl in Fig. 100). This is a pink, ultra-fine grained, homogeneous biotite granite mylonite. Its ribbon structure is only visible to the naked eye on delicately etched, glacially smoothed surfaces. Note that the swarm of 2640 ± 20 Ma granite sheets, to which the Felsic Lake granite apparently belongs, is syntectonic with respect to the amphibolite facies mylonitization (see "Hornblende-biotite granitoid bodies"). Northeast of Reeve Lake (Fig. 3), the hornblende-porphyroclastic and Felsic Lake granite ultramylonites can be traced across strike into chlorite-bearing mylonite (Fig. 123). These observations are best interpreted in terms of the reworking of higher temperature mylonite by younger, colder mylonite. The 15 km wide belt of granulite facies mylonite has been reworked to produce a 2 km wide amphibolite facies belt, which was itself reworked to form a belt of lower greenschist facies mylonite, several hundreds of metres wide. This reflects the progressive narrowing of the active zone of shearing with cooling through time (e.g. Hanmer, 1988a).

This progressive localization contrasts with the lower amphibolite facies sinistral ribbon mylonite on the east side of the Chipman batholith which clearly cuts across and truncates the older, higher temperature mylonite in an abrupt manner. On

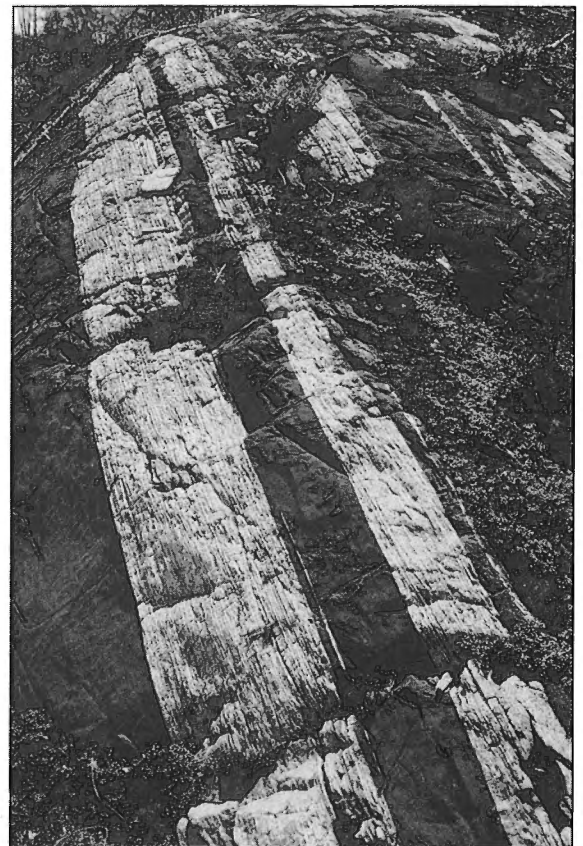


Figure 124. Hornblende-bearing tonalite ribbon mylonite with transposed Chipman dykes, Bompas Lake. Hammer for scale. GSC 1994-111

the east shore of southern Bompas Lake (Fig. 3), the Chipman tonalitic straight gneiss and mafic dykes are deformed into a finely banded, hornblende-bearing ribbon mylonite (Fig. 124) with extensively developed 0.1 to 5.0 m scale sheath folding of both the dykes and the mylonite fabric (Fig. 125, 126). This mylonite forms a 0.5 to 1.0 km wide belt which extends along the east shore and south of Bompas Lake, truncating the fabrics and lithological contacts in the high temperature mylonite of the sinistral shear zone. While some of the mylonitized mafic dykes may be part of the Chipman dyke swarm, the presence of the Fehr dykes, and the local occurrence of minor mafic dykes in greenschist facies mylonite (see "Low temperature flow"), suggests that some mafic mylonite may be derived from younger dykes.

Taylor Bay fault

The Taylor Bay fault (Fig. 127) is well exposed as a less than 100 m thick zone of fine grained, hornblende-feldspar porphyroclastic ribbon mylonite, along the western contact of the McGillivray granite. It dips moderately to the west and carries a down-dip extension lineation associated with winged porphyroclasts, up to 5 cm long, which indicate a top-side-down sense of shear.

Low temperature flow

The pattern of high and medium temperature conjugate shear zones in the lower deck, and dip-slip shearing at the upper deck/lower deck interface, is reflected in the distribution of greenschist facies mylonites (Fig. 113). They represent the ultimate stage of the progressive localization of flow already noted at higher metamorphic grade (see "Medium temperature flow"). The presence of these mylonites was noted by earlier workers (see "Previous and recent work"). For ease of reference, this report will employ a terminology which reflects the fault names used by them (Fig. 127). The mylonites are spatially associated with remarkably discrete brittle faults. Pseudotachylite is practically absent, cataclasite is very rare, and quartz-carbonate veining is infrequent.

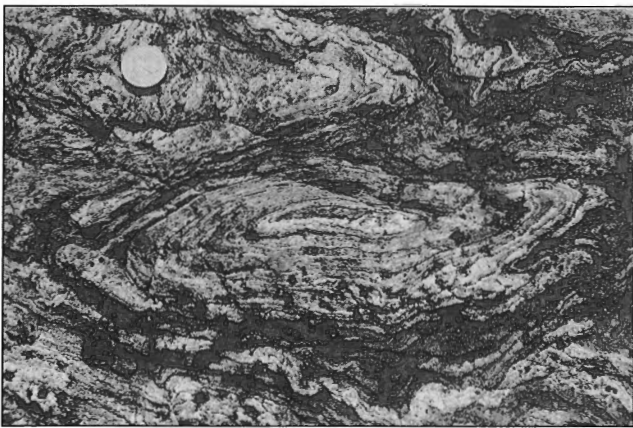


Figure 125. Hornblende-bearing tonalite ribbon mylonite, Bompas Lake, observed looking along the extension lineation. Note the sheath folding of the ribbon mylonite fabric and the dark bands, interpreted to be Chipman dyke material. Coin for scale 2.5 cm. GSC 1994-196

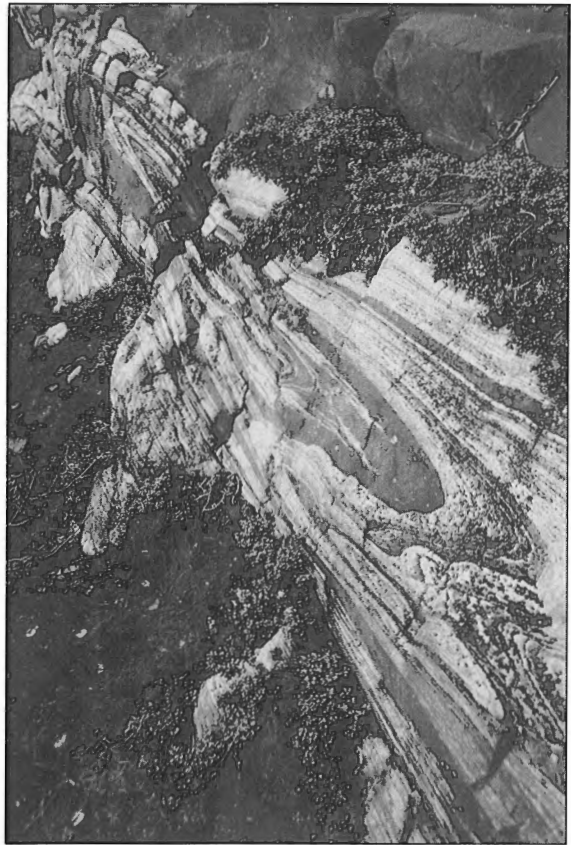


Figure 126. Hornblende-bearing tonalite ribbon mylonite with transposed Chipman dykes, Bompas Lake, observed looking along the extension lineation. Note the sheath folding of the ribbon mylonite fabric and the Chipman dykes. A smaller sheath fold occurs in the foreground, just below the principal fold. Note that the mafic band just to the left of the smaller sheath fold can be traced into the principal dark band marking the larger sheath fold. In other words, despite the magnitude of the finite strain, the original branching configuration of the dykes is locally preserved in the YZ section of the finite strain ellipsoid. Long dimension of principal fold is about 2 m. GSC 1994-112

Black-Bompas fault

Biotite-chlorite and chlorite-sericite mylonite occurs discontinuously along the northwestern side of the dextral shear zone and along the eastern side of the sinistral shear zone. In the sinistral shear zone, the transition from the high temperature mylonite is abrupt, albeit progressive. The Black-Bompas fault, the main belt of greenschist facies chlorite-sericite mylonite (Fig. 127), is 100 to 200 m thick. It is derived, in large part, at the expense of the Hearne metatextitic paragneiss to the east, which was itself intruded by Bompas leucogranite. The mylonite (Fig. 128) is often so fine grained that no ribbon structure is discernible to the naked eye. The foliation dips moderately to steeply to the west and the lineation rakes southward across the foliation plane at approximately 40°. It contains few, sinistral, shear-sense indicators and has accommodated a component of east-side-up displacement. At a distance of 100 to 200 m east of the greenschist

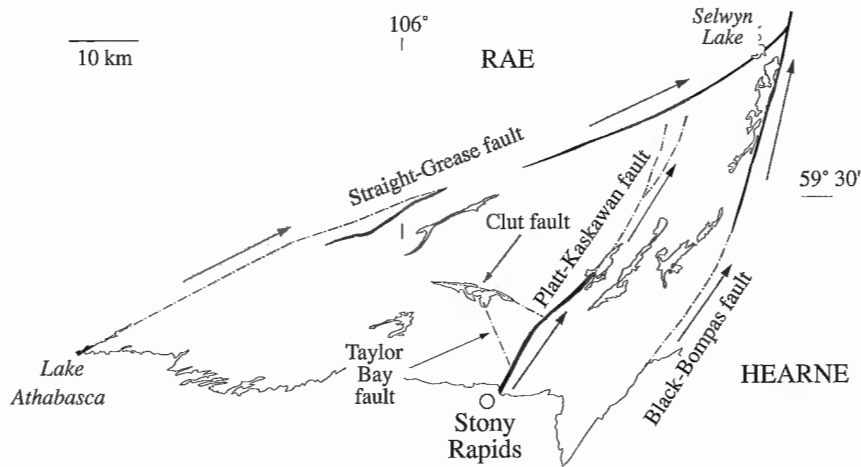


Figure 127. Distribution of low temperature mylonite zones and faults in the East Athabasca mylonite triangle. Arrows indicate relative displacements of wall rock across the faults.

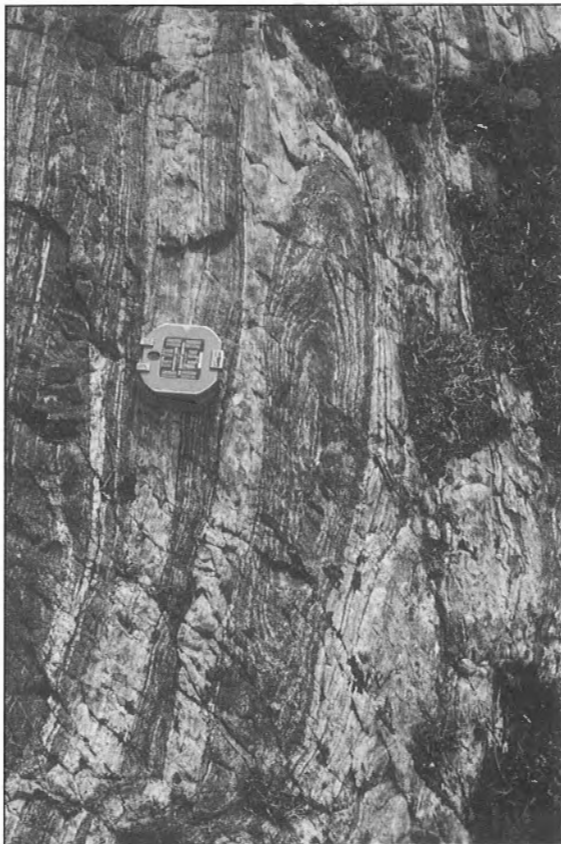


Figure 128. Tonalite ribbon mylonite, Bompas Lake, observed looking along the extension lineation. Note the sheath folding of the ribbon mylonite fabric and the dark chlorite-actinolite-bearing bands, interpreted to be Chipman dyke material. Compass for scale. GSC 1994-197

mylonite belt, the migmatitic paragneiss is tectonically reduced to a biotite-muscovite schist with scattered feldspar porphyroclasts and metre-scale boudins of hornblende-bearing amphibolite. In this state it has been intruded by an array of 1 to 50 m thick subconcordant sheets of equigranular, medium grained Bompas leucogranite. These rocks pass westward into the main belt of chlorite mylonite, centred upon the main about 50 m wide sheet of leucogranite with inclusions of chlorite schist. The leucogranite is syntectonic and its approximate magmatic crystallization age of ca. 2600 Ma is indicative of the timing of greenschist mylonitization (see "Hornblende-biotite granitoid bodies"). Within the greenschist mylonite, a single occurrence of a 4 cm thick, syntectonic, crosscutting, foliated mafic dyke was observed. Combined with the ca. 3.13 Ga Chipman dykes and the ca. 2.6 Ga Fehr dykes, this small dyke suggests that the east side of the lower deck has been the site of repeated syntectonic mafic dyke emplacement for over 500 Ma. To the south, the greenschist mylonite is present as several strands. While it is reasonable to suggest that it forms part of a linked strike-slip system (e.g. Woodcock and Fischer, 1986), it has not been possible to demonstrate this.

Straight-Grease fault

The Straight-Grease fault (Fig. 127) is an array of low temperature dextral mylonite bodies and anastomosing fault strands which preserve a progressive, retrograde relationship with the high temperature mylonite of the lower deck (see "Medium temperature flow"). The chlorite-sericite mylonite is similar in appearance to that described from the Black-Bompas fault. The foliation dips steeply to either side of the vertical and is associated with a subhorizontal to moderately southwest-plunging extension lineation. Shear-sense indicators are scarce, but consistently dextral (Fig. 129). The greatest thickness of greenschist mylonite, 500 m, occurs along the southeastern shore of Grease Bay (Fig. 3). Between Grease

Bay and Felsic Lake, outcrop is moderate to very poor. The mylonite at Grease Bay is succeeded along strike by a pair of brittle faults, the more southeasterly of which appears to follow a rather sinuous trace to Felsic Lake. However, it is possible that this study has simply highlighted certain components of a complex fault array and has failed to identify the master fault strand. At Felsic Lake (Fig. 3) the fault roots into a simple 100 to 200 m thick strand of chlorite-bearing mylonite. In contrast to the Black-Bompas fault, this mylonite is everywhere concordant to its high temperature equivalents within the dextral shear zone. However, as at Bompas Lake, there are two components to the protolith. A quartzofeldspathic component, derived in part from the amphibolite facies mylonite of the lower deck, and a banded, often phyllonitic component, derived from the sillimanite-garnet metapelitic rocks and associated granite units of the Rae wall rocks. Thorough mylonitization and retrogression of the wall rocks occurred over a short distance (<100 m).

Other faults

Greenschist mylonite also occurs within the interior of the lower deck, along the Platt-Kaskawan and Clut faults (Fig. 127). The faults are not well exposed, but their influence on the map pattern of the lower deck is immediately apparent. The poorly exposed Platt-Kaskawan fault trends parallel to the trace of the Black-Bompas fault. Outcrops of actinolitic and chlorite-bearing mylonite, up to 100 m across, occur along Platt Creek and at Cora Lake (Fig. 3). Smaller outcrops of fine grained chloritic mylonite are present at a number of localities along the trace of the fault. However, over most of its length, the presence and location of the fault is only apparent from contrasts in the map pattern on either side of its trace (see Hanmer, 1994). Foliations are vertical and, with the marked exception of an isolated dip-lineated outcrop just north of Fond du Lac (Fig. 3), the extension lineation plunges gently to the southwest. A single shear-sense determination

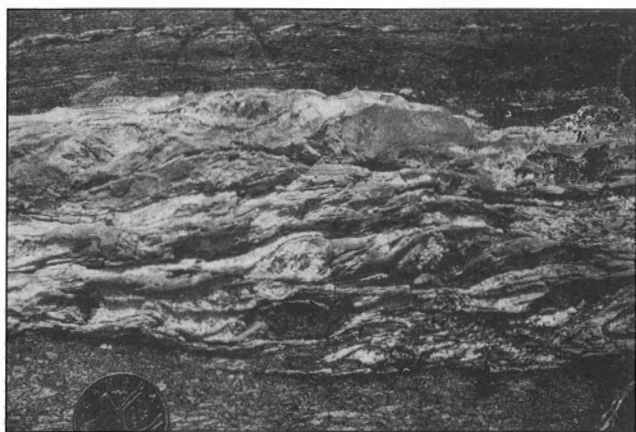


Figure 129. Concordant pegmatite in chlorite mylonite, Straight River, northeast of Tantato Lake. Looking down at horizontal surface. Note the well preserved composite *CIS* fabric indicative of dextral shear sense (see Hanmer and Passchier, 1991). Coin for scale 2.5 cm. GSC 1994-191

in the field, combined with the sense of offset of piercing points related to the contacts of a prominent belt of diatexite, indicate a sinistral, strike-slip sense of displacement.

At Clut Lakes (Fig. 3), the Clut fault dips at 70° to the south (Fig. 127). A 10 to 50 m thick, dip-lineated, actinolite-chlorite mylonite section of the fault occurs at west Clut Lake. No shear-sense indicators were found. Colborne (1961) projects the Clut fault across the trace of the Platt-Kaskawan fault, without offsetting the latter. South of Steinhauer Lake (Fig. 3), it was not possible to map the range of fabrics in the Chipman tonalite noted to the north (see "Chipman batholith"). However, this may in part be a function of inadequate sampling due to poor access and exposure. Nevertheless, over the 10 km distance from the southwest end of Lytle Lake (Fig. 3) to the southeast margin of the Chipman batholith, the average volumetric proportion of dykes is more than 50%, with local kilometre-scale swaths of 80%. Anorthosite inclusions, while present, are much less common. It would appear that Steinhauer Lake marks a structural break in the Chipman batholith. The axis of the lake lies along the east-southeastward projection of the trace of the Clut fault. However, any suggestion that the Clut fault extends along Steinhauer Lake would require an explanation of the clear lack of offset of the Platt-Kaskawan fault, and *vice versa* (Fig. 127). The sudden increase in the density of Chipman dykes south of Steinhauer Lake is suggestive of an extension of the Clut fault, but no direct evidence has been found. Dip-slip displacement along a possible 110° trending extension of the Clut fault *could* result in zero offset of the 020° striking vertical Platt-Kaskawan fault. However, the gravity data (Fig. 27) would suggest that the density of the dyke swarm should increase downward and that the dip-slip movement is south-side-up. If the Clut fault, at Clut Lakes is south-side-down, as are its higher temperature predecessors, there is either a contradiction or the fault accommodates a scissors-type displacement.

Heterogeneous flow

The Archean deformation fabrics developed within the East Athabasca mylonite triangle are remarkable for their homogeneity over a range of scales, from outcrop to 1:100 000 map scale. The most obvious exceptions are the strain variation between map units within the Chipman batholith, and in the central septum. However, a pattern of heterogeneous, partitioned flow is evident within the ribbon mylonite in the southwestern parts of both the lower and upper decks. In the lower deck, between Reeve Lake and Lake Athabasca (Fig. 3), map-scale lenses of ribbon gneiss (Fig. 88, 89) are enclosed by belts of mylonite, unusually rich in feldspar porphyroclasts (Fig. 90-94; see "Anastomosing flow"). Flow appears to have been partitioned between the relatively slowly deforming ribbon gneiss, and narrow zones of faster strain rate in which the feldspar component acted as stiff porphyroclasts. In the upper deck, homogeneous ribbon mylonite fabrics are penetratively developed throughout the Pine Channel diatexite, except for the low-strain lenses near Sucker Bay. In the vicinity of the lenses, the plunge of the extension lineation is markedly steeper than elsewhere (see "Dip-slip shear zone (upper deck)").

At least two speculative, nonexclusive scenarios could account for these observations (Fig. 130). Distribution of strain and strain rate may be heterogeneous where (i) bulk deformation is relatively low and all the potentially deformable material has not yet been incorporated into the maturing shear zone, or (ii) the imposed bulk strain rate is too fast for all of the shear zone material to participate equally. In either case, localization of flow is enhanced. In the first case, bulk deformation could decrease toward the southwest as one approaches the stiff core of the Athabasca lozenge. Alternatively, strain rate could be particularly fast in the southwestern corner of the East Athabasca mylonite triangle because of the constructive interference of two independent driving forces. Late Archean granulite facies deformation on the conjugate strike-slip shear zones in the lower deck acted to accommodate a northwest-southeast, subhorizontal direction of principal shortening. However, contemporaneous, granulite facies extensional shearing within the upper deck represents a response to a steeply-plunging direction of principal shortening. Because of the geometrical configuration of the upper and lower decks, the two independent directions of principal shortening combine to produce locally resolved dextral shearing on a common shear plane *only* in the southwestern part of the East Athabasca mylonite triangle. If the interface between the upper and lower decks was reasonably cohesive, constructive re-enforcement of the driving forces would lead to an enhancement of the strain rate and favour localization of the flow.

SYNTECTONIC MAGMATISM

The relationship between magma emplacement and deformation has long been a topic of intense debate (e.g. Hanmer and Vigneresse, 1980; Brun and Pons, 1981; Hanmer et al., 1982; Bateman, 1984; Castro, 1985; Van den Eeckhout et al., 1986; Paterson, 1988; Ramsay, 1989; Paterson and Fowler, 1993a) which, at least recently, has been couched in terms of the room problem associated with the introduction of large volumes of new material into the continental crust (e.g. Guinberteau et al., 1987; Hutton et al., 1990; Clemens and Mawer, 1992; Morand, 1992; Paterson and Tobisch, 1992; Cox, 1993; Paterson and Fowler, 1993b). Indeed, it appears to be axiomatic that the presence of a swarm of parallel dykes is *prima facie* evidence for extension across the average trend of the swarm, to the extent that dyke swarms are commonly taken to indicate *de facto* the orientation of the least compressive regional stress (e.g. Escher et al., 1976; Emerman and Marrette, 1990; Wolf and Saleeby, 1992; Meyer et al., 1992). This debate is particularly pertinent to the study and analysis of the East Athabasca mylonite triangle for three principal reasons. First, the synkinematic nature of much of the granitoid magma is the geological basis for isotopically dating the deformation events responsible for the mylonitization. Secondly, as will be examined below, the emplacement of the voluminous mafic and granitoid magmas presents a potential mechanism for the transfer of heat required for the high temperature granulite facies metamorphism which accompanied the deformation. Thirdly, the mafic dykes recorded here were emplaced into active transpressive shear zones.

This report has already dealt with the simple aspects of syntectonic magmatic emplacement, mostly to justify the use of U-Pb data to date deformation. However, there are other

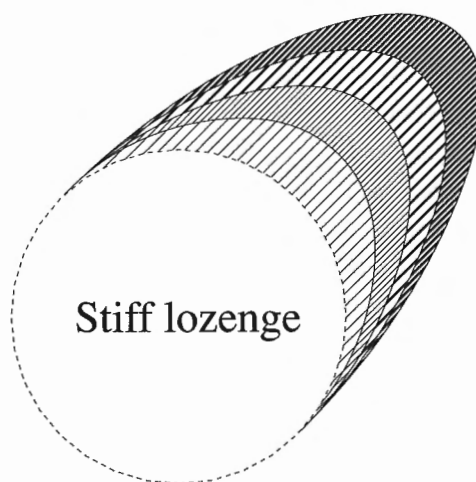


Figure 130. Schematic illustration of the concept of the distribution of finite strain where a stiff object is in cohesive contact with a deforming softer matrix which was tectonically extended along the direction of the hatching. The effect of the cohesive boundary is to strengthen the matrix adjacent to the stiff inclusion compared to the matrix further away. Therefore, as indicated by the progressively lighter shading, the magnitude of the finite strain in the matrix decreases towards the inclusion; in this case the Athabasca lozenge.

features of the synkinematic emplacement of some of the granite units and mafic dykes which warrant closer examination, for example, the control exerted by the displacement of the upper deck on the emplacement of the Clut, Melby-Turnbull, and McGillivray granites. This entails a certain degree of feedback because examination of the emplacement of these granite bodies also sheds light on the complex structural evolution of the upper deck/lower deck interface. Subsequently, the relationship between transpressive shear and the emplacement of the Chipman dykes will be addressed.

Granites, extension, and accretion

The eastern part of the interface between the upper and lower decks is occupied by the Clut granite (Fig. 131). The granite was mylonitized at amphibolite facies, during extensional shearing which accommodated southwest-directed displacement of the upper deck. Because the Clut granite contains no trace of relict pyroxenes, it was emplaced after granulite facies mylonitization of the East Athabasca mylonite triangle. Therefore, during the amphibolite facies mylonitization, the upper deck was apparently displaced as a coherent, relatively stiff hanging wall above a localized extensional shear zone. The spatial relationship between the thickest part of the Clut granite and the trailing edge of the upper deck is more than a coincidence. The granite is located at the site of dilation which would result from the top-down to the southwest displacement of the stiff upper deck (Fig. 131). In other words, the emplacement of the Clut granite was syntectonic with respect to the amphibolite facies displacement of the upper deck.

The Clut granite extends westward into the lower deck as the Melby-Turnbull granites (Fig. 131). The latter were syn-tectonically emplaced exclusively within narrow dextral shear belts and variably mylonitized at amphibolite facies (see "Hornblende-biotite granitoid bodies"). Because the dextral shear plane in the Melby-Turnbull granites is subparallel to the dextral lateral ramp of the upper deck, the deformation within the lower deck is kinematically compatible, as well as materially continuous, with the deformation fabric in the Clut granite beneath the upper deck (Fig. 131). However, because the mylonite zones containing the Melby-Turnbull granite sheets lie clockwise of the lateral ramp, they would have experienced a component of dilation across the shear plane in response to the displacement of the upper deck,

which would have assisted magma emplacement. In other words, the Clut and Melby-Turnbull granites were emplaced into a belt of anastomosing dilational loci, dynamically determined by the relative displacement of the upper deck.

The McGillivray granite is also located adjacent to the trailing edge of the upper deck (Fig. 132). It cuts and includes xenoliths and rafts of already mylonitic Clut granite. However, the mylonitic foliation within the Clut granite bifurcates around the McGillivray pluton (Fig. 110). This indicates that the McGillivray granite exerted a mechanical influence on the pattern of tectonic flow within its wall rocks prior to its final emplacement, presumably during its ascent. It appears that the McGillivray granite was emplaced into a steeply oriented dilational zone, during the amphibolite facies displacement

Figure 131.

Distribution of the Clut and Melby-Turnbull granites in relation to the displacement (arrows) and disposition of the lateral ramp and trailing edge (see Fig. 10) of the upper deck. See Figure 113 for location.

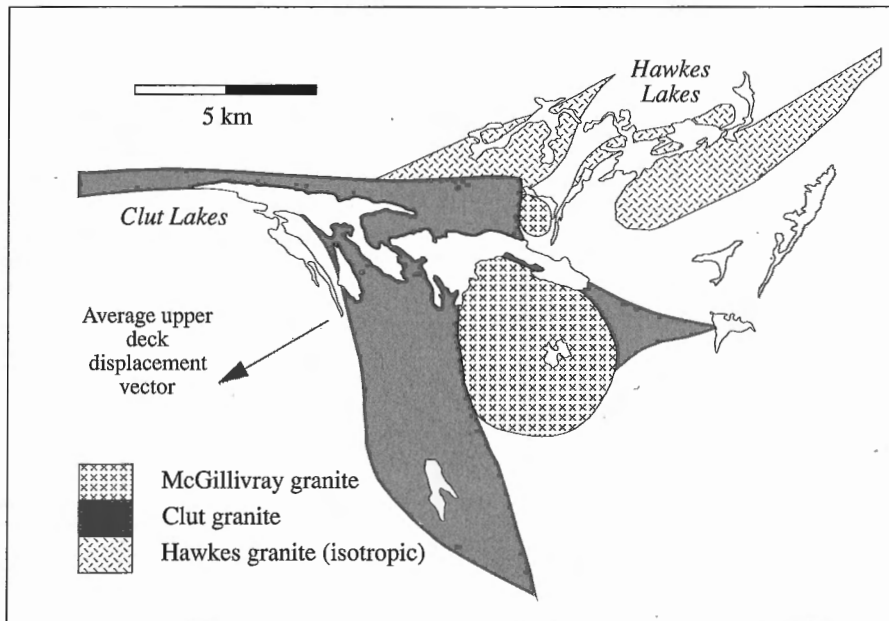
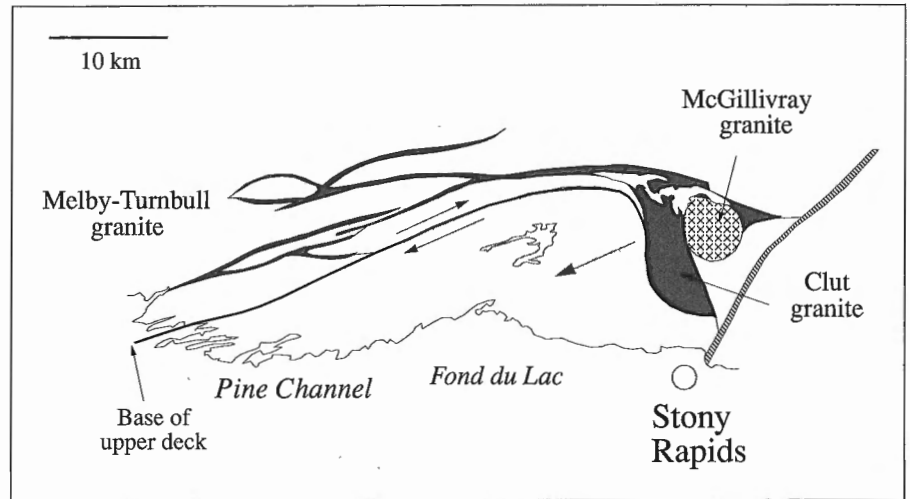


Figure 132.

Detail of Figure 131 to highlight the bifurcation of the Clut granite around the apparently younger McGillivray granite and the location of the thickest part of the Clut granite, the McGillivray granite, and the isotropic Hawkes granite opposite the trailing edge of the upper deck. See Figure 100 for location.

of the upper deck, while the Clut granite was actively deforming along a shallowly dipping shear plane. The present postkinematic outcrop pattern simply reflects the final stages of its emplacement history.

As already explained, the initial lower contact of the upper deck was probably located along the line now occupied by the Robillard-Patterson gneiss and the Godfrey granite (Fig. 115; see “Dip-slip shear zone (upper deck)”). Subsequent granulite facies flow in the upper deck was decoupled from flow in the lower deck, as evidenced by the discordant relationships in the Clut Lakes area. The southern branch of the amphibolite facies Melby-Turnbull granites lies parallel to the interface between the upper and lower decks, but within the lower deck (Fig. 131). In effect, during the amphibolite facies displacement, part of the lower deck was parautochthonously accreted to the upper deck. This is the reverse of the normal sequence observed in extensional faults (e.g. Davis et al., 1986; Gaudemer and Tapponier, 1987; Davis, 1988; Harms and Price, 1992). It is suggested that this is, in part, a reflection of the influence of earlier structures in the footwall, but also a consequence of complex mechanical interaction between the regional deformation field and local deformation fields associated with the intruding magmas. If this is valid, then deep-seated segments of extensional shear zones may not conform to the simple distribution of temperature-sensitive and pressure-sensitive deformation structures associated with their shallower equivalents.

Mafic dykes and transpression

The emplacement of mafic dyke swarms is commonly interpreted in terms of extensional tectonics (e.g. Wolf and Saleeby, 1992). In view of the dilation required to permit emplacement of dykes tens of metres thick, this would seem to be a reasonable interpretation. However, this interpretation assumes that the dilation vector was oriented at a high angle to the dyke wall. Such an assumption is not necessarily justified (e.g. Beach and Jack, 1982). It has already been noted that the Chipman dykes present a range of deformation states and are demonstrably syntectonic with respect to the formation of the annealed (straight gneiss) mylonites in the tonalitic Chipman batholith (see “Chipman dykes”). The transposition and dismemberment of the most strongly deformed dykes precludes interpretation of the mechanism and kinematics of their emplacement. However, the least deformed examples preserve a systematic and kinematically significant geometry. Although statistically significant, quantitative measurements were not made, it is clear that the majority of the least deformed Chipman dykes were initially emplaced along fractures oriented 15-25° anticlockwise with respect to the banding of the tonalitic straight gneiss host rocks (Fig. 133). The rest were either concordant to the host banding, or made a clockwise angle of about 15-20° (Fig. 134).

When present, the asymmetry of flame-like apophyses (horns or bayonets) is constant on a given dyke contact, and is mirrored from one side of the dyke to the other. The asymmetry of the apophyses is a direct reflection of the systematic offset and overlap of the initial crack array from which the dyke-filled fracture developed (Fig. 135; e.g. Nicholson and Pollard, 1985). The

sense of offset, or stepping, of en-relais cracks, making a very low angle with the boundaries of the array, is a function of the sign of the shear stress resolved along the array (e.g. Segall and Pollard, 1980). Because of the asymmetrical distribution of the mean stress around the tip of a crack along which shear stress is resolved, sinistral shear favours left-stepping fracture arrays (Fig 135). In the field, asymmetrical apophyses systematically indicate that the anticlockwise dykes were emplaced into left-stepping (sinistral) fracture arrays. Of the clockwise dykes which preserve asymmetrical apophyses, most were emplaced into right-stepping (dextral) fracture arrays. However, two examples where clockwise dykes were clearly emplaced into left-stepping (sinistral) arrays were observed.

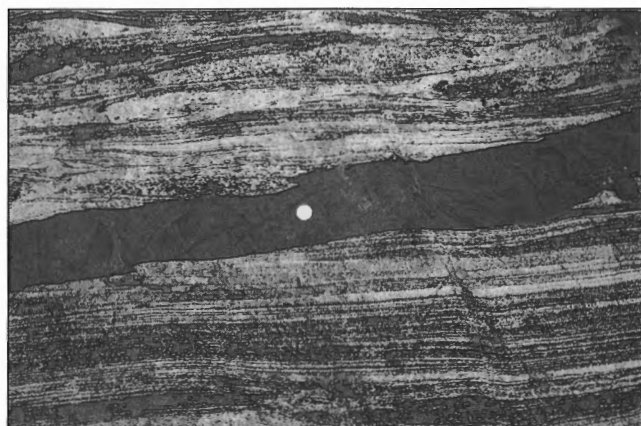


Figure 133. Chipman dyke cutting anticlockwise across annealed tonalite mylonite (straight gneiss) at low angle, Chipman tonalite batholith, Chipman Lake. Note the opposed asymmetrical apophyses on either side of the dyke indicative of magma emplacement into a left-stepping array of en relais fractures (see Fig. 135). Coin for scale 2.5 cm. GSC 1993-221B



Figure 134. Chipman dyke cutting clockwise across annealed tonalite mylonite (straight gneiss) at low angle, Chipman tonalite batholith, Woolhether Lake. Hammer for scale. GSC 1994-151

These observations indicate that the Chipman dykes were emplaced into the tonalitic straight gneiss of the Chipman batholith during active sinistral shear. Fracturing of the otherwise plastic gneisses would have occurred during transient excursions into the brittle deformation field (Sibson, 1980), possibly induced by the effect of the forcible emplacement of the pressurized dyking magma on strain rate, or on effective

pressure. The angular symmetry of the dykes with respect to the straight gneiss banding, and the opposing sense of shear resolved on some of the clockwise and anticlockwise dykes, are suggestive of a component of shortening along the obtuse bisector, i.e. normal to the flow plane in the tonalitic host rocks. However, this raises a classical problem in fracture mechanics wherein the shortening direction should theoretically lie along the acute bisector of a pair of conjugate cracks. Moreover, one must account for the skewness of the orientation frequency distribution in favour of the anticlockwise dykes, and for the presence of left-stepping (sinistral) clockwise fracture arrays.

It is suggested here that the fracture arrays into which the Chipman dykes were emplaced correspond to the Riedel R and P planes predicted for sinistral shear (e.g. Logan, 1979; Gamond, 1983), which formed under conditions of sinistral transpression (Fig. 135). The transpressive component is required to account for the antithetic slip along many of the P planes. It is also predictable from the S>L symmetry of the straight gneiss fabrics. Synthetic slip along P planes requires that the system is able to extend (dilate) across the bulk shear plane (Gamond, 1983). Such transverse dilation would not be favoured by transpression and may only occur transiently in response to fluctuations in effective pressure. On the other hand, synthetic slip along R planes requires that the system can extend along the bulk shear plane and would be compatible with transpression. In brief, the Riedel model would predict that the majority of fracture arrays in the Chipman example should lie anticlockwise with respect to the host gneiss fabric, and be composed of left-stepping segments, as is indeed the case. Post-emplacement sinistral shearing would result in the synthetic rotation of the clockwise dykes into the bulk flow plane, whereas the anticlockwise dykes would rotate antithetically toward the same final orientation (e.g. Hanmer and Passchier, 1991).

A transpressive Riedel fracture model for dyke emplacement has important consequences for the tectonic significance of dyke swarms in general. Rather than assuming that they are indicative of far-field tectonic extension, dyke swarms should be investigated for compatibility with shearing deformations where the stretching direction, or fracture dilation vector, makes a low angle with respect to the bulk flow plane. With respect to the East Athabasca mylonite triangle, a practical outcome of this discussion is the identification of the Chipman dykes as widespread shear-sense criteria to further justify that the Chipman straight gneiss formed in a sinistral shear zone.

STRIDING MYLONITE BELT

In contrast to the East Athabasca mylonite triangle, which represents a volume of tectonite developed at the northeastern apex of the Athabasca lozenge, exposure of the Snowbird tectonic zone in the Northwest Territories offers ready access to the interior of the Selwyn lozenge, as well as to the flanking mylonite (Fig. 136; Hanmer and Kopf, 1993). The quality of exposure decreases rapidly northeast of Snowbird Lake, to the extent that the location of a single large outcrop along the

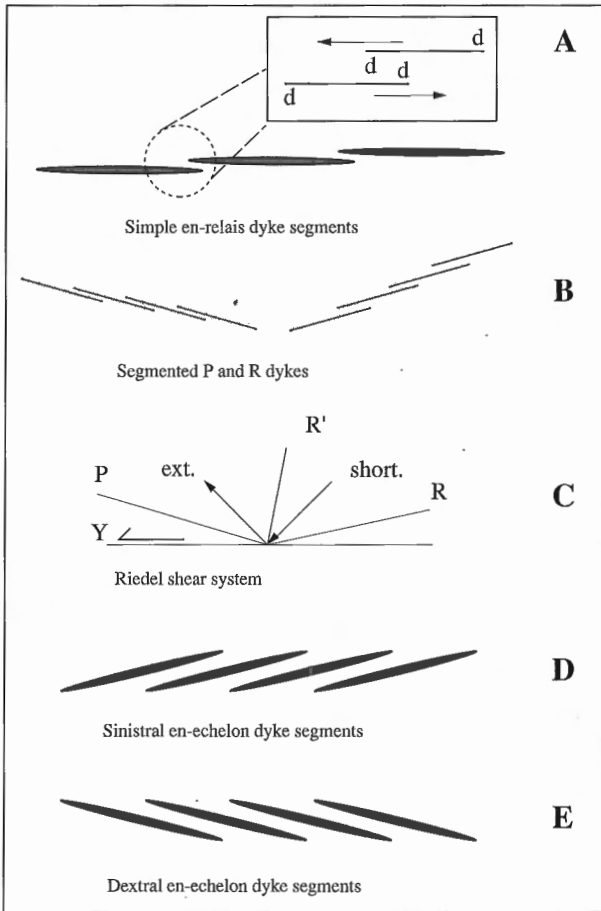


Figure 135. Schematic illustrations of the relationships between en relais fracture patterns, Riedel faults, and segmented dykes, and the contrast with en echelon arrays. The bulk shear plane is horizontal in all cases. **A:** The sense of stepping of overlapping en relais fractures is influenced by the shear sense of the bulk deformation (inset) because initiation of successive fractures is enhanced in the dilatational quadrants (d) at the tips of existing fractures in the array. Therefore, sinistral en relais fracture arrays are left-stepping. Dilation of such fracture arrays by mafic magmas will lead to formation of simple en relais dyke segments. **B:** By combining the concept of en relais fractures with the Riedel fault system **C:** one can account for segmented dykes which lie both clockwise (Riedel P) and anticlockwise (Riedel R) with respect to the bulk shear plane, but show a consistent sense of stepping (ext. and short. are the principal directions of instantaneous extension and shortening, respectively). **D and E:** Compare en echelon dyke segments formed during sinistral and dextral shear with the en relais patterns of A.

magnetically determined southeastern flank of the Three Esker lozenge is truly serendipitous (Fig. 136). Accordingly, Selwyn lozenge offers the best opportunity to directly examine the geology of the geophysically defined lozenges in the study area (however, see Lewry and Sibbald, 1977, 1980 and references therein). Because the lozenges strongly influence the distribution and orientation of the mylonite (see below), the description of the Striding mylonite belt will begin with an examination of the Selwyn lozenge.

Selwyn lozenge

The Selwyn lozenge (125 x 50 km) is lithologically diverse. Its western and northern parts are principally composed of homogeneous to banded amphibolite, abundant hornblende, and diopside pyroxenite, all intruded by a network of leucodiorite to tonalite veins (Fig. 137), or metagabbro intruded by folded granitic veins and crosscutting lamprophyre dykes. Its eastern margin at Striding River (Fig. 136) is composed of an extensive, monotonous, fine grained, annealed mafic granulite of uncertain origin. The extent of the mafic to intermediate lithologies has been underestimated in previous mapping, where they

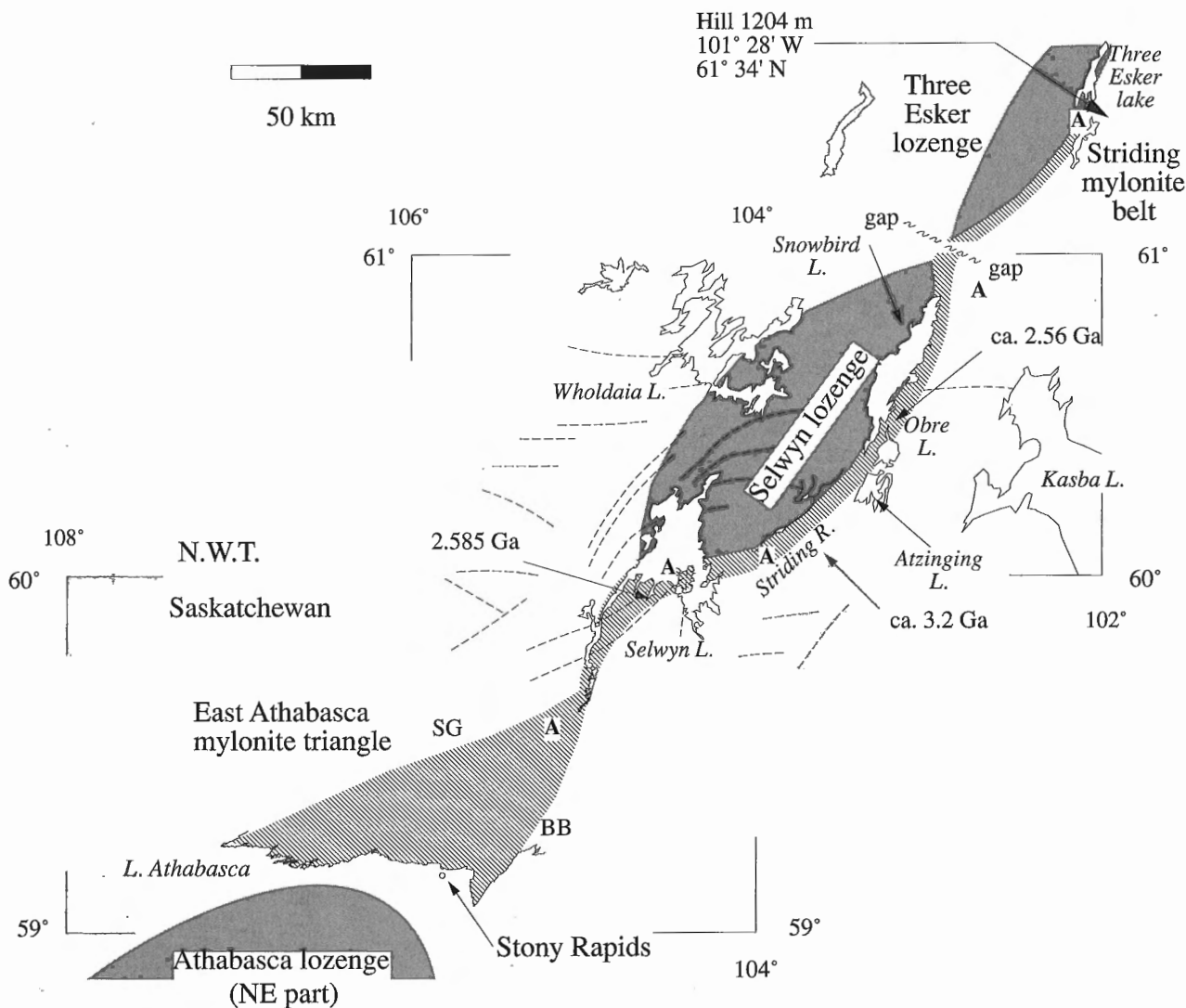


Figure 136. Schematic diagram of the Striding mylonite belt to illustrate its relationship to the principal tectonic elements of the Striding-Athabasca mylonite zone. Uranium-lead zircon magmatic crystallization ages are indicated in Ga. Note the spatial distribution of laterally continuous, extensive high grade mylonites (oblique line rule) with respect to the magnetically defined crustal-scale Athabasca, Selwyn, and Three Esker lozenges (grey shading; drawn from Geological Survey of Canada, 1987). SG, Straight-Grease fault; BB, Black-Bompas fault. Occurrences of anorthosite (A) are indicated. Note also that the grid of latitudes and longitudes is only valid south of Snowbird Lake.

have generally been represented as undifferentiated paragneiss (Taylor, 1963, 1970). The southern end of the lozenge at Selwyn Lake (Fig. 136) is composed of variably deformed hornblende diorite to granodiorite. West of Snowbird Lake (Fig. 136), the lozenge is predominantly composed of irregularly folded migmatitic granitoid orthogneiss, or granodioritic gneiss with multiple phases of variably deformed granitoid veins and intrusions (Fig. 138). Coarse grained garnet-sillimanite diatexite and foliated gneissic granitoid rocks occur throughout the lozenge.

Within the Selwyn lozenge, foliation trends are curvilinear with a significant east-west component, clearly discordant to the magnetically determined lozenge boundaries, and not noticeably distinct from the structural trend pattern in the wall rocks (Fig. 136). For the most part, the rocks are not strongly deformed. They preserve crosscutting relationships, open fold profiles, and igneous textures in foliated plutonic rocks (Fig. 139, 140). In the case of the plutonic rocks, it is uncertain whether their deformation state is a reflection of the magnitude of the total regional strain, or the timing of their intrusion with respect to the deformation history (Fig. 141). The principal exception to the foregoing concerns the monotonous mafic granulite facies rocks northwest of Striding River (Fig. 136) which texturally and compositionally resemble

the annealed granulite facies ultramylonite derived from a norite protolith in the East Athabasca mylonite triangle (e.g. Fig. 71). However, no protolith was identified in the Striding River case and the structural significance of the textures there remains unresolved.



Figure 137. Weakly deformed array of tonalite veins cutting amphibolite, Wholdaia Lake. Lens cap for scale. GSC 1992-241Q

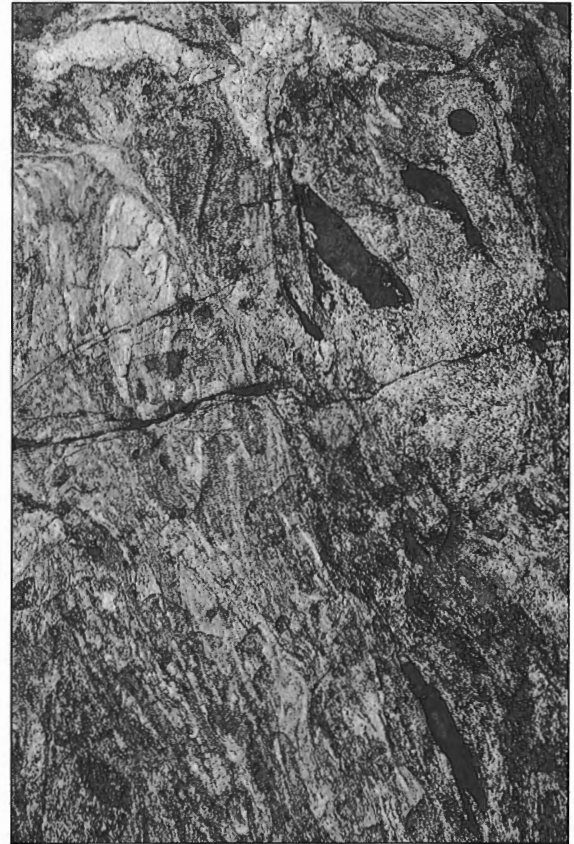


Figure 138. Geometrically complex migmatitic gneiss with irregularly shaped, angular inclusions, Wholdaia Lake, to illustrate absence of transposition. Lens cap for scale. GSC 1992-241C

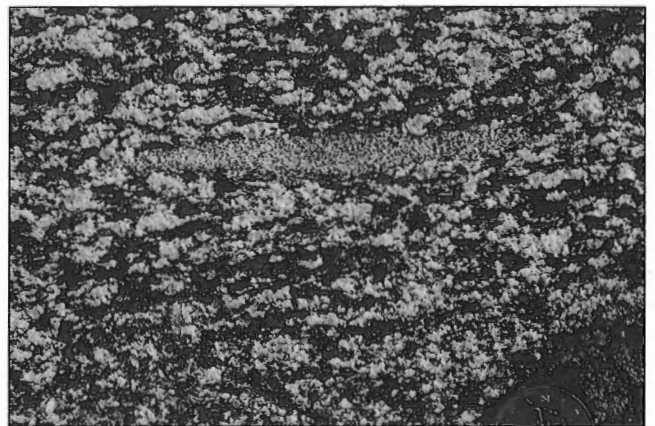


Figure 139. Microgranular xenolith in garnetiferous gabbro/diorite to illustrate weakly developed foliation, Lone Lake, east of Wholdaia Lake. Coin for scale 2.5 cm. GSC 1992-241D

Striding mylonite belt

A belt of through-going upper amphibolite to granulite facies (two pyroxene-garnet±sillimanite) mylonite occurs along the southeastern side of the Selwyn lozenge, from Selwyn Lake, via Striding River, to the north end of Snowbird Lake (Fig. 136). The trace of the mylonite belt is remarkably sinuous, describing two right-angle bends as it closely follows the margin of the Selwyn lozenge. The mylonite (Fig. 142) runs from the East Athabasca mylonite zone, north along the southern arm of Selwyn Lake. The belt swings eastward across the middle of Selwyn Lake (Fig. 143, 144), then returns to a northeast trend along Striding River (Fig. 145, 146) and southern Snowbird Lake (Fig. 147). Approaching the northern part of the Snowbird Lake (Fig. 148-151), the mylonite turns to a northward strike. The isolated outcrop at Three Esker Lake (Fig. 152), in combination with regional geological trends (see Wright, 1967), suggests that the highly sinuous character of the trace of the mylonite belt persists to, at least, 61°30'N latitude.

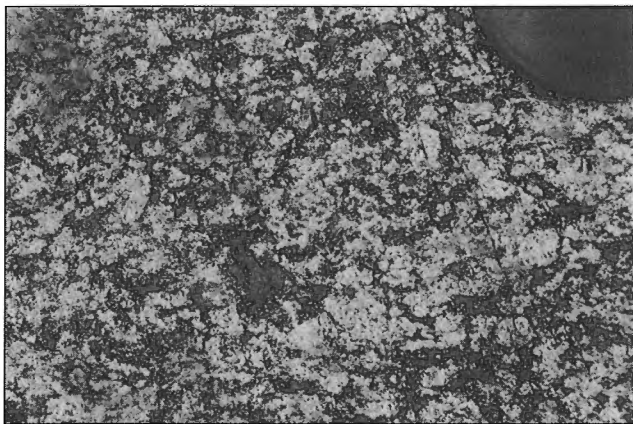


Figure 140. Near-isotropic garnet-clinopyroxene granite, Wholdaia Lake. Lens cap for scale. GSC 1992-241J

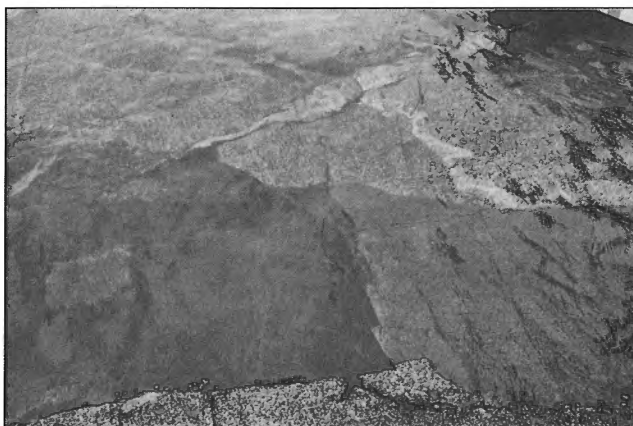


Figure 141. Postkinematic lamprophyre dyke (foreground, about 1 m thick) cutting across granitic veins (light grey) intruded into weakly foliated gabbro/diorite (see Fig. 139), Lone Lake, east of Wholdaia Lake. GSC 1994-165



Figure 142. Granitic ribbon mylonite with large feldspar porphyroclast (centre), south arm of Selwyn Lake. Coin for scale 2.5 cm. GSC 1994-200



Figure 143. Flaggy banded ribbon mylonite derived from diatexite, central Selwyn Lake. Note absence of porphyroclasts. Reflection of outboard motor for scale. GSC 1992-241F

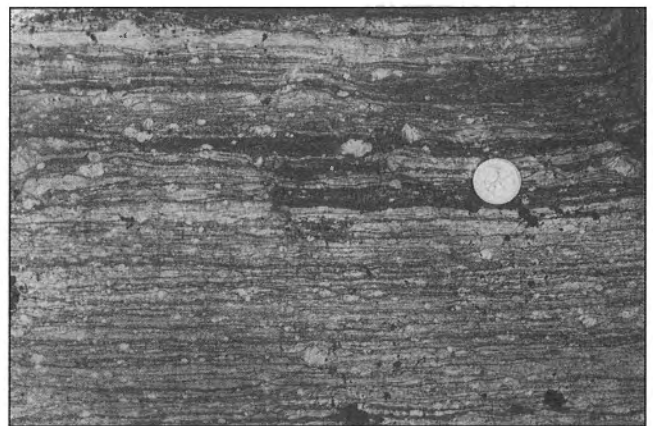


Figure 144. Porphyroclastic ribbon mylonite derived from granite protolith, Parkhurst Peninsula, east Selwyn Lake. Coin for scale 2.5 cm. GSC 1992-241B



Figure 145. Garnet-clinopyroxene anorthosite ribbon mylonite, Striding River. Note absence of porphyroclasts and the thin garnet clinopyroxenite layer (bottom). Coin for scale 2.5 cm. GSC 1992-241P



Figure 148. Garnet-clinopyroxene anorthosite ribbon mylonite with garnet-clinopyroxenite bands, north Snowbird Lake. Coin for scale 2.5 cm. GSC 1994-211

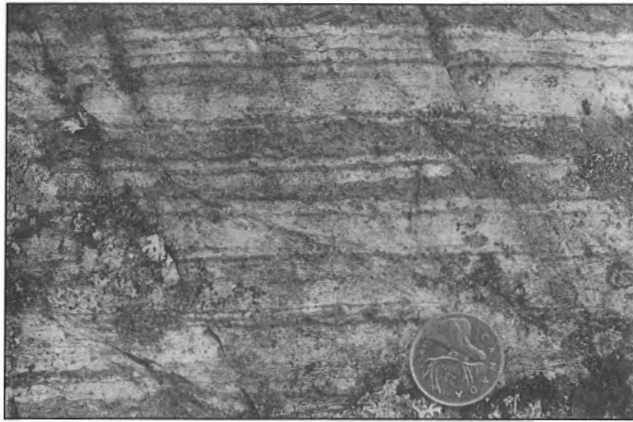


Figure 146. Garnet-clinopyroxene anorthosite ribbon mylonite with garnet clinopyroxenite bands, Striding River. Coin for scale 2.5 cm. GSC 1994-203

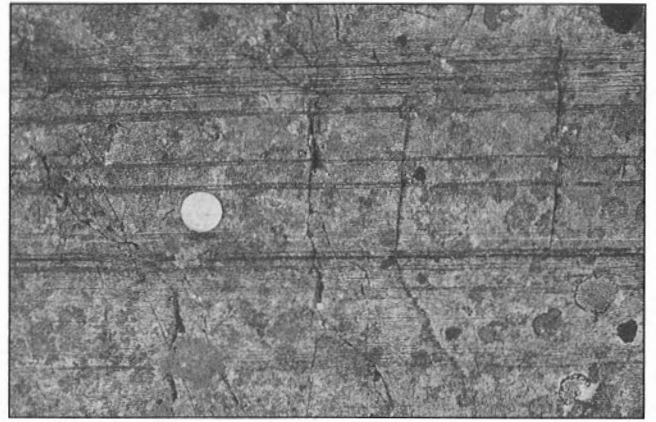


Figure 149. Garnet-clinopyroxene anorthosite ribbon mylonite with extremely thin attenuated garnet clinopyroxenite bands, north Snowbird Lake. Note absence of porphyroclasts. Coin for scale 2.5 cm. GSC 1994-163



Figure 147. Sheets of leucogranite ribbon mylonite (white) in ribbon mylonite of paragneissic origin, south Snowbird Lake. Note absence of porphyroclasts. Coin for scale 2.5 cm. GSC 1994-210



Figure 150. Detail of garnet-clinopyroxene anorthosite ribbon mylonite, north Snowbird Lake. The dark grey streaks are garnet-clinopyroxene aggregates. Coin for scale 2.5 cm. GSC 1992-241V

The belt of penetratively developed mylonite is apparently 5 to 10 km thick, except at Selwyn Lake where it bifurcates into two thinner strands (Fig. 153). It is associated with an upright S>>L mylonitic foliation and layering, a subhorizontal extension lineation and consistently dextral shear sense (Fig. 154, 155). Although compositionally diverse along the southwest arm of Selwyn Lake, from mid-Selwyn Lake to Three Esker Lake, the mylonite is principally derived from diatexite, anorthosite and mafic rocks, and granite (Hanmer and Kopf, 1993).

At three locations along the Striding mylonite belt, U-Pb analysis of magmatic zircon in syntectonic granite indicates that the mylonite is Archean in age (Table 1). First, at the southern end of Snowbird Lake (Fig. 136), ribbon mylonite of uncertain, perhaps diatexitic, protolith is cut by coarse grained, white leucogranite. An earlier phase of leucogranite is a ribbon mylonite (Fig. 147), cut by a later, more porphyroclast-rich mylonitic phase of similar granite. The leucogranite bodies are considered to be related, and thereby contemporaneous with mylonitization. Accordingly, the approximate magmatic crystallization age of 2558 ± 25 Ma (Table 1) obtained from the porphyroclastic granite mylonite suggests that the mylonitization is Late Archean.

The Striding mylonite belt bifurcates in the southern half of Selwyn Lake (Fig. 153). To the south, the two strands coalesce just north of their confluence with the apex of the East Athabasca mylonite triangle (Fig. 136). In the north-western strand, north-trending mylonite occurs along the south arm of Selwyn Lake and swings progressively to strike east across the centre of the lake, while the southeastern strand strikes about 045° . Most of the mylonite is present as annealed, slabby quartz leucodioritic-amphibolite straight gneiss (Hanmer, 1988b), locally with excellent preservation of feldspar porphyroclasts and quartz or feldspar ribbons. However, the east-striking mylonite in the central part of the lake is principally ribbon ultramylonite, derived from garnet-sillimanite diatexite and garnet anorthosite protoliths (Fig. 143). The annealed mylonite is cut by an array of 1 to 10 m thick sheets of generally concordant pink biotite granite in various states of deformation, even within a given outcrop.

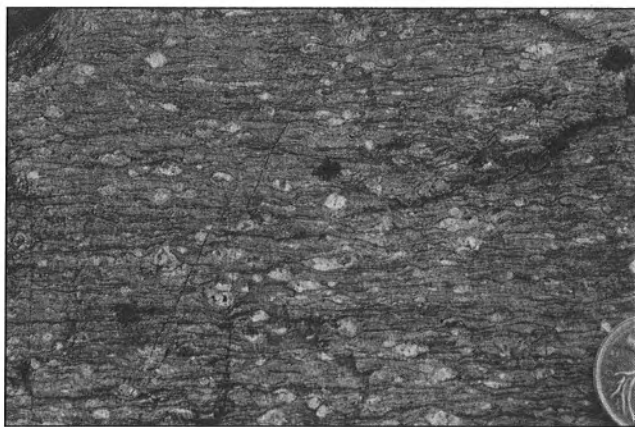


Figure 151. Porphyroclastic granite ribbon mylonite, north Snowbird Lake. Coin for scale 2.5 cm. GSC 1992-241U

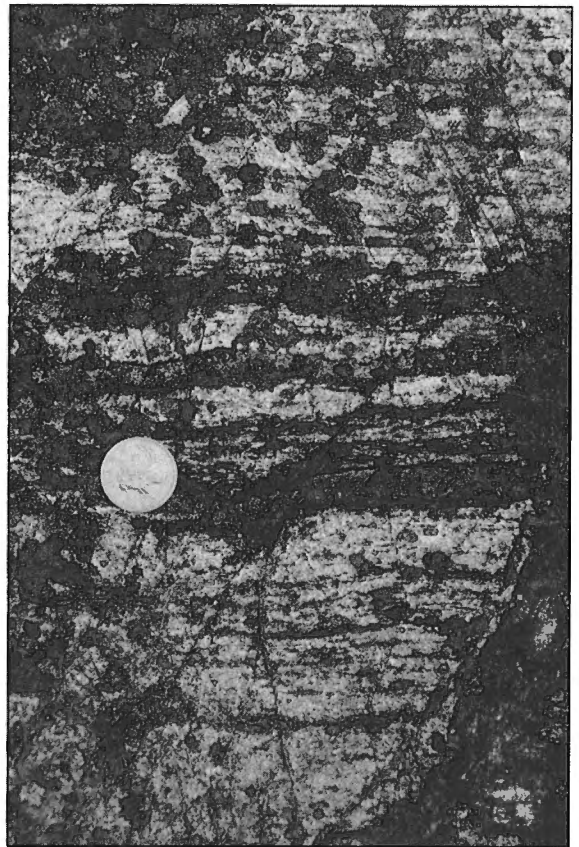


Figure 152. Garnet-clinopyroxene anorthosite ribbon mylonite, Three Esker Lake. Compare with Figure 145. Coin for scale 2.5 cm. GSC 1994-164

The most strongly deformed granite sheets are garnetiferous ribbon ultramylonite (Fig. 142), which are themselves locally cut by less deformed sheets of similar granite. The mylonite in both strands dips moderately to the west and north, carries a subhorizontal extension lineation, and was formed by dextral transcurrent shear.

The two strands of mylonite are separated by a body of coarse-grained, isotropic biotite granite (Fig. 153). The marginal zone between the granite and the mylonites is composed of the isotropic to poorly foliated granite with large (hundreds of metres long by tens of metres thick) rafts of annealed leucodioritic-amphibolite straight gneiss, somewhat coarser grained than the adjacent material outside of the granite, but still recognizable as the same rocks. The rafts are oriented parallel to the external mylonite, except at the northeastern termination of the granite where they have been re-oriented into parallelism with the pluton contact. The location of the granite just south of a right-handed, near-right angle bend in the dextral mylonite is surely no coincidence. Such a position would correspond to a releasing bend, or dilational jog (e.g. Sibson, 1986a, b), an excellent site for magma emplacement (e.g. Guinberteau et al., 1987; Hutton, 1988; Hutton et al., 1990; Morand, 1992). Therefore, it is suggested that emplacement of the granite was late syntectonic with respect to the high grade mylonitization. As noted above, outside of

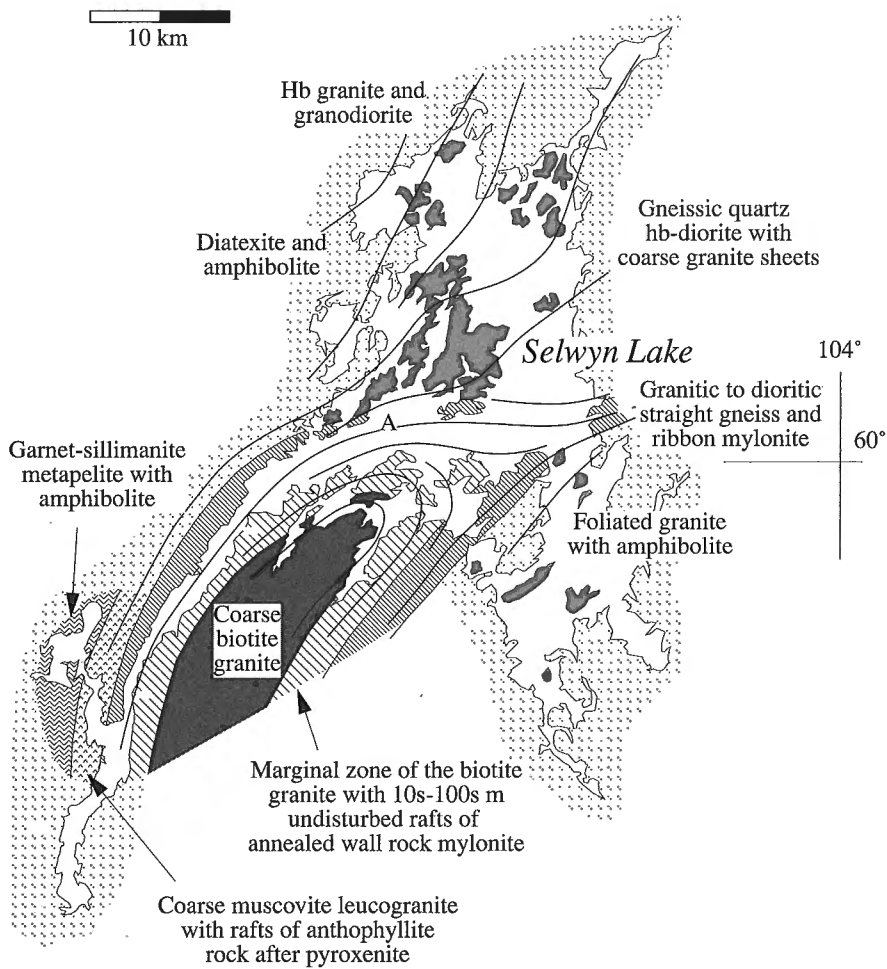


Figure 153. Geological sketch of the bifurcation and 90° bend in the mylonite of the Striding mylonite belt at Selwyn Lake. Thin lines are foliation trajectories. A = anorthosite, hb = hornblende. Discussed in text.



Figure 154. Porphyroclastic granitic ribbon mylonite, central Selwyn Lake. Looking down at horizontal surface. The disposition of the polycrystalline wings on the two feldspar porphyroclasts in the centre indicate dextral shear sense. Coin for scale 2.5 cm. GSC 1992-241A

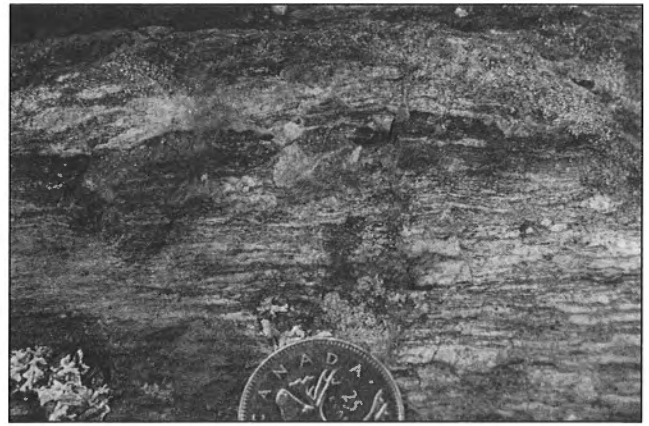


Figure 155. Porphyroclastic granitic ribbon mylonite, Striding River. Looking down at horizontal surface. The disposition of the polycrystalline wings on the feldspar porphyroclast (top centre) indicates dextral shear sense. Coin for scale 2.5 cm. GSC 1994-209

the main body of granite, the straight gneiss wall rocks are cut by veins of similar granite, which vary from isotropic and crosscutting, to concordant ribbon mylonite. If these granite sheets were related to the main granite, it would imply that the final emplacement of the pluton was preceded by its own vein cortege, and that the granite is in fact syntectonic with respect

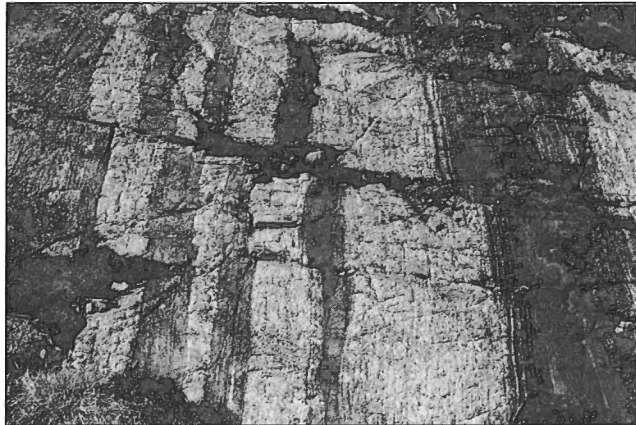


Figure 156. Leucogranite ribbon mylonite with straight bands of mafic granulite, east of Striding River (Fig. 136). Fore-ground long side of photograph about 3 m. GSC 1992-241H

to the Striding mylonite belt. Accordingly, the magmatic crystallization age of 2585 ± 2 Ma (Table 1) obtained from the granite would indicate the approximate time of mylonitization.

Five kilometres east of the Striding River (Fig. 136), pink leucogranite ribbon mylonite with locally boudined garnet-amphibolite and mafic granulite bands (Fig. 156; 2 pyroxene-garnet) contains coarse grained, foliated pink leucogranite in the interboudin necks. The syntectonic interboudin material has been dated at ca. 3.3-3.1 Ga. Allowing for the imprecision of the determined ages (see Hanmer et al., 1994), the three syntectonic age determinations (Table 1) indicate that the high grade Middle and Late Archean deformation events in the contiguous East Athabasca mylonite triangle (Hanmer et al., 1994) are broadly correlative with those recorded by the Striding mylonite belt. The important point being made here is that the mylonite units are not Early Proterozoic.

Selwyn lozenge, northwest margin

The magnetic expression of the northwestern margin of the Selwyn lozenge is discrete and trends north-northeast through the middle of Wholdaia Lake (Fig. 136). However, it does not coincide with any simple geological feature (Fig. 157). The western shore of the lake is underlain by a

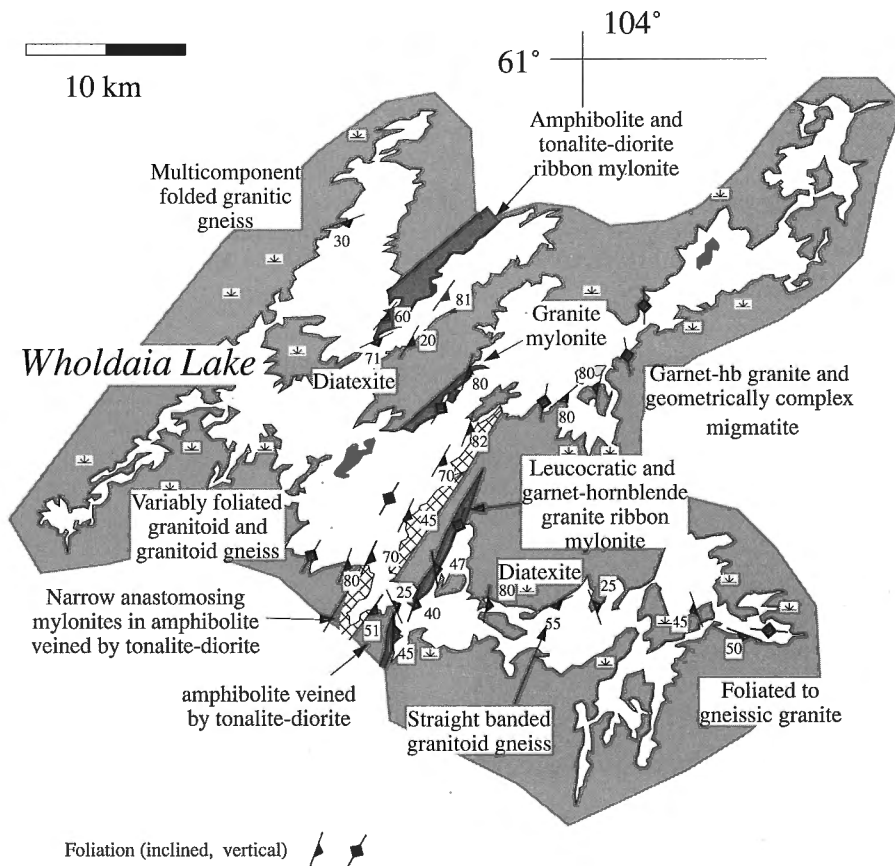


Figure 157. Sketch of the geology at Wholdaia Lake with foliation data marked (discussed in text); hb = hornblende.

granitic gneiss, with folded banding and folded, crosscutting granitic veins. The overall strike of foliation and layering here is discordant to the general trends of laterally discontinuous mylonite strands (Fig. 158) in the central part of the lake, associated with an upright foliation, subhorizontal extension lineation, and dextral sense of shear (see Fig. 160). Similarly, in the southeast arm of the lake, poorly foliated diatexite and foliated to gneissic granite are also structurally discordant with respect to the mylonite. It would appear that the mylonite *should* define the geological limit of the Selwyn lozenge, separating wall rock gneiss on the western lake shore from the lozenge interior on the eastern side of the lake. Although the mylonite is very well developed at the outcrop scale, it does *not* define the lozenge boundary. Thickness may exceed hundreds of metres, but the mylonite is discontinuous and does not extend beyond Wholdaia Lake.

The best developed individual strand of mylonite underlies a recently burned ridge, 10 km long (cross hatched pattern in Fig. 157). Ribbon mylonite units, developed from two distinct granite bodies are penetratively developed in a 500 m thick

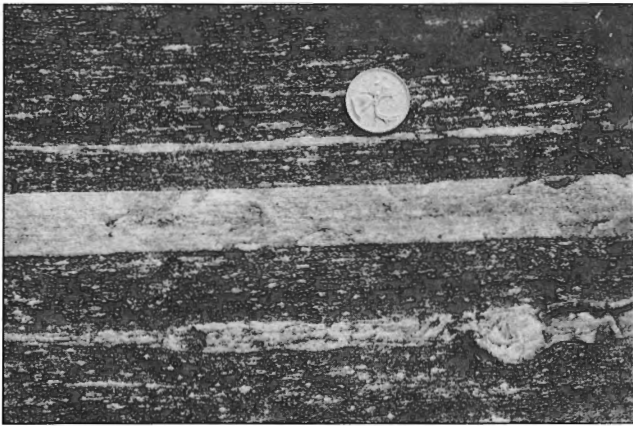


Figure 158. Porphyroclastic ribbon mylonite derived from diorite and granitic sheets (light grey), Wholdaia Lake. Coin for scale 2.5 cm. GSC 1992-241R

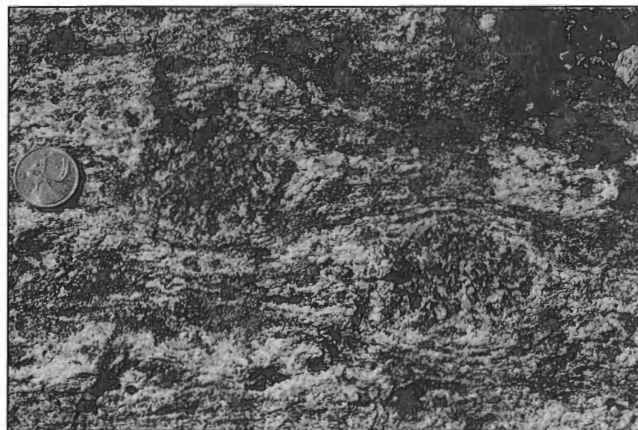


Figure 159. Large garnets, riddled with quartz inclusions, in streaky mylonite derived from garnet-pyroxene granite, Wholdaia Lake. Coin for scale 2.5 cm. GSC 1994-167

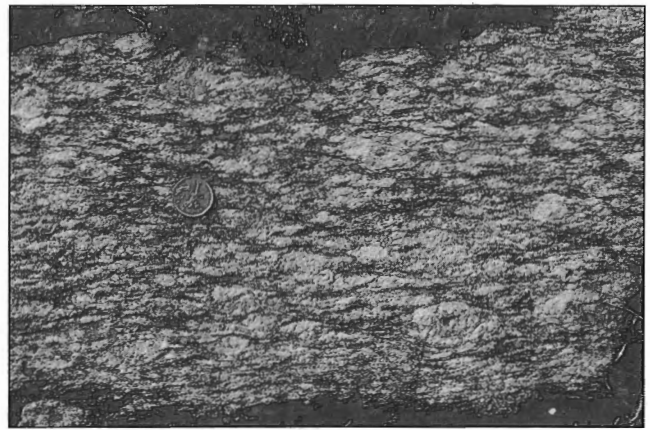


Figure 160. Protomylonite with well preserved, very coarse feldspar porphyroclasts, Wholdaia Lake. Looking down on horizontal surface. Note the asymmetrical extensional shear bands (top-left to bottom-right), cutting across the principal foliation (horizontal) and indicating dextral shear sense. Coin for scale 2.5 cm. GSC 1994-168

belt. The older granite is superficially very similar to melanocratic parts of the Mary granite in the East Athabasca mylonite zone. It is hornblende-garnet-clinopyroxene-orthopyroxene-bearing, with well defined ribbons and streaky feldspar aggregates. Relict feldspar porphyroclasts indicate that the parent rocks grain size was coarse, on the order of 2 to 4 cm, but the mylonite may contain 5 cm garnet crystals (Fig. 159). This mylonite is cut by a very coarse protomylonitic garnet-clinopyroxene-bearing leucogranite with feldspar megacrysts larger than 5 cm (Fig. 160). In low strain windows, it forms concordant sheets of foliated granite to protomylonite in a uniformly mylonitic host. Mostly, it forms concordant pink bands of garnet-clinopyroxene ribbon ultramylonite (Fig. 161). This field relationship suggests that the leucogranite was emplaced during granulite facies mylonitization. The 1907 ± 8 Ma (Table 1) magmatic crystallization age for the granite indicates the approximate timing of granulite facies mylonitization.

MYLONITIZATION

Shear zone geometry

Mylonite fabrics are penetratively developed throughout the Striding-Athabasca mylonite zone. Unlike other large-scale shear zones (e.g. Great Slave Lake shear zone; Hanmer, 1988a; Hanmer et al., 1992a), the geometry and the kinematic pattern of the Striding-Athabasca mylonite zone are complex (Fig. 10, 11, 136), though tractable. Shear-sense indicators are present throughout the mylonite (see above). Many examples of these shear-sense indicators are diagnostic of transpressive general noncoaxial flow (kinematical vorticity number $w_k < 1$; e.g. Means et al., 1980; Hanmer and Passchier, 1991) at the scale of observation (e.g. in-plane δ -porphyroclasts and asymmetrical extensional shear bands; see detailed discussions in Hanmer, 1990; Hanmer and Passchier, 1991). At the map scale, combined, apparently complex flow along the



Figure 161. Garnet-clinopyroxene granite ribbon mylonite, Wholdaia Lake. The garnets form dark clusters while the clinopyroxene forms narrow chain-like ribbons. Coin for scale 2.5 cm. GSC 1994-166

three coeval shear zones in the East Athabasca mylonite triangle indicates that the bulk finite strain ellipsoid lies in the prolate symmetry field. This corresponds to the flow pattern expected adjacent to the apical region of a rigid ellipse subjected to northeast directed extensional flow. In comparison, the relatively simple $S \gg L$ fabrics in the Striding mylonite belt indicate more oblate finite strains. However, the apparent simplicity of the Striding mylonite belt is complicated by the existence of the two near right-angle bends in the map trace of the mylonite zone along the southeastern margin of the Selwyn lozenge (Fig. 136). If these bends are primary, rather than the result of modification of a once straight shear zone, they must have imposed severe constraints on the ability of the mylonite to accommodate significant wall rock displacements. Alternatively, there are three principal deformation scenarios which could have led to the geometrical modification of a hypothetically initially straight Striding mylonite belt: (i) heterogeneous shortening (folding), (ii) heterogeneous extension (boudinage) and (iii) brittle disruption (Fig. 162). In what follows, each of these scenarios is critically evaluated.

Crustal-scale folding of the mylonite belt could be accomplished by flexural slip or by internal tangential longitudinal strain (e.g. Ramsay, 1967, p. 391-403). The simplest argument against modification of an initially straight mylonite zone by heterogeneous shortening is provided by the colinearity of the long axes of the Athabasca, Selwyn, and Three Esker lozenges (Fig. 11, 136). If the relatively stiff lozenges had been subjected to bulk shortening along their line of centres, they would have rotated toward the corresponding plane of flattening; clearly, they did not. Moreover, in the flexural slip model, clockwise rotation of the mylonite fabrics from their initial northeast trend would have engendered sinistral shear along the rotating foliation planes. Accordingly, the east-trending mylonite in the mid-section of Selwyn Lake (Fig. 136) should show indications of sinistral shear imposed upon earlier dextral shear fabrics (Fig. 162). This is not the case. Alternatively, in the internal tangential longitudinal strain model, the buckling of the initially straight mylonite belt would have been accommodated by layer-parallel and

layer-normal extensional strains on the outer and inner arcs of the folds, respectively. No such accommodation structures are present (see also Taylor, 1963, 1970).

Formation of the discrete lozenges by crustal-scale boudinage at a relatively late stage in the mylonitization history would also lead to a predictable spatial distribution of shear fabrics and shear sense (Fig. 162). First, the lozenges should be bounded by continuous mylonite belts, with minimum boudinage-related deformation in their midsections. Although high grade mylonite belts, up to 500 m wide, occur along the northwestern side of the Selwyn lozenge at Wholdaia Lake (Fig. 136), they do not extend more than 20 km along the lozenge boundary. Secondly, indications of sinistral shear sense should be present along the lozenge boundaries in the southwest and northeast quadrants

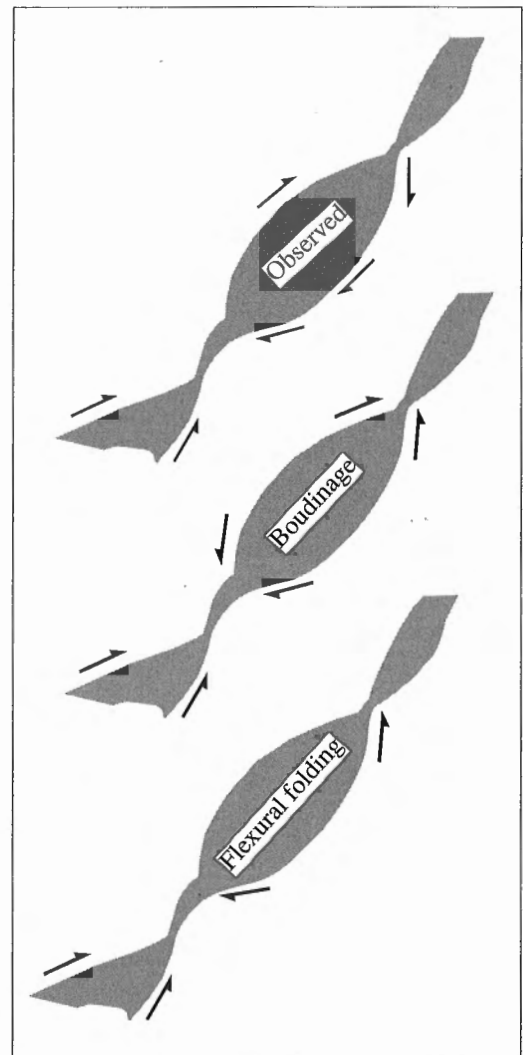


Figure 162. Observed distribution of shear sense in the Striding-Athabasca mylonite zone and adjacent to the Selwyn lozenge, compared with those distributions predicted by models based on boudinage and flexural folding to account for the present geometry of the Striding-Athabasca mylonite zone. Discussed in text.

(Fig. 162). However, there is no mylonite in the southwest quadrant and there is no evidence for sinistral shear sense in the northeastern quadrant, i.e. at Snowbird Lake (Fig. 136).

It is possible to produce a strong deflection (bending) of an initially straight deformation belt by the action of superposed brittle faulting (e.g. Cunningham, 1993). Such a mechanism would obviate the requirement for sinistral shear-sense indicators and inner arc/outer arc accommodation strains. The faults could either be long and discrete, or short components of a closely spaced array. In the former case, they would clearly dislocate the initially straight mylonite belt. No such offsets are present (see also Taylor, 1963, 1970). In the latter case, rotations of the order of 90° would lead to severe disruption and dilation of the mylonite belt and its wall rocks. This is not observed.

To summarize, in the absence of brittle dislocation and dilation, ductile models for the deformation of a once straight Striding mylonite belt (Fig. 162) either predict mylonite where there is none (southwest quadrant), poor mylonite development where excellent mylonite is present (mid-points on either side of the lozenge), or sinistral shear where the vorticity is consistently dextral (northeast quadrant). Furthermore, the absence of through-going, continuous mylonite along the northwestern margin of the Selwyn lozenge (Fig. 136) demonstrates that the lozenge is older than, and has served to localize, the Striding mylonite belt. It may be suggested that the same conclusion applies to the Three Esker lozenge (Fig. 136). Accordingly, the bends in the Striding mylonite belt are considered to be primary and represent the initial structural configuration, dictated by the geometry and distribution of the lozenges. This conclusion is compatible with that drawn above regarding the causal relationship between the pattern of flow in the East Athabasca mylonite triangle and the Athabasca lozenge (Fig. 10).

Fault localization

The Striding-Athabasca mylonite zone does not appear to extend much beyond the strike length examined in this report. Granulite facies mylonite, indeed thick belts of mylonite at any metamorphic grade, is absent along the trace of the Snowbird tectonic zone to the south of the Athabasca Basin (e.g. Crocker et al., 1993), as well as between Three Esker lozenge and Baker Lake (Tella and Eade, 1985; Eade, 1985; see Fig. 1). Either the lateral extensions of the Striding-Athabasca mylonite zone were cut out by subsequent Early Proterozoic faulting along the Virgin River shear zone (e.g. Crocker et al., 1993) and the Tulemalu fault (Eade, 1985; Tella and Eade, 1985, 1986), or the mylonite zone never extended much beyond its present length (400-500 km). The absence of relics of high grade mylonite does not favour the former hypothesis. Accordingly, the latter possibility is examined below.

The Selwyn and Three Esker lozenges have clearly influenced the sinuous trace of the Striding mylonite belt and its oblate fabrics, and the Athabasca lozenge has played a pivotal role in the location and complex kinematic development of the East Athabasca mylonite triangle and its prolate bulk flow (Fig. 136). The control exerted by the lozenges over the

complex trace of the mylonite indicates that they have been instrumental in provoking a partitioning of the flow. In other words, they behaved as relatively strong rheological heterogeneities (e.g. Bell, 1981, 1985; Bell et al., 1989). This interpretation is supported by the lithological contrast between the granodioritic to granitic wall rocks on the one hand, and the more mafic to intermediate composition of the Athabasca and Selwyn lozenges on the other (see also Crocker and Collerson, 1988; Crocker et al., 1993).

Theoretical treatments of plane strain (Vilotte et al., 1984) and three dimensional flow (England and Houseman, 1985) have examined the role of lithospheric variation in rheology in the localization of strike-slip faults. Both studies sought to model the formation of the Altyn Tagh fault on the southeastern margin of the relatively stiff Tarim Basin, north of the Himalayas. The study by Vilotte et al. (1984) specifically addressed the question of the size of the rheological heterogeneity and determined that even small strength perturbations are significant. The Athabasca-Selwyn-Three Esker lozenges, can be viewed collectively as a small-scale rheological analogue of the Tarim Basin in the above cited theoretical studies. This is not to suggest that these features are *homologous*. For example, in the theoretical treatments, the Tarim Basin is modelled as a clockwise rotating object in front of a rigid indenter. The absence of through-going mylonite on the northwest side of the Selwyn lozenge eliminates the possibility of significant rotation. Moreover, there is no geological evidence for Late Archean indenter tectonics in the western Churchill province.

Modest movements, spectacular fabrics

The geometry of the Striding-Athabasca mylonite zone imposed an important constraint on its potential to accommodate significant strike-slip displacements between the Rae and Hearne crusts. The sinuous course of the Striding mylonite belt (Fig. 136), and the conjugate character of the lower deck in the East Athabasca mylonite triangle (Fig. 10), combine to represent an extremely inefficient geometry for transcurrent movements (e.g. Lamouroux et al., 1991; Saucier et al., 1992). The bends in the fault trace represent a high amplitude relief on the fault plane and would have acted to impede easy strike-slip motion along the mylonite zone and prevent the accumulation of significant lateral displacements of the wall rocks. The apparent kinematic inefficiency of the Striding-Athabasca mylonite zone, predicated upon direct observation of the geometry of the structure, raises important questions: (i) *why didn't a favourably oriented segment of the mylonite zone propagate to form a straight, through-going shear zone?* and (ii) *how were spectacular ribbon fabrics generated in what is essentially a failed fault?*

It has been noted above that the deformation fabrics and shear-sense indicators of the Striding-Athabasca mylonite zone as a whole are indicative of shortening across a bulk dextral shear plane. In the Striding mylonite belt, this is principally expressed as oblate finite strains, with some supporting evidence from shear criteria. Most of the shear-sense indicators in the East Athabasca mylonite triangle occur in the lower deck. At the local scale they show that deformation occurred

by progressive general noncoaxial flow, rather than simple shear. The coeval operation of the large scale conjugate shear zones, which make up much of the lower deck, combined to accommodate a component of shortening approximately normal to the general trend of the Striding-Athabasca mylonite zone (Fig. 163). Together, these observations indicate that, whereas the local fabrics can reflect the immediate influence of the stiff lozenges (e.g. prolate flow at the tip of the Athabasca lozenge; see "Central septum (lower deck)"), the bulk of the Striding-Athabasca mylonite zone accommodated a transpressive deformation (e.g. Sanderson and Marchini, 1984). Displacement on a fault which terminates within continental crust must, by definition, attenuate to zero at the fault tips (Chinnery, 1969; Freund, 1974). Fault tips propagate in response to the accumulation of increments of displacement on the main part of the fault (e.g. Swanson, 1992; Cowie and Scholz, 1992). However, in a strongly transpressive deformation regime, coupled with a kinematically inefficient geometry, the simple shear/pure shear ratio will be low. Accordingly, even in a wide shear zone, displacements may be modest and the fault is unlikely to propagate very far from the rheological heterogeneities upon which it initially localized.

The evolution of mylonite fabrics is a reflection of the partitioning of flow within the rock (e.g. Hanmer, 1987b). The number of attempts to define 'mylonite' is partly a reflection of the historical ambivalence regarding a genetic designation (e.g. Higgins, 1971; Bell and Etheridge, 1973; Zeck, 1974; White et al., 1980; White, 1982; Tullis et al., 1982; Wise et al., 1984; Mawer, 1986; Hanmer, 1987b). However, it is probably also a reflection of the diversity of mylonitic fabrics and microstructures developed in different lithologies, deformed at different conditions of strain rate, flow regime, and metamorphic environment (PTX). Many, though by no means all, descriptions of mylonite include a reference to the presence of monomineralic ribbons, often of quartz or feldspar which, at least partially, define the mylonitic foliation (e.g. Boullier and Bouchez, 1978). They are commonly interpreted as the highly attenuated, deformed equivalents of rock-forming minerals of the initially coarse parent material. The most spectacular ribbons are developed in ultramylonite where the scarcity of porphyroclasts allows the ribbons to adopt a homogeneous planar aspect. The development of relatively fine grained ultramylonite from an initially coarse protolith is classically described in terms of a fabric path whereby porphyroclastic phases are progressively refined and incorporated into the microstructural matrix by dynamic recrystallization (e.g. Sibson, 1977; White, 1982; Wise et al., 1984). The magnitude of the finite strain required for the elimination of the porphyroclast population is therefore a partial function of the rate of dynamic recrystallization of the porphyroclastic materials within the aggregate (Hanmer, 1987b). However, this perspective is a reflection of the historical bias toward the study of mylonitization in relatively low grade metamorphic environments.

Compared with low temperature mylonite, few studies have specifically focussed upon the microstructural evolution and fabric paths of high temperature mylonite fabrics (e.g. Etheridge, 1975; Bell and Etheridge, 1976; Brodie, 1981; Hanmer, 1982, 1984a, 1987b; Biermann and van Roermund, 1983; Brodie and Rutter, 1985, 1987; White and Mawer, 1986, 1988).

It is clear that the size, or even the existence, of porphyroclasts in any mylonitic rock is a function of the scale of deformation partitioning within the grain-scale aggregate (Hanmer, 1987b; Bell and Johnson, 1989). Extrinsic factors which influence the deformation partitioning include those governing the strength of minerals, i.e. P , T , P_{H_2O} and strain rate. The persistence of stiff feldspar porphyroclasts in low temperature mylonite and ultramylonite is well known, but at appropriately high temperatures and slow strain rates, feldspar can become as soft as quartz (Tullis and Yund, 1980, 1985; Tullis, 1983; Tullis et al., 1990). Under appropriate conditions, a fabric path may lead directly from the protolith to an ultramylonite without the intermediate development of a matrix/porphyroclast bimodality. In other words, if high *recrystallization rate/strain rate ratios* pertain throughout the grain-scale aggregate, a straight, planar ribbon fabric can develop at relatively low finite strain magnitudes (Fig. 3a in Hanmer, 1987b; Fig. 13 in Hanmer et al., 1992b; cf. Ramsay and Graham, 1970). If, in addition, the deformation is the product of a progressive general noncoaxial flow (kinematical vorticity number $W_k < 1$; e.g. Hanmer and Passchier, 1991), with a significant component of shortening across the flow plane ($W_k \ll 1$), *longitudinal strain* along the flow plane can accumulate very quickly (Pfiffner and Ramsay, 1982). Accordingly, the development of a ribbon mylonite fabric could represent even lower magnitudes of *shear strain* than in the case of progressive simple shear. Field observations indicate that feldspar porphyroclasts are poorly preserved throughout most of the voluminous mylonite of the Striding-Athabasca mylonite zone. Thermobarometric determinations of metamorphic conditions in the East Athabasca mylonite triangle indicate very high temperatures (850-1000°C; see Williams et al., 1995; Snoeyenbos et al., 1995), and structural observations indicate significant deviation from ideal simple shear. Therefore, in a transpressive regime, under high temperature granulite facies metamorphic conditions, a thick mylonite zone such as the Striding-Athabasca example need not represent major wall rock displacements.

Interpretation of the Striding-Athabasca mylonite zone as a deep-crustal, transpressive fault during the Late Archean begs the question of how the coaxial component of the flow was accommodated, given the shallow to moderate plunges of the associated extension lineations. Under conditions of constant volume deformation and significant extension of the flow plane along the transport direction, a subhorizontal principal extension direction would generate an important room problem at the fault terminations. Moreover, a strongly transpressive, volume-constant, progressive deformation would tend to generate steeply plunging extension lineations (Sanderson and Marchini, 1984). However, in the Striding-Athabasca mylonite zone, melts were moving through the presently exposed structural level. Crustal (granite) and probable mantle melts (gabbro/norite) were emplaced from below, but potentially voluminous granitic melts from the diatexites would have migrated upward to higher structural levels. It is unlikely that one will ever be able to evaluate the bulk volume change in the Striding-Athabasca mylonite zone. However, it is suggested that significant volume loss by magma migration may be a fundamental process in deep-crustal, high temperature shear zones (Hanmer et al., 1995b).

TECTONIC SIGNIFICANCE

The present study of the northern Saskatchewan/District of Mackenzie segment of the Snowbird tectonic zone has established the existence and the nature of the Striding-Athabasca mylonite zone. Briefly, it is a geometrically and kinematically complex, Archean right-lateral transpressive structure, 400 to 500 km long, formed at granulite facies in the deep crust. Early Proterozoic tectonic activity is recorded as extremely weakly developed and localized plastic deformation, and relatively minor granitoid intrusion. The granulite facies mineral assemblages in the mylonite contrast sharply with the lower metamorphic grade of the adjacent Hearne crust. As argued above, the sinuous and branching geometry of the Striding-Athabasca mylonite zone is not the result of modification of an initially straight shear zone. Therefore, it could not have accommodated significant transcurrent displacement of its wall rocks, despite the associated spectacular mylonite fabrics.

However, the mylonite is but one component of this segment of the Snowbird tectonic zone. The other component is the train of three lozenges (Fig. 136), lithologically, and at least in part isotopically, distinct from their wall rocks (Table 2; Crocker et al., 1993).

Lozenges

Although much of the interior of the Athabasca lozenge is obscured by younger rocks and Quaternary deposits, the East Athabasca mylonite triangle at the northern apex (Fig. 136), and the gneisses of the Caren Lake area near the southwestern apex (Fig. 11), are accessible. These rocks are both lithologically and isotopically distinct from the Rae and Hearne wall rocks. The petrological sequence of early sedimentary supracrustal rocks, intruded sequentially by Middle Archean tonalite, dismembered anorthosite plus mafic dykes, Late Archean mafic plutons and granite bodies in the East Athabasca mylonite triangle is petrologically very similar to the sequence described from the south end of the lozenge at Caren Lake (Lewry and Sibbald, 1977 and references therein; Crocker et al., 1993). Taken together, these observations suggest that the Athabasca lozenge is lithologically quite similar to the Selwyn lozenge. Both lozenges are mafic to intermediate in composition and bounded by granitic to granodioritic Rae and Hearne wall rocks (e.g. Taylor, 1963, 1970; Gilboy, 1980b; Slimmon, 1989). Moreover, it appears that the occurrence of anorthosite is associated with the eastern margin of both lozenges. Within the East Athabasca mylonite triangle, anorthosite is confined to the sinistral shear zone on the eastern side of the lower deck, and anorthosite at Caren Lake is located adjacent to the eastern margin of the lozenge (Fig. 136). In the case of the Selwyn lozenge, anorthosite is a common protolith in the Striding mylonite belt. Recalling the distribution of anorthosite along the southeastern margin of the Selwyn lozenge, the available data, while not definitive, allow one to draw parallels between the Athabasca and Selwyn lozenges. The occurrence of diatexite-anorthosite-garnet pyroxenite ribbon mylonite on the southeastern margin of the Three Esker lozenge (Fig. 136) suggests that all three lozenges may share a similar internal architecture.

Preliminary Nd data support the proposed lithological correlation of the lozenges. With one exception, Nd model ages for the Middle Archean tonalite and associated anorthosite-pyroxenite assemblage in the East Athabasca mylonite triangle, and the margin of the Three Esker lozenge, fall in the range 3.45-3.30 Ga (Table 2). Crocker et al. (1993) report similar Nd model ages of ca. 3.5-3.1 Ga from Middle Archean rocks at Caren Lake (Fig. 11), in the southern window into the Athabasca lozenge (however, see Bickford et al., 1994).

Stiff Middle Archean crust

It has been argued above that the present geometries of the East Athabasca mylonite triangle and the Striding mylonite belt are primary, as opposed to the product of the modification of an initially straight shear zone, and that, because the lozenges are not defined on both sides by the bounding mylonite, they are older and have acted to localize the shear zones (see "Shear zone geometry"). The Selwyn and, by extrapolation, Three Esker lozenges have controlled the sinuous trace of the Striding mylonite belt, and the Athabasca lozenge has played a pivotal role in the complex kinematic development of the East Athabasca mylonite triangle (Fig. 136). Granulite facies mylonite of the East Athabasca mylonite triangle formed in two stages; annealed mylonite at ca. 3.13 Ga preserved in the eastern part of the lower deck, and widespread ribbon mylonite at ca. 2.62-2.60 Ga. A similar two stage mylonitization history has been established for the Striding mylonite belt (Tables 1 and 2). Preliminary U-Pb zircon data for the East Athabasca mylonite triangle suggest that tonalitic, mafic, and at least some anorthositic protolith of the Athabasca lozenge are Middle Archean.

It has been suggested that the lozenges behaved as relatively strong rheological heterogeneities (see "Fault localization"). This interpretation is supported by their lithological composition relative to that of the wall rocks. However, it raises the question as to why the mylonite should be derived at the expense of relatively stiff lozenge material, for example, anorthosite, rather than the relatively soft wall rocks. I have shown that in the East Athabasca mylonite triangle, emplacement of the voluminous Late Archean mafic and granitoid protoliths was contemporaneous with mylonitization. I suggest that their Nd model ages (ca. 3.0-2.7 Ga; Table 2) indicate juvenile magmas which may have interacted to varying degrees with older, more evolved crust. This suggestion is supported by the ϵ_{Nd} values calculated for 2.6 Ga (Table 2). It is suggested here that deformation, localized at the lozenge boundaries, may have focussed the emplacement of mantle and crustally derived magmas, thereby creating a hot, soft zone favourable to the continued localization of plastic deformation (e.g. Simpson, 1986; Segall and Simpson, 1986). In such a scenario, the evolved continental crust would be represented by the lozenges, with which isotopic interaction would be favoured by the channelled emplacement process.

Nd model ages (Table 2; Crocker et al., 1993) suggest that Middle Archean mafic and intermediate composition rocks along the southeast margin of the lozenges were derived from a relatively uniform mantle source, without significant interaction

with older crust. The lozenges may represent fragments of Middle Archean, or older, crust within the western Churchill continent. If they ever formed a single body, dismemberment would have occurred prior to the ca. 2.6 Ga ribbon fabrics of the Striding-Athabasca mylonite zone. Middle Archean (ca. 3.13 Ga) sinistral mylonite is preserved in the Chipman tonalite batholith in the eastern part of East Athabasca mylonite triangle (Fig. 9). Dextral mylonite of similar vintage (ca. 3.3-3.1 Ga) occurs on the same side of the Selwyn lozenge, across the inter-lozenge gap (Fig. 162 and 163). Therefore, it is kinematically possible that the Athabasca and Selwyn lozenges were pulled apart along the Middle Archean mylonite units at ca. 3.13 Ga.

Middle Archean arc?

Combining the observations of this study with those of Crocker et al. (1993), one can construct a schematic sequence for the Middle Archean rocks of the Snowbird tectonic zone. Early semipelitic to pelitic rocks were intruded by a layered mafic complex composed of gabbro/norite, pyroxenite, and anorthosite. The mafic rocks were dismembered by tonalite batholiths. Two attempts to date the tonalite batholith in the East Athabasca mylonite triangle have yielded poorly constrained Middle Archean ages: 3149 ± 100 Ma and $3466 +327/-80$ Ma (Table 1). In order to obtain a preliminary indication of the magmatic history of these Middle Archean rocks, ϵ_{Nd} values have been calculated for 3.3 Ga, the average

Table 2. Samples come from the lower deck of the East Athabasca mylonite zone (Fig. 9 and 10), except for the Mafic granulite (upper deck; Fig. 9 and 10) and the Three Esker anorthosite (Fig. 136). Values for $\epsilon_{Nd(3.3)}$ and $\epsilon_{Nd(2.6)}$ were calculated for times of magmatic crystallization based upon the ca. 3.4-3.2 Ga U-Pb zircon ages determined for the Chipman tonalite, and the ca. 2.6 Ga ages for the granulite metagranites and mafic rocks (Table 1). Attribution of a Mid-Archean age to the Three Esker anorthosite is an extrapolation based upon geological and model age similarity to anorthosite inclusions within the Chipman tonalite. All measurements are by T.I.M.S. at the University of California at Santa Cruz. The Sm and Nd concentrations were determined by isotope dilution (Kopf, unpublished data). The $T_{(DM)}$ ages are calculated after the method of DePaolo (1981).

Sm/Nd data for the East Athabasca mylonite triangle								
Sample	Sm (ppm)	Nd (ppm)	$^{147}\text{Sm}/^{144}\text{Nd}$	$^{143}\text{Nd}/^{144}\text{Nd}$	$\epsilon_{Nd(3.3)}$	$\epsilon_{Nd(2.6)}$	$\epsilon_{Nd(0)}$	$T_{(DM)}$ Ma
Chipman tonalite (ca. 3.4-3.2 Ga)								
CK90 SB	0.88	5.87	0.0906	0.510397	1.42		-43.72	3326
CK90 M076	1.32	13.19	0.0605	0.509628	-0.76		-58.72	3444
CK90 M063	10.20	64.31	0.0959	0.510420	-0.38		-43.27	3452
Pyroxenite (ca. 3.4-3.2 Ga): inclusions in Chipman tonalite								
CK90 J099	0.86	3.32	0.1566	0.511807	0.85		-16.21	3402
Anorthosite (ca. 3.4-3.2 Ga): inclusions in Chipman tonalite								
CK90 S137	0.46	1.85	0.1503	0.511687	1.18		-18.55	3349
Three Esker anorthosite (ca. 3.4-3.2 Ga?)								
CK92 S197	0.51	2.02	0.1527	0.511754	1.50		-17.25	3304
Bohica mafic complex (ca. 2.6 Ga)								
CK91 C531	0.26	1.25	0.1258	0.511373		-0.95	-24.68	2931
CK91 S527	0.79	4.43	0.1078	0.511114		0.00	-29.73	2803
CK91 C534	0.43	1.98	0.1313	0.511502		-0.28	-22.16	2886
CK91 S574	3.66	14.32	0.1545	0.511955		0.78	-13.33	2847
CK91 S576	3.18	11.97	0.1606	0.512016		-0.07	-12.13	3012
CK91 S525	2.54	12.48	0.1231	0.511415		0.78	-23.86	2764
Granulite facies metagranites (ca. 2.6 Ga)								
CK91 C664a	4.44	25.39	0.1057	0.510984		-1.84	-32.26	2938
CK91 C728	10.25	55.78	0.1111	0.511249		1.55	-27.09	2686
CK90 S177	8.23	37.98	0.1310	0.511429		-1.62	-23.58	3019
CK91 S762	8.00	43.51	0.1112	0.511220		0.96	-27.66	2733
Mafic granulite (ca. 2.6 Ga): upper deck								
CK91 C780b	1.37	5.60	0.1479	0.511809		0.15	-16.16	2902
CK90 M205	1.02	4.58	0.1347	0.511589		0.30	-20.46	2837
CK90 S075	1.58	6.96	0.1373	0.511638		0.37	-19.52	2837
CK90 S210	0.91	4.37	0.1259	0.511446		0.43	-23.25	2802
CK90 S251	3.66	20.02	0.1105	0.511097		-1.24	-30.06	2906

of the two ages (Table 2). The results are suggestive of juvenile magmas with little assimilation of evolved continental crustal material. However, the younger of the two U-Pb determinations is similar to the ca. 3.13 Ga age of emplacement of a spatially associated syntectonic, syngranulite facies dyke swarm and associated granite sheets (Table 1). It is therefore possible that the layered mafic rocks and anorthosite, tonalite, mafic dykes, and granite were emplaced in a sequence of events which culminated in the formation of the Middle Archean mylonite at ca. 3.13 Ga. Allowing that the age constraints remain fairly loose, this synthetic picture is reminiscent of published descriptions of more recently constructed, metamorphosed and deformed magmatic arcs, for example, Kohistan (Jan and Howie, 1981; Jan, 1988; Khan et al., 1989) and Wrangellia (Beard and Barker, 1989), as well as Archean examples in the Limpopo Belt and Southwest Greenland (e.g. Windley et al., 1981). In Kohistan, the anorthosite bodies represent relatively small masses that were emplaced into the lower part of the arc, which has subsequently been rotated through 90° about an arc-parallel horizontal axis (Coward et al., 1982). By analogy, the anorthosite in the present study area could represent the lower parts of an arc-related magmatic pile which has been tilted to expose its base along the southeastern margins of the lozenges. This interpretation would imply that the emplacement of the vertical, late tectonic components of the Chipman mafic dyke swarm was relatively late.

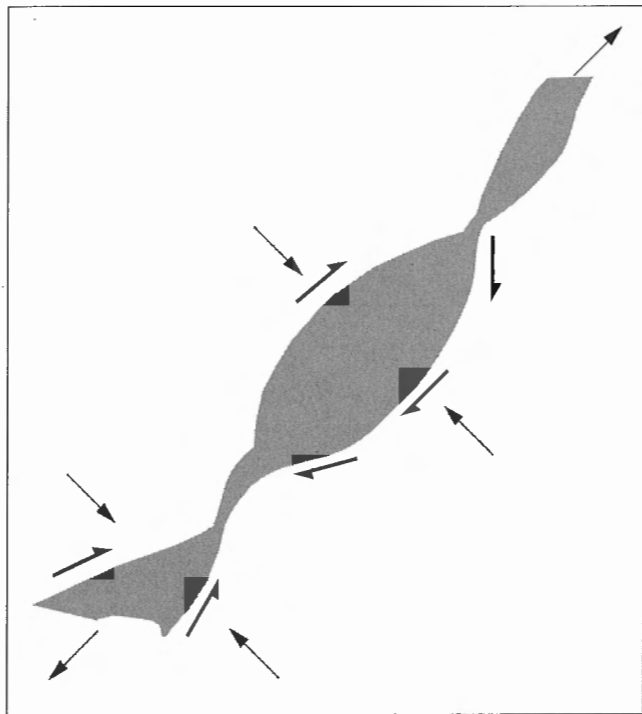


Figure 163. Distribution of shear sense, and coaxial shortening and extension, in the Striding-Athabasca mylonite zone and adjacent to the Selwyn lozenge. Discussed in text.

According to this scenario, if the Striding-Athabasca segment of the Snowbird tectonic zone was associated with a tectonic suture at anytime during its history, it would have been at the time of incorporation of the arc within the growing western Churchill continent during the Archean. It is already noted that the Athabasca, Selwyn, and Three Esker lozenges (Fig. 11 and 136) may represent large fragments of Middle Archean crust which are quite distinct from the rocks of the surrounding western Churchill continent. If they once formed a single body, it would have been dismembered prior to the formation of the ca. 2.6 Ga ribbon mylonite which was localized by the three lozenges in their present configuration. Middle Archean annealed sinistral mylonite is preserved in the Chipman tonalite batholith in the eastern part of the lower deck of the East Athabasca mylonite triangle (Fig. 162). Dextral mylonite of similar vintage (ca. 3.3-3.1 Ga) occurs on the same side of the Selwyn lozenge, across the inter-lozenge gap. It is kinematically possible that the Athabasca and Selwyn lozenges were pulled apart along the Middle Archean mylonite at ca. 3.13 Ga. Alternatively, if the location and shear sense of the Middle Archean mylonite were controlled by crustal-scale rheological variations, in the same way as the Late Archean ribbon mylonite, it would imply that the present configuration of the Athabasca and Selwyn lozenges is older than 3.13 Ga. In any event, the absence of a systematic array of mylonite bounding the lozenges on all sides is readily explained if the lozenges were separated from each other prior to their final tectonic incorporation within the evolving western Churchill continent.

Whatever the relationship of the ca. 3.13 Ga mylonite to the lozenges, the shearing was accompanied by high pressure granulite facies metamorphism (850°C, 1.0 GPa; Williams et al., 1995) and, in the East Athabasca mylonite triangle at least, by the emplacement of an important mafic dyke swarm. The dykes were emplaced throughout the shearing event and could be responsible for the high temperatures of metamorphism (e.g. Barton et al., 1990; Williams et al., 1995).

Late Archean intracontinental shear zone

Three independent data sets point to an intracontinental setting for the Striding-Athabasca mylonite zone in the Late Archean. First, the Rankin-Ennadai greenstone belt, the largest Archean tectonic entity identified to date in this part of the Canadian Shield, extends as a zone of outliers across the Hearne crust, over 600 km from Hudson Bay toward the Selwyn lozenge (Fig. 1). Uranium-lead zircon data from both its northeastern and southwestern parts show that the volcanic rocks of the greenstone belt are ca. 2.7 Ga old (Chiarenzelli and Macdonald, 1986; Mortensen and Thorpe, 1987; Tella et al., 1992). Very little is currently known about the tectonic context of the formation and deformation of the Rankin-Ennadai greenstone belt. Preliminary work suggests that the northeastern part of the belt may have originated as an island arc, which was tectonically stacked as a pre-2.65 Ga thrust-nappe pile (Park and Ralser, 1992). Syn- to late tectonic granitoid rocks were intruded into the arc, prior to its juxtaposition with its present continental wall rocks. However, it is important to note that the tectonic, stratigraphic, or intrusive nature of the gneiss-greenstone belt boundary as a whole

remains unresolved. Dating of the granites indicates that thrust-stacking occurred at 2.677 Ga, followed by upright shearing and folding just prior to 2.666 Ga (Park and Ralser, 1992; see also Cavell et al., 1991). The salient point here is that, according to Park and Ralser (1992), the basin in which the greenstone belt formed had closed prior to ca. 2.67-2.66 Ga. Because there is no evidence for any other major Late Archean basin in either the Hearne or the Rae crusts, I suggest that the western Churchill continent was a discrete tectonic entity by ca. 2.67-2.66 Ga.

Secondly, although the present data set is far from complete, Late Archean granitic bodies, ca. 2.63-2.58 Ga, broadly contemporaneous with high grade mylonitization in the Striding-Athabasca mylonite belt, do not appear to be arranged in the belt-like configuration typical of magmatic arcs associated with plate margins (Fig. 164; e.g. Windley, 1984). Thirdly, the same spatial pattern of Archean Nd model age variation, ca. 4.0-2.4 Ga in the southwest *versus* ca. 2.9-2.5 Ga in the northeast, is present in both the Rae and Hearne crusts (Fig. 6). This observation would be further supported if the basement rocks beneath the westernmost parts of the Trans-Hudson orogen

(Fig. 1) are indeed part of the Hearne crust (see Bickford et al., 1992). This suggests that the southwestern parts of both the Rae and Hearne crusts are fundamentally different from their northeastern parts. For such a distribution pattern of Nd model ages to accommodate a Late Archean suture along the Snowbird tectonic zone would require some very special boundary conditions, for example, a narrow, short lived basin, and similar drift and convergence vectors. Taken together, these arguments suggest that, by ca. 2.62-2.60 Ga, the site of the Striding-Athabasca mylonite zone was not located at a suture, but lay well within the interior of the Late Archean western Churchill continent.

It is argued above that the Striding-Athabasca mylonite zone is a relatively short (400-500 km), kinematically inefficient, deep-crustal intracontinental shear zone, which acted as an accommodation structure in response to convergence, collision, and shortening at the far-field plate margin (see "Modest movements, spectacular fabrics"). The problem now is to account for the Late Archean granulite facies metamorphism, and the subsequent uplift of the mylonite, in an intracontinental setting.

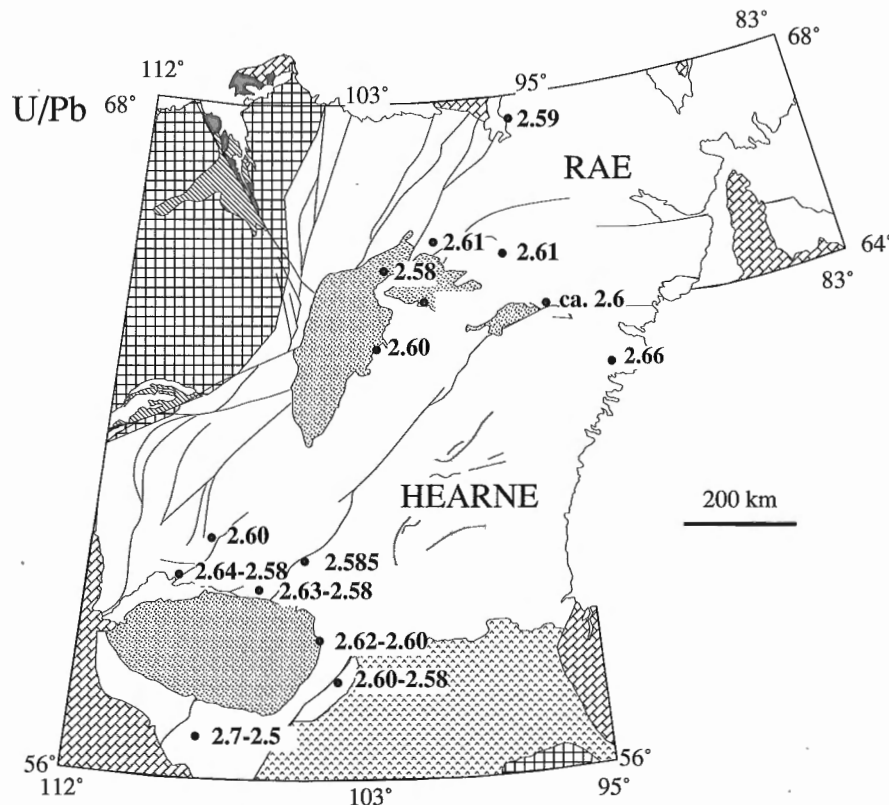


Figure 164. Distribution of available U-Pb zircon dates (Ga) for magmatic crystallization of granitic rocks in the range 2.63-2.58 Ga, approximately contemporaneous with granulite facies mylonitization in the East Athabasca mylonite triangle. Note the absence of an obvious belt-like disposition. Discussed in text. Data from Bickford et al. (1986), Van Schmus et al. (1986), Stevenson et al. (1989), Dudas et al. (1991), LeCheminant and Roddick (1991), Frisch and Parrish (1992), Roddick et al. (1992), Bickford et al. (1992), Annesley et al. (1992), and Tella et al. (1992). Patterns as in Figure 1.

Metamorphism and uplift

Several lines of evidence suggest that the localization of Late Archean high grade deformation in the Striding-Athabasca mylonite zone, post-thermal peak uplift and regional granitoid plutonism may be genetically linked to a common cause: continental deformation and lower lithospheric delamination of the western Churchill continent.

Delamination and metamorphism

The distribution of Late Archean granite across the western Churchill continent is reminiscent of that of the Lachlan Fold Belt, southeastern Australia, and the Pan-African Saharan domain. In those examples, extensive uniform metamorphism and granitoid production has been attributed by some workers to continental-scale delamination of the lower lithosphere, heating of the lower crust by injection of mafic magma, and widespread crustal melting (e.g. Wyborn, 1992; Black and Liegeois, 1993). If such a scenario were applicable to the western Churchill continent, the Axis mafic granulite (Fig. 26) of the upper deck and the Bohica mafic complex (Fig. 69) of the lower deck of the East Athabasca mylonite triangle (Fig. 9, 10) might represent the heat-carrying mafic magmas emplaced into the lower crust. As in the case of the Chipman mafic dykes (Fig. 42), coeval with the Middle Archean mylonite, these magmas may represent the mafic underplating frequently associated with granulite facies metamorphism in other terranes (e.g. Glikson, 1986; Bohlen and Mezger, 1989; Carney et al., 1991; Martignole, 1992; Ashwal et al., 1992). Widespread upper mantle melting associated with a Late Archean delamination event of this scale could represent a component of the upper mantle depletion invoked by Hoffman (1991; see also Grand, 1987) to account for the existence of a cold, yet buoyant tectospheric root beneath the exposed Canadian Shield.

Uplift and exhumation

High grade (850-1000°C, 1.0 GPa; Williams et al., 1995; Snoeyenbos et al., 1995) ribbon mylonite of the East Athabasca mylonite triangle formed during the Late Archean at ca. 2.62-2.60 Ga. However, within that time window, initial pervasive granulite facies mylonitization was sequentially succeeded by more localized amphibolite and greenschist facies shearing. Throughout the Striding-Athabasca mylonite zone, the reaction of garnet to produce rims of radial symplectitic clinopyroxene-plagioclase, monomineralic plagioclase rims, quartz-plagioclase-kyanite/sillimanite, and undistorted pseudomorphs of plagioclase-biotite, are all indicative of high temperature, postkinematic decompression during cooling. Rare examples of oriented pyroxene-plagioclase symplectite in pressure shadows on garnets indicate that decompression began at the end of high grade mylonitization.

Within the time/temperature constraints available, it is possible to attempt a very simplistic evaluation of the order of magnitude of cooling rates. A minimum temperature decrease from 850°C (granulite) to 450°C (greenschist) during the about 20 Ma time window (2.62-2.60 Ga) would suggest a time averaged cooling rate of 20°C/Ma. However,

in light of the statistical error envelopes associated with the age determinations of syntectonic granites in the Striding-Athabasca mylonite zone, it may be more appropriate to consider a time window of about 40 Ma and time averaged cooling rates of about 10°C/Ma. Although these are grossly oversimplified estimates, such cooling rates are apparently fast compared with similar structural levels in some other strike-slip shear zones. For example, geothermobarometric and geochronological data for the Great Slave Lake shear zone (Hanmer, 1988a; Hanmer et al., 1992a) indicate that temperatures dropped 250°C, from about 900°C to about 650°C, during the interval 1975-1925 Ma. This corresponds to a time averaged cooling rate of 5°C/Ma, half the apparent rate for the Striding-Athabasca mylonite zone. However, the estimated time averaged cooling rate for this study is unremarkable compared with the approximately 100°C/Ma obtained for the strike-slip fault Red River (Leloup and Kienast, 1993). Nevertheless, rapid cooling of the Striding-Athabasca mylonite zone, if valid, would imply uplift and exhumation.

Continental deformation and uplift

Without significant shortening and crustal thickening, delamination does not necessarily result in significant uplift (compare Clemens, 1988, Collins and Vernon, 1992 with Powell, 1986). Even so, it is unlikely that delamination alone could cause uplift in excess of a few kilometres (England and Molnar, 1990; England, 1993; Platt and England, 1993), hardly sufficient to account for the present juxtaposition of the Striding-Athabasca mylonite belt and the Rankin-Ennadai greenstone belt. One must look for other possible contributions to the uplift history of the Striding-Athabasca mylonite belt.

Since the initial formulation of modern geological models of crustal thickening by penetrative continental deformation (e.g. Dewey and Burke, 1973), there have been a number of theoretical treatments of the subject. Of particular interest here is the three dimensional simulation by England and Houseman (1985) who examined the role of lithospheric variation in rheology in the localization of intracontinental strike-slip faults, the generation of anomalously high topography, and erosional uplift. Their study modelled the localization of the Altyn Tagh fault and highlands, and the Tien Shan, at the margins of the relatively stiff lithosphere underlying the Tarim Basin, north of the Himalayas. The location and sinuous configuration of the Striding-Athabasca mylonite zone (Fig. 136) was controlled by the presence of relatively stiff, anomalously old Middle Archean material, now disposed in three crustal-scale lozenges (Fig. 11), which may constitute a small-scale rheological analogue of the Tarim Basin (see "Fault localization"). As fragments of older Middle Archean crust, the lozenges may have had deeper, colder, stiffer, and potentially denser roots than the adjacent western Churchill continent. Such lithospheric fragments could have acted as privileged sites for delamination, thereby focussing magmatism and metamorphism, as well as deformation and the generation of surface topography (cf. England, 1993). The principal weak link in the analogy is the paucity of information concerning the timing and distribution of metamorphism and deformation in the western Churchill continent.

However, if the analogy is valid, penetrative Late Archean continental deformation, with localized flow centred on a crustal-scale strength heterogeneity, may offer a partial explanation for the exposure of Late Archean relatively high pressure assemblages, and associated deep-crustal mafic intrusions, by anomalous postkinematic erosionally driven uplift and exhumation of the Striding-Athabasca mylonite zone.

Apparent vertical throw (Rae)

Within the Striding-Athabasca mylonite zone, postkinematic retrogression and hydration are widespread, as witnessed by the abundance of soft polycrystalline amphibole and phyllosilicate pseudomorphs which preserve the shapes of euhedral garnets wrapped around by the ribbon mylonite fabric. However, the preservation of fresh granulite facies mineral assemblages shows that the retrogression was not pervasive. Extensive development of granulite facies assemblages is reported from the Rae crust in Saskatchewan (e.g. Fraser et al., 1978; Lewry et al., 1978; Slimmon, 1989). During this study, field reconnaissance, up to 100 km west of the East Athabasca mylonite triangle, indicated that the Rae wall rocks have been subjected to severe hydration and retrogression, compared with the Striding-Athabasca mylonite zone. For example, the wall rocks contain coarsely recrystallized, biotite-muscovite migmatite with postkinematic pegmatitic aggregates of andalusite-sillimanite, indicative of severe retrogression under hydrostatic conditions. Initial transmission electron microscope study suggests that the preservation of granulite assemblages in the fine grained mylonite reflects the tightness of the grain boundary network and the consequent difficulty for the postkinematic penetration of water (J.C. White, pers. comm., 1993). Accordingly, the present metamorphic contrast between the Striding-Athabasca mylonite zone and the Rae wall rocks is interpreted as a reflection of the state of preservation of granulite facies assemblages, rather than an abrupt difference in crustal level.

Real vertical throw (Hearne)

In the Hearne wall rocks of Saskatchewan, metamorphism in the sillimanite-cordierite-bearing metapelitic component has not exceeded the stage of incipient partial melting, indicating that the rocks never reached granulite grade (however, see Lewry and Sibbald, 1977, 1980). In the Northwest Territories, regional metamorphism in the Late Archean Rankin-Ennadai greenstone belt, which is exposed within 15 km of the Striding mylonite belt (Fig. 1), never exceeded uppermost greenschist to lowermost amphibolite facies throughout its 600 km strike length (Taylor, 1963; Park and Ralser, 1992). Clearly, there is a significant metamorphic contrast between the wall rock assemblages and the Late Archean metamorphism in the Striding-Athabasca mylonite zone. The shallow to subhorizontal plunge of the transport direction in the mylonite makes it extremely improbable that the granulites were uplifted by the shearing which produced the mylonite. Moreover, it has been argued above that the mylonitization was not associated with tectonically significant shearing displacements. Therefore, the present distribution of

metamorphic assemblages within and east of the Striding-Athabasca mylonite zone must involve important postmylonite fault movements.

Brittle dip-slip faulting

Greenschist facies regional metamorphism at the northeastern end of the Rankin-Ennadai greenstone belt occurred at ca. 2.68-2.65 Ga (Park and Ralser, 1992). Assuming that metamorphism in the greenstone outlier just east of the Striding-Athabasca mylonite zone is of the same vintage, the present close juxtaposition of greenschist and granulite facies rocks requires important post-2.6 Ga fault movements. Regional mapping shows that such faults, if they exist, are cryptic. They are not marked by dip-slip mylonite, cataclasite, breccia, gouge, or quartz veining. They do not offset or disrupt the Striding-Athabasca mylonite belt (Fig. 136), nor are they visible in the immediately adjacent Hearne wall rocks (Taylor, 1963). If they are hidden at the eastern margin of the mylonite, they must follow the same sinuous trace. Right-angle bends in the map trace of a strike-slip fault render non-dilatational displacements extremely difficult (Fig. 136; see Saucier et al., 1992), to the extent that such faults are unlikely to have accommodated important transcurrent displacements. Although the relief on the fault surfaces would have allowed them to accommodate significant northwest-side-up dip-slip movement, the cryptic faults must dip as steeply as the vertical mylonites. The unacceptable alternative is to propose that the three surfaces (mylonitic, fault, and erosional) serendipitously intersect in a single line. At present, it is not possible to adequately explain how significant dip-slip movement could be accommodated on such unfavourably oriented faults, even if the displacement was kinematically controlled, as opposed to stress controlled. Most importantly, there is no geological evidence for an appropriately located, regional-scale, shallowly dipping extensional or contractional fault system into which such faults might be rooted. Even assuming that cryptic dip-slip faults are present, there are two constraints on their timing. First, the localization of deformation with cooling from granulite to greenschist facies in the East Athabasca mylonite zone occurred during the Late Archean (ca. 2.6 Ga; Table 1). Accordingly, uplift of the granulite facies mylonite could have occurred at that time, although there is no supporting evidence for this along the Striding mylonite belt. Second, the minimum age of uplift is given by the ca. 1.85 Ga volcanic and sedimentary rocks of the Baker basin (Fig. 1) which straddle the northeastward extension of these putative faults with relatively minor offset (Hoffman, 1988).

Implications for Proterozoic tectonics

Differences between the Archean geological features of the Rae and Hearne crusts, and the apparent truncation of the pronounced magnetic signature of the 1.99-1.90 Ga Taltson magmatic arc beneath the Phanerozoic cover, led Hoffman (1988) to interpret the Snowbird tectonic zone as an Early Proterozoic suture (Fig. 1, 165; Hoffman, 1988; see also Ross et al., 1991; Theriault, 1992). This interpretation derives considerable support from the combined geophysical and

geochronological evidence for important Early Proterozoic plate tectonic activity in the vicinity of the Snowbird tectonic zone as it is defined in the subsurface of Alberta (Ross et al., 1991). However, geological study of the Striding-Athabasca mylonite zone indicates that the tectonometamorphic history of a 400 to 500 km long segment of the Snowbird tectonic zone is essentially Archean in age. Accordingly, differences between the Rae and Hearne crusts could reflect several factors, including possible juxtaposition of different crustal levels in continental blocks during the Middle Archean. However, the fact remains that Early Proterozoic tectonic activity to the west, and along strike to the southwest of the Striding-Athabasca mylonite zone in the time range 2.0-1.80 Ga, and possibly younger, is in apparent contradiction with the absence of significant Early Proterozoic ductile deformation in the Striding-Athabasca mylonite zone itself (Fig. 165; see also Bickford et al., 1994). In order to address this question, it is necessary to briefly review the evidence for tectonic activity along the Alberta segment of the Snowbird tectonic zone.

Ross et al. (1991) have identified a fan-like bundle of alternating wedge-shaped magnetic anomalies to the southwest of the Athabasca lozenge (Fig. 165). They suggest that the Wabamun High is bounded on the southeast by a broad shear zone, the Thorsby Low, and by a more discrete fault on its northwest margin. Sheared gneiss from the Thorsby Low has yielded a U-Pb zircon age of 2.29 Ga, and a deformed pegmatite has given 1.91 Ga. On the southeastern side of the Thorsby Low, the Rimbey High, composed of biotite granite has yielded U-Pb magmatic crystallization ages between 1.85 and 1.78 Ga. At least some of this granite was derived from old,

highly evolved continental crust (Villeneuve et al., 1993; Bickford et al., 1994). The northeastern termination of the Rimbey High (Fig. 165) corresponds to the poorly foliated Junction granite, itself dated at 1.82 Ga (Bickford et al., 1986, 1994), and considered to be late syntectonic with respect to greenschist facies mylonite of the Virgin River shear zone (Lewry and Sibbald, 1977, 1980; Macdonald, 1987; Carolan and Collerson, 1988, 1989). Using geometry to infer a kinematic analogy with the East Athabasca mylonite triangle, Ross et al. (1991) suggest that the Wabamun High is an escape wedge of Rae crust, expelled to the southwest during Early Proterozoic southeastward subduction and continental collision at ca. 1.85-1.82 Ga. In this scenario the Rimbey High would represent a continental arc constructed at the leading edge of the Hearne crust (Fig. 165).

There are at least two possible solutions to the apparent temporal contradiction between the Alberta and Striding-Athabasca segments of the Snowbird tectonic zone: (i) southeastward subduction associated with the closure of a basin initially formed in the dilational quadrant of a strike-slip fault (Ross, 1992), and (ii) eastward subduction beneath a jagged continental margin (see below).

Dilational basin

Ross (1992) suggested that the southeastward subduction beneath the Rimbey High was related to closure of a basin floored by thin continental to oceanic crust. In this model, the opening of the basin is related to strike-slip displacements along north-south oriented faults within the Taltson arc,

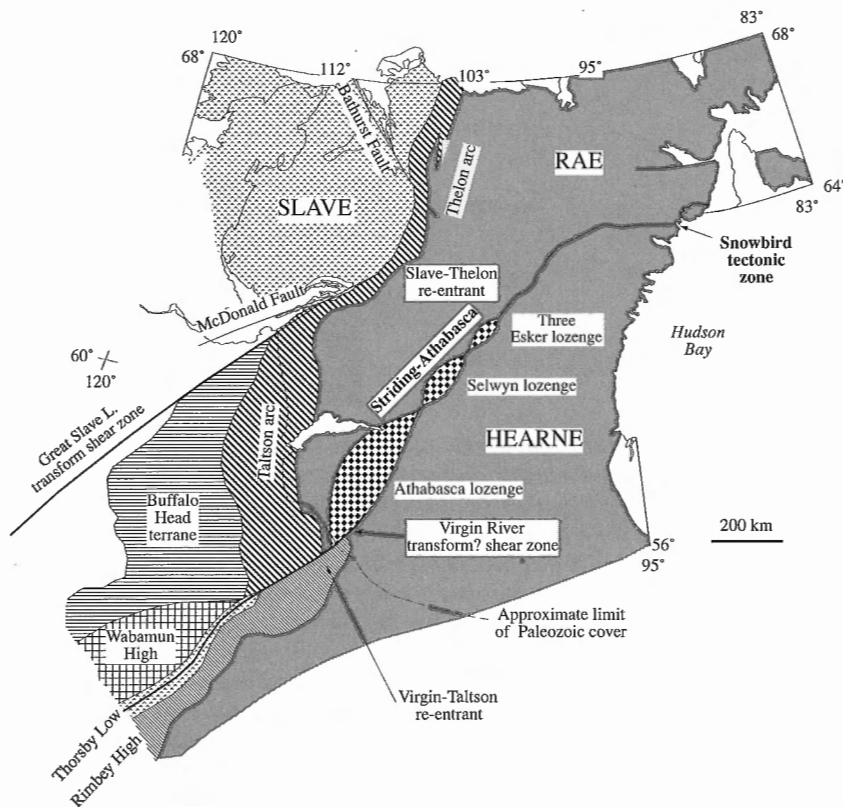


Figure 165.

Sketch of the jagged boundary between Archean western Churchill continent (Rae and Hearne crusts) and the Early Proterozoic Thelon arc, Taltson arc, Rimbey High, the Buffalo Head terrane, Wabamun High, and Thorsby Low, Athabasca, Selwyn and Three Esker lozenges, Virgin-Taltson and Slave-Thelon re-entrants, Great Slave Lake shear zone and Virgin River shear zone transforms. Modified from Ross et al. (1991). Discussed in text.

analogous to recent basins related to major Himalayan faults, such as the South China Sea (Red River Fault) and the Andaman Sea (Sagaing Transform). However, in order to open a basin which extended to the southwest of the Taltson magmatic zone, this model requires the existence of a north-trending, crustal-scale, dextral fault, of appropriate age (pre-1.85 Ga). The basin must be large enough to sustain southeastward subduction and generation of the Rimbey magmas for a period of at least ca. 70 Ma (1.85-1.78 Ga). Accordingly, the fault displacements must be correspondingly important. Even for a simple orthogonal geometry (maximum basin opening/fault slip ratio), and a conservative rate of plate motion (1 cm/a), the basin width and corresponding fault displacement should both be of the order of 700 km, at least. To close the basin, similar magnitude sinistral displacements are required, perhaps along the same fault, during the period 1.85-1.78 Ga. However, the faults within the Taltson magmatic zone form an anastomosing system of discontinuous segments, with both dextral and sinistral elements, for which no through-going master fault has yet been proposed (Bostock, 1987, 1988; McDonough, 1993a, b). The cited authors also show that, where it can be determined, dextral shearing postdates sinistral shearing (see also Hanmer et al., 1992b), the converse of Ross' (1992) model. Moreover, the shear zones appear to be contemporaneous with plutonism in the ca. 1.99-1.90 Ga Taltson magmatic arc (McDonough et al., 1993a; McNicoll et al., 1993) and are thereby too old to have accommodated the ca. 1.85-1.78 Ga closure of the proposed basin.

Re-entrants, jagged margins, and transform faults

An alternative hypothesis is suggested here. The Virgin River shear zone, exposed just north of the Paleozoic cover (Fig. 165), is a narrow greenschist to lower amphibolite facies mylonite zone. It is located on the same side of the Athabasca lozenge as the mylonitic Black-Bompas fault in the lower deck of the East Athabasca mylonite triangle (Fig. 127). If the mylonite along this margin of the lozenge was part of a through-going master fault, it should show the same sense of shear. The Virgin River mylonite is strike-lineated and associated with strike-slip displacements, but in contrast to the sinistral Black-Bompas fault, it has a dextral shear sense (Carolan and Collerson, 1988, 1989; Hanmer et al., 1994). This implies that the Virgin River shear zone does not extend along the boundary of the Athabasca lozenge: *it must terminate south of Lake Athabasca*. Even if it was suggested that the Virgin River shear zone is more properly related to the mylonitic Straight-Grease fault on the northwest (dextral) side of the East Athabasca mylonite triangle (Fig. 1, 3; Hanmer et al., 1994), the kinematic consequences remain unchanged. Such a relationship would imply that the shear zone was composed of discontinuous, left-stepping segments, and the Virgin River segment would still terminate south of Lake Athabasca. Regardless, the initial geochronological data indicate that the Straight-Grease fault has only suffered minor re-activation during the Early Proterozoic (see Table 1).

The orientations of the Early Proterozoic rocks, and their collective boundary with the Archean western Churchill continent in the Alberta subsurface, describe a 120° angle (Fig. 165, 166; Ross et al., 1991). Jagged continental margins,

comprised of promontories and re-entrants, are common features (e.g. Burke and Dewey, 1973; Dewey and Burke, 1974; Rankin, 1976; Thomas, 1977). In some cases it has been shown that primary offsets in the rifted continental margin directly reflect the intersection of the average plane of rifting and pre-existing planes of weakness, such as old faults within the initially intact continent (e.g. Haworth, 1977, 1980).

It is suggested here that the generally meridional (present-day co-ordinates) initial Early Proterozoic margin of the western Churchill continent was jagged with a sharp re-entrant in what is now Alberta, possibly related to the southwest continuation of the train of Middle Archean lozenges (Fig. 165). It is proposed that the Virgin River shear zone acted as a dextral transform fault along the southern arm of the re-entrant (Fig. 166). The restriction of the Rimbey High to the Hearne edge of the Alberta re-entrant (Fig. 165) suggests that the Virgin River shear zone acted to localize intrusion of the Rimbey granite, as has been shown in fault zones elsewhere (e.g. Strong and Hanmer, 1981; Hanmer et al., 1982; Guinberteau et al., 1987; Hutton, 1988; Hutton et al., 1990; Tikoff and Teyssier, 1992). This scenario predicts that the Virgin River shear zone was active over much of its length throughout the period of plutonism (ca. 1.85-1.78 Ga). If the Virgin River shear zone was inherited from the geometry of the initial rifted western Churchill continental margin (Fig. 165), one can predict that it would have influenced the accretion of pre-Rimbey crustal fragments.

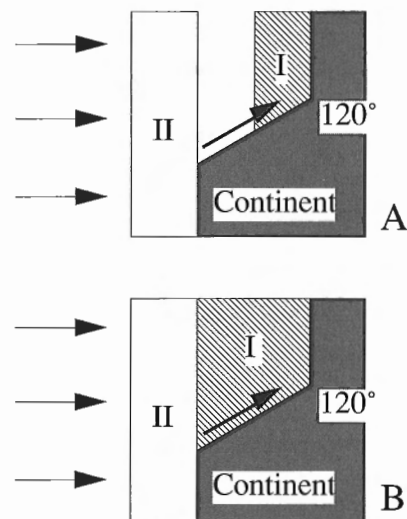


Figure 166. Model of terrane (I), docked at a jagged continental margin, and arrival of a second outboard terrane (II). This hypothesis predicts that the Virgin River shear zone was a long-lived, initially transform fault, which accommodated relative displacements both at the active continental edge and within the accreted terranes. Compare with Figure 165. A fault can remain active during subduction, convergence, and accretion if (i) terrane (I) does not fill the re-entrant (A), or (ii) if it is softer than the continental material (grey) and the rigid re-entrant/promontory pair continues to act as a strength heterogeneity within the continental margin during subsequent compression (B). The initial transform fault may evolve in (B) to become an intraplate strike-slip fault.

Accordingly, the Buffalo Head terrane (Fig. 165), which docked as early as 2.08-2.05 Ga (Bostock and van Breemen, 1994), should be offset or truncated by the proposed transform fault. Ross et al. (1991) present a clear geometrical interpretation of the aeromagnetic data which indicates that this could well be the case. Therefore, it is predicted that further geochronological work should show that parts of the Virgin River shear zone were active for 300 million years (2.08-1.78 Ga; see also Bickford et al., 1994).

The abrupt termination of the magnetic expression of the buried southern segment of the ca. 1.99-1.90 Ga Taltson magmatic arc (Fig. 165) has been taken as *prima facie* evidence for truncation by important Early Proterozoic displacements across the trace of the Snowbird tectonic zone (e.g. Hoffman, 1988; Ross et al., 1991). However, the hypothesis presented here allows for an alternative explanation. Dewey and Lamb (1992) describe a relationship between gaps in the lateral continuity of subduction-related magmatic arcs in the Andes which reflect variations in the dip of the subducting plate. One might envisage segmentation and variable dip of the subducting plate beneath the leading edge of the western Churchill continent, on either side of a Virgin River transform fault, resulting in primary termination of the Taltson arc at the geophysical trace of the Snowbird tectonic zone.

An internal test

The hypothesis stemming from the present study makes two further predictions which one can compare with the available regional geological data. First, a collisional event in the time range ca. 1.85-1.78 Ga must have occurred to the west of the accreted terranes in order to drive the displacements along the Virgin River shear zone after accretion of the Buffalo Head terrane (Fig. 165). Secondly, a jagged continental margin would be expected to contain more than one re-entrant/promontory pair. Regarding the first prediction, the ca. 1.85-1.78 Ga Rimbey plutonism was broadly contemporaneous with latitudinal (present-day co-ordinates) shortening and low temperature faulting adjacent to the Slave Craton (Fig. 1, 165; Hoffman, 1988; Henderson et al., 1990). The dextral McDonald Fault and its sinistral conjugate, the Bathurst Fault, are genetically related and coeval with a network of faults generated by collision of the Nahanni terrane with the Wopmay orogen, west of the Slave Craton, at ca. 1845 Ma (Fig. 1, 165; Villeneuve and Thériault, 1991; see also Hoffman, 1988; Henderson et al., 1990). It is suggested that the docking of the Nahanni terrane is a component of the western collisional event required by this hypothesis. Note, however, that the same prediction is made by Ross et al. (1992).

Regarding the second prediction, the reader's attention is called to the deflections of the western margin of the Rae crust, highlighted by the 2.0-1.9 Ga Taltson-Thelon magmatic arc in the vicinity of Great Slave Lake (Fig. 165). They have been attributed entirely to ca. 1.97-1.90 Ga postcollisional indentation by the Slave Craton indenter (Fig. 165; Hoffman, 1987; Hanmer et al., 1992b). However, the northeast-trending segment of the Rae-Slave boundary, marked by the ca. 2.0-1.9 Ga

Great Slave Lake shear zone, contains an apparently anomalous belt of concordant pre-2.56 Ga mylonite (Hanmer et al., 1992b). In the context of the present discussion, this Late Archean mylonite may have localized a second re-entrant in the initial Early Proterozoic margin of the western Churchill continent which controlled the orientation of Great Slave Lake shear zone, albeit modified by collision and indentation. Note that both Great Slave Lake shear zone and the younger McDonald fault have been interpreted as transform faults (Hoffman, 1987; Henderson et al., 1990). Significantly, the proposed Slave-Thelon and Virgin-Taltson re-entrants are of similar scale. Finally, if the jagged margin hypothesis holds, the remarkable spatial coincidence between Great Slave Lake shear zone and an associated syntectonic granite batholith (Hanmer and Connelly, 1986; Hanmer, 1988a; Hanmer et al., 1992b) is perhaps a well exposed analogue of the relationship I propose here between the Virgin River shear zone and emplacement of the Rimbey plutons.

REFERENCES

- Alcock, F.J.**
1936: Geology of Lake Athabasca region, Saskatchewan; Geological Survey of Canada, Memoir 196, 41 p.
- Annesley, I.R., Madore, C., and Krogh, T.E.**
1992: U-Pb zircon, titanite, and monazite ages from the Wollaston domain: a summary; in Summary of Investigations 1992, Saskatchewan Geological Survey; Saskatchewan Energy and Mines, Miscellaneous Report 92-4, p. 61-65.
- Ashwal, L.D., Morgan, P., and Hoisch, T.D.**
1992: Tectonics and heat sources for granulite metamorphism of supracrustal-bearing terranes; *Precambrian Research*, v. 55, p. 525-538.
- Baer, A.J.**
1969: The Precambrian geology of Fond-du-Lac map-area (74-O), Saskatchewan; Geological Survey of Canada, Paper 68-61, 17 p.
- Bailes, A.H. and McRitchie, W.D.**
1978: The transition from low to high grade metamorphism in the Kisseynew sedimentary gneiss belt, Manitoba; in Metamorphism in the Canadian Shield, Geological Survey of Canada, Paper 78-10, p. 155-179.
- Barton, J.M., van Reenen, D.D., and Roering, C.**
1990: The significance of 3000 Ma granulite-facies mafic dikes in the central zone of the Limpopo belt, southern Africa; *Precambrian Research*, v. 48, p. 299-308.
- Bateman, R.**
1984: On the role of diapirism in the segregation, ascent and final emplacement of granitoid magmas; *Tectonophysics*, v. 110, p. 211-231.
- Beach, A. and Jack, S.**
1982: Syntectonic vein development in a thrust sheet from the external French Alps; *Tectonophysics*, v. 81, p. 67-84.
- Beard, J.S. and Barker, F.**
1989: Petrology and tectonic significance of gabbros, tonalites, shoshonites, and anorthosites in a Late Paleozoic arc-root complex in the Wrangellia terrane, southern Alaska; *Journal of Geology*, v. 87, p. 667-683.
- Bell, T.H.**
1981: Foliation development – the contribution, geometry and significance of progressive, bulk, inhomogeneous shortening; *Tectonophysics*, v. 75, p. 273-296.
1985: Deformation partitioning and porphyroblast rotation in metamorphic rocks: a radical reinterpretation; *Journal of Metamorphic Geology*, v. 3, p. 109-118.
- Bell, T.H. and Etheridge, M.A.**
1973: Microstructures of mylonites and their descriptive terminology; *Lithos*, v. 6, p. 337-348.
1976: The deformation and recrystallisation of quartz in a mylonite zone, Central Australia; *Tectonophysics*, v. 32, p. 235-267.

- Bell, T.H. and Johnson, S.E.**
1989: The role of deformation partitioning in the deformation and recrystallization of plagioclase and K-feldspar in the Woodroffe Thrust mylonite zone, central Australia; *Journal of Metamorphic Geology*, v. 7, p. 151-168.
- Bell, T.H., Duncan, A.C., and Simmons, J.V.**
1989: Deformation partitioning, shear zone development and the role of undeformable objects; *Tectonophysics*, v. 158, p. 163-171.
- Bickford, M.E., Collerson, K.D., and Lewry, J.F.**
1994: Crustal history of the Rae and Hearne provinces, southwestern Canadian Shield, Saskatchewan: constraints from geochronologic and isotopic data; *Precambrian Research*, v. 68, p. 1-21.
- Bickford, M.E., Collerson, K.D., Lewry, J.F., and Orrell, S.E.**
1992: Pegmatites and leucogranites as probes of crust beneath allochthonous orogenic rocks in the Glennie and La Ronge domains; in *Summary of Investigations 1992*, Saskatchewan Geological Survey; Saskatchewan Energy and Mines, Miscellaneous Report 92-4, p. 124-129.
- Bickford, M.E., Van Schmus, W.R., Collerson, K.D., and Macdonald, R.**
1987: U-Pb zircon geochronology project: new results and interpretations; in *Summary of Investigations 1987*, Saskatchewan Geological Survey; Saskatchewan Energy and Mines, Miscellaneous Report 87-4, p. 76-86.
- Bickford, M.E., Van Schmus, W.R., Macdonald, R., Lewry, J.F., and Pearson, J.G.**
1986: U-Pb zircon geochronology project for the Trans-Hudson Orogen: current sampling and recent results; in *Summary of Investigations 1986*, Saskatchewan Geological Survey; Saskatchewan Energy and Mines, Miscellaneous Report 86-4, p. 101-107.
- Biermann, C. and van Roermund, H.L.M.**
1983: Defect structures in naturally deformed clin amphiboles – a TEM study; *Tectonophysics*, v. 95, p. 267-278.
- Black, R. and Liegeois, J.P.**
1993: Cratons, mobile belts, alkaline rocks and continental lithospheric mantle: the Pan-African testimony; *Journal of the Geological Society of London*, v. 150, p. 89-98.
- Bohlen, S.R. and Mezger, K.**
1989: Origin of granulite terranes and the formation of the lowermost continental crust; *Science*, v. 244, p. 326-329.
- Bostock, H.H.**
1987: Geology of the south half of the Taltson Lake map area, District of Mackenzie; in *Current Research, Part A*; Geological Survey of Canada, Paper 87-1A, p. 443-450.
1988: Geology of the north half of the Taltson Lake map area, District of Mackenzie; in *Current Research, Part C*; Geological Survey of Canada, Paper 88-1C, p. 189-198.
- Bostock, H.H. and van Breemen, O.**
1994: Ages of detrital and metamorphic zircons and monazites from a pre-Taltson magmatic zone basin at the western margin of the Rae Province; *Canadian Journal of Earth Sciences*, v. 31, p. 1353-1364.
- Boullier, A.M. and Bouchez, J.L.**
1978: Le quartz en rubans dans les mylonites; *Bulletin de la Société géologique de France*, vol. 7, p. 253-262.
- Brodie, K.H.**
1981: Variation in amphibole and plagioclase composition with deformation; *Tectonophysics*, v. 78, p. 385-402.
- Brodie, K.H. and Rutter, E.H.**
1985: On the relationship between deformation and metamorphism, with special reference to the behaviour of basic rocks; in *Metamorphic reactions, kinetics, textures & deformation*, (ed.) A.B. Thompson and D.C. Rubie; Springer-Verlag, p. 138-179.
1987: Deep crustal extensional faulting in the Ivrea Zone of northern Italy; *Tectonophysics*, v. 140, p. 193-212.
- Brown, I.C. and Wright, G.M.**
1957: Proterozoic rocks of the Northwest Territories and Saskatchewan; in *The Proterozoic in Canada*, (ed.) J.E. Gill; University of Toronto Press, Toronto, p. 79-92.
- Brown, M.**
1973: The definition of metatexis, diatexis and migmatite; *Proceedings of the Geological Association*, v. 84, p. 371-382.
- Brown, R.J.E.**
1967: Permafrost in Canada; Geological Survey of Canada, Map 1246A, scale 1:7 603 200.
- Brun, J.P. and Pons, J.**
1981: Strain patterns of pluton emplacement in a crust undergoing non-coaxial deformation, Sierra Morena, southern Spain; *Journal of Structural Geology*, v. 3, p. 219-230.
- Burke, K. and Dewey, J.F.**
1973: Plume-generated triple junctions: key indicators in applying plate tectonics to old rocks; *Journal of Geology*, v. 81, p. 406-433.
- Burwash, R.A. and Culbert, R.R.**
1976: Multivariate geochemical and mineral patterns in the Precambrian basement of western Canada; *Canadian Journal of Earth Sciences*, v. 13, p. 1-18.
- Byers, A.R.**
1962: Major faults in western part of Canadian Shield with special reference to Saskatchewan; in *The Tectonics of the Canadian Shield*, (ed.) J.S. Stevenson; University of Toronto Press, Toronto, p. 40-59.
- Carney, J.N., Treloar, P.J., Barton, C.M., Crow, M.J., Evans, J.A., and Simango, S.**
1991: Deep-crustal granulites with migmatitic and mylonitic fabrics from the Zambesi Belt, northeastern Zimbabwe; *Journal of Metamorphic Geology*, v. 9, p. 461-479.
- Carolan, J. and Collerson, K.D.**
1988: The Virgin River Shear Zone in the Careen Lake area: field relationships and kinematic indicators; in *Summary of Investigations 1988*, Saskatchewan Geological Survey; Saskatchewan Energy and Mines, Miscellaneous Report 88-4, p. 92-96.
1989: Field relationships and kinematic indicators in the Virgin River Shear Zone; in *Summary of Investigations 1989*, Saskatchewan Geological Survey; Saskatchewan Energy and Mines, Miscellaneous Report 89-4, p. 98-101.
- Castro, A.**
1985: Structural pattern and ascent model in the Central Extremadura batholith; *Journal of Structural Geology*, v. 8, p. 633-645.
- Cavanaugh, M.D. and Seyfert, C.K.**
1977: Apparent polar wander paths and the joining of the Superior and Slave Provinces during Proterozoic time; *Geology*, v. 5, p. 207-211.
- Cavell, P.A., Baadsgaard, H., Wijbrans, J.R., and Compston, W.**
1991: The Archean carbonatite-bearing alkaline intrusion at Kaminak Lake, N.W.T., Canada – an ion microprobe age; in *Proceedings of the 9th International Conference on Geochronology*, Perth, Australia, September 1990, p. 100.
- Chiarenzelli, J.R. and Macdonald, R.**
1986: A U-Pb zircon date for the Ennadai Group; in *Summary of Investigations 1986*, Saskatchewan Geological Survey; Saskatchewan Energy and Mines, Miscellaneous Report 86-4, p. 112-113.
- Chinnery, M.A.**
1969: Secondary Faulting, I. Theoretical aspects; *Canadian Journal of Earth Sciences*, v. 3, p. 163-174.
- Clemens, J.D.**
1988: Volume and composition relationships between granites and their lower crustal source regions: an example from central Victoria, Australia; *Australian Journal of Earth Sciences*, v. 35, p. 445-449.
- Clemens, J.D. and Mawer, C.K.**
1992: Granitic magma transport by fracture propagation; *Tectonophysics*, v. 204, p. 339-360.
- Colborne, G.L.**
1960: The geology of the Clut Lakes area (west half), Saskatchewan; Saskatchewan Department Mineral Resources, Report 43, 22 p.
1961: The geology of the Clut Lakes area (east half), Saskatchewan; Saskatchewan Department of Mineral Resources, Report 58, 31 p.
1962: The geology of the Wiley Lake area (east half), Saskatchewan; Saskatchewan Department of Mineral Resources, Report 69, 44 p.

- Colborne, G.L. and Rosenberger, E.**
1963: The geology of the Wiley Lake area (west half), Saskatchewan; Saskatchewan Department of Mineral Resources, Report 79, 29 p.
- Collerson, K.D., Lewry, J.F., Van Schmus, W.R., and Bickford, M.E.**
1989: Sm-Nd isotopic constraints on the age of the buried basement in central and southern Saskatchewan: implications for diamond exploration; *in* Summary of Investigations 1989, Saskatchewan Geological Survey; Saskatchewan Energy and Mines, Miscellaneous Report 89-4, p. 168-171.
- Collerson, K.D., Van Schmus, R.W., Lewry, J.F., and Bickford, M.E.**
1988: Buried Precambrian basement in south-central Saskatchewan: provisional results from Sm-Nd model ages and U-Pb zircon geochronology; *in* Summary of Investigations 1988, Saskatchewan Geological Survey; Saskatchewan Energy and Mines, Miscellaneous Report 88-4, p. 142-150.
- Collins, W.J. and Vernon, R.H.**
1992: Palaeozoic arc growth, deformation and migration across the Lachlan Fold Belt, southeastern Australia; *Tectonophysics*, v. 214, p. 381-400.
- Coward, M.P., Jan, M.Q., Rex, D., Tarney, J., Thirlwall, M., and Windley, B.F.**
1982: Geo-tectonic framework of the Himalaya of N. Pakistan; *Journal of the Geological Society of London*, v. 139, p. 299-308.
- Cowie, P.A. and Scholz, C.H.**
1992: Growth of faults by accumulation of seismic slip; *Journal of Geophysical Research*, v. 97, p. 11085-11095.
- Cox, S.C.**
1993: Inter-related plutonism and deformation in South Victoria Land, Antarctica; *Geological Magazine*, v. 130, p. 1-14.
- Crocker, C.H. and Collerson, K.D.**
1988: Archean and Early Proterozoic field relationships in the Careen Lake area of the Western Granulite Domain; *in* Summary of Investigations 1988, Saskatchewan Geological Survey; Saskatchewan Energy and Mines, Miscellaneous Report 88-4, p. 97-102.
- Crocker, C.H., Collerson, K.D., Lewry, J.F., and Bickford, M.E.**
1993: Sm-Nd, U-Pb, and Rb-Sr geochronology and lithostructural relationships in the southwestern Rae province: constraints on crustal assembly in the western Canadian shield; *Precambrian Research*, v. 61, p. 27-50.
- Cumming, G.L. and Krstic, D.**
1992: The age of unconformity-related uranium mineralization in the Athabasca Basin, northern Saskatchewan; *Canadian Journal of Earth Sciences*, v. 29, p. 1623-1639.
- Cumming, G.L., Krstic, D., and Wilson, J.A.**
1987: Age of the Athabasca Group, northern Alberta (abstract); *in* Program with Abstracts, Joint Annual Meeting, Geological Association of Canada-Mineralogical Association of Canada, v. 12, p. 35.
- Cunningham, W.D.**
1993: Strike-slip faults in the southernmost Andes and the development of the Patagonian orocline; *Tectonics*, v. 12, p. 169-186.
- Darnley, A.G.**
1981: The relationship between uranium distribution and some major crustal features in Canada; *Mineralogical Magazine*, v. 44, p. 425-431.
- Davidson, A.**
1972: The Churchill Province; *in* Variations in Tectonic Styles in Canada, (ed.) R.A. Price and R.J.W. Douglas; Geological Association of Canada, p. 381-434.
- Davis, G.A.**
1988: Rapid upward transport of mid-crustal mylonitic gneisses in the footwall of a Miocene detachment fault, Whipple Mountains, southeastern California; *Geologische Rundschau*, v. 77, p. 191-209.
- Davis, G.A., Lister, G.S., and Reynolds, S.J.**
1986: Structural evolution of the Whipple and South Mountains shear zones, southwestern United States; *Geology*, v. 14, p. 7-10.
- DePaolo, D.J.**
1981: A neodymium and strontium isotope study of the Mesozoic calc-alkaline granitic batholiths of the Sierra Nevada and Penninsular Ranges, California; *Journal of Geophysical Research*, v. 86, p. 10478-10488.
- Dewey, J.F. and Burke, K.**
1974: Hot spots and continental breakup: implications for collisional orogeny; *Geology*, v. 2, p. 57-60.
- Dewey, J.F. and Burke, K.C.A.**
1973: Tibetan, Variscan and Precambrian basement reactivations: products of continental collision; *Journal of Geology*, v. 81, p. 683-692.
- Dewey, J.F. and Lamb, S.H.**
1992: Active tectonics in the Andes; *Tectonophysics*, v. 205, p. 79-95.
- Douglas, R.J.W.**
1969: Geological map of Canada; Geological Survey of Canada, Map 1250A, scale 1:5 000 000.
- Dudas, F.O., LeCheminant, A.N., and Sullivan, R.W.**
1991: Reconnaissance Nd isotopic study of granitoid rocks from the Baker Lake region, District of Keewatin, N.W.T., and observations on analytical procedures; *in* Radiogenic Age and Isotopic Studies: Report 4; Geological Survey of Canada, Paper 90-2, p. 101-112.
- Eade, K.E.**
1978: Notes on metamorphism in the Churchill Province, District of Keewatin; Geological Survey of Canada, Paper 78-10, p. 191-194.
1985: Geology, Tulemalu Lake-Yathkyed Lake, District of Keewatin, Northwest Territories; Geological Survey of Canada, Map 1604A, scale 1:250 000.
1986: Precambrian geology of the Tulemalu Lake-Yathkyed Lake area, District of Keewatin; Geological Survey of Canada, Paper 84-11, 31 p.
- Emerman, S.H. and Marrett, R.**
1990: Why dikes?; *Geology*, v. 18, p. 231-233.
- England, P.**
1993: Convective removal of thermal boundary layer of thickened continental lithosphere: a brief summary of causes and consequences with special reference to the Cenozoic tectonics of the Tibetan Plateau and surrounding regions; *Tectonophysics*, v. 223, p. 67-73.
- England, P. and Houseman, G.**
1985: Role of lithospheric strength heterogeneities in the tectonics of Tibet and neighbouring regions; *Nature*, v. 315, p. 297-301.
- England, P. and Molnar, P.**
1990: Surface uplift, uplift of rocks, and exhumation of rocks; *Geology*, v. 18, p. 1173-1177.
- Escher, A., Jack, S., and Watterson, J.**
1976: Tectonics of the North Atlantic Proterozoic dyke swarm; *Philosophical Transactions of the Royal Society of London*, v. A280, p. 529-539.
- Etheridge, M.A.**
1975: Deformation and recrystallization of orthopyroxene from the Giles Complex, central Australia; *Tectonophysics*, v. 25, p. 87-114.
- Fraser, J.A., Heywood, W.W., and Mazurski, M.A.**
1978: Metamorphic map of the Canadian Shield; Geological Survey of Canada, Map 1475A, scale 1:5 000 000.
- Freund, R.**
1974: Kinematics of transform and transcurrent faults; *Tectonophysics*, v. 21, p. 93-134.
- Frisch, T. and Parrish, R.R.**
1992: U-Pb zircon ages from the Chantrey Inlet area, northern District of Keewatin, Northwest Territories; *in* Radiogenic Age and Isotopic Studies: Report 4; Geological Survey of Canada, Paper 91-2, p. 35-41.
- Furnival, G.M.**
1940: Stony Rapids and Porcupine River areas, Saskatchewan; Geological Survey of Canada, Paper 40-10, p. 1-10.
1941a: Porcupine River, northern Saskatchewan; Department of Mines and Resources, Mines and Geology Branch, Map 658A, scale 1:253 440.
1941b: Stony Rapids, northern Saskatchewan; Department of Mines and Resources, Mines and Geology Branch Map 658A, scale 1:253 440.
- Gamond, J.F.**
1983: Displacement features associated with fault zones: a comparison between observed examples and experimental models; *Journal of Structural Geology*, v. 5, p. 33-46.
- Gaudemer, Y. and Tapponier, P.**
1987: Ductile and brittle deformations in the northern Snake Range, Nevada; *Journal of Structural Geology*, v. 9, p. 159-180.

Geological Survey of Canada

1987: Magnetic anomaly map of Canada; Geological Survey of Canada, Map 1255A, scale 1:500 000.

Gibb, R.A.

1978: Slave-Churchill collision tectonics; *Nature*, v. 271, p. 50-52.

1983: Model for suturing of Superior and Churchill plates: an example of double indentation tectonics; *Geology*, v. 11, p. 413-417.

Gibb, R.A. and Halliday, D.W.

1974: Gravity measurements in southern District of Keewatin and south-eastern District of Mackenzie, with maps; Earth Physics Branch Gravity Map Series, 124-131, 36 p.

Gibb, R.A., Thomas, M.D., Lapointe, P.L., and Mukhopadhyay, M.

1983: Geophysics of proposed Proterozoic sutures in Canada; *Precambrian Research*, v. 19, p. 349-384.

Gibb, R.A., Thomas, M.D., and Mukhopadhyay, M.

1980: Proterozoic sutures in Canada; *Geoscience Canada*, v. 7, p. 149-154.

Gilboy, C.F.

1978a: Reconnaissance bedrock geology, Stony Rapids area (parts of NTS area 74P); *in* Summary of Investigations 1978, Saskatchewan Geological Survey, Saskatchewan Mineral Resources, Miscellaneous Report 78-10, p. 35-42.

1978b: Reconnaissance bedrock geology, Stony Rapids North (part of NTS 74P); *in* Summary of Investigations 1978, Saskatchewan Geological Survey, Saskatchewan Mineral Resources, Miscellaneous Report 78-10, p. 12-18.

1979: Reconnaissance bedrock geology, Stony Rapids North (part of NTS 74P); *in* Summary of Investigations 1979, Saskatchewan Geological Survey, Saskatchewan Mineral Resources, Miscellaneous Report 79-10, p. 12-18.

1980a: Reconnaissance bedrock geology: Chambeuil Lake East area (part of NTS 74P); *in* Summary of Investigations 1980, Saskatchewan Geological Survey, Miscellaneous Report 80-4, p. 14-16.

1980b: Bedrock compilation geology: Stony Rapids area (NTS 74P). Saskatchewan Geological Survey, Saskatchewan Energy and Mines, Preliminary Geological Map, scale 1: 250 000.

Gilboy, C.F. and Ramaekers, P.

1981: Compilation bedrock geology: Stony Rapids area (NTS 74P); *in* Summary of Investigations 1981, Saskatchewan Geological Survey, Saskatchewan Mineral Resources, Miscellaneous Report 81-4, p. 6-11.

Glikson, A.Y.

1986: An upthrust Early Proterozoic basic granulite-anorthosite suite and anatectic gneisses, south-west Arunta block, Central Australia: evidence on the nature of the lower crust; *Transactions of the Geological Society of South Africa*, v. 89, p. 263-283.

Goodacre, A.K., Grieve, R.A.F., Halpenny, J.F., and Sharpton, V.L.

1987: Horizontal gradient of the Bouguer gravity anomaly map of Canada; Geological Survey of Canada, Canadian Geophysical Atlas, Map 5, scale 1:10 000 000.

Gordon, T.M.

1988: Precambrian geology of the Daly Bay area, District of Keewatin; Geological Survey of Canada, Bulletin 422, p. 21.

Grand, S.

1987: Tomographic inversion for shear velocity beneath the North American plate; *Journal of Geophysical Research*, v. 92, p. 14065-14090.

Guinbertau, B., Bouchez, J.L., and Vigneresse, J.L.

1987: The Mortagne granite pluton (France) emplaced by pull-apart along a shear zone: structural and gravimetric arguments and regional implication; *Geological Society of America Bulletin*, v. 99, p. 763-770.

Hanmer, S.

1982: Microstructure and geochemistry of plagioclase and microcline in naturally deformed granite; *Journal of Structural Geology*, v. 4, p. 197-213.

1984a: Strain – insensitive foliations in polymineralic rocks; *Canadian Journal of Earth Sciences*, v. 21, p. 1410-1414.

Hanmer, S. (cont.)

1984b: The potential use of planar and elliptical structures as indicators of strain regime and kinematics of tectonic flow; *in* Current Research, Part B; Geological Survey of Canada, Paper 84-1B, p. 133-142.

1986: Asymmetrical pull-aparts and foliation fish as kinematic indicators; *Journal of Structural Geology*, v. 8, p. 111-122.

1987a: Granulite facies mylonites: a brief structural reconnaissance north of Stony Rapids, northern Saskatchewan; *in* Current Research, Part A; Geological Survey of Canada, Paper 87-1A, p. 563-572.

1987b: Textural map-units in quartzofeldspathic mylonitic rocks; *Canadian Journal of Earth Sciences*, v. 24, p. 2065-2073.

1988a: Great Slave Lake Shear Zone, Canadian Shield: reconstructed vertical profile of a crustal-scale fault zone; *Tectonophysics*, v. 149, p. 245-264.

1988b: Ductile thrusting at mid-crustal level, southwestern Grenville Province; *Canadian Journal of Earth Sciences*, v. 25, p. 1049-1059.

1989: Initiation of cataclastic flow in a mylonite zone; *Journal of Structural Geology*, v. 11, p. 751-762.

1990: Natural rotated inclusions in non-ideal shear; *Tectonophysics*, v. 176, p. 245-255.

1991: Great Slave Lake shear zone, District of Mackenzie, Northwest Territories; Geological Survey of Canada, Map 1740A, scale 1:150 000.

1994: Geology, East Athabasca mylonite triangle, Saskatchewan; Geological Survey of Canada, Map 1859A, scale 1:100 000.

Hanmer, S. and Connelly, J.N.

1986: Mechanical role of the syntectonic Laloche Batholith in the Great Slave Lake Shear Zone, District of Mackenzie, N.W.T.; *in* Current Research, Part B; Geological Survey of Canada, Paper 86-1B, p. 811-826.

Hanmer, S. and Kopf, C.F.

1993: The Snowbird tectonic zone in District of Mackenzie, Northwest Territories; *in* Current Research, Part C; Geological Survey of Canada, Paper 93-1C, p. 41-52.

Hanmer, S. and Lucas, S.B.

1985: Anatomy of a ductile transcurrent shear: the Great Slave Lake Shear Zone, District of Mackenzie, N.W.T. (preliminary report); *in* Current Research, Part B; Geological Survey of Canada, Paper 85-1B, p. 7-22.

Hanmer, S. and Needham, T.

1988: Great Slave Lake shear zone meets Thelon Tectonic Zone, District of Mackenzie, N.W.T.; *in* Current Research, Part C; Geological Survey of Canada, Paper 88-1C, p. 33-49.

Hanmer, S. and Passchier, C.W.

1991: Shear-sense indicators: a review; Geological Survey of Canada, Paper 90-17, 72 p.

Hanmer, S. and Scott, D.J.

1990: Structural observations in the Gilbert River belt, Grenville Province, southeastern Labrador; *in* Current Research, Part C; Geological Survey of Canada, Paper 90-1C, p. 1-12.

Hanmer, S. and Vigneresse, J.L.

1980: Mise en place de diapirs syntectoniques dans la chaîne hercynienne: exemple des massifs de Locronan et de Pontivy (Bretagne centrale); *Bulletin de la Société géologique de France*, vol. 22, p. 193-202.

Hanmer, S., Berthé, D., and LeCorre, C.

1982: The role of granite emplacement in the Hercynian of Central Brittany; *Journal of the Geological Society of London*, v. 139, p. 85-93.

Hanmer, S., Bowring, S., van Breemen, O., and Parrish, R.

1992a: Great Slave Lake shear zone, northwest Canada: mylonitic record of Early Proterozoic continental convergence, collision and indentation; *Journal of Structural Geology*, v. 14, p. 757-773.

Hanmer, S., Darrach, M., and Kopf, C.

1992b: The East Athabasca mylonite zone: an Archean segment of the Snowbird tectonic zone in Northern Saskatchewan; *in* Current Research, Part C; Geological Survey of Canada, Paper 92-1C, p. 19-29.

- Hanmer, S., Ji, S., Darrach, M., and Kopf, C.**
1991: Tantato domain, northern Saskatchewan: a segment of the Snowbird tectonic zone; *in* Current Research, Part C; Geological Survey of Canada, Paper 91-1C, p. 121-133.
- Hanmer, S., Parrish, R., Williams, M., and Kopf, C.**
1994: Striding-Athabasca mylonite zone: complex Archean deep-crustal deformation in the East Athabasca mylonite triangle, N. Saskatchewan; Canadian Journal of Earth Sciences, v. 31, p. 1287-1300.
- Hanmer, S., Williams, M., and Kopf, C.**
1995a: Striding-Athabasca mylonite zone: implications for Archean and Early Proterozoic tectonics of the western Canadian Shield; Canadian Journal of Earth Sciences, v. 32, p. 178-196.
1995b: Modest movements, spectacular fabrics in an intracontinental deep-crustal strike-slip fault: Striding-Athabasca mylonite zone, NW Canadian Shield; Journal of Structural Geology, v. 17, p. 493-507.
- Harms, T.A. and Price, R.A.**
1992: The Newport fault: Eocene listric normal faulting, mylonitisation, and crustal extension in northeast Washington and northwest Idaho; Geological Society of America Bulletin, v. 104, p. 745-761.
- Haworth, R.T.**
1977: The continental crust northeast of Newfoundland and its ancestral relationship to the Charlie Fracture Zone; Nature, v. 266, p. 246-249.
1980: Appalachian structural trends northeast of Newfoundland and their trans-Atlantic correlation; Tectonophysics, v. 64, p. 111-130.
- Heaman, L.M. and Parrish, R.R.**
1991: U-Pb geochronology of accessory minerals; Mineralogical Association of Canada Handbook on the Application of Radiogenic Isotope Systems to Problems in Geology, v. 19, p. 59-102.
- Henderson, J.B., McGrath, P.H., Theriault, R.J., and van Breemen, O.**
1990: Intracratonic indentation of the Archean Slave Province into the early Proterozoic Thelon Tectonic Zone of the Churchill Province, north-western Canadian Shield; Canadian Journal of Earth Sciences, v. 27, p. 1699-1713.
- Higgins, M.W.**
1971: Cataclastic rocks; United States Geological Survey, Professional Paper 687, 97 p.
- Hoffman, P.F.**
1987: Continental transform tectonics: Great Slave Lake shear zone (ca 1.9 Ga), northwest Canada; Geology, v. 15, p. 785-788.
1988: United plates of America, the birth of a craton: Early Proterozoic assembly and growth of Laurentia; Annual Review of Earth and Planetary Sciences, v. 16, p. 543-603.
1990: Subdivision of the Churchill Province and Extent of the Trans-Hudson Orogen; Geological Association of Canada, Special Paper 37, p. 15-39.
1991: Geological constraints on the origin of the mantle root beneath the Canadian Shield; *in* Allochthonous Terranes, (ed.) J.F. Dewey, I.G. Gass, G.B. Curry, N.B.W. Harris, and A.M.C. Sengor; Cambridge University Press, Cambridge, p. 67-76.
- Hulbert, L.**
1988: Investigation of mafic and ultramafic rocks for nickel-copper and platinum group elements in northern Saskatchewan: preliminary findings; *in* Summary of Investigations 1988, Saskatchewan Geological Survey, Saskatchewan Energy and Mines, Miscellaneous Report 88-4, p. 152-154.
- Hutton, D.H.W.**
1988: Granite emplacement mechanisms and tectonic controls: inferences from deformation studies; Transactions of the Royal Society of Edinburgh, v. 79, p. 245-255.
- Hutton, D.H.W., Dempster, T.J., Brown, P.E., and Becker, S.D.**
1990: A new mechanism of granite emplacement: intrusion in active extensional shear zones; Nature, v. 343, p. 452-455.
- Jan, M.Q.**
1988: Geochemistry of amphibolites from the southern part of the Kohistan arc, N. Pakistan; Mineralogical Magazine, v. 52, p. 147-159.
- Jan, M.Q. and Howie, R.A.**
1981: The mineralogy and geochemistry of the metamorphosed basic and ultrabasic rocks of the Jijal Complex, Kohistan, NW Pakistan; Journal of Petrology, v. 22, p. 85-126.
- Johnston, F.J.**
1960: The geology of the Tantato Lake area, Saskatchewan; Saskatchewan Department of Mineral Resources, Report 44, 32 p.
1961: The geology of the Astrolabe Lake area (west half), Saskatchewan; Saskatchewan Department of Mineral Resources, Report 59, 26 p.
1962: The geology of the Chambeuil Lake area (west half), Saskatchewan; Saskatchewan Department of Mineral Resources, Report 68, 32 p.
1963: The geology of the Lytle Lake area (west half), Saskatchewan; Saskatchewan Department of Mineral Resources, Report 80, 20 p.
1964: The geology of the Lytle Lake area (east half), Saskatchewan; Saskatchewan Department of Mineral Resources, Report 90, 8 p.
- Khan, M.A., Jan, M.Q., Windley, B.F., Tarney, J., and Thirlwall, M.F.**
1989: The Chilas mafic-ultramafic igneous complex: the root of the Kohistan island arc in the Himalaya of northern Pakistan; *in* Tectonics of the Western Himalaya, (ed.) L.L. Malinconico and R.J. Lillie; Geological Society of America, Boulder, Colorado, p. 75-94.
- Kranck, S.H.**
1955: Geology of the Stony Rapids norite area, northern Saskatchewan; MSc. thesis, McGill University, Montreal, Quebec, 100 p.
- Lamouroux, C., Ingles, J., and Debat, P.**
1991: Conjugate ductile shear zones; Tectonophysics, v. 185, p. 309-323.
- LeCheminant, A.N. and Roddick, J.C.**
1991: U-Pb zircon evidence for widespread 2.6 Ga felsic magmatism in the central District of Keewatin, NWT; *in* Radiogenic Age and Isotopic Studies: Report 4; Geological Survey of Canada, Paper 90-2, p. 91-99.
- Leloup, P.H. and Kienast, J.R.**
1993: High-temperature metamorphism in a major strike-slip shear zone, the Ailo Shan-Red River, People's Republic of China; Earth and Planetary Science Letters, v. 118, p. 213-234.
- Lewry, J.F. and Sibbald, T.I.I.**
1977: Variation in lithology and tectonometamorphic relationships in the Precambrian basement of northern Saskatchewan; Canadian Journal of Earth Sciences, v. 14, p. 1453-1467.
1980: Thermotectonic evolution of the Churchill Province in Northern Saskatchewan; Tectonophysics, v. 68, p. 45-82.
- Lewry, J.F., Sibbald, T.I.I., and Rees, C.J.**
1978: Metamorphic patterns and their relation to tectonism and plutonism in the Churchill Province in Northern Saskatchewan; Geological Survey of Canada, Paper 78-10, p. 139-154.
- Lewry, J.F., Sibbald, T.I.I., and Schledewitz, D.C.P.**
1985: Variation in character of Archean rocks in the western Churchill province and its significance; *in* Evolution of Archean Supracrustal sequences, (ed.) L.D. Ayres, P.C. Thurston, K.C. Card, and W. Weber; Geological Association of Canada, p. 239-261.
- Lister, G.S. and Williams, P.F.**
1983: The partitioning of deformation in flowing rock masses; Tectonophysics, v. 92, p. 1-33.
- Logan, J.M.**
1979: Brittle phenomena; Reviews of Geophysics and Space Physics, v. 17, p. 1121-1132.
- Lord, C.S.**
1953: Geological notes on southern District of Keewatin, Northwest Territories; Geological Survey of Canada, Paper 53-22, 11 p.
- Macdonald, R.**
1980: New edition of the geological map of Saskatchewan, Precambrian Shield area; *in* Summary of Investigations 1980, Saskatchewan Geological Survey, Miscellaneous Report 80-4, p. 19-21.
1987: Update on the Precambrian geology and domain classification of northern Saskatchewan; *in* Summary of Investigations 1987, Saskatchewan Geological Survey; Saskatchewan Energy and Mines, Miscellaneous Report 87-4, p. 87-104.

- Macdonald, R. and Sibbald, T.I.I.**
1988: Highlights of the Northern Geoscience Program 1988-89; *in* Summary of Investigations 1988, Saskatchewan Geological Survey; Saskatchewan Energy and Mines, Miscellaneous Report 88-4, p. 1-6.
- Martignole, J.**
1992: Exhumation of high-grade terranes - a review; *Canadian Journal of Earth Sciences*, v. 29, p. 737-745.
- Mawdsley, J.B.**
1949: Pine Channel area, Lake Athabasca District, Saskatchewan; Geological Survey of Canada, Paper 49-27, p. 46.
1957: Charlebois Lake area, Saskatchewan; Saskatchewan Department of Mineral Resources, Geology Branch, Map 24A, scale 1:63 360.
- Mawer, C.K.**
1986: What is a mylonite?; *Geoscience Canada*, v. 13, p. 33-34.
- McDonough, M.R., Grover, T.W., McNicoll, V.J., and Lindsay, D.D.**
1993a: Preliminary report of the geology of the southern Taltson magmatic zone, northeastern Alberta; *in* Current Research, Part C; Geological Survey of Canada, Paper 93-1C, p. 221-232.
- McDonough, M.R., Grover, T.W., McNicoll, V.J., Lindsay, D.D., Kelly, K.L., and Guerstein, P.G.**
1993b: Geology, Mercredi Lake, Alberta (74M/15); Geological Survey of Canada, Open File 2629, scale 1:50 000.
- McLelland, J.M., Chiarenzelli, J., and Perham, A.**
1992: Age, field, and petrological relationships of the Hyde School Gneiss, Adirondack Lowlands, New York: criteria for an intrusive origin; *Journal of Geology*, v. 100, p. 69-90.
- McNicoll, V., McDonough, M., and Grover, T.**
1993: Preliminary U-Pb geochronology of the southern Taltson magmatic zone, northeastern Alberta; *in* Lithoprobe report of transect workshop, Alberta basement transects, v. 31, 129 p.
- Means, W.D., Hobbs, B.E., Lister, G.S., and Williams, P.F.**
1980: Vorticity and non-coaxially in progressive deformations; *Journal of Structural Geology*, v. 2, p. 371-378.
- Mehnert, K.R.**
1971: *Migmatites and the Origin of Granitic Rocks*; Elsevier, Amsterdam, 405 p.
- Meyer, M.T., Bickford, M.E., and Lewry, J.F.**
1992: The Wathaman batholith: an Early Proterozoic continental arc in the Trans-Hudson orogenic belt, Canada; *Geological Society of America Bulletin*, v. 104, p. 1073-1085.
- Mezger, K., Rawnsley, C.M., Bohlen, S.R., and Hanson, G.N.**
1991: U-Pb garnet, sphene, monazite and rutile ages: implications for the duration of high-grade metamorphism and cooling histories, Adirondack Mts, New York; *Journal of Geology*, v. 99, p. 415-428.
- Morand, V.J.**
1992: Pluton emplacement in a strike-slip fault zone: the Doctors Flat Pluton, Victoria, Australia; *Journal of Structural Geology*, v. 14, p. 205-213.
- Mortensen, J.K. and Thorpe, R.I.**
1987: U-Pb zircon ages of felsic volcanic rocks in the Kaminak Lake area, District of Keewatin; *in* Radiogenic Age and Isotope Studies: Report 1; Geological Survey of Canada, Paper 87-2, p. 123-128.
- Nicholson, R. and Pollard, D.D.**
1985: Dilation and linkage of echelon cracks; *Journal of Structural Geology*, v. 7, p. 583-590.
- Nicolas, A. and Poirier, J.P.**
1976: *Crystalline Plasticity and Solid State Flow in Metamorphic Rocks*; Wiley, New York, 444 p.
- Nyman, M.W., Law, R.D., and Smelik, E.A.**
1992: Cataclastic deformation mechanism for the development of core-mantle structures in amphibole; *Geology*, v. 20, p. 455-458.
- Orrell, S.E. and Bickford, M.E.**
1989: Geology of Early Proterozoic gneissic rocks, Black Birch Lake area: progress report 2; *in* Summary of Investigations 1989, Saskatchewan Geological Survey; Saskatchewan Energy and Mines, Miscellaneous Report 89-4, p. 105-109.
- Park, A.F. and Ralser, S.**
1992: Precambrian geology of the southwestern part of the Tavani map area, District of Keewatin, Northwest Territories; Geological Survey of Canada, Bulletin 416, 81 p.
- Parrish, R.R.**
1990: U-Pb dating of monazite and its application to geological problems; *Canadian Journal of Earth Sciences*, v. 27, p. 1431-1450.
- Passchier, C.W. and Simpson, C.**
1986: Porphyroclast systems as kinematic indicators; *Journal of Structural Geology*, v. 8, p. 831-844.
- Paterson, S. and Tobisch, O.T.**
1992: Rates of processes in magmatic arcs: implications for the timing and nature of pluton emplacement and wall rock deformation; *Journal of Structural Geology*, v. 14, p. 291-300.
- Paterson, S.R.**
1988: Cannibal Creek granite: post-tectonic "ballooning" pluton or pre-tectonic piercement diapir?; *Journal of Geology*, v. 96, p. 730-736.
- Paterson, S.R. and Fowler, T.K.**
1993a: Re-examining pluton emplacement processes; *Journal of Structural Geology*, v. 15, p. 191-206.
1993b: Extensional pluton-emplacement models: do they work for large plutonic complexes?; *Geology*, v. 21, p. 781-784.
- Peterson, T.D. and Hamner, S.**
1992: Digital cartography with the Macintosh computer, in and out of the field; *in* Current Research, Part E; Geological Survey of Canada, Paper 93-1E, p. 309-314.
- Pfiffner, O.A. and Ramsay, J.G.**
1982: Constraints on geological strain rates: arguments from finite strain states of naturally deformed rocks; *Journal of Geophysical Research*, v. 87, p. 311-321.
- Pilkington, M.**
1989: Variable-depth magnetization mapping: application to the Athabasca basin, northern Alberta and Saskatchewan, Canada; *Geophysics*, v. 54, p. 1164-1173.
- Pitcher, W.S. and Berger, A.R.**
1972: *The Geology of Donegal: a Study of Emplacement and Unroofing*; Wiley Interscience, London, 435 p.
- Platt, J.P. and England, P.C.**
1993: Convective removal of lithosphere beneath mountain belts: thermal and mechanical consequences; *American Journal of Science*, 293, p. 307-336.
- Platt, J.P. and Vissers, R.L.M.**
1980: Extensional structures in anisotropic rocks; *Journal of Structural Geology*, v. 2, p. 397-410.
- Poirier, J.P.**
1985: *Creep of Crystals: High Temperature Deformation Processes in Metals, Ceramics and Minerals*; Cambridge University Press, 260 p.
- Powell, C.M.**
1986: Continental underplating model for the rise of the Tibetan Plateau; *Earth and Planetary Science Letters*, v. 81, p. 79-94.
- Ramsay, J.G.**
1967: *Folding and Fracturing of Rocks*; McGraw Hill, New York, 568 p.
1989: Emplacement kinematics of a granite diapir: the Chindamora batholith, Zimbabwe; *Journal of Structural Geology*, v. 11, p. 191-209.
- Ramsay, J.G. and Graham, R.H.**
1970: Strain variation in shear belts; *Canadian Journal of Earth Sciences*, v. 7, p. 786-813.
- Rankin, D.W.**
1976: Appalachian salients and recesses: Late Precambrian continental breakup and the opening of the Iapetus Ocean; *Journal of Geophysical Research*, v. 81, p. 5605-5619.
- Roddick, J.C., Henderson, J.R., and Chapman, H.J.**
1992: U-Pb ages from Archean Whitehills-Tehek lakes supracrustal belt, Churchill Province, District of Keewatin, Northwest Territories; *in* Radiogenic Age and Isotopic Studies: Report 4; Geological Survey of Canada, Paper 92-2, p. 31-40.

- Ross, G.M.**
1992: Tectonic evolution of crystalline basement along the central transect; *in* Lithoprobe report of transect workshop, Alberta basement transects, v. 28, p. 120-138.
- Ross, G.M., Parrish, R.R., Villeneuve, M.E., and Bowring, S.A.**
1991: Geophysics and geochronology of the crystalline basement of the Alberta Basin, western Canada; *Canadian Journal of Earth Sciences*, v. 28, p. 512-522.
- Roy, J.L., Morris, W.A., Lapointe, P.L., Irving, E., Park, J.K., and Schmidt, P.W.**
1978: Apparent polar wanderpaths and the joining of the Superior and Slave Provinces during early Proterozoic time: Comment; *Geology*, v. 6, p. 132-133.
- Sanderson, D.J. and Marchini, W.R.D.**
1984: Transpression; *Journal of Structural Geology*, v. 6, p. 449-458.
- Saucier, F., Humphreys, E., and Welldon, R.**
1992: Stress near geometrically complex strike-slip faults: application to the San Andreas Fault at Cajon Pass, Southern California; *Journal of Geophysical Research*, v. 97, p. 5081-5094.
- Schau, M. and Ashton, K.E.**
1979: Granulites and plutonic complexes northeast of Baker Lake, District of Keewatin; *in* Current Research, Part A; Geological Survey of Canada, Paper 79-1A, p. 311-316.
- Schau, M., Tremblay, F., and Christopher, A.**
1982: Geology of Baker Lake map area, District of Keewatin: a progress report; *in* Current Research, Part A; Geological Survey of Canada, Paper 82-1A, p. 143-150.
- Segall, P. and Pollard, D.D.**
1980: The mechanics of discontinuous faults; *Journal of Geophysical Research*, v. 85, p. 4337-43540.
- Segall, P. and Simpson, C.**
1986: Nucleation of ductile shear zones on dilatant fractures; *Geology*, v. 14, p. 56-59.
- Seyfert, C.K. and Cavanaugh, M.D.**
1978: Apparent polar wander paths and the joining of the Superior and Slave Provinces during Proterozoic time: Reply; *Geology*, v. 6, p. 133-135.
- Sibson, R.H.**
1977: Fault rocks and fault mechanisms; *Journal of the Geological Society of London*, v. 133, p. 191-213.
1980: Transient discontinuities in ductile shear zones; *Journal of Structural Geology*, v. 2, p. 165-171.
1986a: Brecciation processes in fault zones: inferences from earthquake rupturing; *Pure and Applied Geophysics*, v. 124, p. 159-175.
1986b: Rupture interaction with fault jogs; *American Geophysical Union, Geophysical Monograph*, v. 37, p. 157-167.
- Simpson, C.**
1986: Fabric development in brittle-to-ductile shear zones; *Pageophysics*, v. 124, p. 269-288.
- Slimmon, W.L.**
1989: Bedrock compilation geology: Fond du Lac (NTS 74-O); Saskatchewan Geological Survey, Saskatchewan Energy and Mines, Map 247A, scale 1: 250 000.
- Slimmon, W.L. and Macdonald, R.**
1987: Bedrock geological mapping, Pine Channel area (Part of NTS 74O-7 and -8); *in* Summary of Investigations 1987, Saskatchewan Geological Survey; Saskatchewan Energy and Mines, Miscellaneous Report 87-4, p. 28-33.
- Snoeyenbos, D.R., Williams, M.L., and Hanmer, S.**
1995: An Archean eclogite facies terrane in the western Canadian Shield; *European Journal of Mineralogy*, v. 7, p. 1251-1272.
- Spear, F.S. and Florence, F.P.**
1992: Thermobarometry in granulites: pitfalls and new approaches; *Precambrian Research*, v. 55, p. 209-241.
- Stevenson, R.K., Patchett, P.J., and Martin, R.F.**
1989: Sm-Nd isochron from a granodiorite-granite complex in the Portman Lake region, Northwest Territories; *Canadian Journal of Earth Sciences*, v. 26, p. 2724-2729.
- Strong, D.F. and Hanmer, S.**
1981: The South Brittany leucogranites: formation by frictional heating, fractional melting and fluid flux; *Canadian Mineralogist*, v. 19, p. 163-176.
- Swanson, M.T.**
1992: Fault structure, wear mechanisms and rupture processes in pseudo-tachylite generation; *Tectonophysics*, v. 204, p. 223-242.
- Symons, D.T.A.**
1991: Paleomagnetism of the Proterozoic Wathaman batholith and the suturing of the Trans-Hudson orogen in Saskatchewan; *Canadian Journal of Earth Sciences*, v. 28, p. 1931-1938.
- Talbot, C.J. and Sokoutis, D.**
1992: The importance of incompetence; *Geology*, v. 20, p. 951-953.
- Tapponier, P. and Molnar, P.**
1976: Slip-line field theory and large scale continental tectonics; *Nature*, v. 264, p. 319-324.
- Tapponier, P., Peltzer, G., and Armijo, R.**
1986: On the mechanics of the collision between India and Asia; *in* Collision Tectonics, Special Publication Geological Society of London, (ed.) M.P. Coward and A.C. Ries; Geological Society of London, p. 115-157.
- Tapponier, P., Peltzer, G., Le Dain, A. Y., Armijo, R., and Cobbold, P.R.**
1982: Propagating extrusion tectonics in Asia: new insights from simple experiments with plasticine; *Geology*, v. 10, p. 611-616.
- Taylor, F.C.**
1963: Snowbird Lake map-area, District of Mackenzie; Geological Survey of Canada, Memoir 333, p. 23.
1970: Geology, Wholdaia Lake, District of Mackenzie; Geological Survey of Canada, Map 1199A, scale 1: 250 000.
- Tella, S. and Eade, K.E.**
1985: Geology, Kamilukuak Lake, District of Keewatin, Northwest Territories; Geological Survey of Canada, Map 1629A, scale 1:250 000.
1986: Occurrence and possible tectonic significance of high-pressure granulite fragments in the Tulemalu fault zone, District of Keewatin, N.W.T., Canada; *Canadian Journal of Earth Sciences*, v. 23, p. 1950-1962.
- Tella, S., Schau, M., Armitage, A.E., Seemayer, B.E., and Lemkow, D.**
1992: Precambrian geology and economic potential of the Meliadine Lake-Barbour Bay region, District of Keewatin, Northwest Territories; *in* Current Research, Part C; Geological Survey of Canada, Paper 92-1C, p. 1-11.
- Teskey, D.J. and Hood, P.J.**
1991: The Canadian aeromagnetic database: evolution and applications to the definition of major crustal boundaries; *Tectonophysics*, v. 192, p. 41-56.
- Theriault, R.J.**
1992: Nd isotopic evolution of the Taltson magmatic zone, Northwest Territories, Canada: insights into the early Proterozoic accretion along the western margin of the Churchill Province; *Journal of Geology*, v. 100, p. 465-475.
- Thomas, D.J.**
1983: Distribution, geological controls and genesis of uraniferous pegmatites in the Cree Lake zone of northern Saskatchewan; MSc. thesis, University of Regina, Regina, Saskatchewan, 100 p.
- Thomas, M.D. and Gibb, R.A.**
1985: Proterozoic plate subduction and collision: processes for reactivation of Archean crust in the Churchill Province; *Geological Association of Canada, Special Paper* 28, p. 264-279.
- Thomas, M.D., Grieve, R.A.F., and Sharpton, V.L.**
1988: Gravity domains and assembly of the North American continent by collisional tectonics; *Nature*, v. 331, p. 333-334.
- Thomas, W.A.**
1977: Evolution of Appalachian-Ouachita salients and recesses from reentrants and promontories in the continental margin; *American Journal of Science*, v. 277, p. 1233-1278.

- Tikoff, B. and Teyssier, C.**
1992: Crustal-scale, en echelon "P-shear" tensional bridges: a possible solution to the batholithic room problem; *Geology*, v. 20, p. 927-930.
- Tullis, J.**
1983: Deformation of feldspars; in *Feldspar Mineralogy*, (ed.) P.H. Ribbe; Mineralogy Society of America, p. 297-323.
- Tullis, J. and Yund, R.A.**
1980: Hydrolytic weakening of experimentally deformed Westerly Granite and Hale albite rock; *Journal of Structural Geology*, v. 2, p. 439-453.
1985: Dynamic recrystallization of feldspar: a mechanism for ductile shear zone formation; *Geology*, v. 13, p. 238-241.
- Tullis, J., Dell'Angelo, L., and Yund, R.A.**
1990: Ductile shear zones from brittle precursors in feldspathic rocks: the role of dynamic recrystallization; in *The Brittle-Ductile Transition in Rocks: The Heard Volume*, (ed.) A. Duba, W.B. Durham, J.W. Handin, and H.F. Wang; American Geophysical Union, Washington, D.C., p. 67-81.
- Tullis, J., Snoke, A.W., and Todd, V.R.**
1982: Penrose Conference Report: significance and petrogenesis of mylonitic rocks; *Geology*, v. 10, p. 227-230.
- Tyrrell, J.B.**
1897a: Report of the Doobaunt, Kazan and Ferguson Rivers and the north-west coast of Hudson Bay and on two overland routes from Hudson Bay to Lake Winnipeg; Geological Survey of Canada, Annual Report 1897, Part F, p. 218.
1897b: Report on the country between Athabaska Lake and Churchill River; Geological Survey of Canada, Annual Report 1895, Part D, p. 120.
- Van den Eeckhout, B., Grocott, J., and Vissers, R.**
1986: On the role of diapirism in the segregation, ascent and final emplacement of granitoid magmas – discussion; *Tectonophysics*, v. 127, p. 161-166.
- Van Schmus, W.R., Persons, S.S., Macdonald, R., and Sibbald, T.I.I.**
1986: Preliminary results from U-Pb zircon geochronology in the Uranium City region; in *Summary of Investigations 1986*, Saskatchewan Geological Survey; Saskatchewan Energy and Mines, Miscellaneous Report 86-4, p. 108-111.
- Villeneuve, M.E. and Thériault, R.J.**
1991: U-Pb ages and Sm-Nd signature of two subsurface granites from the Fort Simpson magnetic high, northwest Canada; *Canadian Journal of Earth Sciences*, v. 28, p. 1003-1008.
- Villeneuve, M.E., Ross, G.M., Thériault, R.J., Miles, W., Parrish, R.R., and Broome, J.**
1993: Tectonic subdivision and U-Pb geochronology of the crystalline basement of the Alberta Basin, western Canada; *Geological Survey of Canada, Bulletin 447*, p. 86.
- Vilotte, J.P., Daignières, M., Madariaga, R., and Zienkiewicz, O.C.**
1984: The role of a heterogeneous inclusion during continental collision; *Physics of the Earth and Planetary Interiors*, v. 36, p. 236-259.
- Walcott, R.I.**
1968: The gravity field of northern Saskatchewan and northeastern Alberta with maps; Dominion Observatory Gravity Map Series Report 16-20.
- Walcott, R.I. and Boyd, J.B.**
1971: The gravity field of northern Alberta, and part of Northwest Territories and Saskatchewan, with maps; Earth Physics Branch, Gravity Map Series 103-111, 13 p.
- Wallis, R.H.**
1970a: A geological interpretation of gravity and magnetic data, northwest Saskatchewan; *Canadian Journal of Earth Sciences*, v. 7, p. 858-868.
- Wallis, R.H. (cont.)**
1970b: The geology of the Dufferin Lake area (west half), Saskatchewan; Saskatchewan Department of Mineral Resources, Report 132, 59 p.
- White, J.C. and Mawer, C.K.**
1986: Extreme ductility of feldspars from a mylonite, Parry Sound, Canada; *Journal of Structural Geology*, v. 8, p. 133-143.
1988: Dynamic recrystallization and associated exsolution in perthites: evidence of deep crustal thrusting; *Journal of Geophysical Research*, v. 93, p. 325-337.
- White, S.H.**
1975: Tectonic deformation and recrystallization of plagioclase; *Contributions to Mineralogy and Petrology*, v. 50, p. 287-304.
1982: Fault rocks of the Moine Thrust zone: a guide to their nomenclature; *Textures and Microstructures*, v. 4, p. 211-221.
- White, S.H., Burrows, S.E., Carreras, J., Shaw, N.D., and Humphreys, F.J.**
1980: On mylonites in ductile shear zones; *Journal of Structural Geology*, v. 2, p. 175-187.
- Williams, M.L., Hanmer, S., Kopf, C., and Darrach, M.**
1995: Syntectonic generation and segregation of tonalitic melts from amphibolite dikes in the lower crust, Striding-Athabasca mylonite zone, Northern Saskatchewan; *Journal of Geophysical Research*, v. 100, p. 15717-15734.
- Windley, B.F.**
1984: *The Evolving Continents*; Wiley, New York, 399 p.
- Windley, B.F., Bishop, F.C., and Smith, J.V.**
1981: Metamorphosed layered igneous complexes in Archean granulite-gneiss belts; *Annual Reviews of Earth and Planetary Science*, v. 9, p. 175-198.
- Wise, D.V., Dunn, D.E., Engelder, J.T., Geiser, P.A., and Hatcher, R.D.**
1984: Fault related rocks: suggestions for terminology; *Geology*, v. 12, p. 391-394.
- Wolf, M.B. and Saleeby, J.B.**
1992: Jurassic Cordilleran dike swarm-shear zones: implications for the Nevadan orogeny and North American plate motion; *Geology*, v. 20, p. 745-748.
- Wolf, M.B. and Wyllie, P.J.**
1993: Garnet growth during amphibolite anatexis: implications of a garnetiferous restite; *Journal of Geology*, v. 101, p. 357-373.
- Woodcock, N.H. and Fischer, M.**
1986: Strike-slip duplexes; *Journal of Structural Geology*, v. 8, p. 725-735.
- Wright, G.M.**
1955: Geological notes on central District of Keewatin, Northwest Territories; Geological Survey of Canada, Paper 55-17, 17 p.
- Wright, G.M. (cont.)**
1967: Geology of the southeastern Barren Grounds, parts of the Districts of Mackenzie and Keewatin (Operations Keewatin, Baker, Thelon); Geological Survey of Canada, Memoir 350, p. 91.
- Wyborn, D.**
1992: The tectonic significance of Ordovician magmatism in the eastern Lachlan Fold Belt; *Tectonophysics*, v. 214, p. 177-192.
- Zeck, H.P.**
1974: Cataclastites, hemiclastites, holoclastites, blasto-ditto and myloblastites – cataclastic rocks; *American Journal of Science*, v. 274, p. 1064-1073.

